

CALIFORNIA INSTITUTE OF TECHNOLOGY

EARTHQUAKE ENGINEERING RESEARCH LABORATORY

**ENGINEERING DATA AND ANALYSES OF
THE WHITTIER, CALIFORNIA
EARTHQUAKE OF JANUARY 1, 1976**

BY

AHMED M. ABDEL-GHAFFAR

EERL 77-05

A REPORT ON RESEARCH CONDUCTED UNDER A
GRANT FROM THE NATIONAL SCIENCE FOUNDATION

PASADENA, CALIFORNIA

NOVEMBER, 1977

CALIFORNIA INSTITUTE OF TECHNOLOGY
EARTHQUAKE ENGINEERING RESEARCH LABORATORY

ENGINEERING DATA AND ANALYSES OF THE WHITTIER,
CALIFORNIA EARTHQUAKE OF JANUARY 1, 1976

By

Ahmed M. Abdel-Ghaffar

EERL 77-05

A Report on Research Conducted under a Grant
from the National Science Foundation

Pasadena, California

November, 1977

TABLE OF CONTENTS

<u>Chapter</u>	<u>Title</u>	<u>Page</u>
I	General Introduction	1
II	The Whittier Building	9
	II-1 Description of the Structure	9
	II-2 Time Domain Analysis	10
	II-3 Frequency Domain Analysis	12
III	Carbon Canyon Dam	76
	III-1 Description of the Structure	76
	III-2 Time Domain Analysis	78
	III-3 Frequency Domain Analysis	79
IV	Brea Dam	143
	IV-1 Description of the Structure	143
	IV-2 Time Domain Analysis	144
	IV-3 Frequency Domain Analysis	145
V	Diemer Filtration Plant	187
	V-1 Description of the Structure	187
	V-2 Time Domain Analysis	189
	V-3 Frequency Domain Analysis	190
VI	Orange County Reservoir	231
	VI-1 Description of the Structure	231
	Conclusions	253
	Acknowledgement	254

CHAPTER I

GENERAL INTRODUCTION

A magnitude 4.2 earthquake occurred near Whittier, California on January 1, 1976 at 09:20 Pacific Standard time. The shock was centered at 33.58°N (Lat.) and 117.53°W (Long.) in the Puente Hills of Los Angeles County. The ground shaking was recorded within a 14 Km (8.7 miles) radius of the instrumentally determined epicenter, and eleven strong-motion accelerograph records were obtained on 70 mm film from SMA-1 accelerographs operated as part of the U.S.G.S. Seismic Engineering Branch network. Although of relatively small magnitude, the earthquake did produce peak ground accelerations as high as 18% g, which merit an engineering analysis. The locations of the strong-motion accelerograph stations at the time of the earthquake are shown in Fig. 1. The eleven records were obtained from different structures as follows: (1) three records from a ten-story modern reinforced-concrete building in Whittier, (2) three records from the Carbon Canyon earth-dam site, (3) two records from the Brea earth-dam site, (4) two records from the Diemer Filtration Plant, and finally (5) one record from the Orange County Reservoir. Instruments located at Whittier Dam (16.4 Km from the instrumental epicenter) and at Puddingstone Dam (15.0 Km from the epicenter) were operational, but were not triggered by the event (Etheredge and Nielson, Ref. 1).

According to the Caltech Seismological Laboratory at Pasadena (2), the earthquake occurred at a depth of approximately 8 Km (5 miles), and the instrumental epicenter was located about 4 Km (2.5 miles)

north of the Whittier fault zone (see Fig. 1); the earthquake apparently occurred along a small fault approximately 2 Km (1.25 miles) in length that strikes $N 26^{\circ} E$ and dips $72^{\circ} NW$. The orientation of this fault is about 90° with respect to the existing Whittier fault; there was no evidence of surface faulting, but a relative movement was observed in the garage of one residence in the earthquake-affected area. The idealized empirical relation between magnitude and fault length (Housner, 1970) would predict a fault length of 1.3 miles for a magnitude of 4.5, and would predict the fault length of this earthquake to be about 1.2 miles, which is in good agreement with the instrumentally estimated length.

Minor damage, which mainly included broken plate glass windows and cracked plaster, was reported at La Habra, about 5 Km (3.1 miles) south of the epicenter (Ref. 1). Telephone service in some areas was temporarily disrupted. And, the earthquake was felt approximately 80 Km (50 miles) eastward into San Bernardino and Riverside Counties as well as in Los Angeles and Orange Counties (Whittier Daily News, January 2, 1976).

Table 1 is a list of the eleven recovered records, showing the maximum accelerations for the three components at each station with locator coordinates, epicentral distances, the type of structure at each site and the specific location of the instruments at the site. The maximum recorded ground acceleration was $18\% g$, at Orange County Reservoir which is 3.5 Km (2.2 miles) south of the epicenter (Fig. 1). All the eleven stations recorded peak accelerations of $0.10 g$ or greater, except the two instruments at

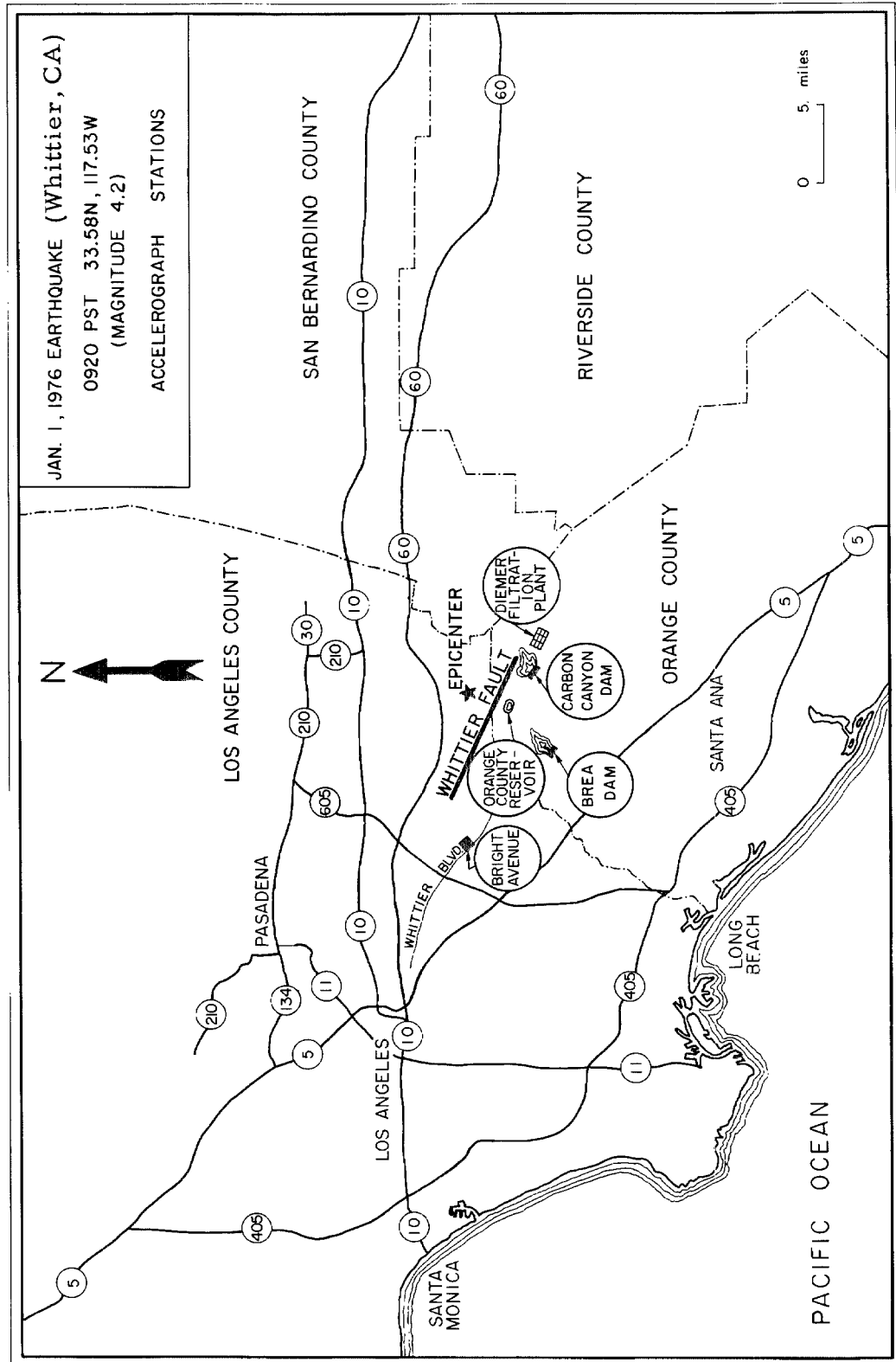


Fig. 1

Diemer Filtration Plant. The maximum recorded acceleration (0.28 g) occurred in Whittier, about 13.8 Km (8.6 miles) west of the epicenter. The accelerograph which recorded it was located at the fifth floor level of the ten-story reinforced concrete building at 7215 Bright Avenue (Fig. 1). The peak acceleration recorded at the basement level was 0.17g and at the tenth floor level was 0.19g. Seismographs from the two Carbon Canyon Dam abutment stations show peak accelerations of 0.14g. The crest station recorded a slightly lower (0.12 g) peak acceleration.

Table 1 and Fig. 1 indicate, for this small earthquake, that close to the fault there is a wide variation in peak acceleration (it ranges from 0.02 g to 0.18 g), and that there is a rapid attenuation of the ground shaking (it decays markedly within a distance of 14 Km (8.7 miles) from the fault). It should be noted that the peak acceleration is only approximately correlated with the general intensity of ground shaking. As indicated by Housner (1974), the variation in peak acceleration depends on such things as depth of faulting, orientation of the fault, the proximity of the site to the portion of the fault that releases significant seismic energy, the source mechanism and the nature of the foundation material. For this earthquake, since the length of the fault over which slipping took place was small, the area affected by strong ground shaking was also small.

For this particular small earthquake, the main ground motion was preceded by less intense shaking (P-wave) which served to start the accelerographs in good time to record a complete picture of significant ground motion as well as structural responses.

TABLE 1

January 1, 1976 Whittier California Earthquake
(33.58 N, 117.53 W), Local Magnitude = 4.2

Station Information			Type of Structure	Distance from Epicenter (Km)	Component	Peak Accl. in g		Peak Ratio I/II	S-Wave Minus Trigger Time(sec)
Station	Name	Coordinate				Vol. I	Vol. II		
The Lutheran Whittier Tower 7215 Bright Ave., Whittier California	Basement	33.97 N	Ten-story Reinforced Concrete Building with shear walls and frames	13.8	North Down West North Down West North Down West	0.06	0.06	1.00	2.5
		118.04 W				0.07	0.06	1.17	
	5th Floor	33.97 N				0.17	0.16	1.06	
						0.07	0.06	1.17	
		118.04 W				0.10	0.09	1.11	2.5
						0.28	0.23	1.22	
	10th Floor	33.97 N				0.04	0.04	1.00	
						0.12	0.11	1.09	
Carbon Canyon Dam		118.04 W	Earth-fill structure 100 ft high and 1,925 ft long	7.4	N50W Down S40W N50W Down S40W N50W Down S40W	0.08	0.06	1.33	1.7
	Crest	33.92 N				0.05	0.05	1.00	
		117.8 W				0.12	0.10	1.20	
		33.92 N				0.10	0.08	1.25	
Brea Dam	R. Abutment	117.8 W		7.4		0.04	0.03	1.33	1.7
						0.14	0.13	1.08	
		33.92 N				0.13	0.10	1.30	
	L. Abutment	117.8 W				0.05	0.04	1.25	
			Zoned earthen embankment 90 ft high and 1,765 ft long	9.3		0.14	0.12	1.17	2.1
	Crest	33.89 N				0.09	0.08	1.13	
		117.93 W				0.06	0.05	1.20	
	Downstream	33.89 N				0.13	0.11	1.18	
Diemer Filtration Plant		117.93 W	Water treatment facility	8.9		0.10	0.08	1.18	1.8
						0.05	0.04	1.25	
	Adm. Bldg. (Basement)	33.91 N				0.06	0.05	1.20	
	Reservoir	117.82 W				0.02	.02	1.00	
Orange County Reservoir		117.82 W	Rectangular reservoir with rounded corners	3.5		0.02	.02	1.00	1.6
						0.02	.02	1.00	
	Abutment	33.94 W				0.02	.02	1.00	
		117.88 W				0.02	.02	1.00	
						0.07	.07	1.00	1.7
						0.18	0.16	1.13	
						0.05	0.04	1.25	
						0.08	0.07	1.14	

The eleven records from the earthquake were digitized, processed and analyzed with the aid of the Caltech standard data-processing procedures. The results are presented in the standard four-volume form: (1) uncorrected digital accelerograms, (2) corrected accelerations, velocities, and displacements, (3) response spectra, and (4) Fourier amplitude spectra.

It is important to point out the appearance of long-period distortion in the integrated velocity and displacement curves in the three components of the eleven records. The standard filtering technique does not remove components having periods of 7 to 10 seconds, hence they show on the integrated curves. These long-period fluctuations could be due to contributions from digitization error, from the digital-filter used in processing the data, and from actual long period ground motions. They could have been removed by a different digital filter, but it was decided not to do so. The results, therefore, illustrate the output of the standard data processing procedure, but the long period components should not be interpreted as representing actual ground motions.

Although this small magnitude earthquake did not cause any damage of engineering significance, there are certain features of the recorded motions that have significance for engineering. The analysis of the recorded motions of the Whittier Building shows that the vibrations of even such a single building excited by moderate shaking are rather complex. The recorded motions at the Diemer Reservoir revealed very significant structural properties of the Reservoir; and the records obtained on the right and left

abutments of Carbon Canyon Dam give valuable information on the degree of correlation between the motions at the two ends of a dam.

REFERENCES

1. "Seismic Engineering Program Report, January - March 1976", Geological Survey Circular 736-A, U.S. Department of the Interior.
2. Personal communication with David Hadley of the Caltech Seismological Laboratory.
3. Housner, G.W.(1970), Strong Ground Motion, Chapter 4 in Earthquake Engineering, edited by R. L. Wiegel, Prentice-Hall, 1970.
4. Housner, G.W. (1974), "Important Features of Earthquake Ground Motion", Proceedings of the Fifth World Conference on Earthquake Engineering, Rome, Italy, Jan. 1974.

CHAPTER II

THE WHITTIER BUILDING

II-1 Description of the Structure

The Lutheran Whittier Tower is a ten-story, reinforced concrete building constructed in 1972 at 7215 Bright Avenue, Whittier, California. The site of the building is approximately 13.8 Km due west of the instrumental epicenter of the January 1, 1976 Whittier, California earthquake. Figure 2 shows a general photograph looking at the north face (short face) and at the east face (long face) of the building, while Fig. 3 shows a structural elevation of the north tower end (south tower end is similar).

The lateral load resisting system of the structure in the east-west direction is composed of two reinforced concrete shear walls comprising the north and south faces (axes 2 and 13 in Figs. 4 and 5) in addition to two small shear walls surrounding the stair-well (axes 7 and 8 in Figs. 4 and 5). The four shear walls extend from the basement level all the way up to the roof level of the building. Other shear walls are provided from the basement level to the second floor to limit deformations and to increase the energy storage capacity of the structure (see Fig. 5-b).

In the longitudinal direction (north-south direction) the structural system of the building is comprised of reinforced concrete frames of column and slab construction with deep beams around the perimeter (axes C, G, 2 and 13 in Figs. 4 and 5). All the columns are of approximately equal stiffness, and are supported by individual spread footings. The east and west faces of the building

consist of columns, beams and reinforced concrete window-wall panels which add appreciable stiffness to the structure for motions in the north-south direction. Interior partitions are constructed of steel studs and drywall (Fig. 4-a).

The foundation of the building consists of spread footings with a design bearing pressure of 5,000 psf. The parking structure consists of prestressed floor deck and columns as shown in Figs. 3 and 4. The building is 183' - 4" by 52' - 8" in plan from the third floor level to the roof level and is 183' - 4" by 64' - 2" from the first floor up to the third floor, while the parking deck is 205' - 4" by 50' - 6" in plane (Fig. 4). The building extends 90 feet above the ground level.

The accelerographs were located in the basement, fifth floor and tenth floor as shown in Figs. 4-a and 5-b. These instruments were designed to start simultaneously when any one of the three reached the threshold level. Each instrument recorded two horizontal and one vertical component of acceleration.

II-2 Time Domain Analysis

The digitized and uncorrected accelerograms recovered from the basement, 5th floor and 10th floor of the building are shown in Figs. 6-a, b and c, while Figs. 7, 8 and 9 show the corrected accelerograms, and the computed velocities and displacements. The maximum recorded acceleration (0.28g) occurred on the 5th floor in the east-west (E-W) direction; the peak acceleration recorded at the basement level in this direction was 0.17g, and at the 10th floor level it was 0.19g. In general, the earthquake ground shaking and

the building response recorded in the E-W direction were markedly stronger than that recorded in the north-south (N-S) direction.

The accelerograms from the upper floors (Figs. 8-a, b, c and 9-a, b, c) of the Whittier building showed that the structure responded in the expected manner. During the earthquake, the N-S motion at the 10th floor reached a peak value of 36 cm/sec^2 (4%g), and clearly showed the motion of the fundamental mode with apparent period of about 0.8 seconds; this is shown in the last seven seconds of the recorded sixteen seconds of motion (Fig. 9-b). The computed velocity shows the motion with this fundamental period superimposed on a long-period fluctuation. Figure 9-b also shows that the higher modes participated significantly in the N-S direction during the first half of the record. The computed velocity curve of the 5th floor in the N-S direction (Fig. 8-b) shows, again, that the structure was vibrating with apparent fundamental period of about 0.8 seconds. There is also a motion with 0.27 seconds period which is very clear in the acceleration curve of Fig. 8-b. The E-W component of the 10th floor shows that a period of about 0.6 seconds dominated between 8 and 16 seconds (Fig. 9-a) which apparently is the natural period of the fundamental mode of vibration in this direction. A significant part of the record in the E-W direction was dominated by this motion of the fundamental mode. From 0 to 4 seconds on the 10th floor (Fig. 9-a) very small response is shown, while from 4 to 8 seconds a contribution from a period of about 0.4 seconds and from a period of about 0.18 seconds is clearly shown. During the strong shaking (approximately 1 second duration), the 5th floor vibrated with a period of about 0.18 seconds.

Then, after 4 seconds of motion, the same floor vibrated with a period of 0.6 seconds as well as a period of 0.4 seconds; this is clearly shown between 4 and 10 seconds (see Fig. 8-a). In general, the duration of the strong phase of ground shaking was relatively short, only about one second, and the peak acceleration pulse in the E-W direction was very narrow (Fig. 7-a), so that the building was not as strongly excited into vibrations as would have happened had the duration been longer and the pulse areas larger.

II-3 Frequency Domain Analysis

The response spectrum curves for the three components of motion of the three floors of the Whittier building are shown in Figs. 10 through 18, while the Fourier amplitude spectrum curves of the recorded accelerations are shown in Figs. 19 through 27. The Fourier amplitude spectrum curves of the accelerations recorded at the 5th and 10th floors reflect the absolute motion of the structure, i. e., the combination of the motion of each floor with respect to the basement and the motion of the basement itself. To isolate the structural motion, the amplification spectra for the 16 seconds of motion were computed by dividing the Fourier amplitude spectrum of the acceleration recorded at the upper floors (5th and 10th) of the building by that recorded at the basement. Before the division, the Fourier amplitude spectrum curves were smoothed with one pass of a Hanning Window ($\frac{1}{4}$, $\frac{1}{2}$, $\frac{1}{4}$ weights). Figures 28 through 30 show the amplification spectra of the three components for the 5th and 10th floors.

The amplification spectrum for the E-W direction of the 10th floor (Fig. 28-a) shows a predominant single peak at 1.66 Hz with a smaller overlapped adjacent peak at 2.34 Hz. The amplitude at 1.66 Hz is greater than three times the next strongest peaks which occur at 5.66, 6.05, 8.40 and 8.79 Hz. The 5th floor amplification spectrum exhibited several well-defined peaks at essentially the same resonant frequencies as the 10th floor (see Fig. 28-b); these well-defined peaks suggest greater participation of the higher modes of vibration at this level of the structure than at the top level.

The N-S component of the 10th floor shows two dominant peaks (Fig. 29-a) at 1.27 and 3.71 Hz; the first peak (at 1.27 Hz) is about 2.5 times greater than the second peak (at 3.71 Hz). The 5th floor amplification spectra (Fig. 29-b) show the two peaks at these same frequencies, but the peak amplitudes were equal.

The amplification spectrum curves of the vertical component (Figs. 30-a and b) show several well-defined peaks at even higher frequencies.

By comparing the peaks (and the associated frequencies) of the Fourier spectrum of the acceleration recorded at each level of the building and those observed from the amplification spectrum curves, it is easy to identify the different modes of vibration of the building, as indicated by Tables 2 and 3.

In trying to identify torsional modes of the building from the amplification spectrum curves, the following points have been taken into account:

- 1 - In the E-W direction, where the resisting structural system is a combination of frames and shear walls, the ratio of the second-mode frequency to the fundamental frequency (1.66 Hz) should be somewhat greater than 3, therefore the peak at 2.34 Hz cannot be the second translational mode. Rather, it has to be either a torsional mode or a mode coupled with the N-S component.
- 2 - This peak at 2.34 Hz was not well-defined in the amplification spectrum of the 10th floor in the N-S direction, so it seems that it is not a major translational mode in this direction since the first and second N-S modes are very clearly shown in Figs. 29-a and b with a frequency ratio of 2.92.
- 3 - Assuming that the floors rotate torsionally as rigid slabs, any twist would have two translational components at the accelerographs (say v and u , as shown in Fig. 31) where $v/u = b/d = 3.48$; i.e., the translational component (caused by torsion) in the E-W direction is about 3.5 times greater than that component in the N-S direction. This argument is consistent with the fact that the peaks (assumed to be torsional) observed in the E-W direction were stronger and clearer than those in the N-S direction.
- 4 - The modes assumed to be purely translational in the E-W direction show frequency ratios (frequency of higher modes/fundamental frequency) of 1.0, 3.41, 5.06 and 6.94 which are typical of a building with frames and shear walls in this direction. In the N-S direction the ratios are 1.0, 2.92 and 5.7.

5 - The amplification spectra for vertical vibrations (Fig. 30-a, b) show more prominent spikes in the higher frequency region than do the spectra for horizontal motions (Fig. 28-a, b and 29-a, b). These prominent spikes reflect the vibration of floor and roof beams, floor and roof slabs, etc., and thus demonstrate that the vertical vibrations of a building are appreciably more complex than the horizontal vibrations.

Some of the mode shapes of vibration as estimated from the amplification spectrum curves are shown in Fig. 32. The ordinates of these modes are the amplification ratios at different floors; in addition, the phase of the response of each floor was compared to that of the basement to determine the signs of the modal displacements. It is clearly shown that the mode shapes in the E-W direction (frame plus shear walls) are different from the mode shapes in the N-S direction (frame only).

Table 4 has a summary of the different identified modes of vibration of the building.

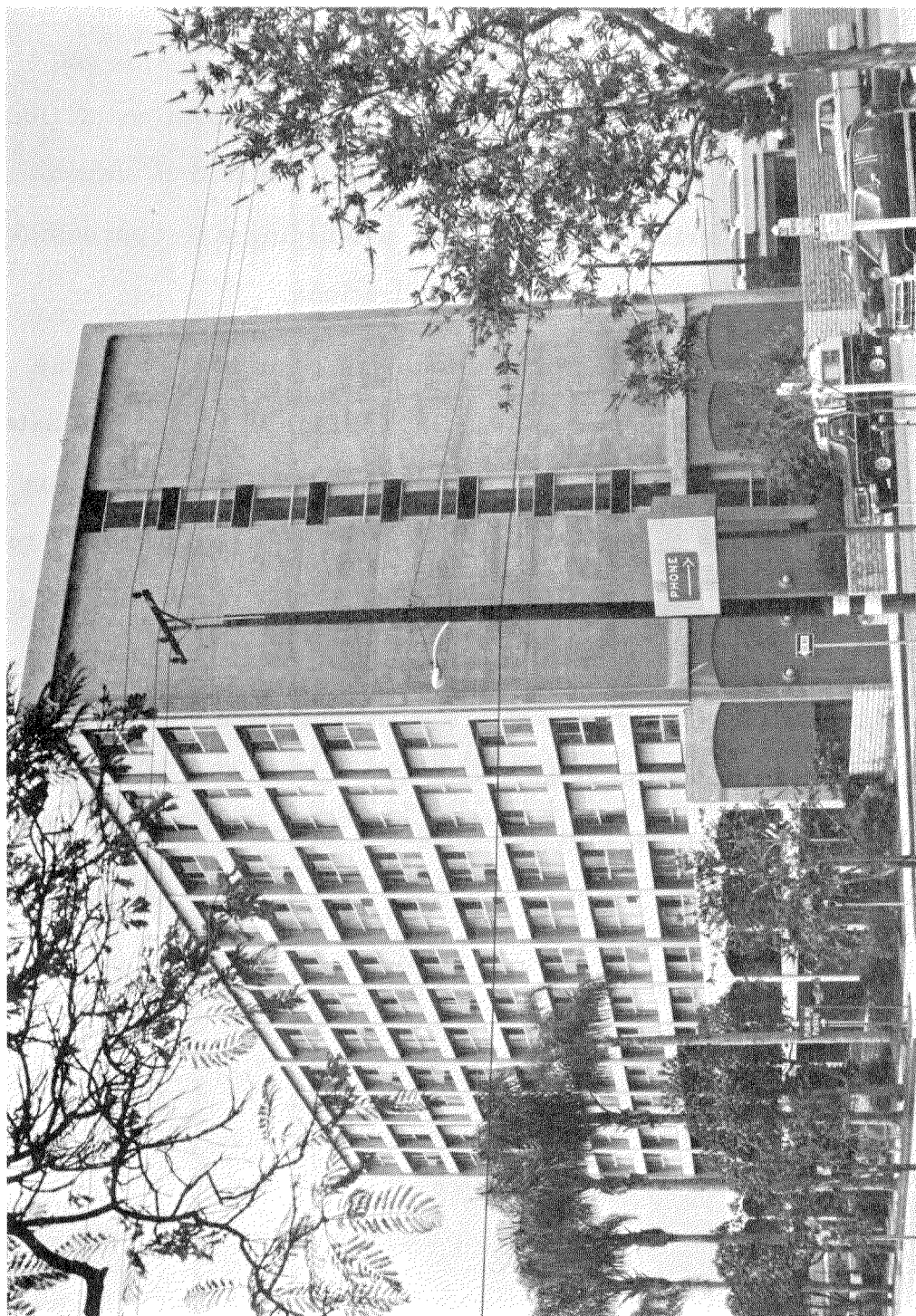
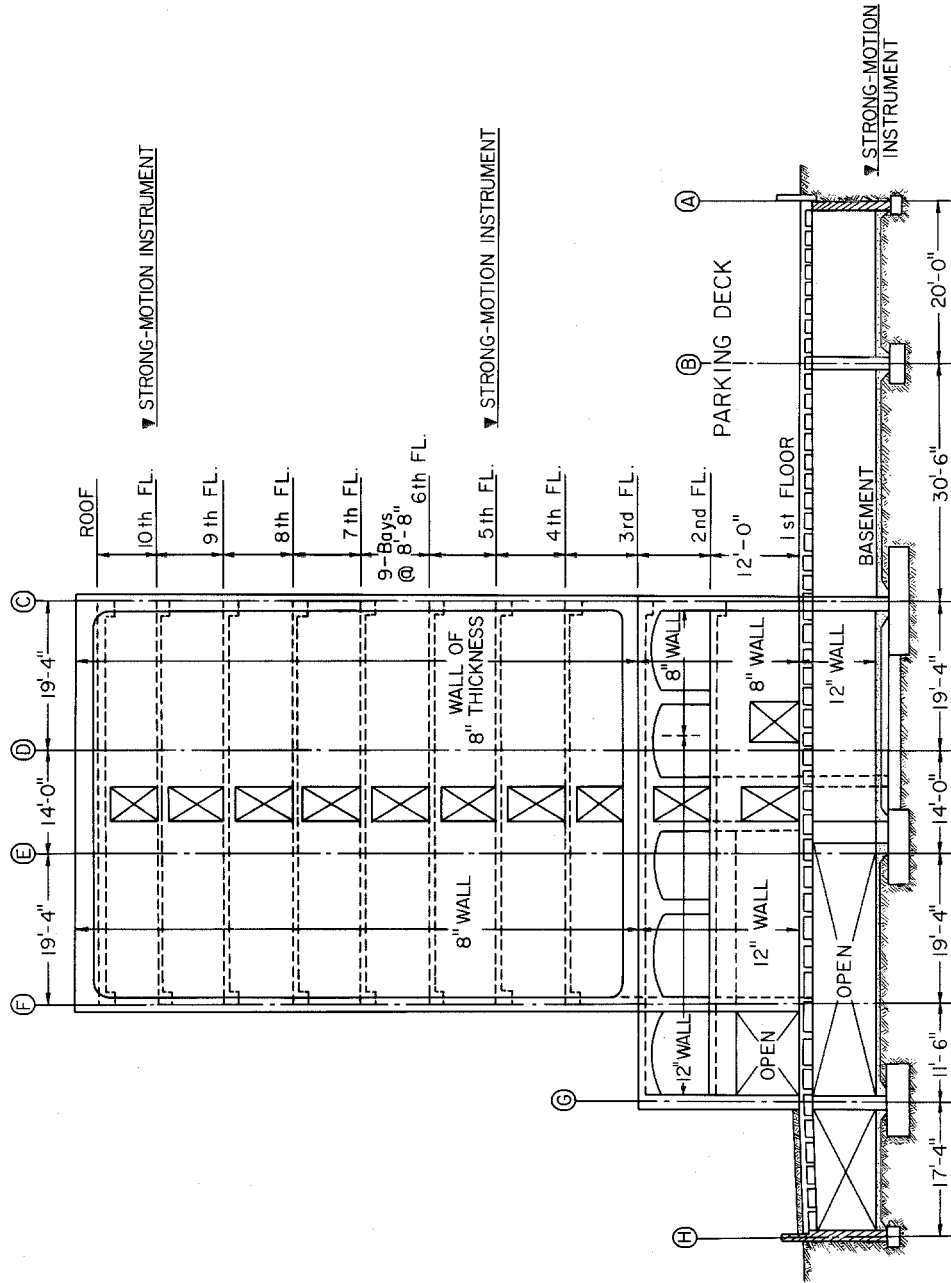
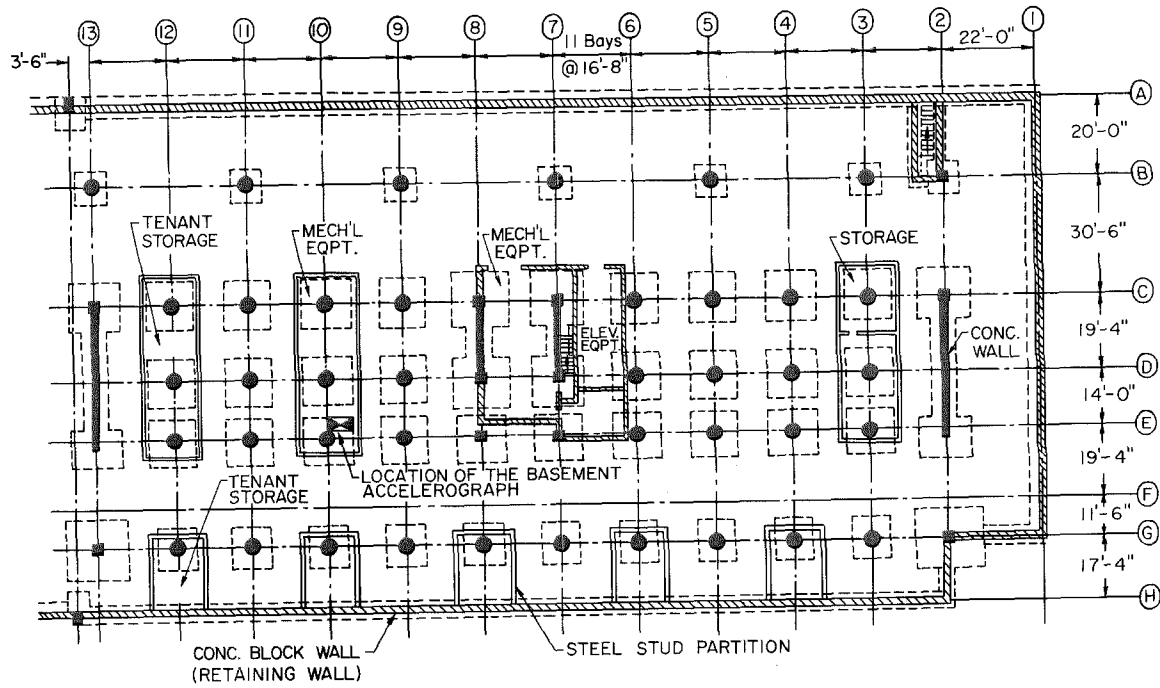


Fig. 2 General view of the Lutheran Whittier Tower, Whittier, California



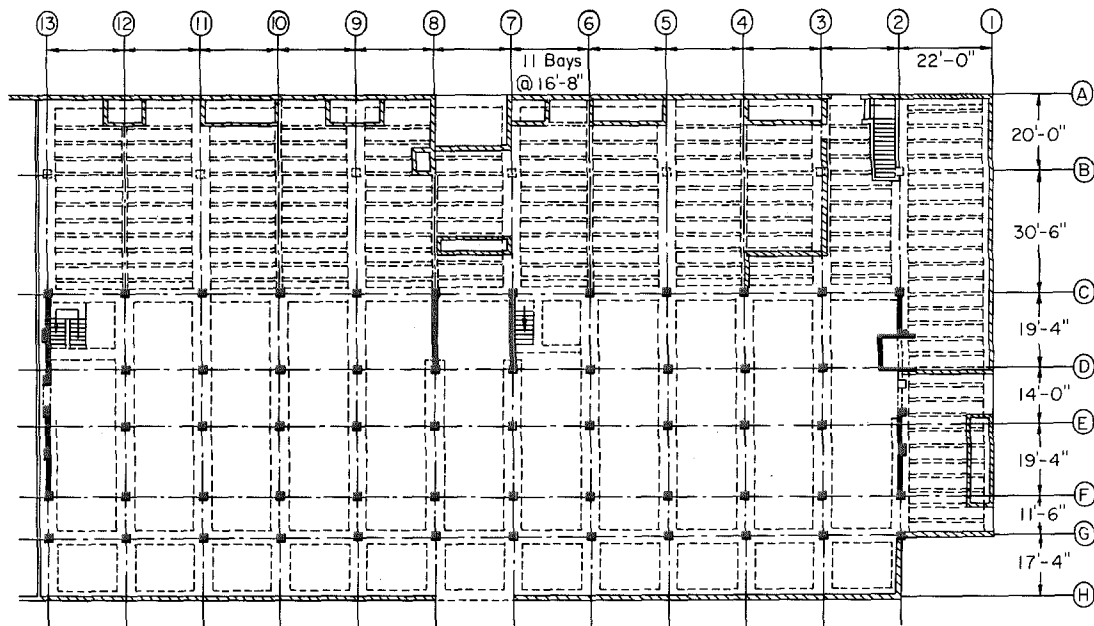
NORTH TOWER END STRUCTURAL ELEVATION
(SOUTH TOWER END SIMILAR)

Fig. 3



BASEMENT - FOUNDATION PLAN

(a)



FIRST FLOOR FRAMING PLAN

(b)

Fig. 4 Structural details of the Basement and First floor

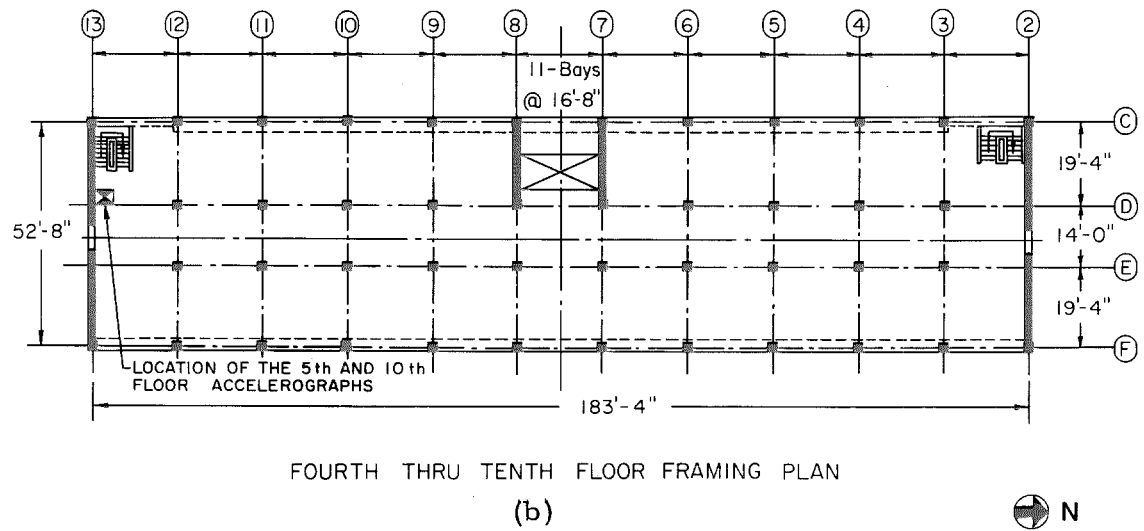
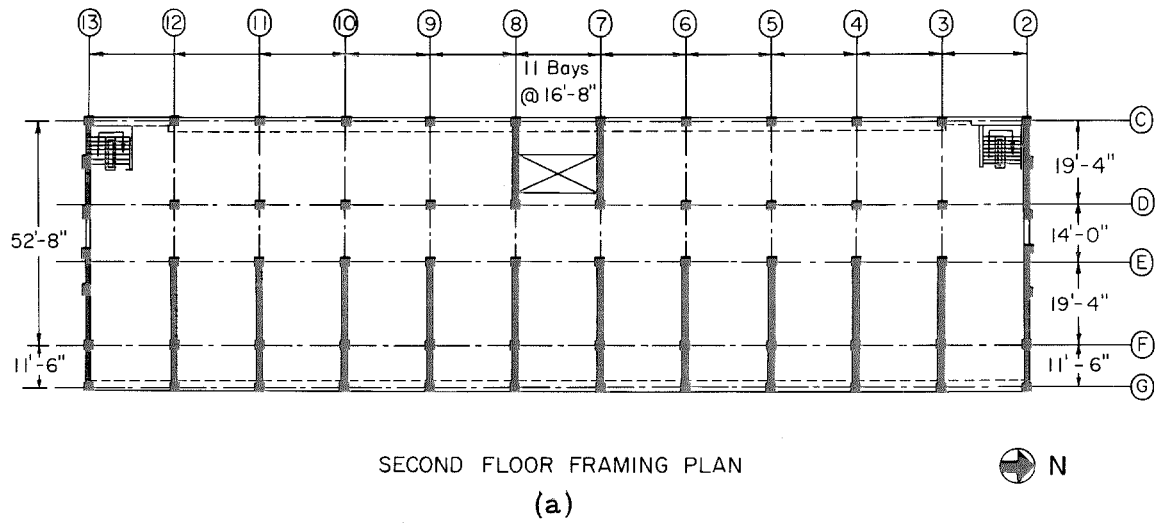


Fig. 5 Structural details of the Second through Tenth floors

WHITTIER, 7215, BRIGHT AVE., BASEMENT, JAN 1 1976 0920 PST

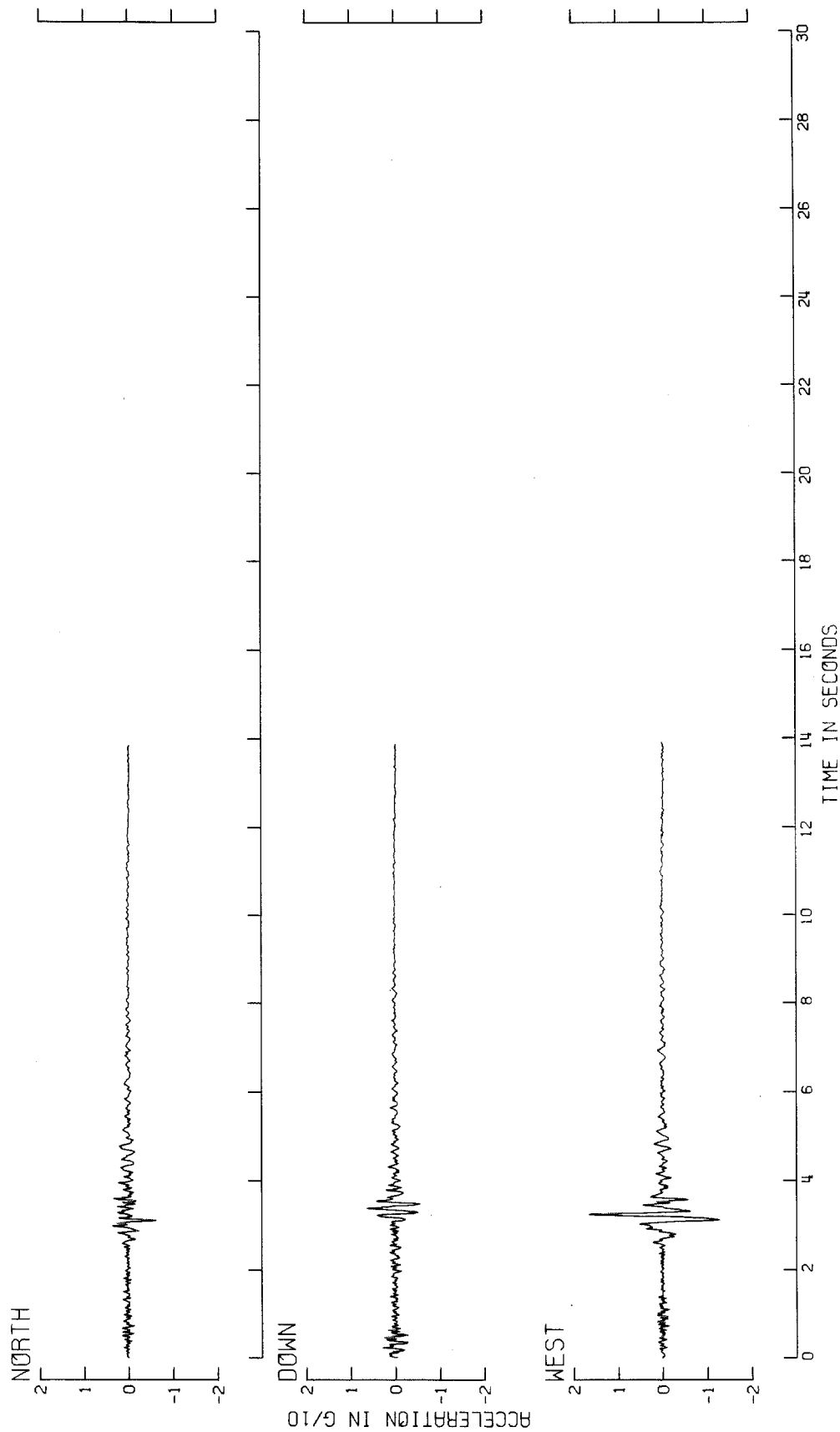


Fig. 6-a Uncorrected Accelerograms (Basement)

WHITTIER, 7215 BRIGHT AVE., 5TH FLOOR, JAN 1 1976 0920 PST

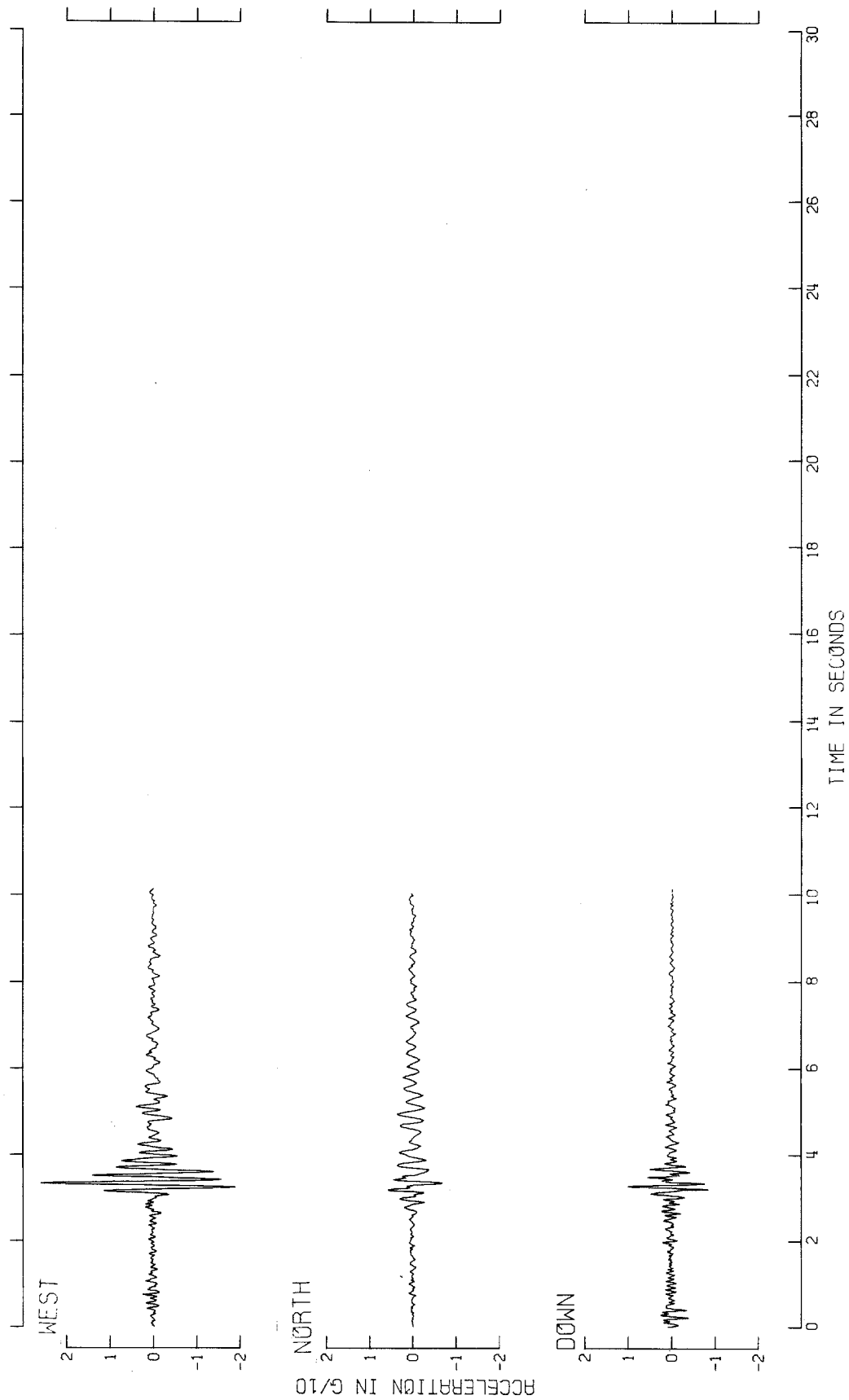


Fig. 6-b Uncorrected Accelerograms (5th Floor)

WHITTIER, 7215 BRIGHT AVE., 10TH FLOOR

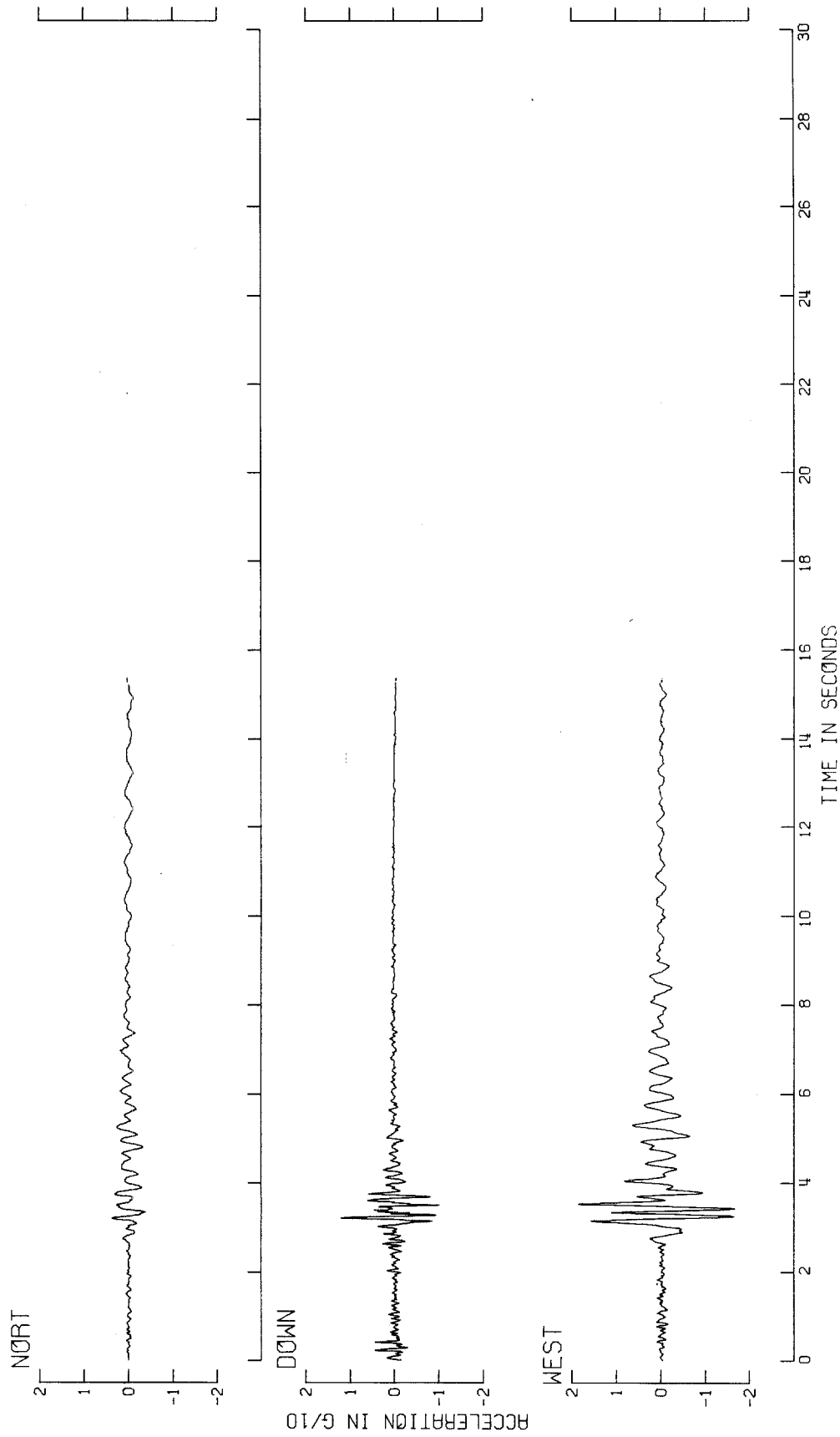


Fig. 6-c Uncorrected Accelerograms (10th Floor)

WHITTIER 7215 BRIGHT AVE. BASEMENT, JANUARY 1, 1976
 IN0001 WHITTIER 7215 BRIGHT AVE. BASEMENT COMP WEST
 Ø PEAK VALUES : ACCEL = -154.8 CM/SEC/SEC VELOCITY = 5.2 CM/SEC DISPL = -1.7 CM

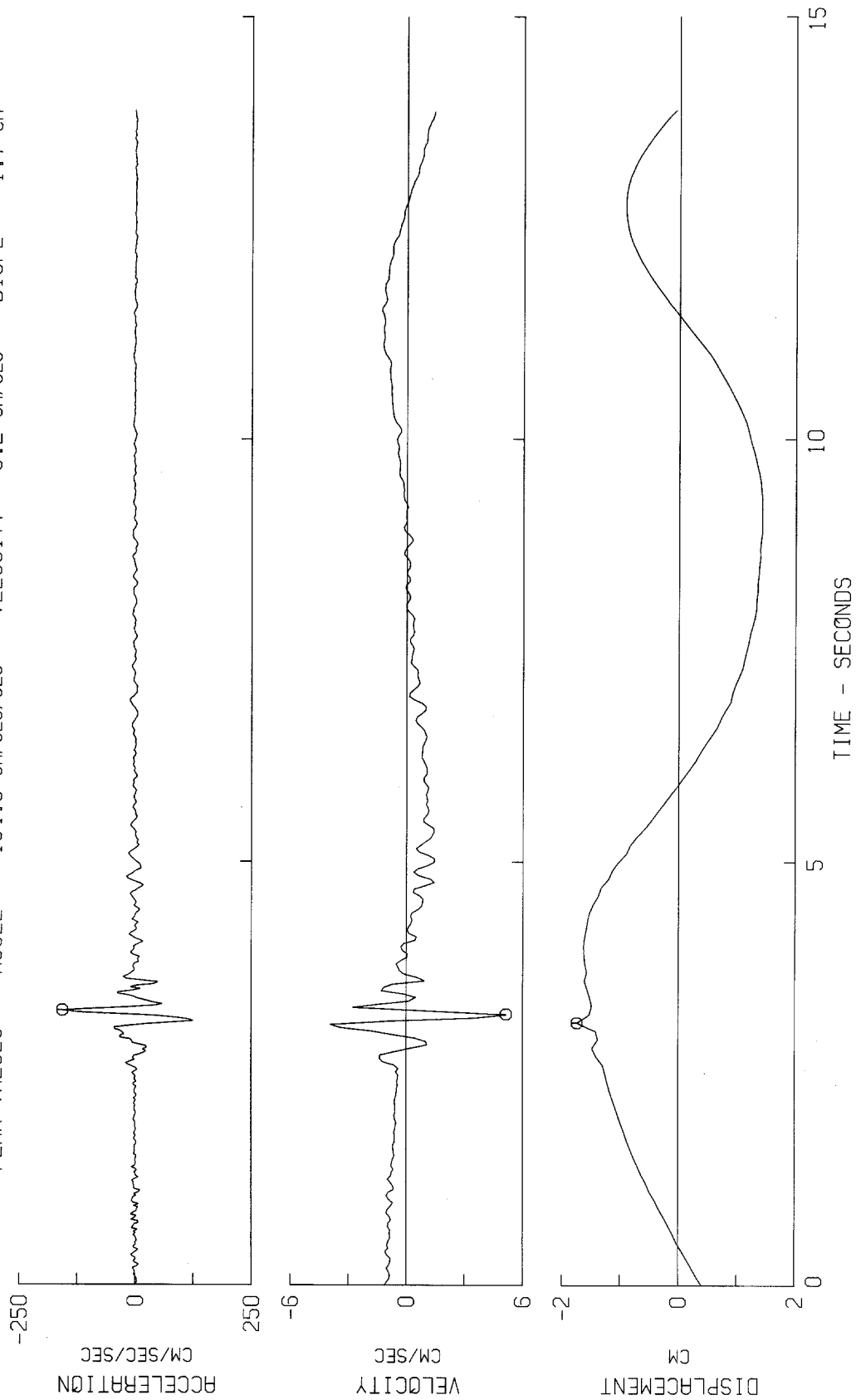


Fig. 7-a

WHITTIER 7215 BRIGHT AVE. BASEMENT, JANUARY 1, 1976
IN0001 WHITTIER 7215 BRIGHT AVE. BASEMENT COMP NORT
Ø PEAK VALUES : ACCEL = 56.8 CM/SEC/SEC VELOCITY = 1.4 CM/SEC DISPL = -1.0 CM

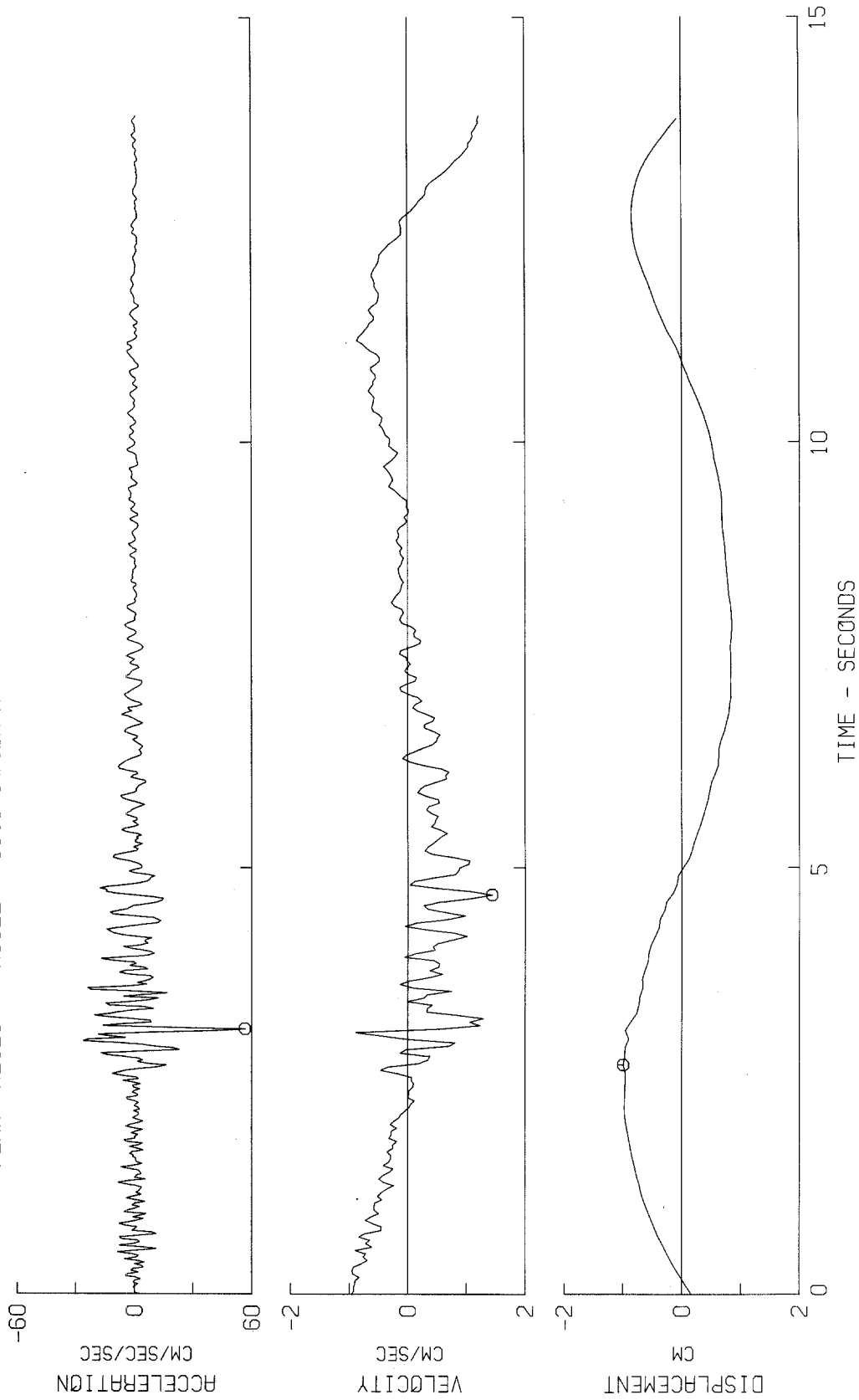


Fig. 7-b

WHITTIER 7215 BRIGHT AVE. BASEMENT, JANUARY 1, 1976
IN0001 WHITTIER 7215 BRIGHT AVE. BASEMENT COMP DOWN
Ø PEAK VALUES : ACCEL = -55.4 CM/SEC/SEC VELOCITY = -1.9 CM/SEC DISPL = -2.1 CM

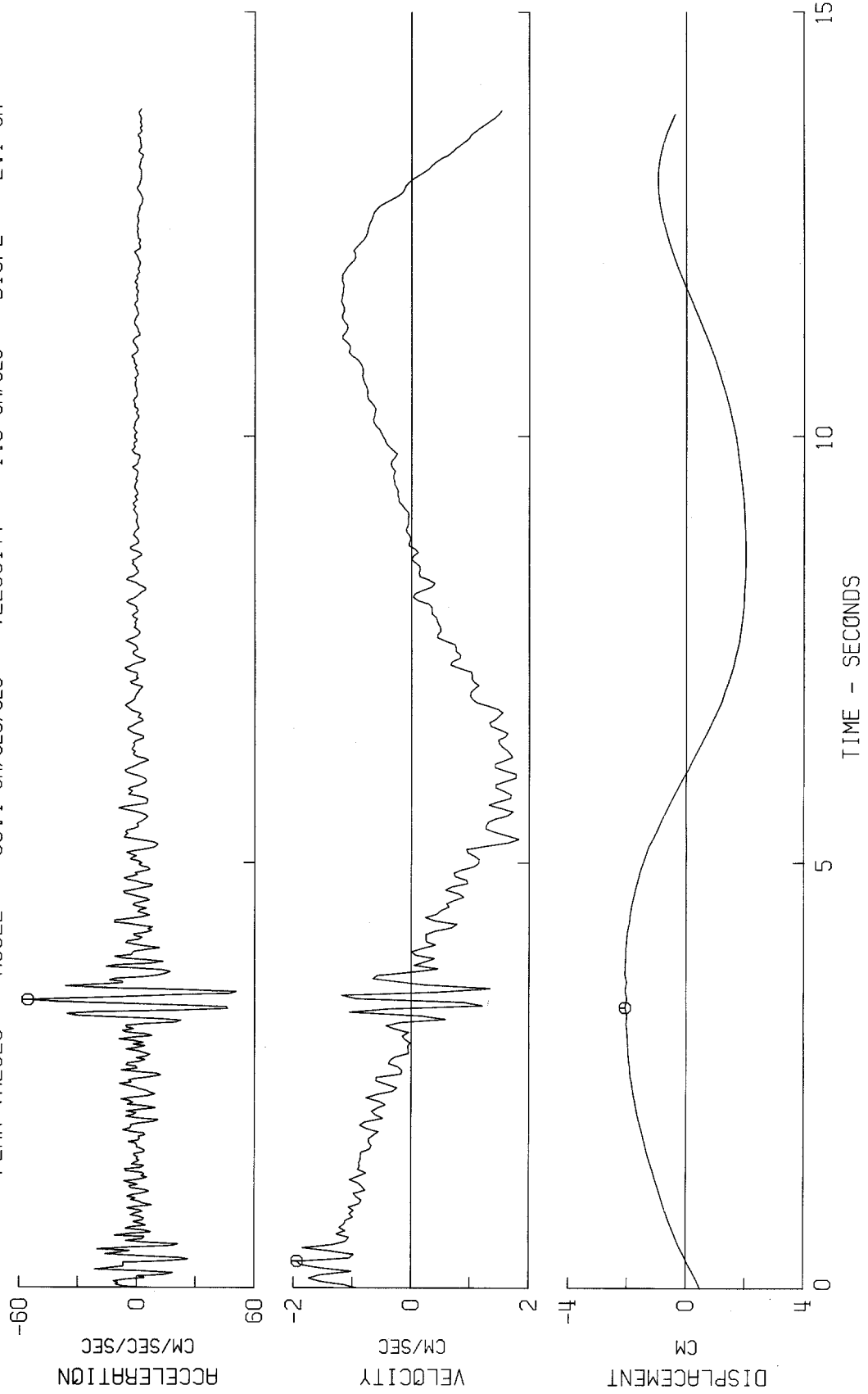


Fig. 7-c

WHITTIER 7215 BRIGHT AVE. 5TH FLOOR, JANUARY 1, 1976
IN0001 WHITTIER 7215 BRIGHT AVE. 5TH FLOOR COMP. WEST

⊙ PEAK VALUES : ACCEL = -228.0 CM/SEC/SEC VELOCITY = -6.1 CM/SEC DISPL = -.8 CM

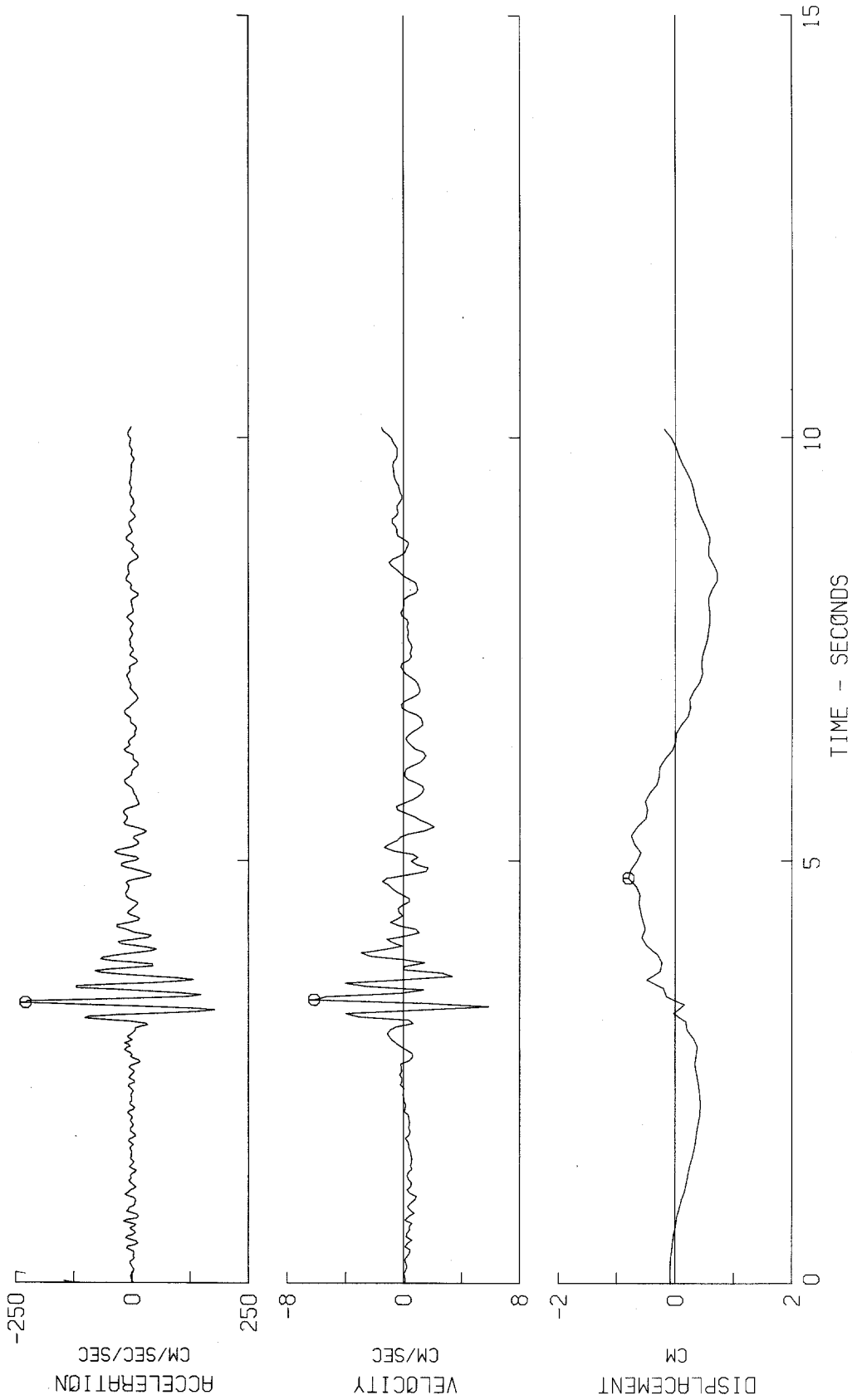


Fig. 8-a

WHITTIER 7215 BRIGHT AVE. 5TH FLOOR, JANUARY 1, 1976
IN0001 WHITTIER 7215 BRIGHT AVE. 5TH FLOOR COMP. NORTH
o PEAK VALUES : ACCEL = 63.5 CM/SEC/SEC VELOCITY = -3.0 CM/SEC DISPL = 1.2 CM

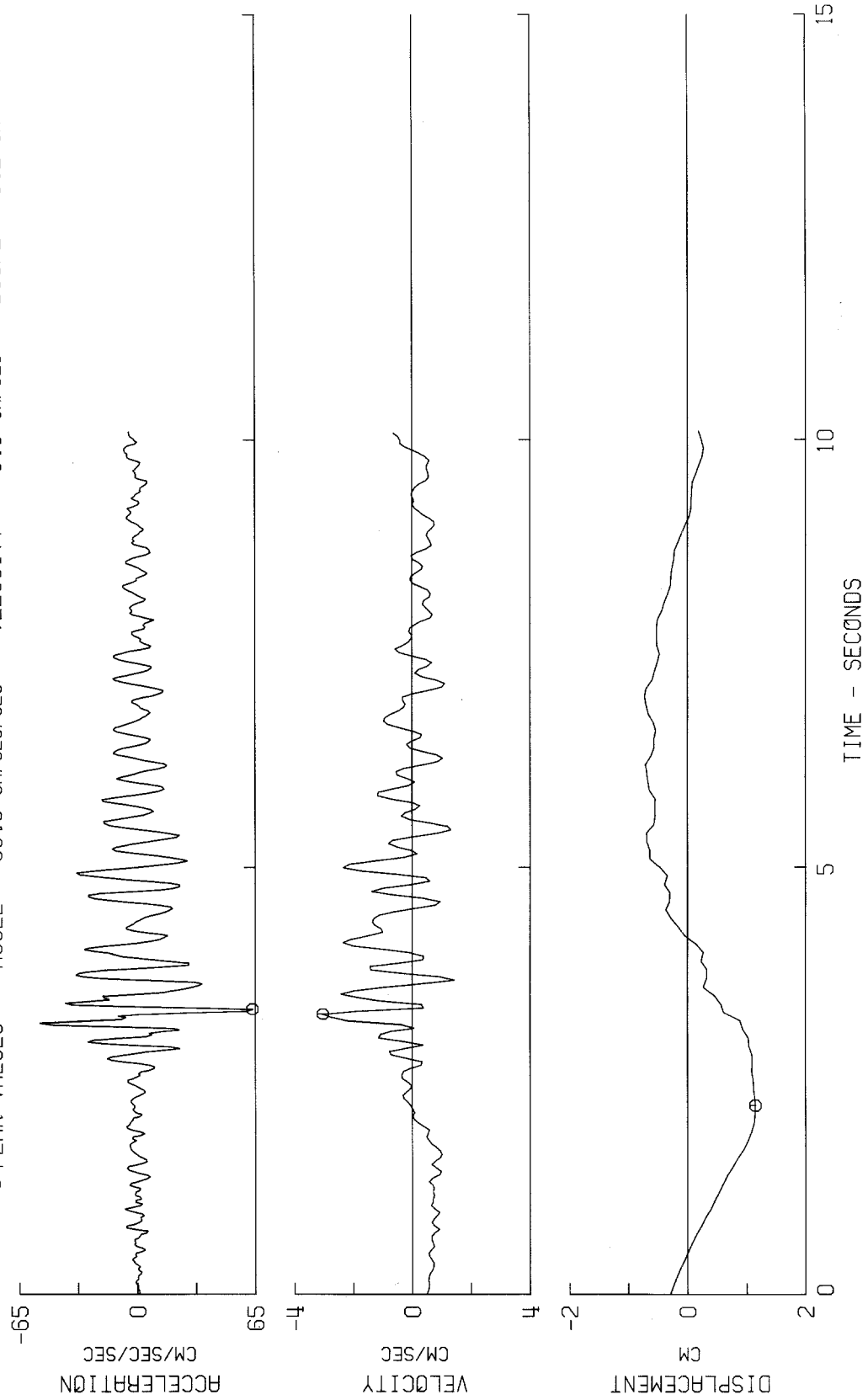


Fig. 8-b

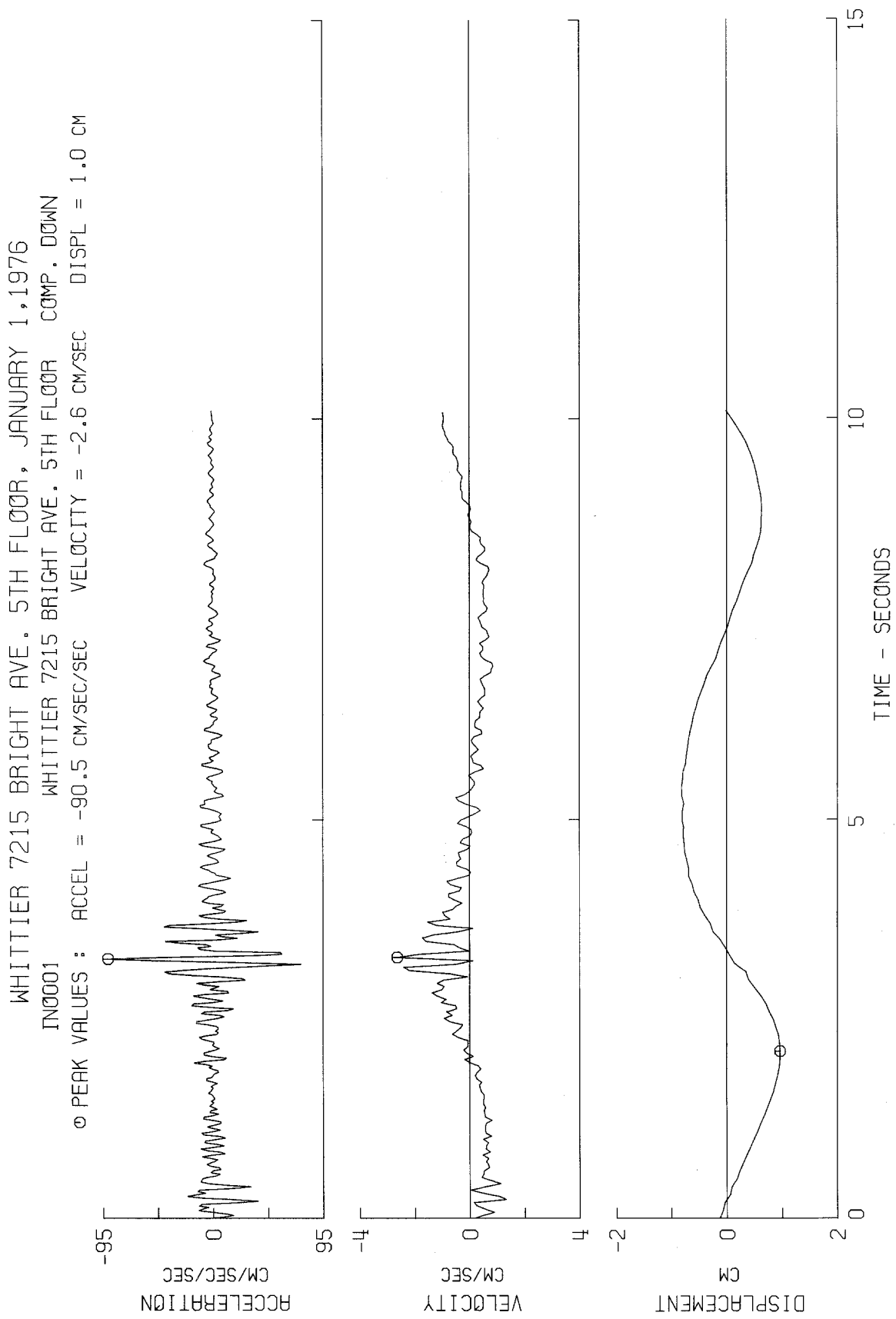


Fig. 8-c

WHITTIER, 7215 BRIGHT AVE., 10TH FLOOR, JANUARY 1, 1976 - 0920 PST
IN00100 WHITTIER, 7215 BRIGHT AVE., 10TH FLOOR WEST
Ø PEAK VALUES : ACCEL = -180.9 CM/SEC/SEC VELOCITY = 10.5 CM/SEC DISPL = -6.4 CM

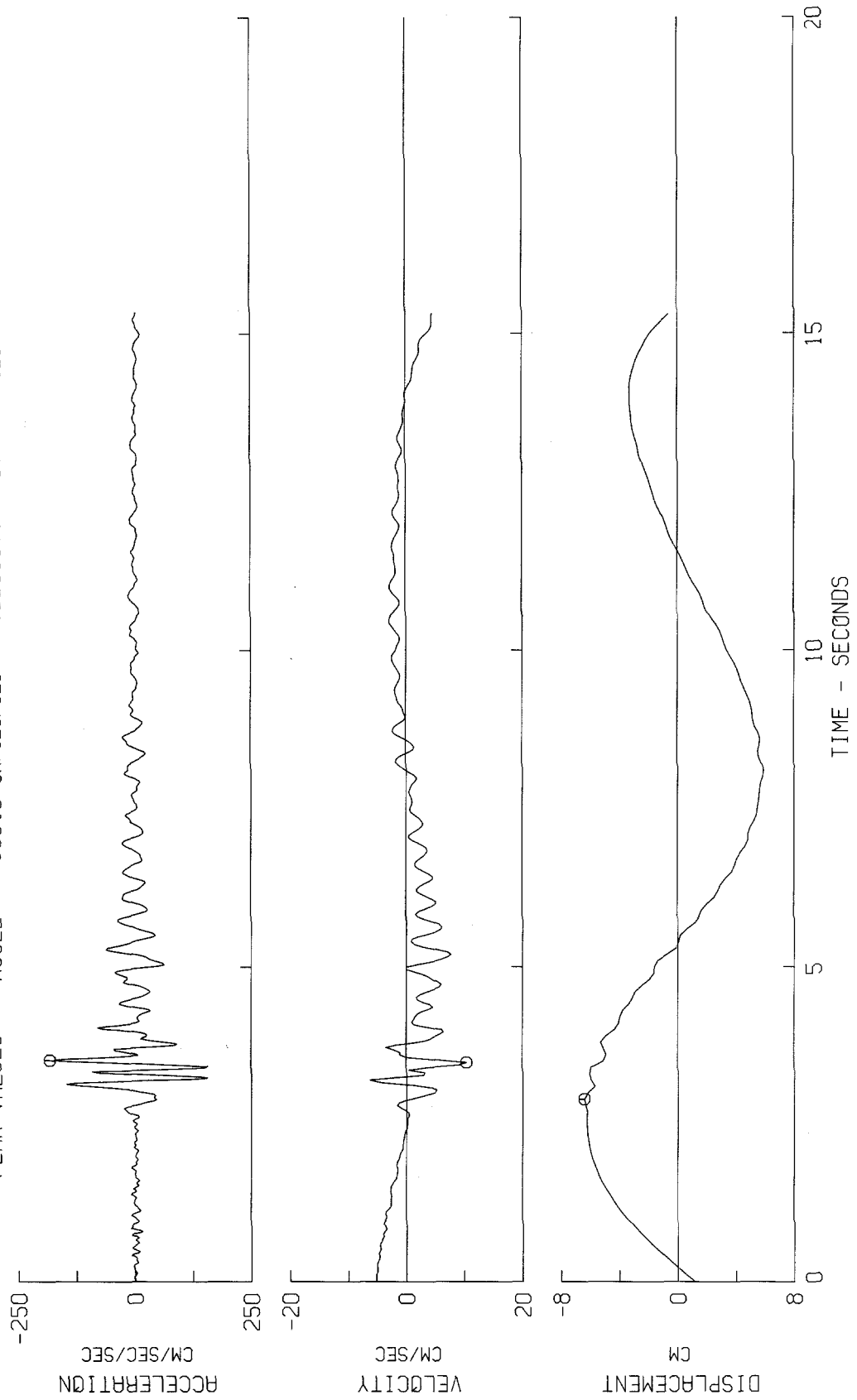


Fig. 9-a

WHITTIER, 7215 BRIGHT AVE., 10TH FLOOR, JANUARY 1, 1976 - 0920 PST
 IN00100
 WHITTIER, 7215 BRIGHT AVE., 10TH FLOOR NORTH
 PEAK VALUES : ACCEL = 35.9 CM/SEC/SEC VELOCITY = 5.8 CM/SEC DISPL = 5.9 CM

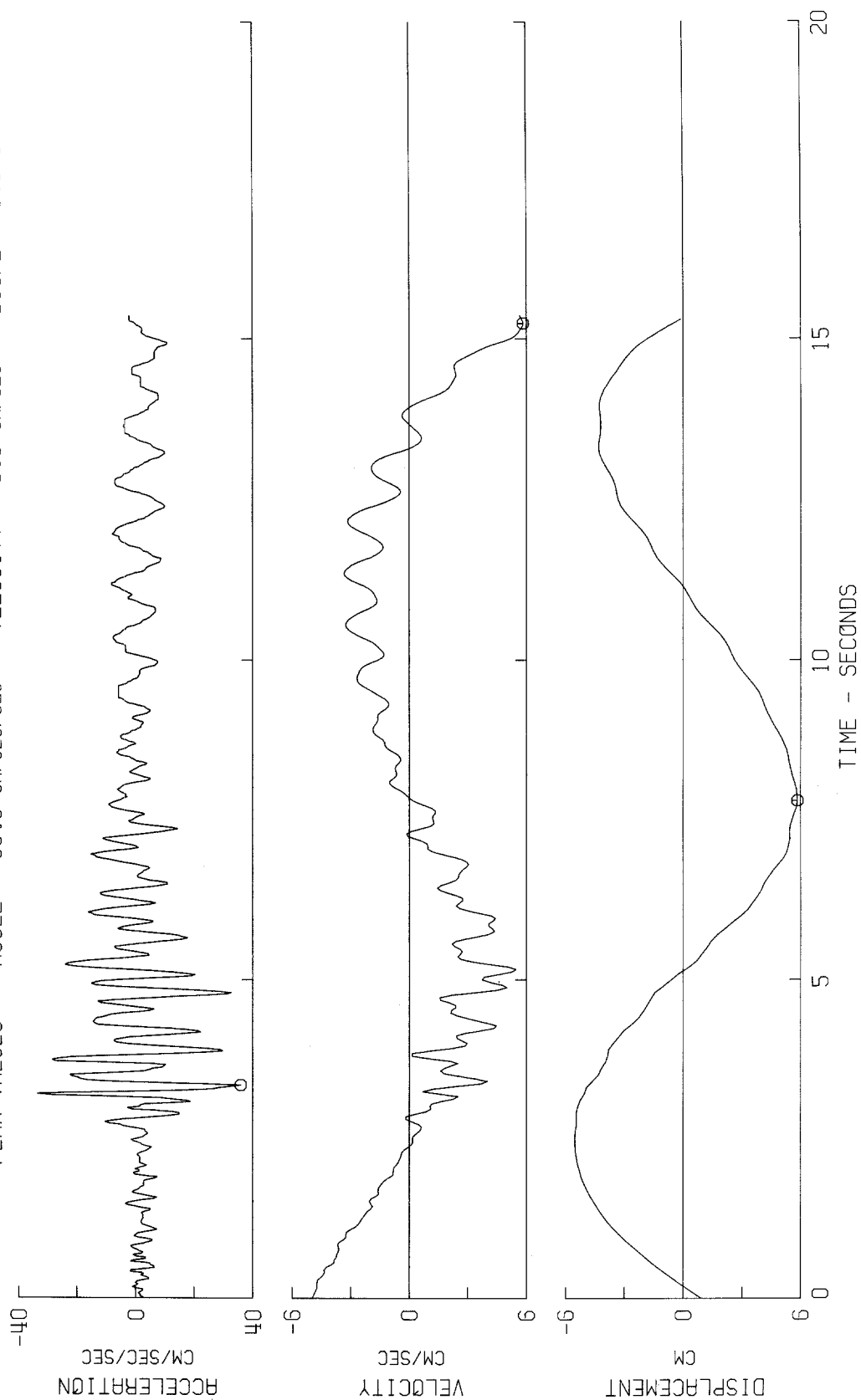


Fig. 9-b

WHITTIER, 7215 BRIGHT AVE., 10TH FLOOR, JANUARY 1, 1976 - 0920 PST
IN00100 WHITTIER, 7215 BRIGHT AVE., 10TH FLOOR DOWN
⊙ PEAK VALUES : ACCEL = -103.9 CM/SEC/SEC VELOCITY = 5.5 CM/SEC DISPL = -4.7 CM

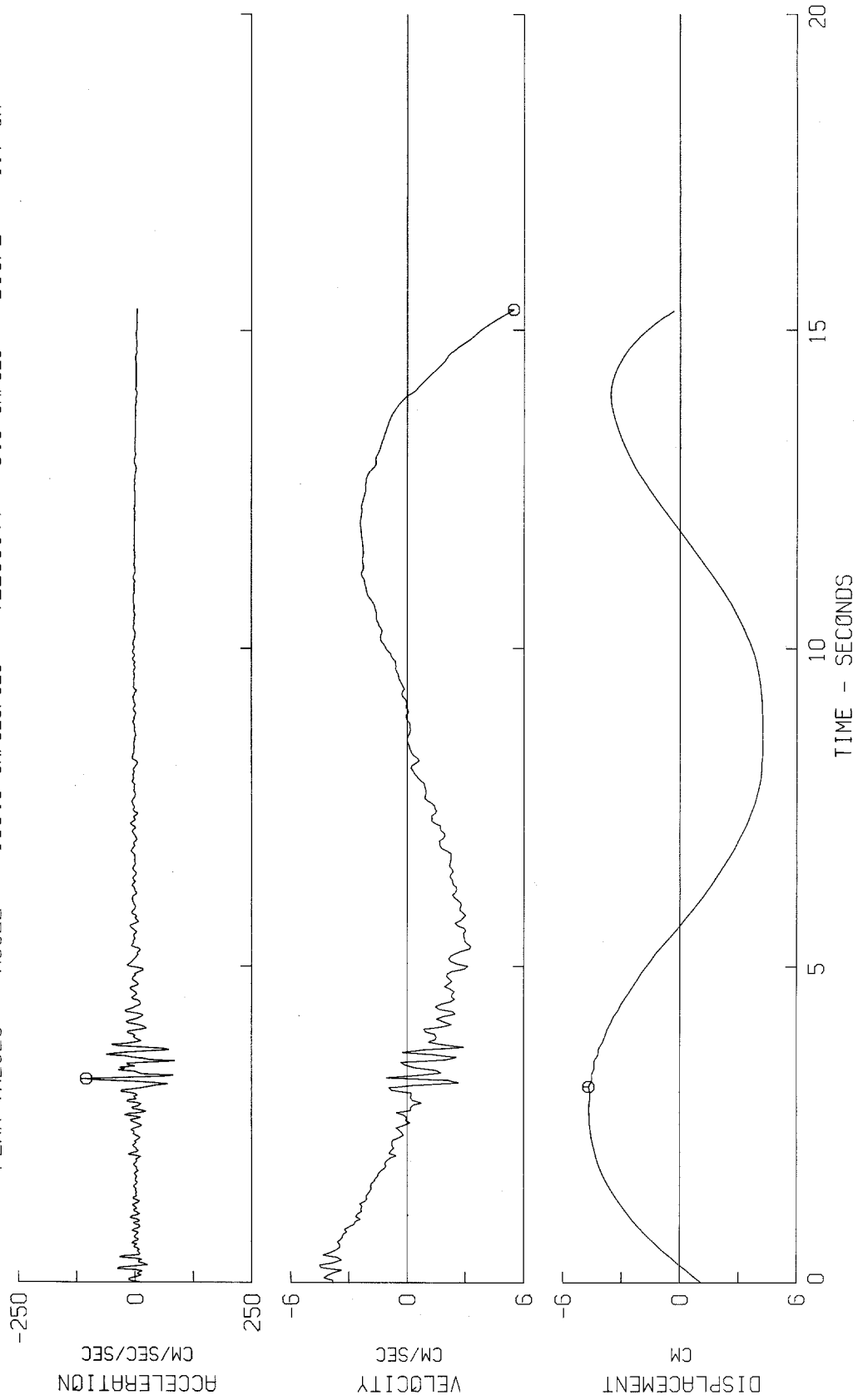


Fig. 9-c

RELATIVE VELOCITY RESPONSE SPECTRUM
WHITTIER 7215 BRIGHT AVE. BASEMENT, JANUARY 1, 1976
11N0001 WHITTIER 7215 BRIGHT AVE. BASEMENT COMP WEST
DAMPING VALUES ARE 0, 2, 5, 10 AND 20 PERCENT OF CRITICAL

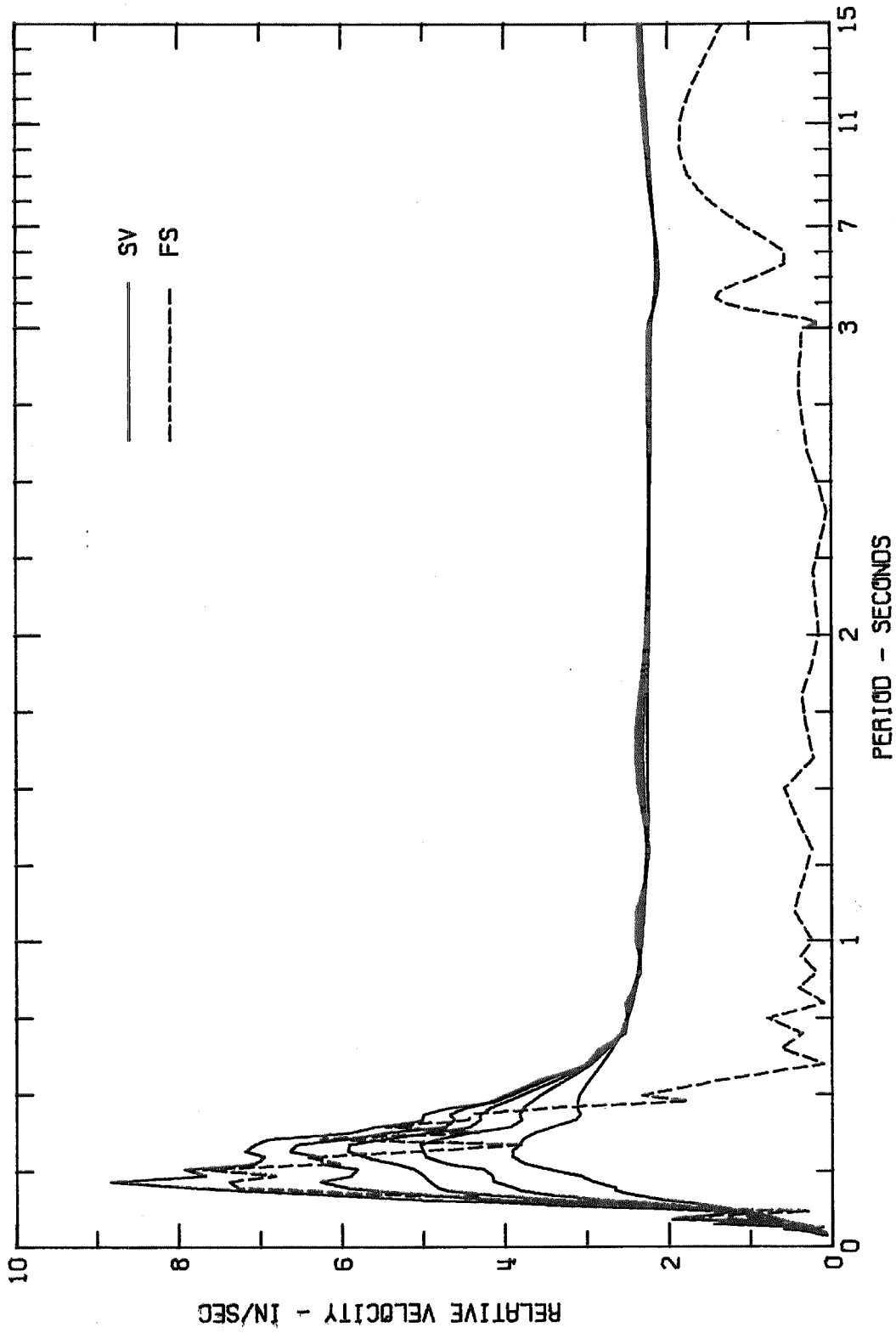


Fig. 10-a

RESPONSE SPECTRUM

WHITTIER 7215 BRIGHT AVE. BASEMENT, JANUARY 1, 1976

IIN0001

WHITTIER 7215 BRIGHT AVE. BASEMENT COMP WEST

DAMPING VALUES ARE 0, 2, 5, 10 AND 20 PERCENT OF CRITICAL

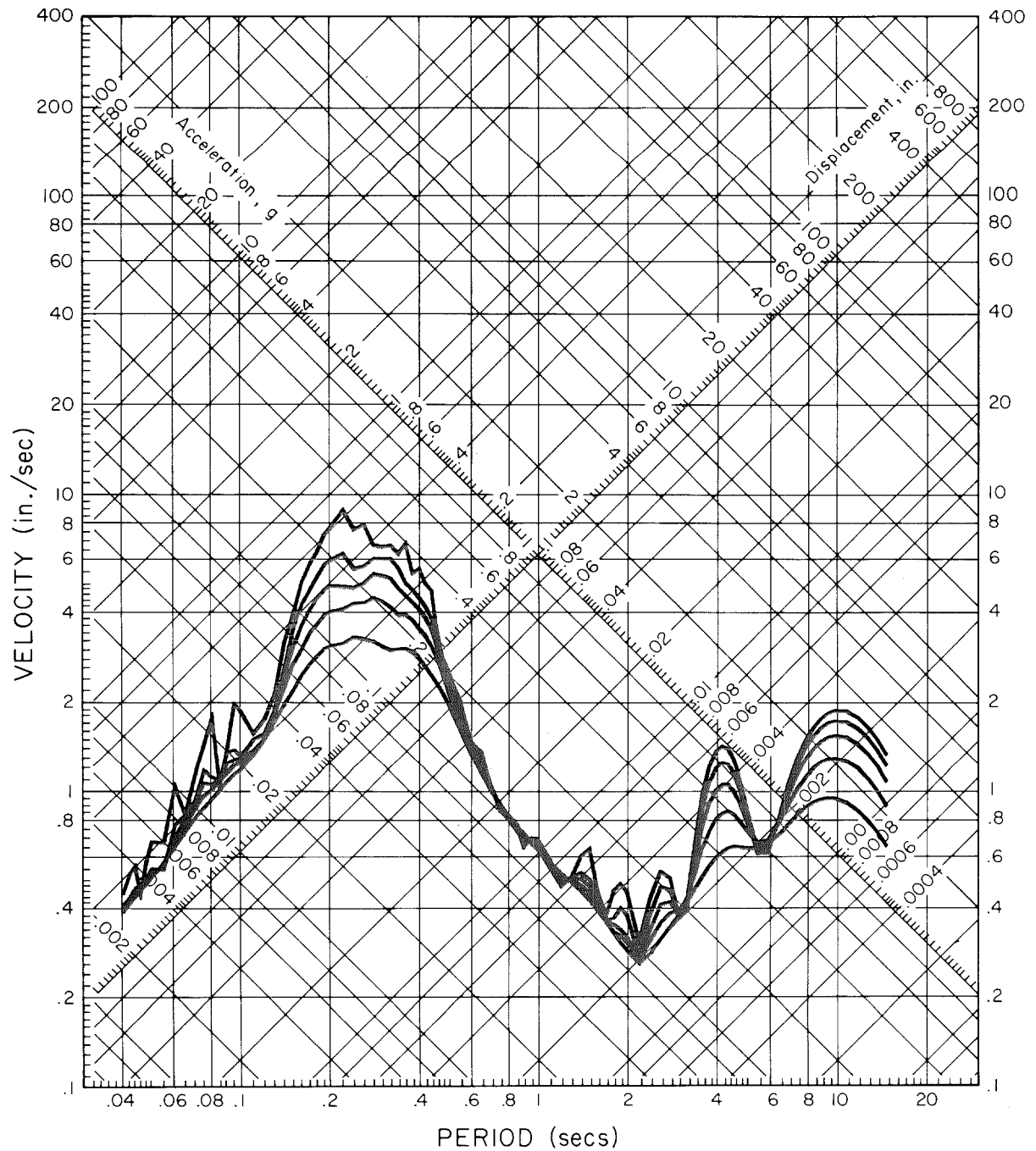


Fig. 10-b

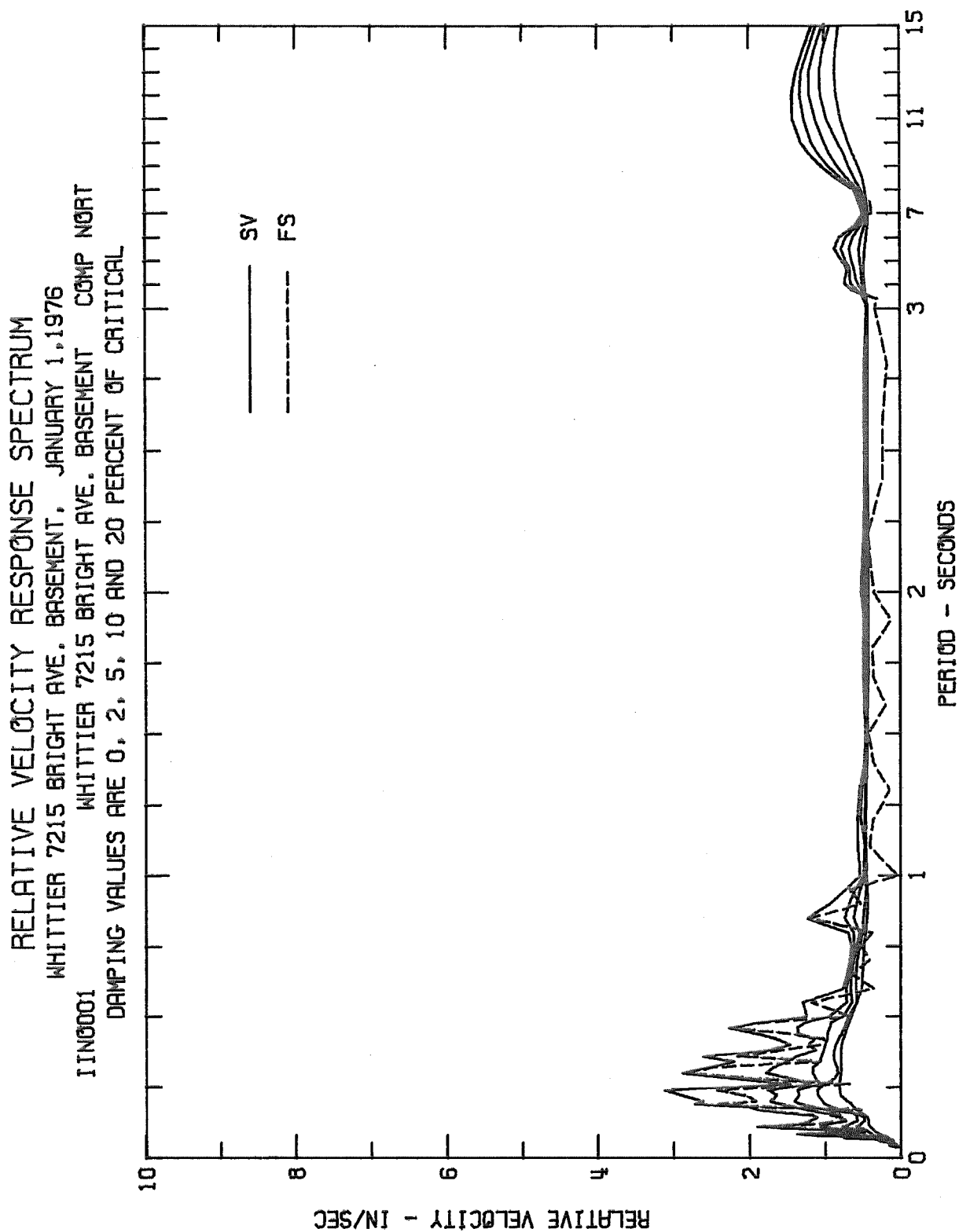


Fig. 11-a

RESPONSE SPECTRUM

WHITTIER 7215 BRIGHT AVE. BASEMENT, JANUARY 1, 1976

IIN0001

WHITTIER 7215 BRIGHT AVE. BASEMENT COMP NORT

DAMPING VALUES ARE 0, 2, 5, 10 AND 20 PERCENT OF CRITICAL

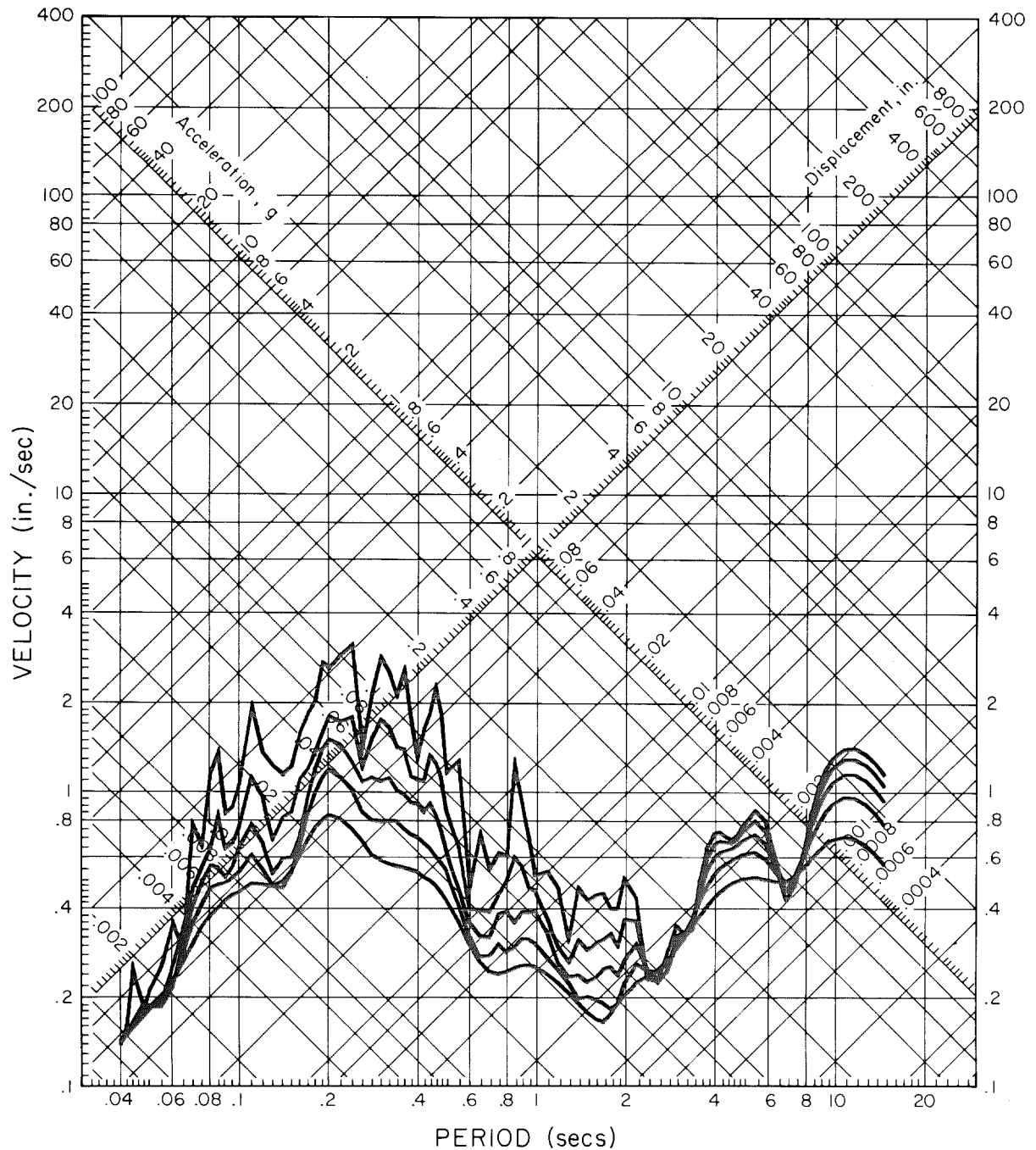


Fig. 11-b

RELATIVE VELOCITY RESPONSE SPECTRUM
 WHITTIER 7215 BRIGHT AVE. BASEMENT, JANUARY 1, 1976
 IING0001 WHITTIER 7215 BRIGHT AVE. BASEMENT COMP DOWN
 DAMPING VALUES ARE 0, 2, 5, 10 AND 20 PERCENT OF CRITICAL

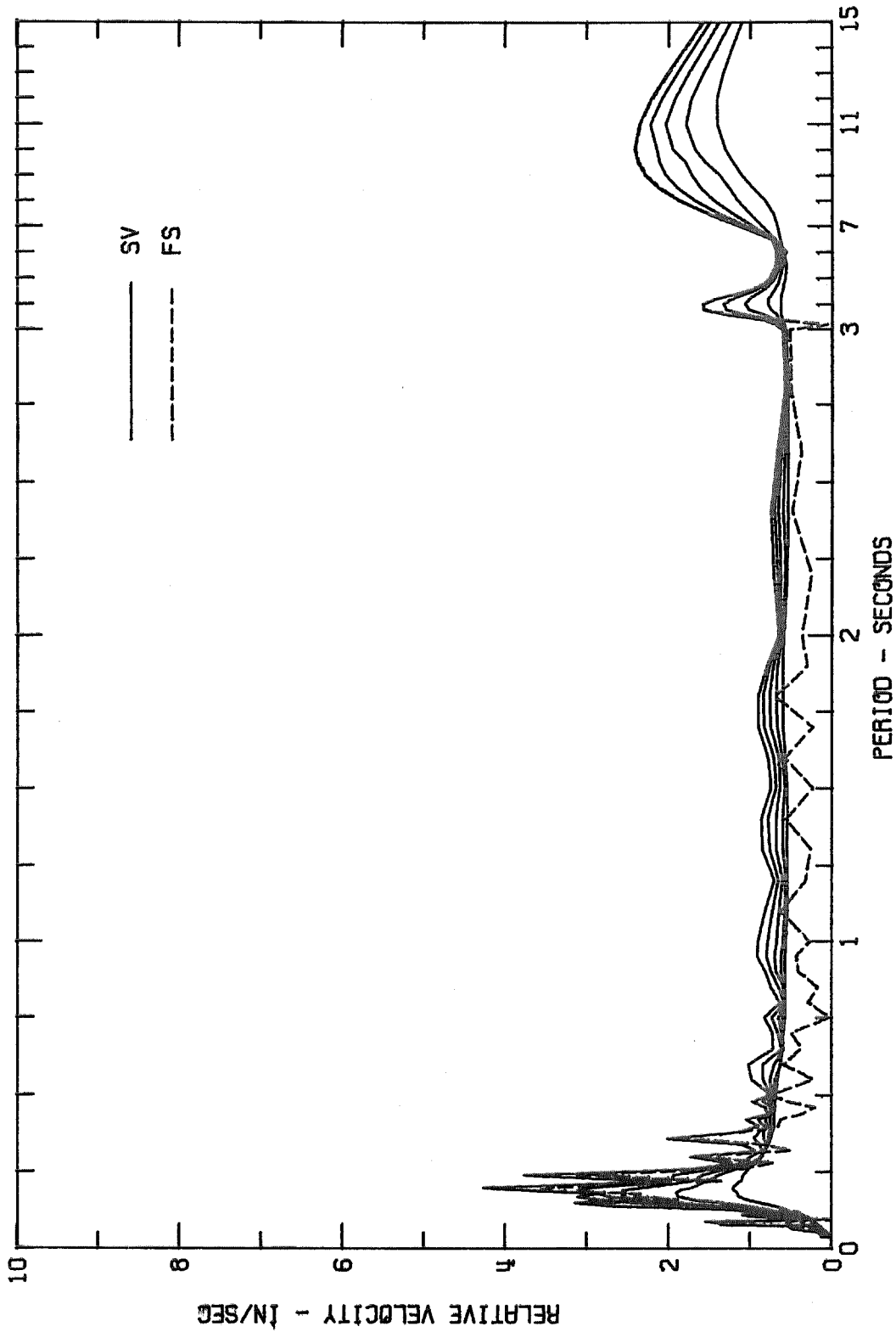


Fig. 12-a

RESPONSE SPECTRUM

WHITTIER 7215 BRIGHT AVE. BASEMENT, JANUARY 1, 1976

IIN0001

WHITTIER 7215 BRIGHT AVE. BASEMENT COMP DOWN

DAMPING VALUES ARE 0, 2, 5, 10 AND 20 PERCENT OF CRITICAL

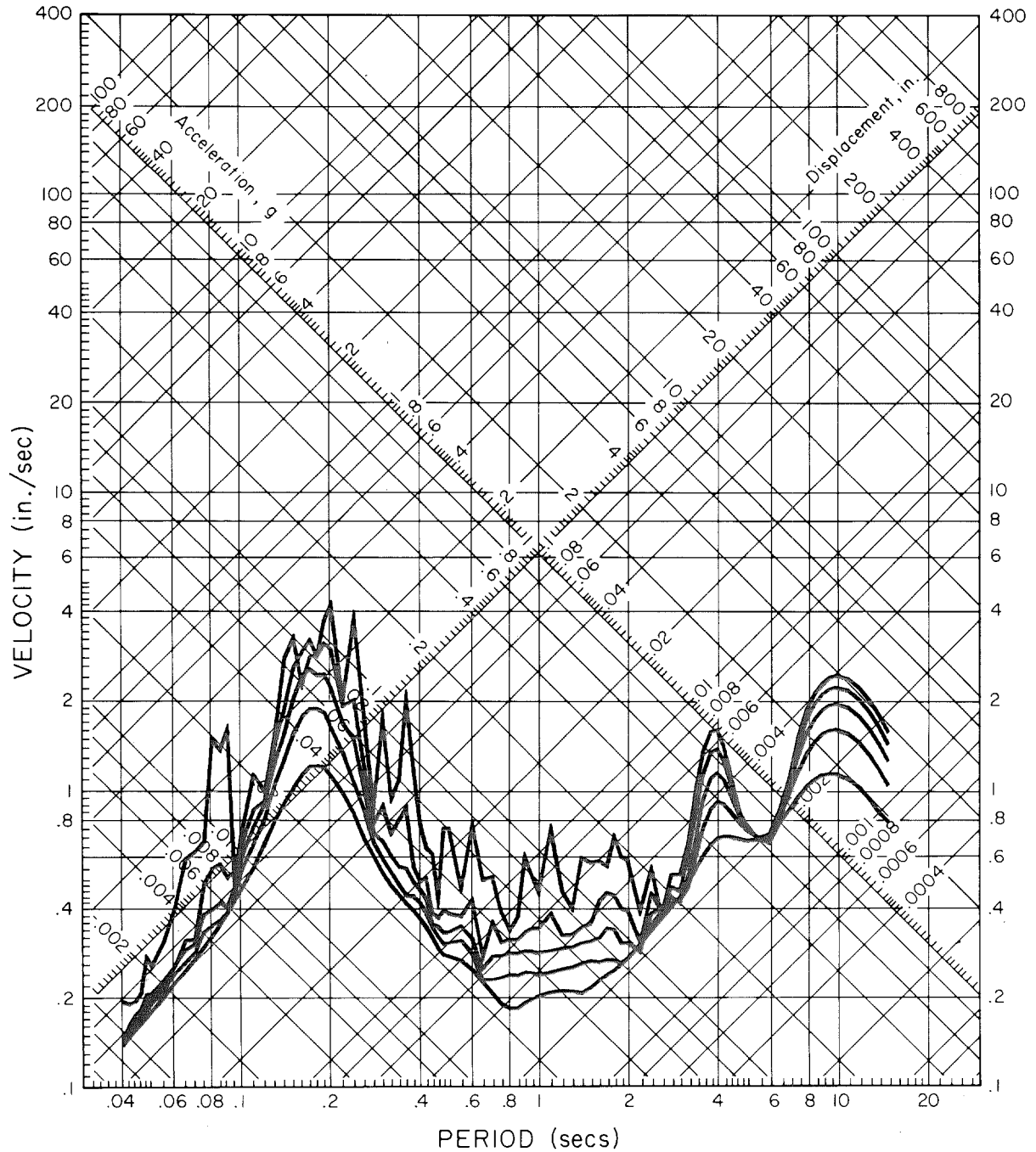


Fig. 12-b

RELATIVE VELOCITY RESPONSE SPECTRUM
WHITTIER 7215 BRIGHT AVE. 5TH FLOOR. JANUARY 1, 1976
IIN0001 WHITTIER 7215 BRIGHT AVE. 5TH FLOOR COMP. WEST
DAMPING VALUES ARE 0, 2, 5, 10 AND 20 PERCENT OF CRITICAL

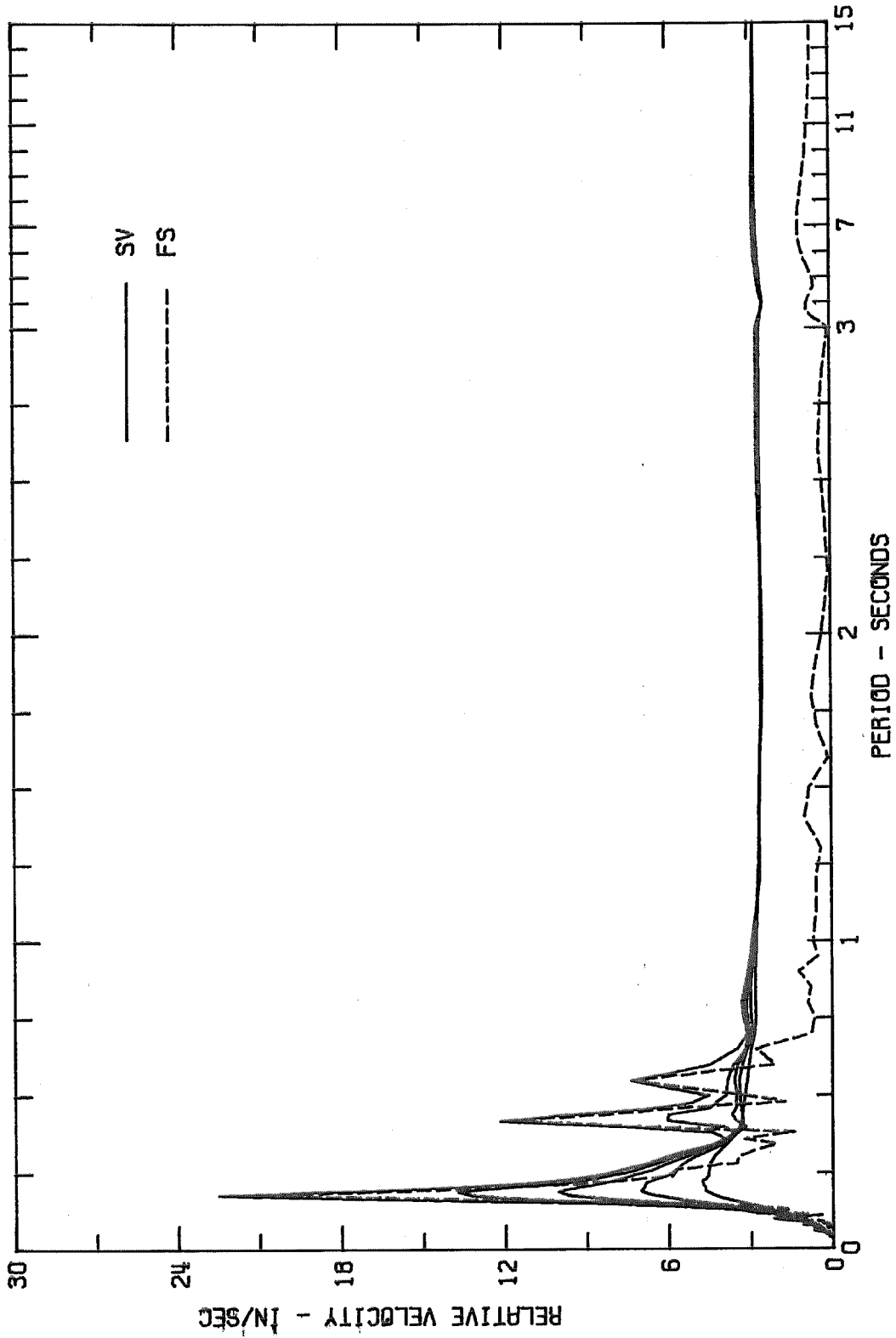


Fig. 13-a

RESPONSE SPECTRUM

WHITTIER 7215 BRIGHT AVE. 5TH FLOOR, JANUARY 1, 1976

IIN0001

WHITTIER 7215 BRIGHT AVE. 5TH FLOOR COMP. WEST

DAMPING VALUES ARE 0, 2, 5, 10 AND 20 PERCENT OF CRITICAL

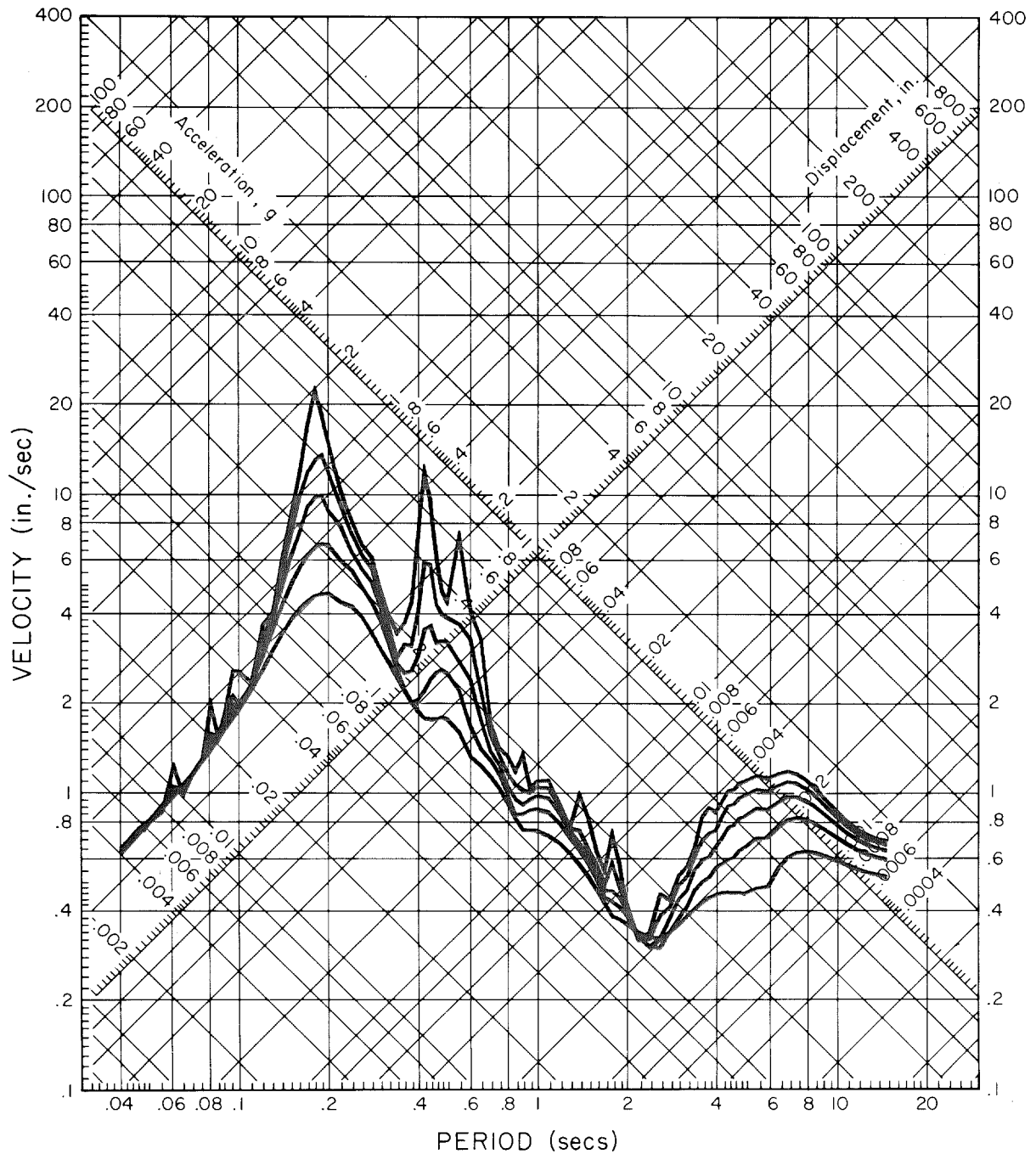


Fig. 13-b

RELATIVE VELOCITY RESPONSE SPECTRUM
 WHITTIER 7215 BRIGHT AVE. 5TH FLOOR, JANUARY 1, 1976
 IING0001 WHITTIER 7215 BRIGHT AVE. 5TH FLOOR COMP. NORT
 DAMPING VALUES ARE 0, 2, 5, 10 AND 20 PERCENT OF CRITICAL

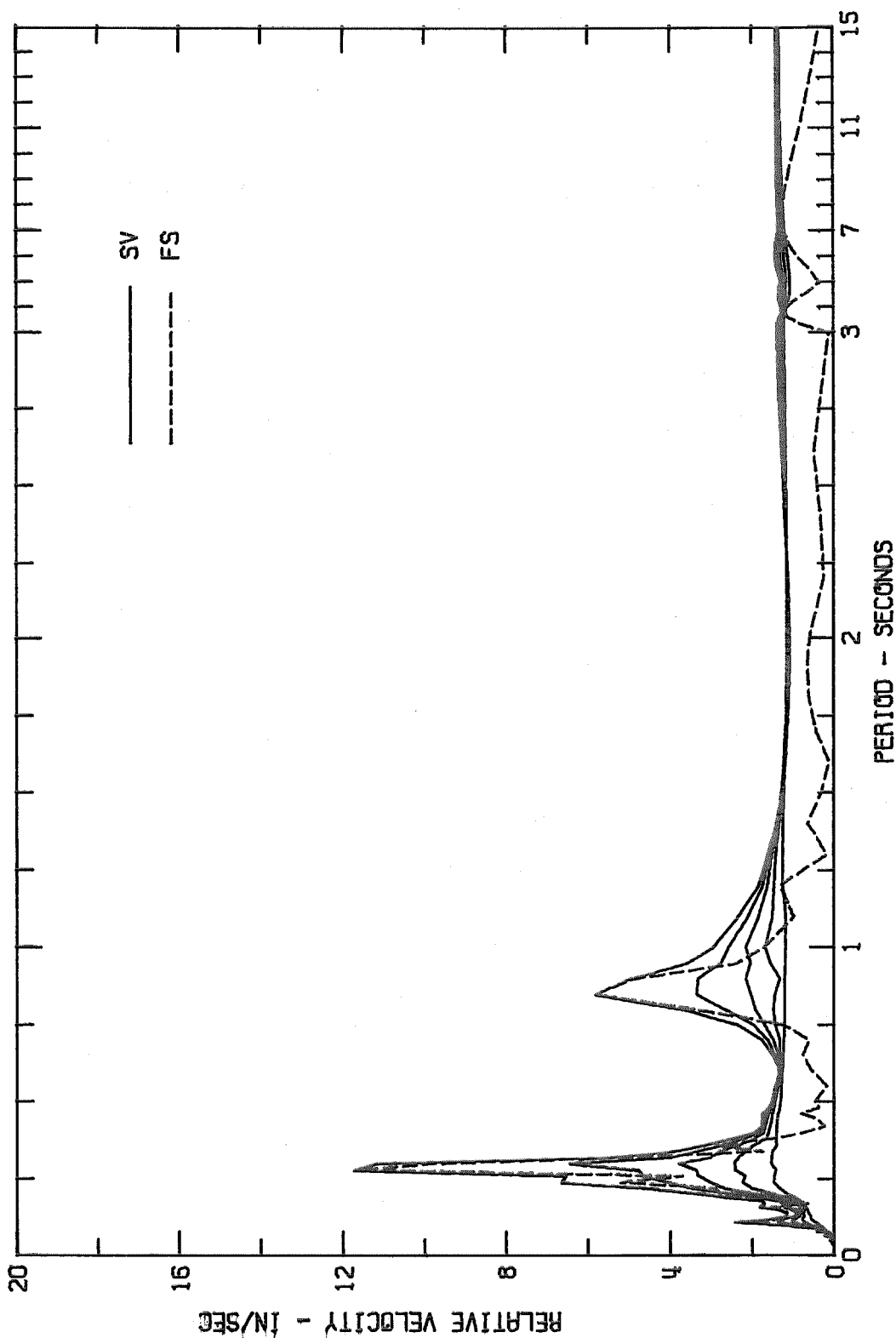


Fig. 14-a

RESPONSE SPECTRUM

WHITTIER 7215 BRIGHT AVE. 5TH FLOOR, JANUARY 1, 1976

IIN0001

WHITTIER 7215 BRIGHT AVE. 5TH FLOOR COMP. NORTH

DAMPING VALUES ARE 0, 2, 5, 10 AND 20 PERCENT OF CRITICAL

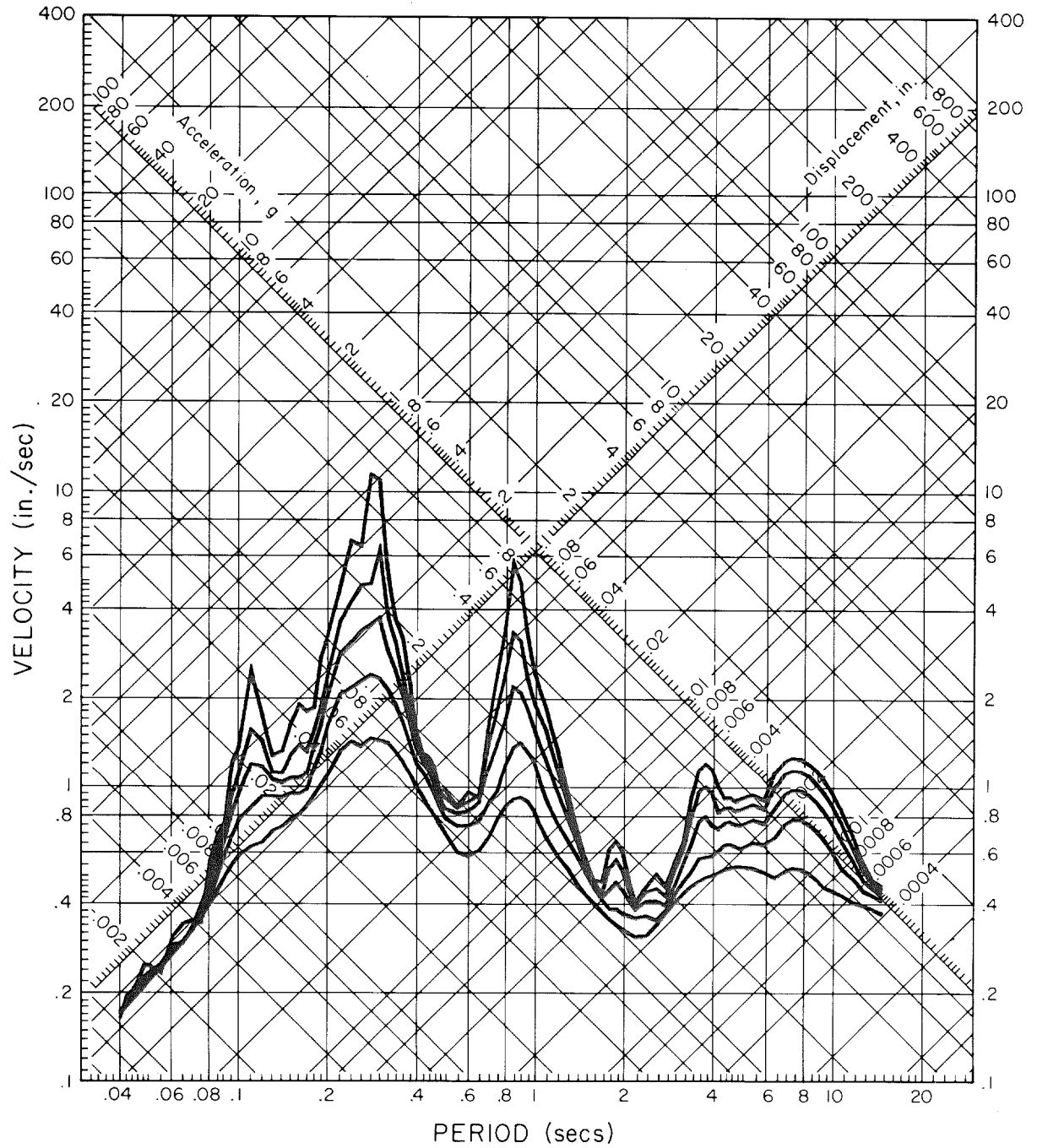


Fig. 14-b

RELATIVE VELOCITY RESPONSE SPECTRUM
WHITTIER 7215 BRIGHT AVE. 5TH FLOOR, JANUARY 1, 1976
IIN0001 WHITTIER 7215 BRIGHT AVE. 5TH FLOOR COMP. DOWN
DAMPING VALUES ARE 0, 2, 5, 10 AND 20 PERCENT OF CRITICAL

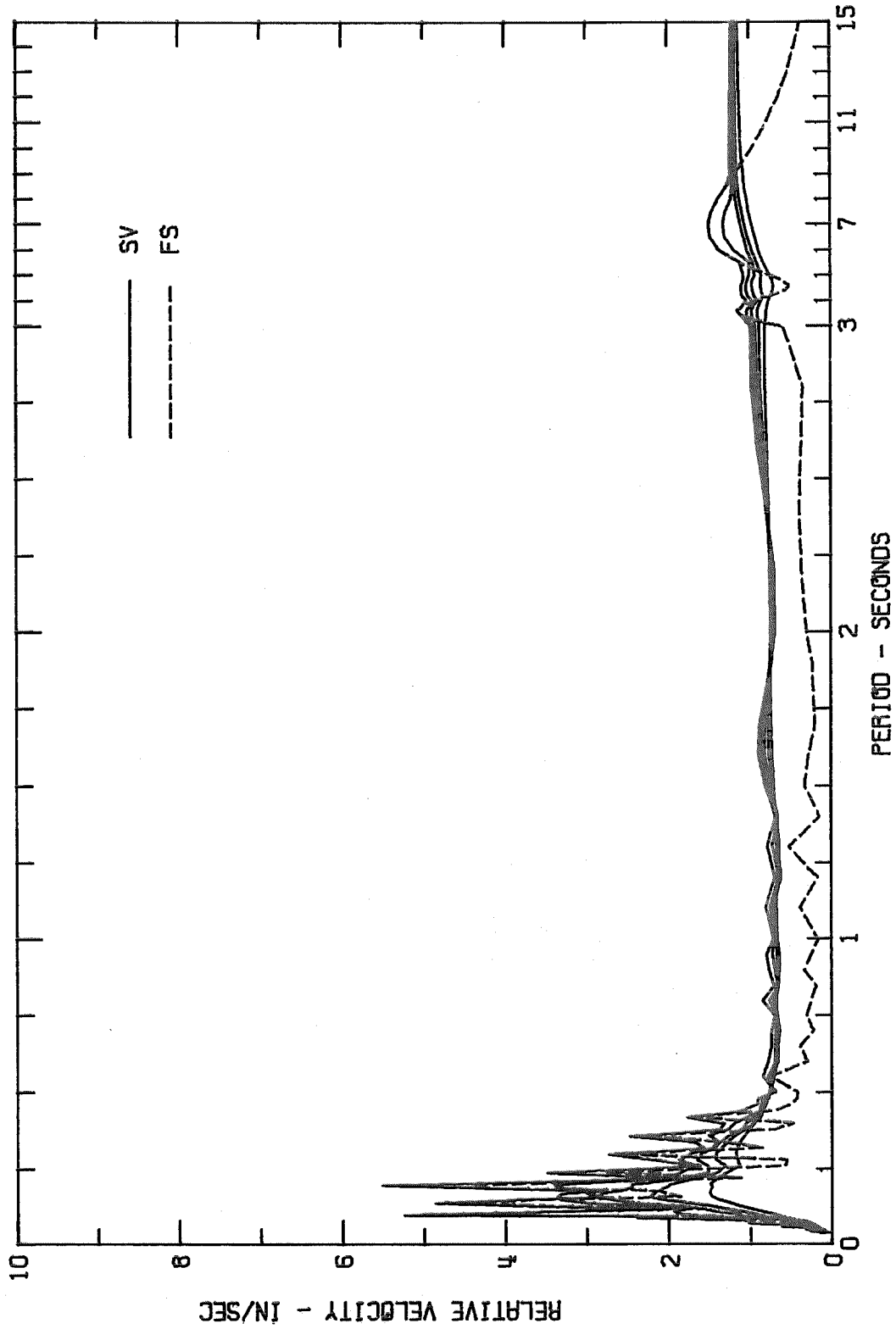


Fig. 15-a

RESPONSE SPECTRUM

WHITTIER 7215 BRIGHT AVE. 5TH FLOOR, JANUARY 1, 1976

IIN0001

WHITTIER 7215 BRIGHT AVE. 5TH FLOOR COMP. DOWN

DAMPING VALUES ARE 0, 2, 5, 10 AND 20 PERCENT OF CRITICAL

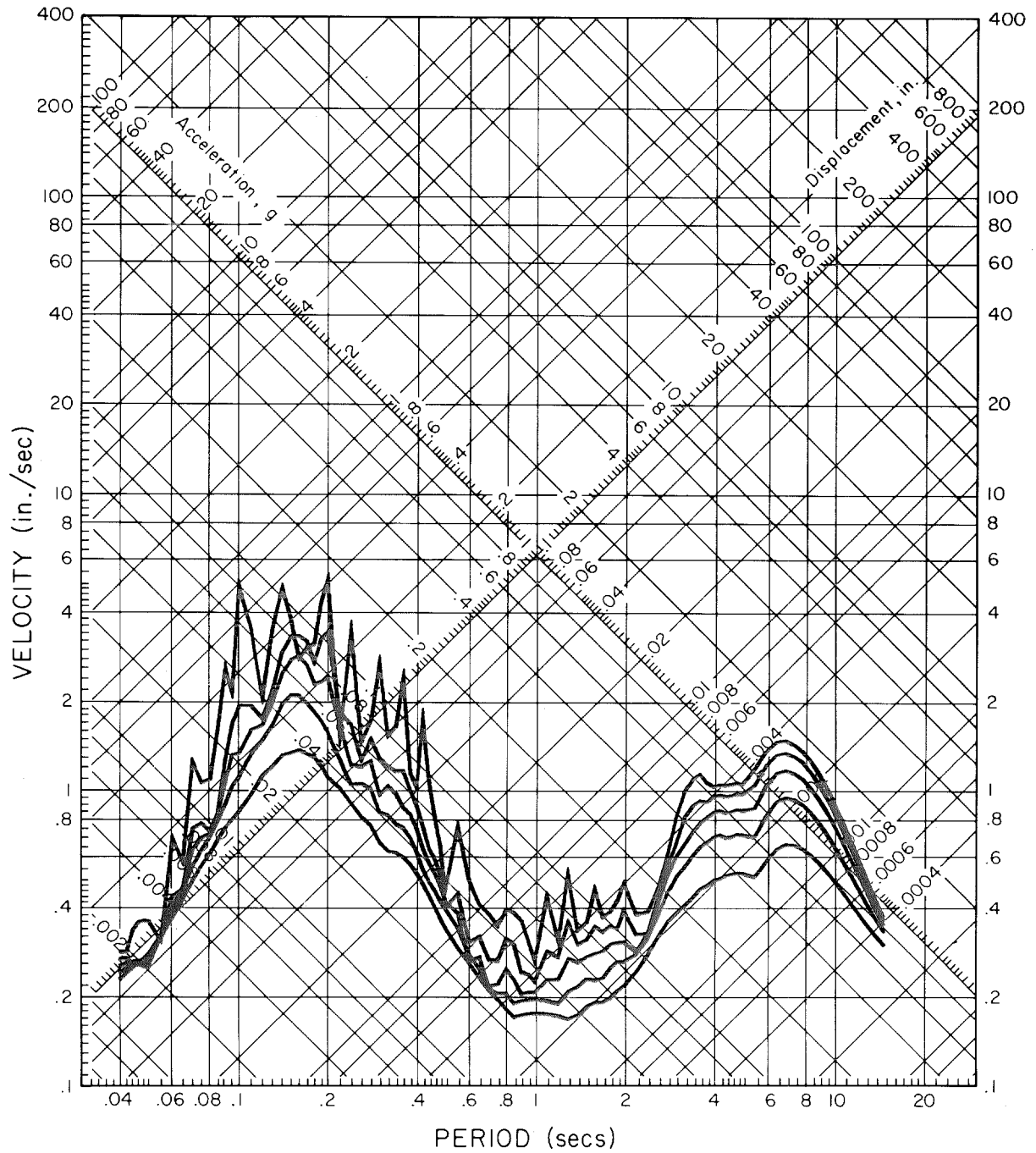


Fig. 15-b

RELATIVE VELOCITY RESPONSE SPECTRUM
WHITTIER, 7215 BRIGHT AVE., 10TH FLOOR, JANUARY 1, 1976 - 0920 PST
IIN00100 WHITTIER, 7215 BRIGHT AVE., 10TH FLOOR WEST
DAMPING VALUES ARE 0, 2, 5, 10 AND 20 PERCENT OF CRITICAL

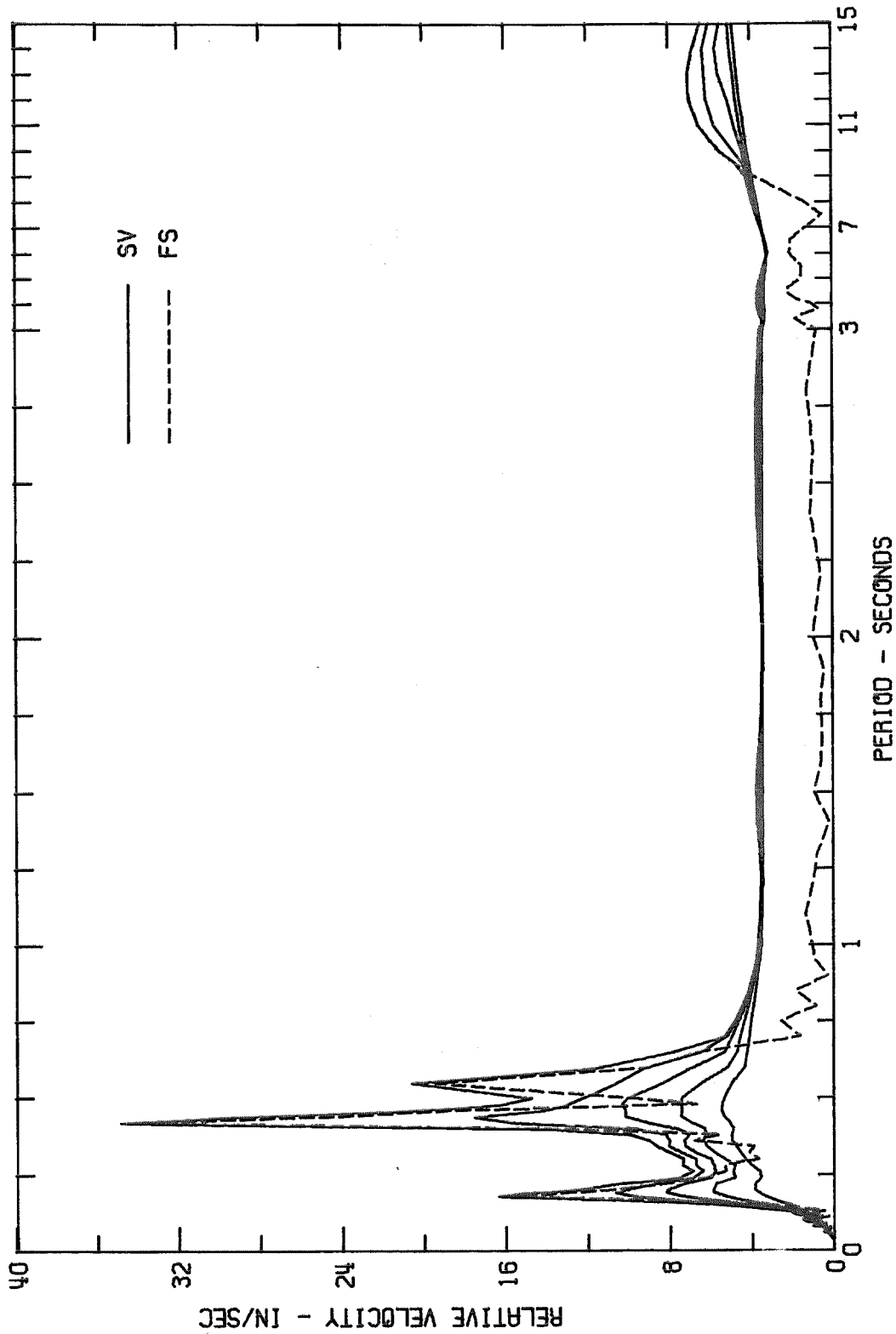


Fig. 16-a

RESPONSE SPECTRUM

WHITTIER, 7215 BRIGHT AVE., 10TH FLOOR, JANUARY 1, 1976 - 0920 PST

IIN00100

WHITTIER, 7215 BRIGHT AVE., 10TH FLOOR WEST

DAMPING VALUES ARE 0, 2, 5, 10 AND 20 PERCENT OF CRITICAL

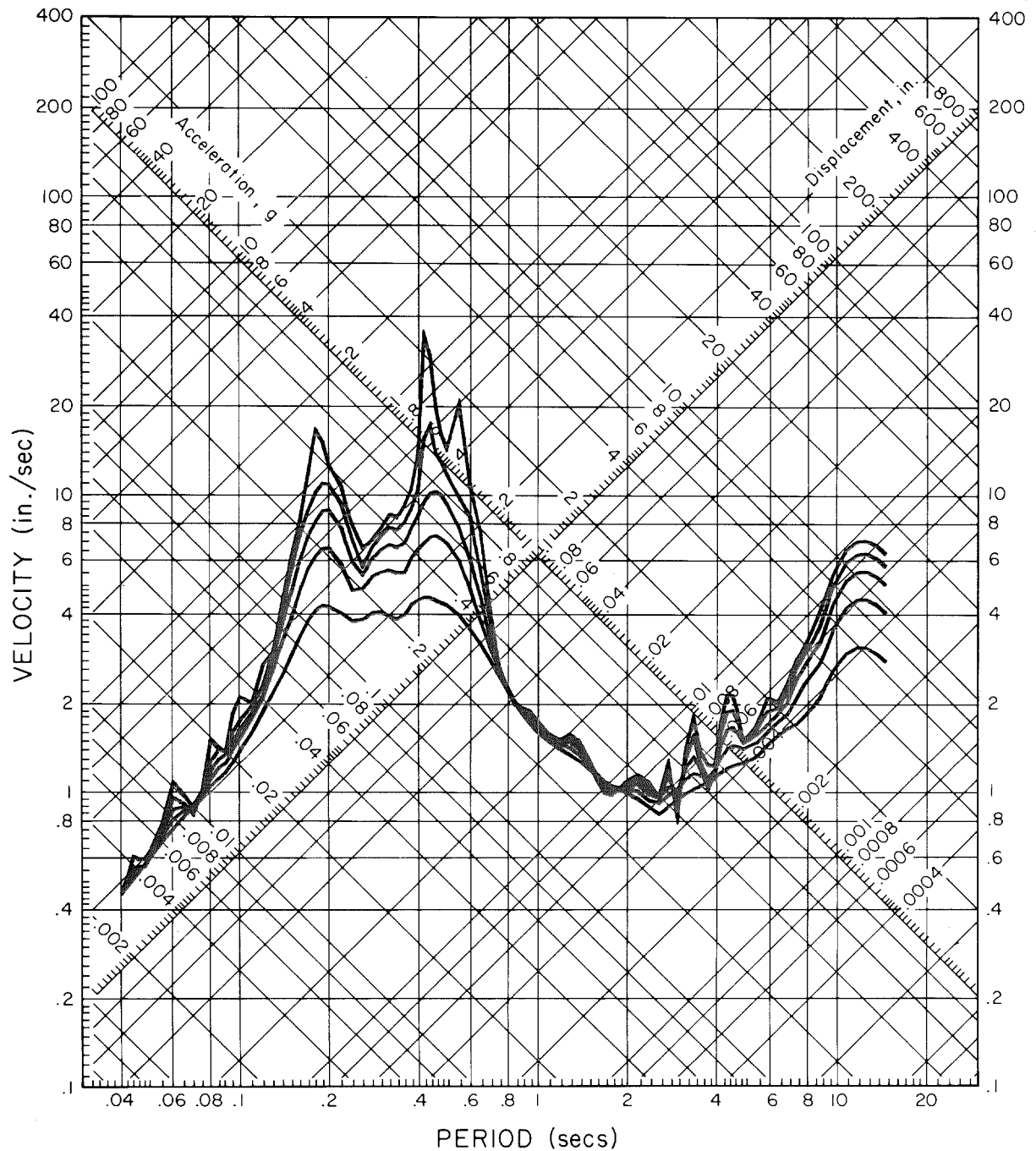


Fig. 16-b

RELATIVE VELOCITY RESPONSE SPECTRUM
WHITTIER, 7215 BRIGHT AVE., 10TH FLOOR, JANUARY 1, 1976 - 0920 PST
IIN00100 WHITTIER, 7215 BRIGHT AVE., 10TH FLOOR NORTH
DAMPING VALUES ARE 0, 2, 5, 10 AND 20 PERCENT OF CRITICAL

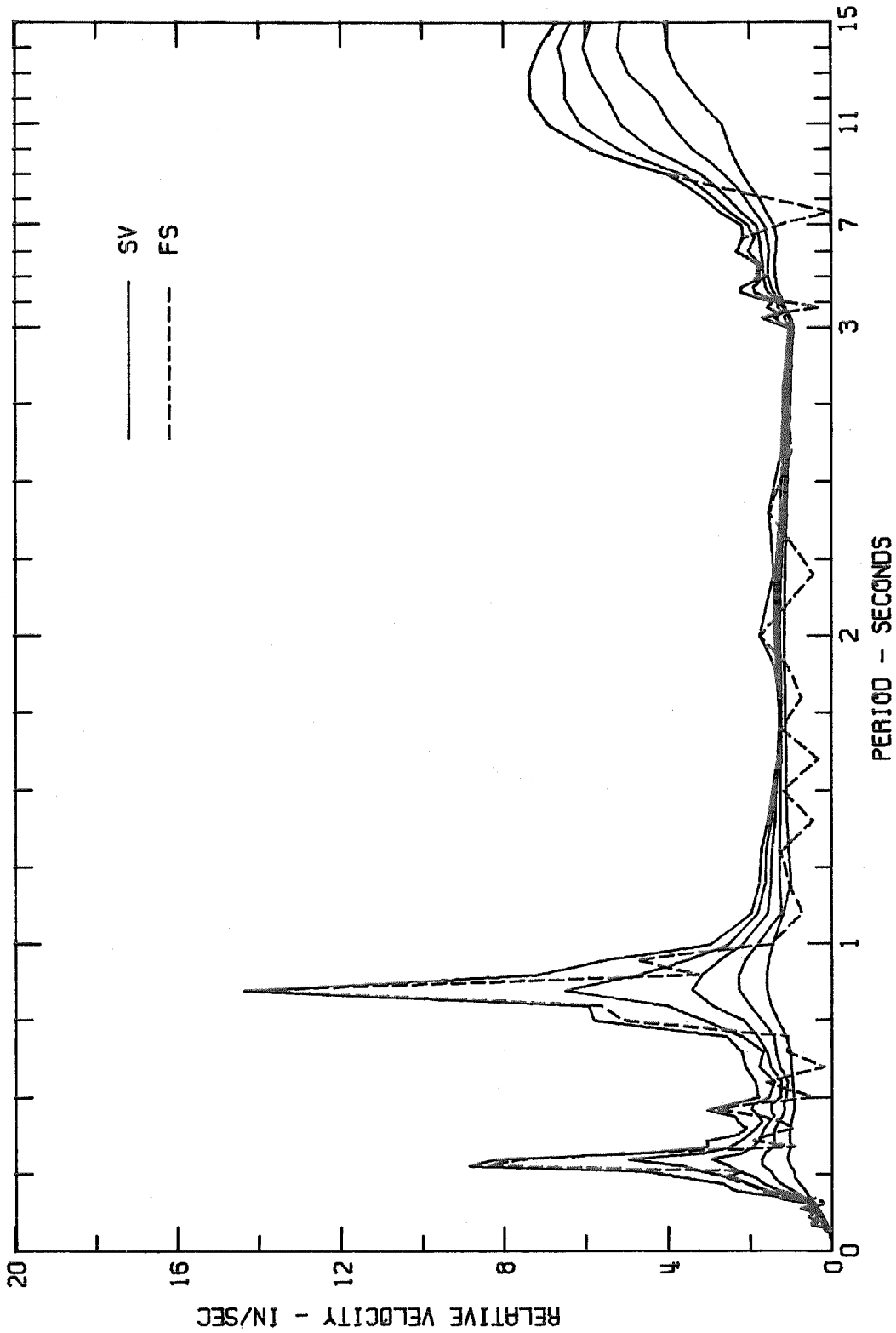


Fig. 17-a

RESPONSE SPECTRUM

WHITTIER, 7215 BRIGHT AVE., 10TH FLOOR, JANUARY 1, 1976 - 0920 PST

IIN00100

WHITTIER, 7215 BRIGHT AVE., 10TH FLOOR NORTH

DAMPING VALUES ARE 0, 2, 5, 10 AND 20 PERCENT OF CRITICAL

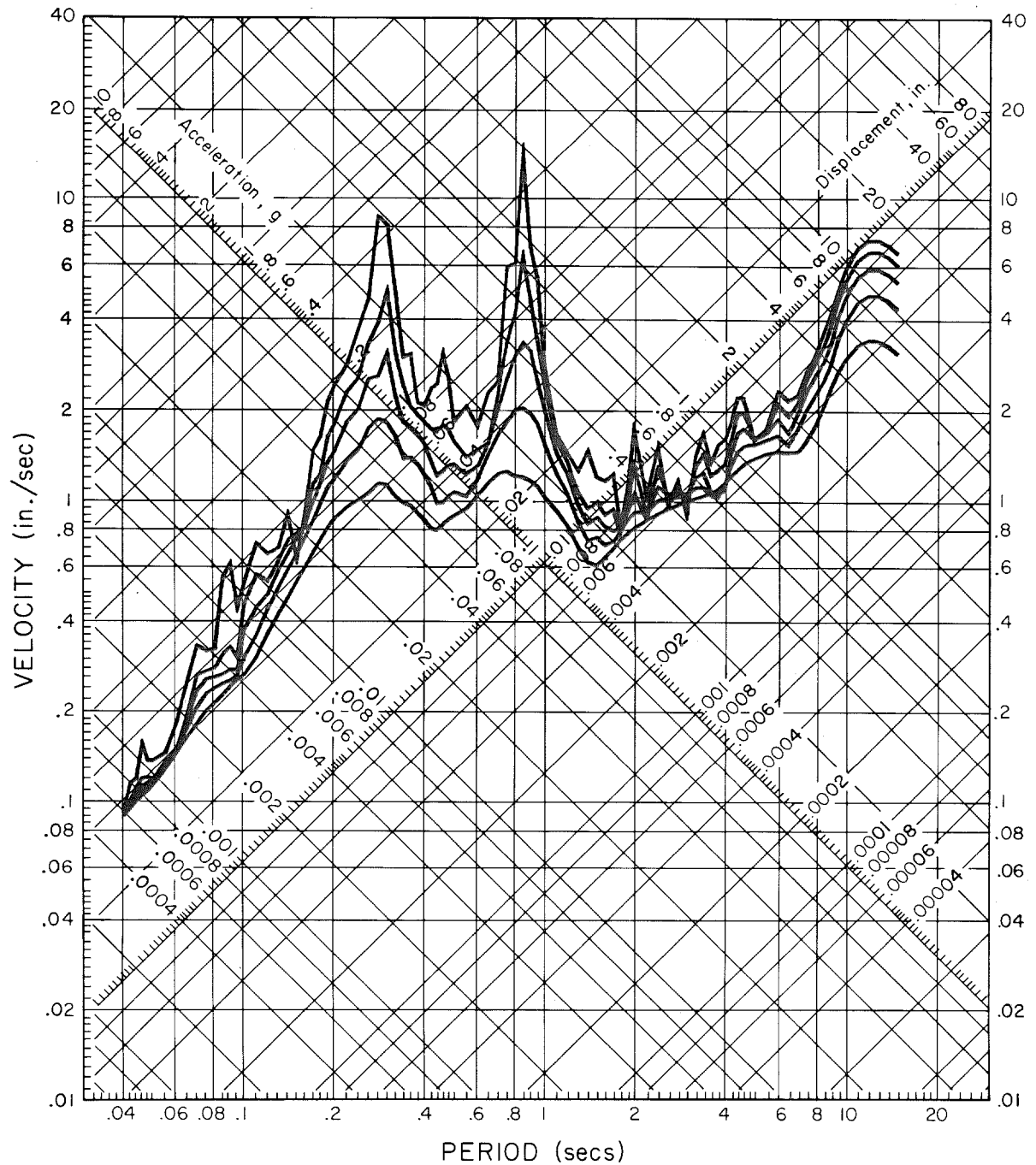


Fig. 17-b

RELATIVE VELOCITY RESPONSE SPECTRUM
WHITTIER, 7215 BRIGHT AVE., 10TH FLOOR, JANUARY 1, 1976 - 0920 PST
11N00100 WHITTIER, 7215 BRIGHT AVE., 10TH FLOOR DOWN
DAMPING VALUES ARE 0, 2, 5, 10 AND 20 PERCENT OF CRITICAL

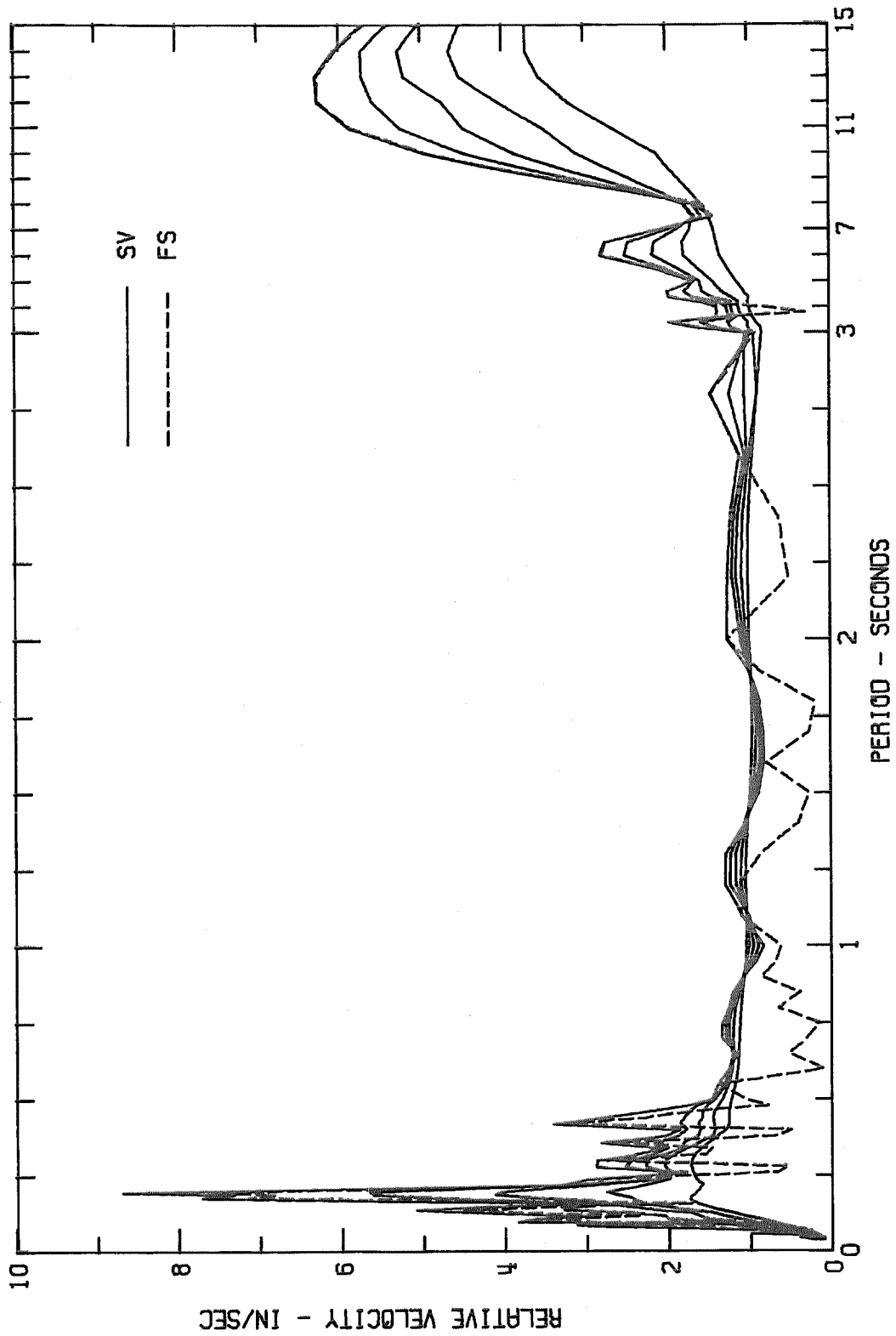


Fig. 18-a

RESPONSE SPECTRUM

WHITTIER, 7215 BRIGHT AVE., 10TH FLOOR, JANUARY 1, 1976 - 0920 PST

IIN00100

WHITTIER, 7215 BRIGHT AVE., 10TH FLOOR DOWN

DAMPING VALUES ARE 0, 2, 5, 10 AND 20 PERCENT OF CRITICAL

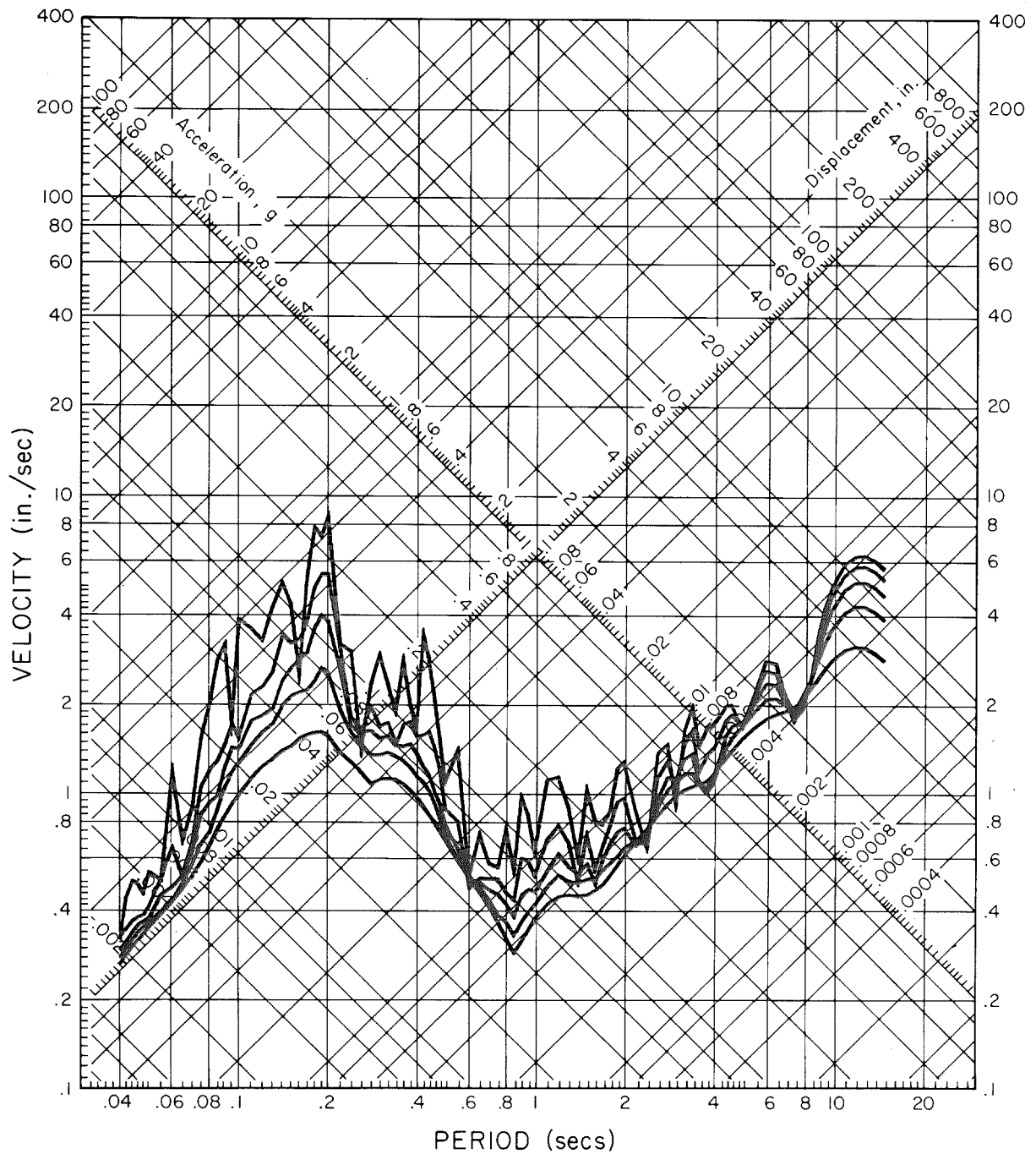


Fig. 18-b

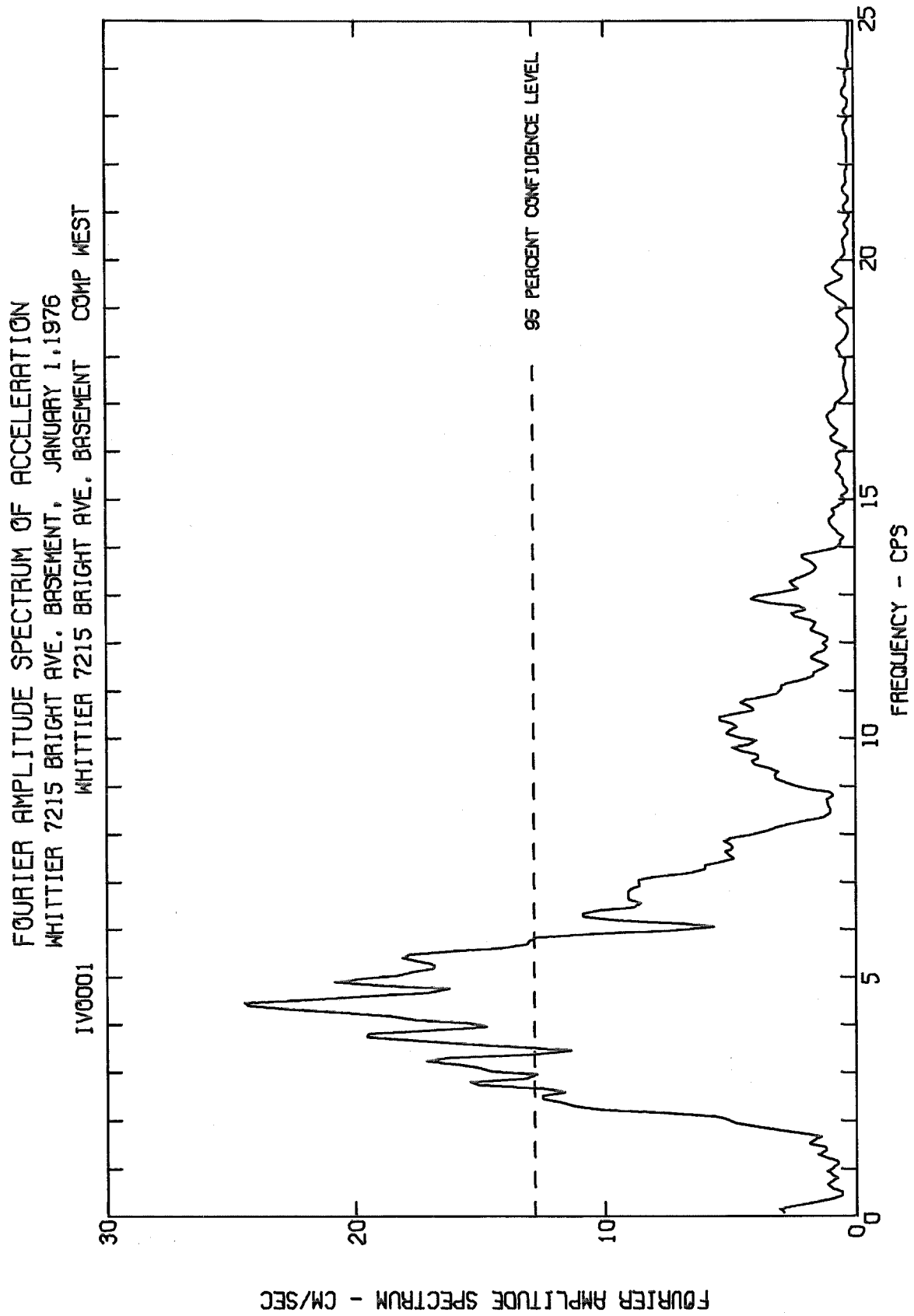


Fig. 19-a

FOURIER AMPLITUDE SPECTRUM OF ACCELERATION
WHITTIER 7215 BRIGHT AVE. BASEMENT, JANUARY 1, 1976
WHITTIER 7215 BRIGHT AVE. BASEMENT COMP WEST

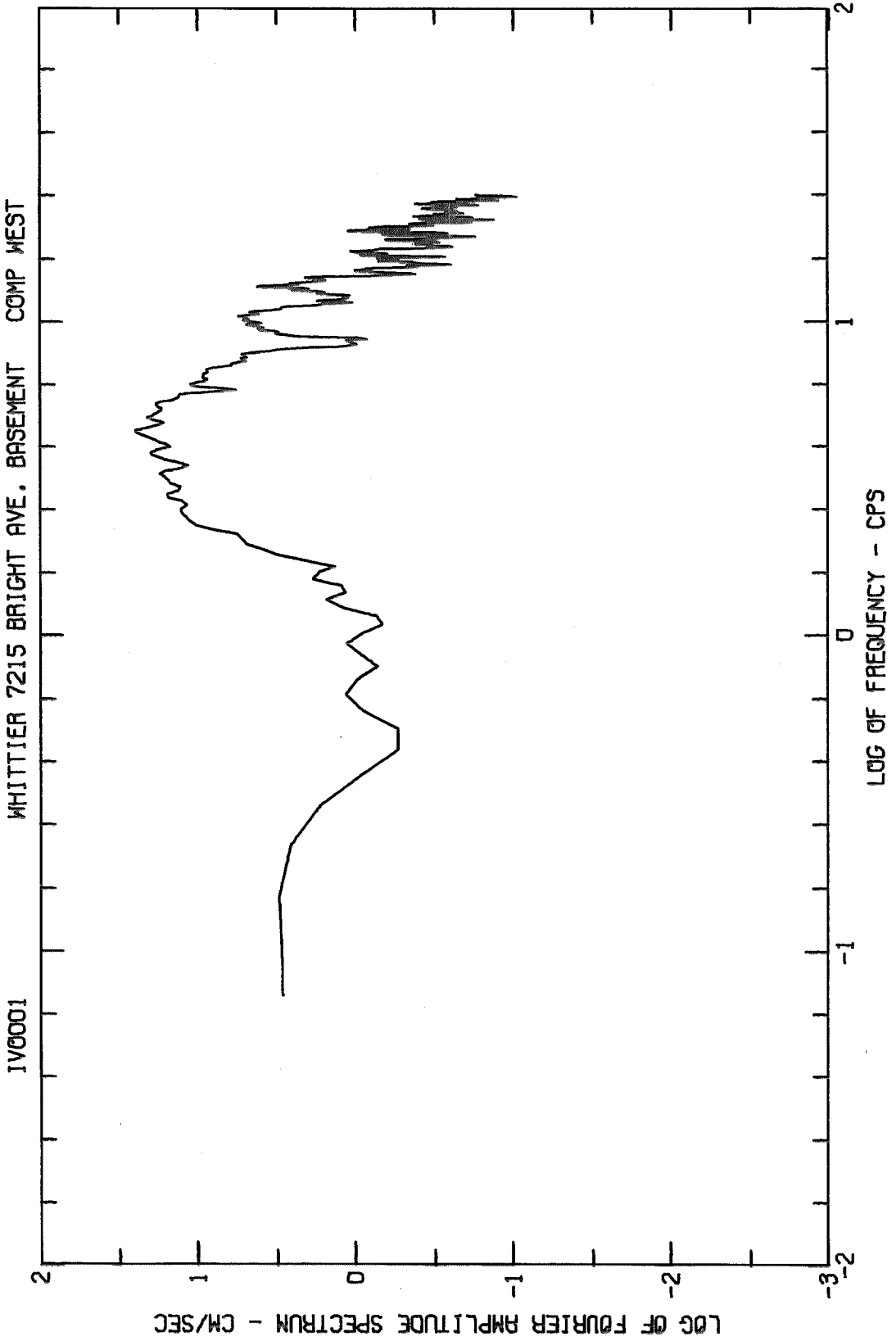


Fig. 19-b

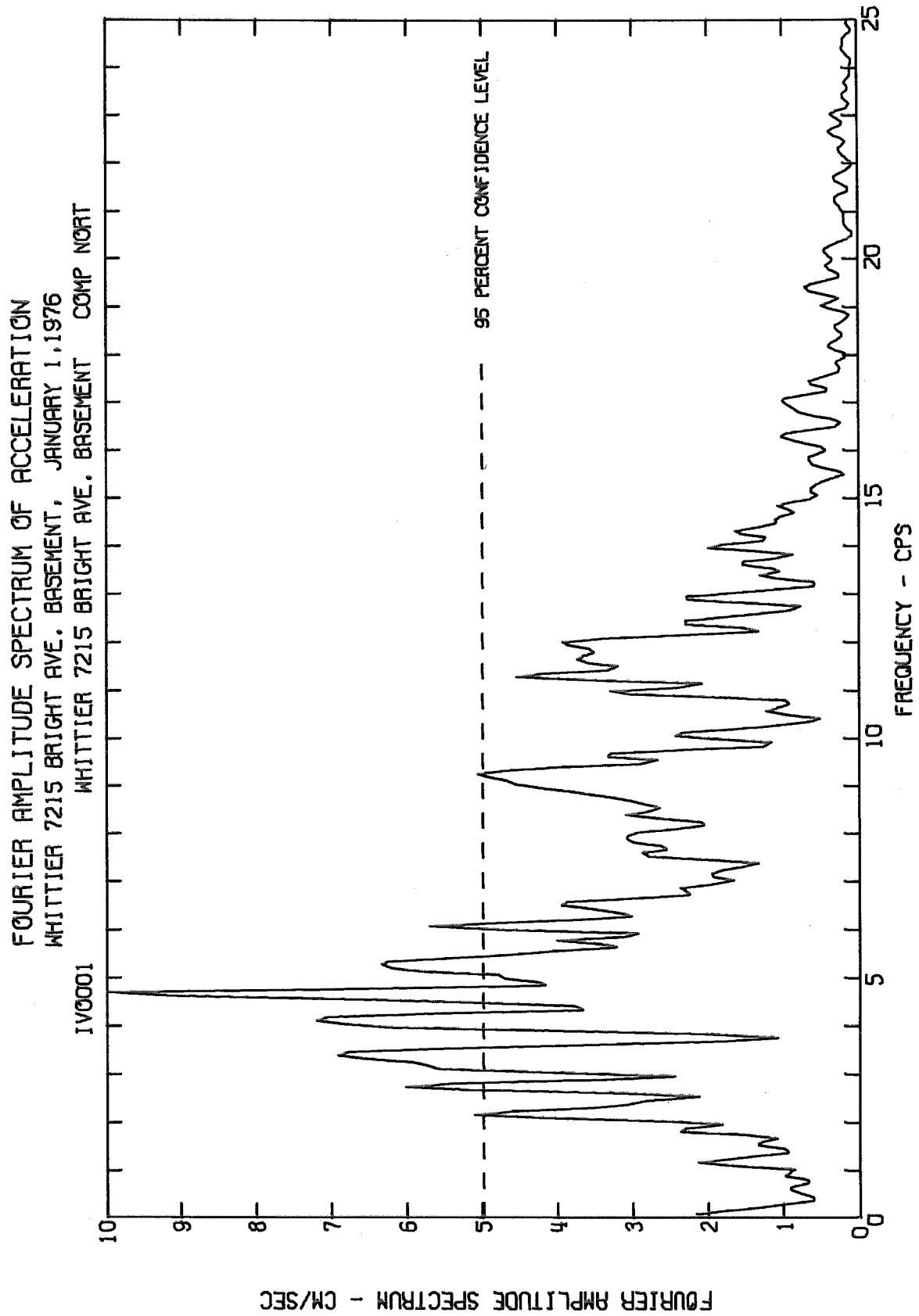


Fig. 20-a

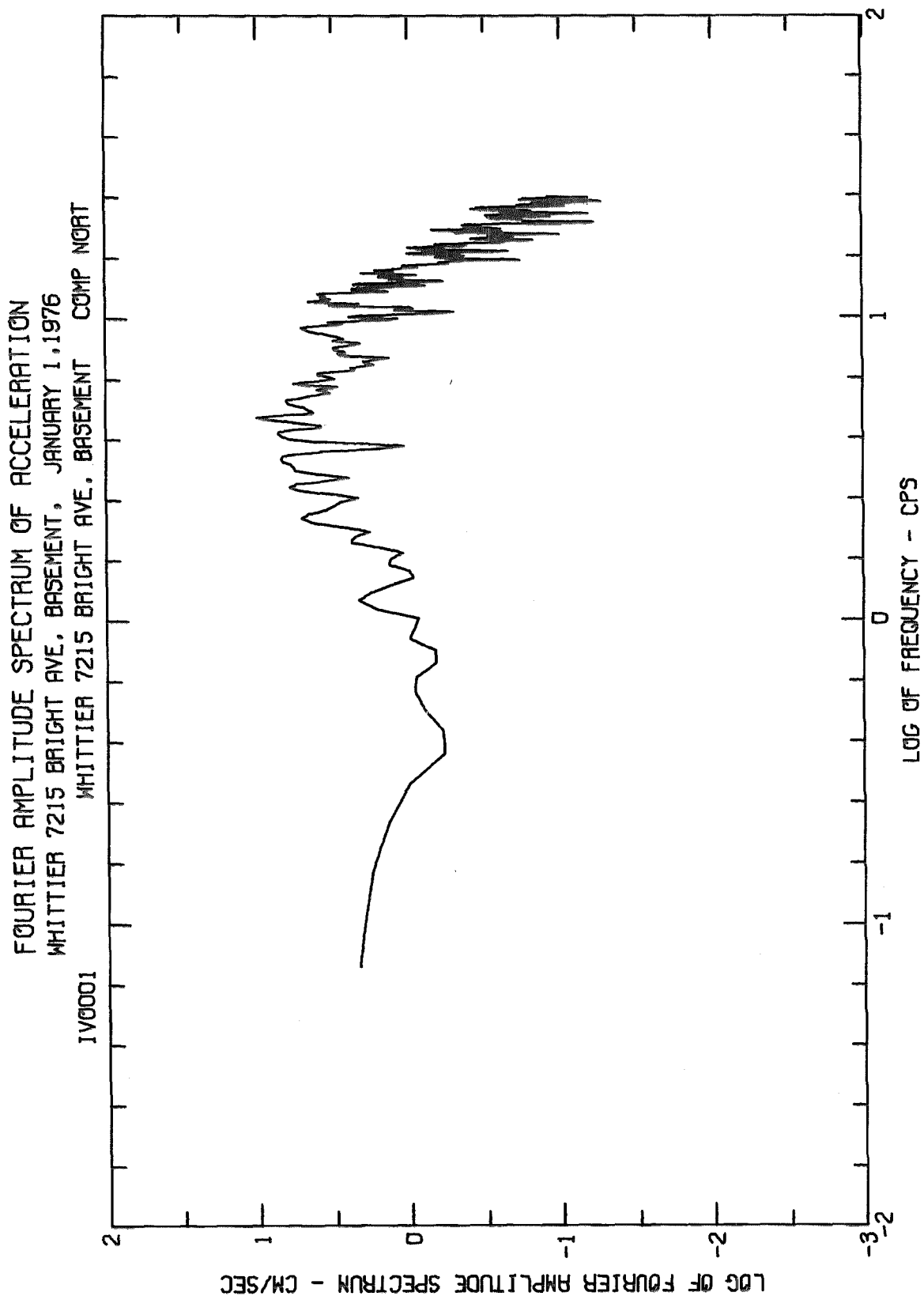


Fig. 20-b

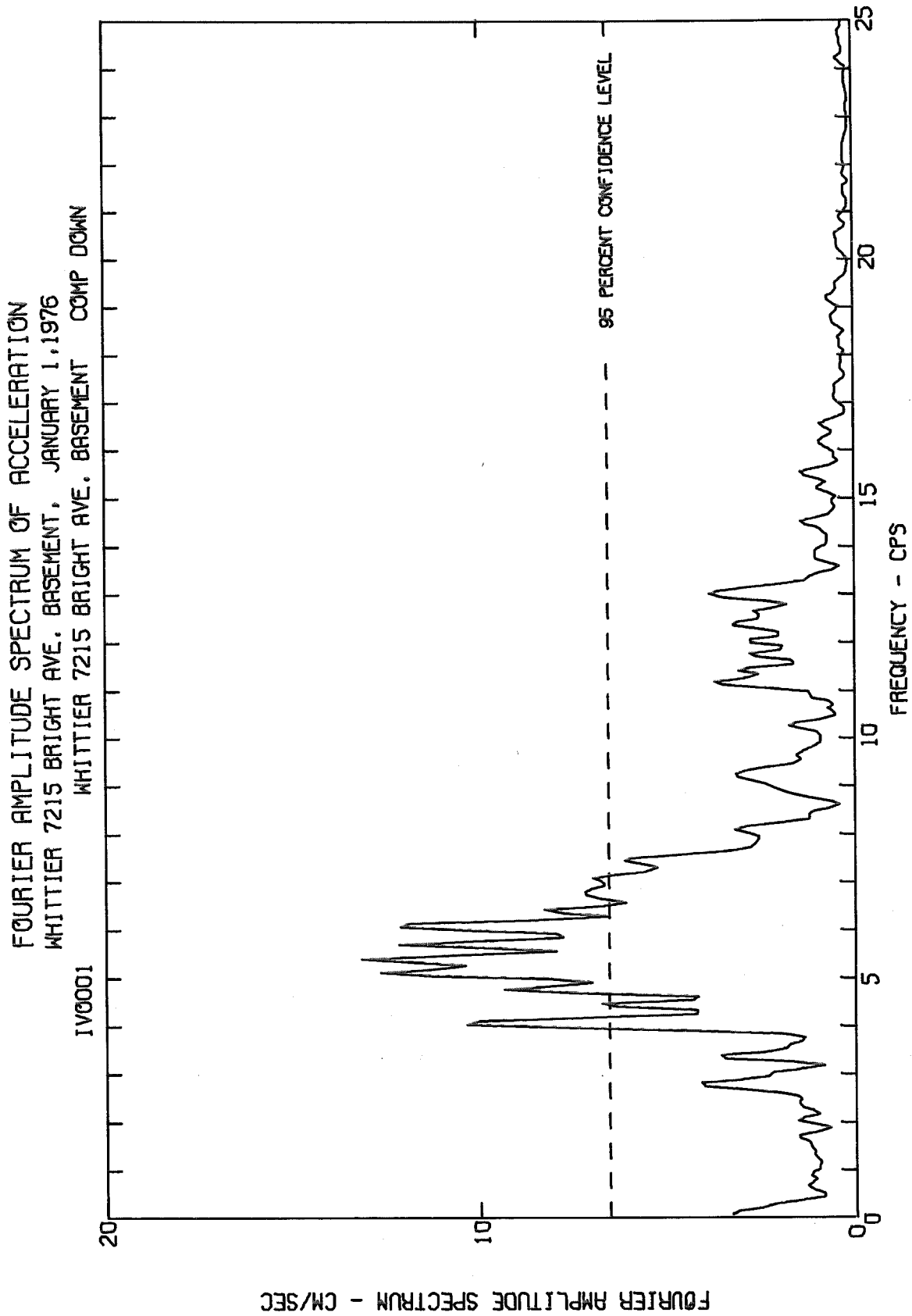


Fig. 21-a

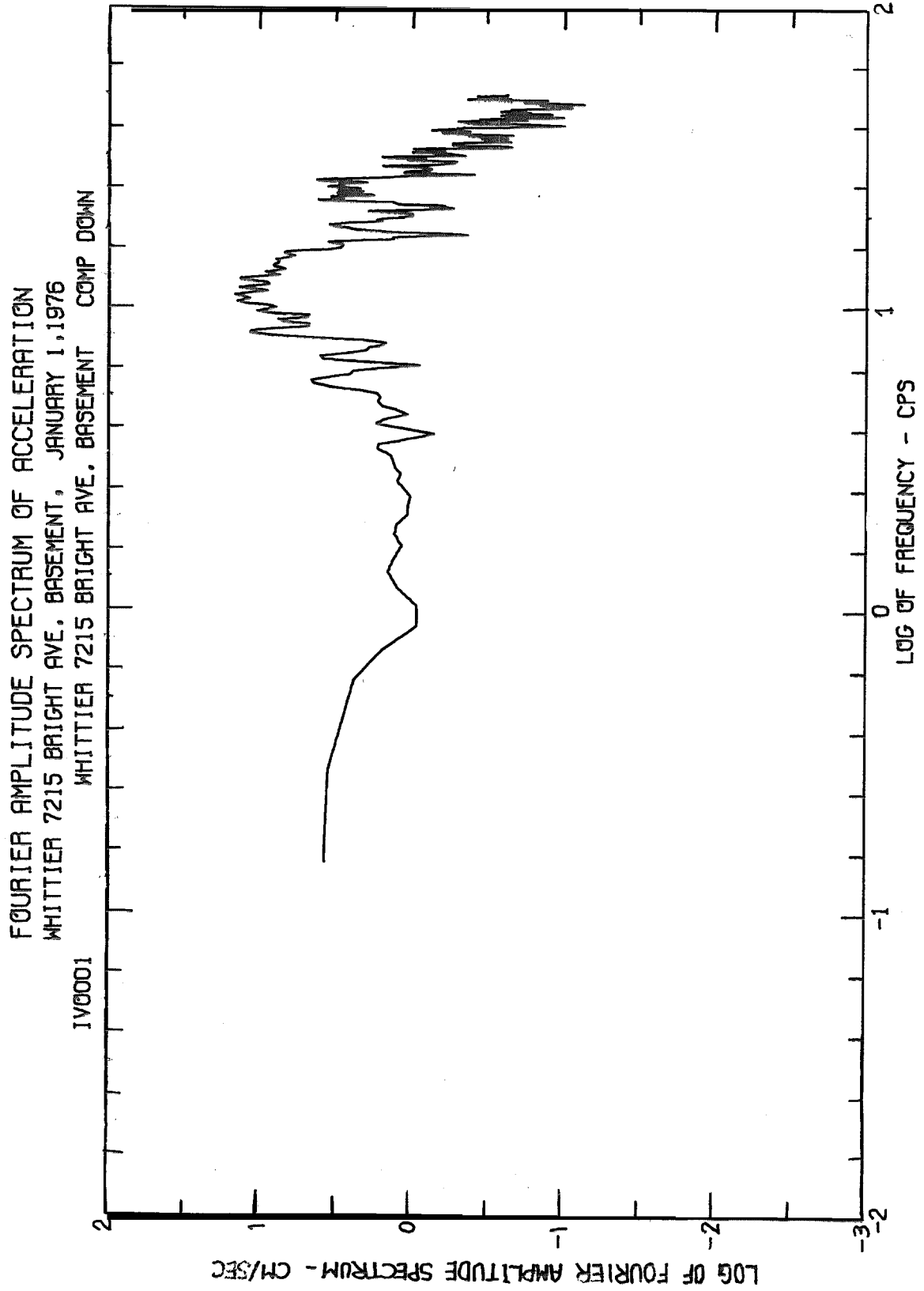


Fig. 21-b

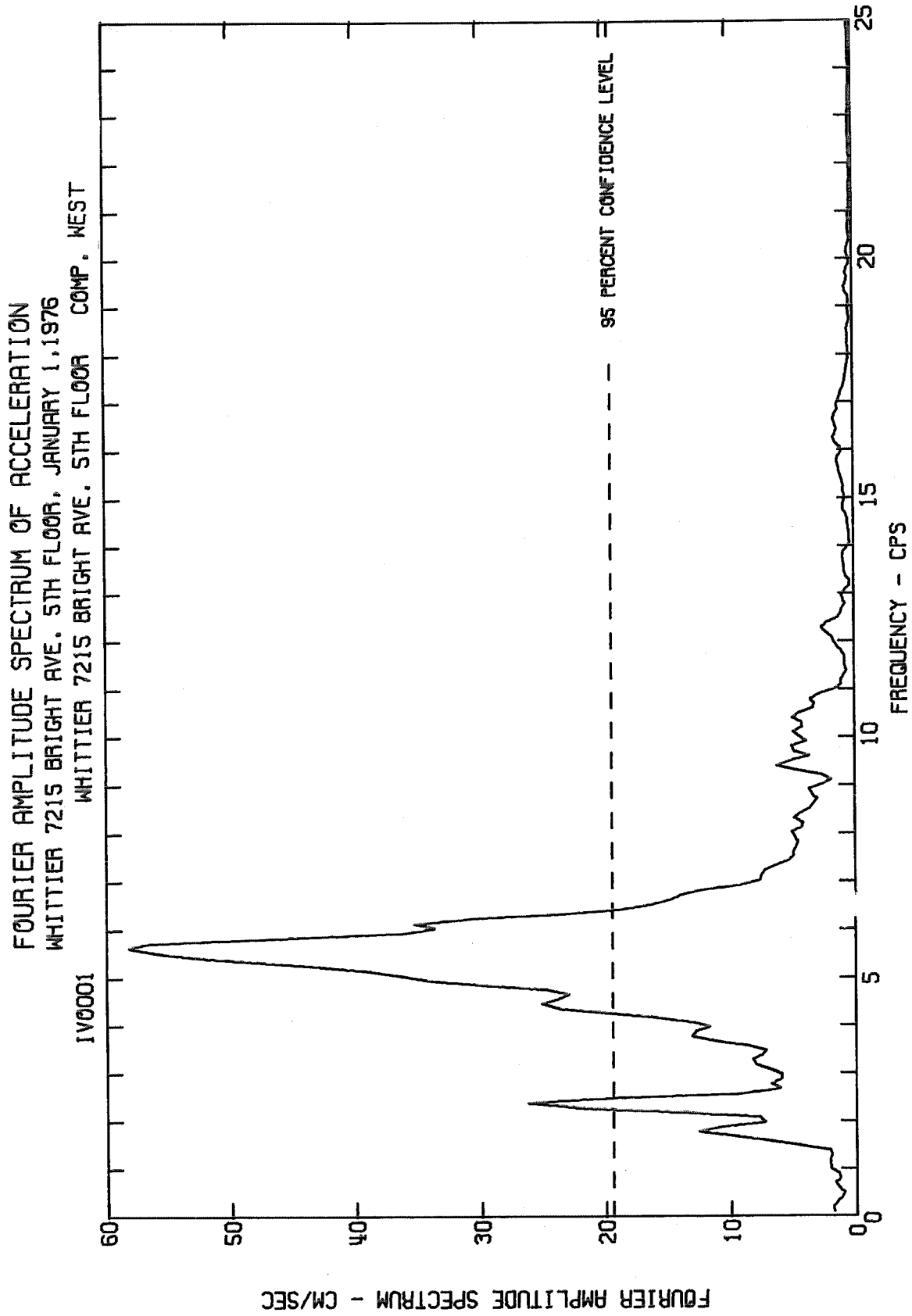


Fig. 22-a

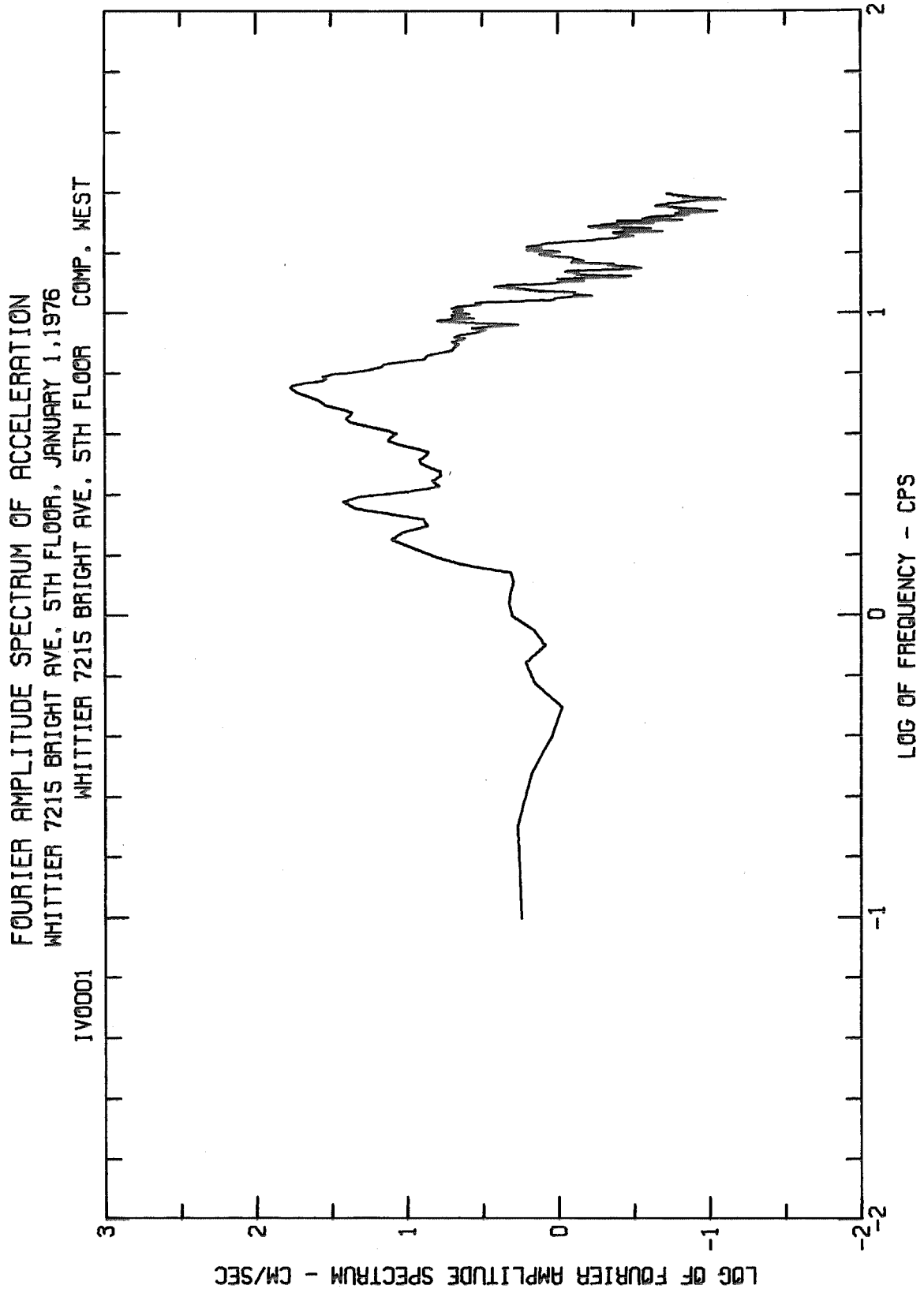


Fig. 22-b

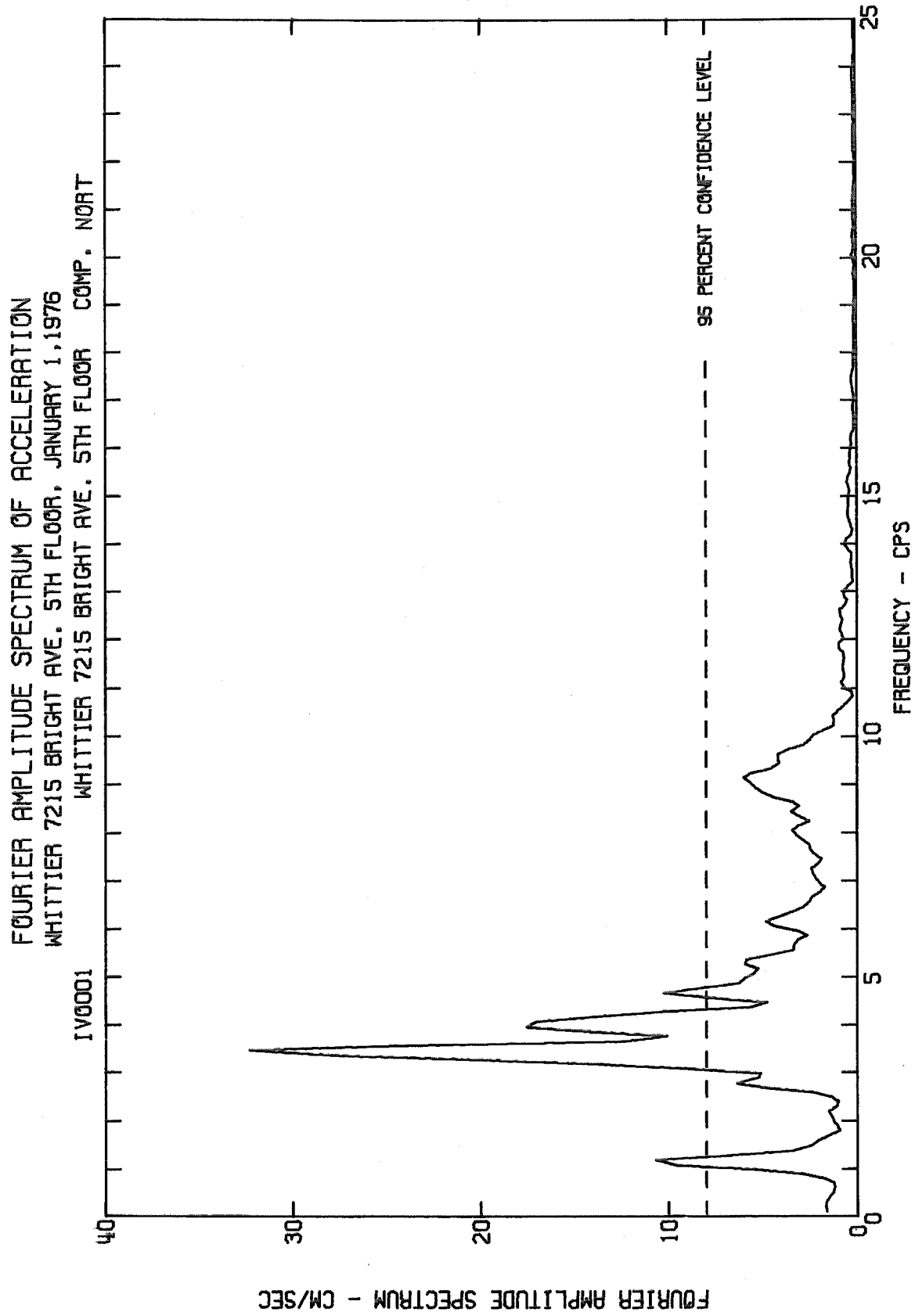


Fig. 23-a

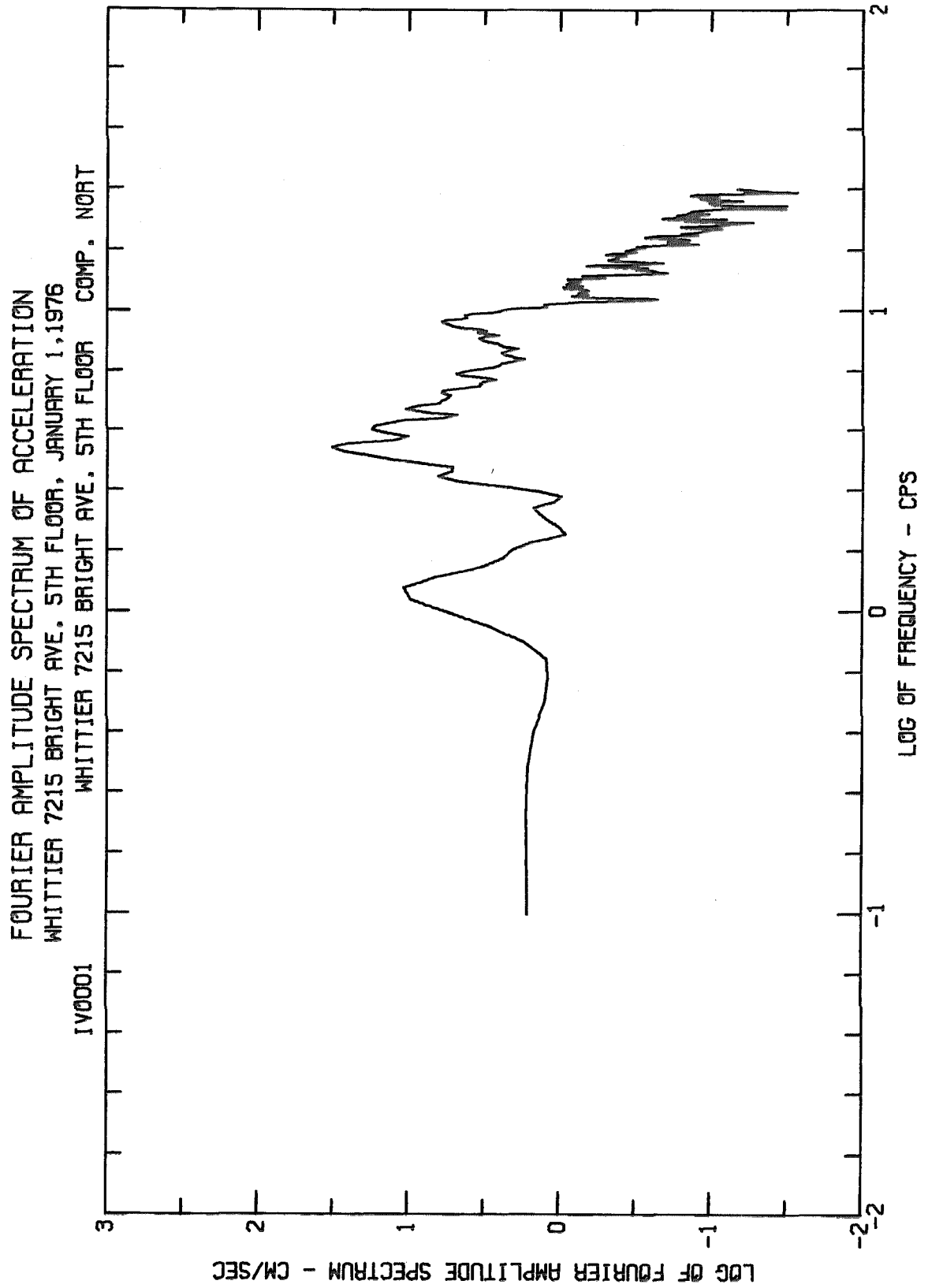


Fig. 23-b

FOURIER AMPLITUDE SPECTRUM OF ACCELERATION
WHITTIER 7215 BRIGHT AVE. 5TH FLOOR, JANUARY 1, 1976
WHITTIER 7215 BRIGHT AVE. 5TH FLOOR COMP. DOWN

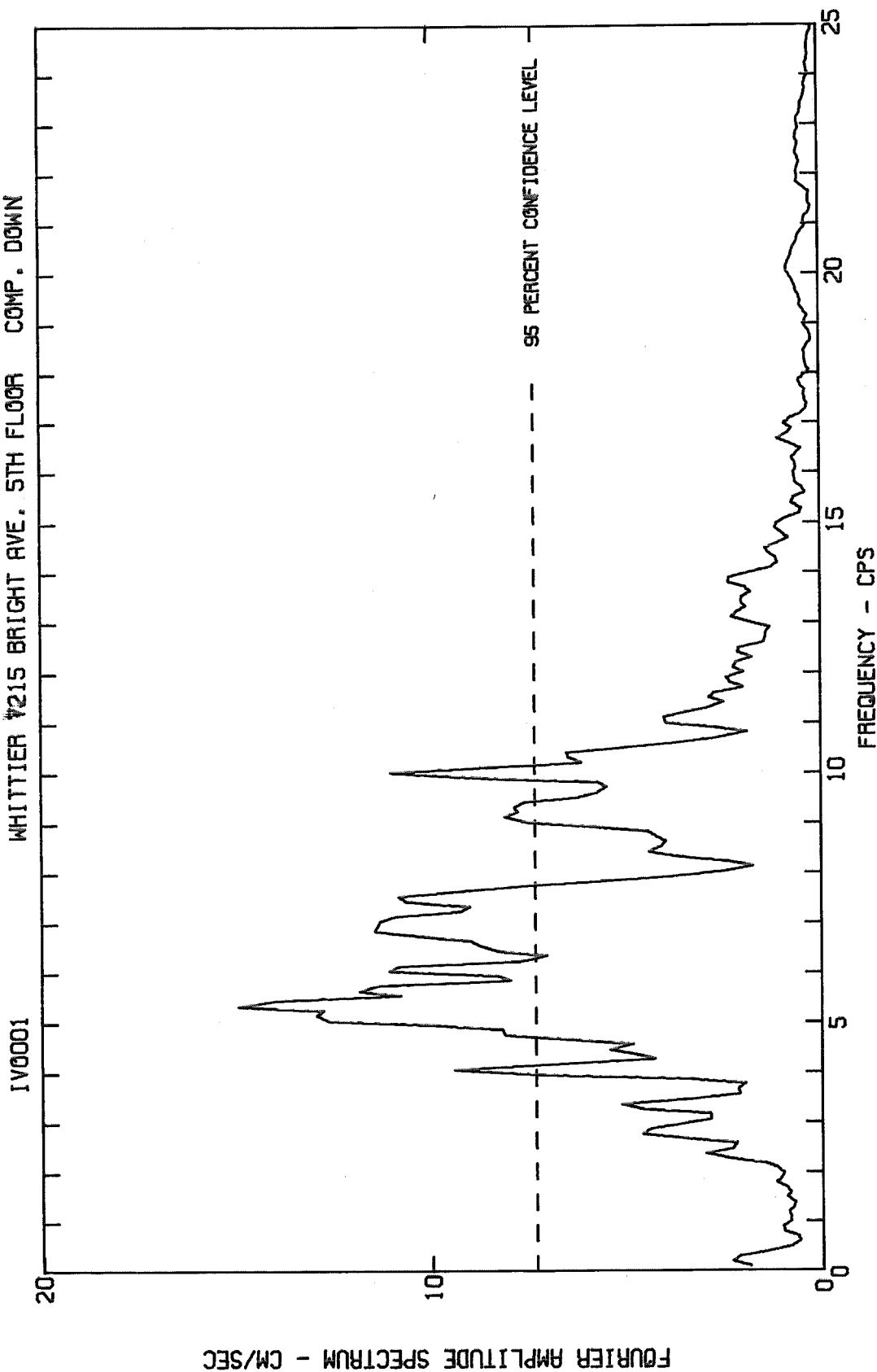


Fig. 24-a

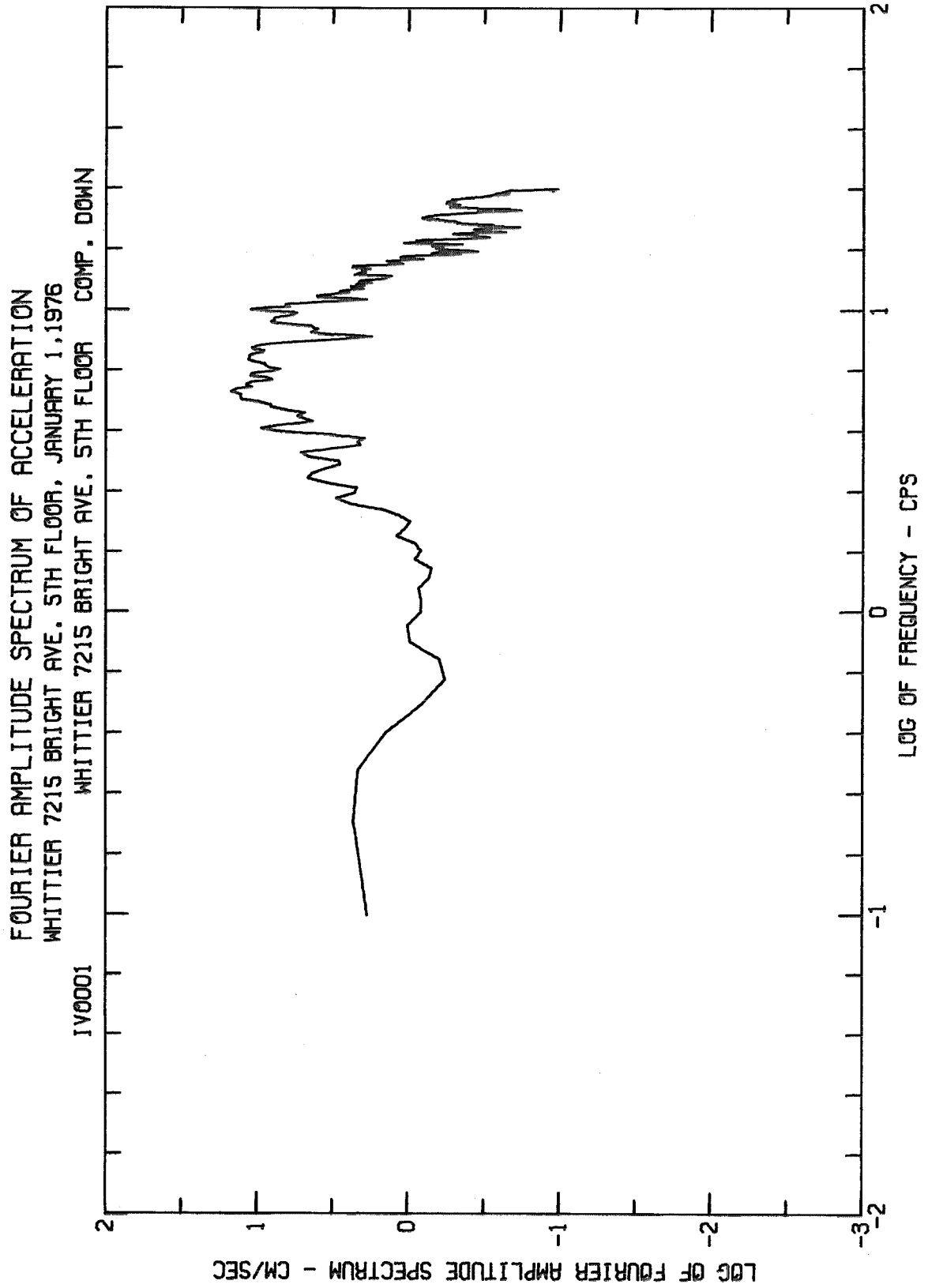


Fig. 24-b

FOURIER AMPLITUDE SPECTRUM OF ACCELERATION
WHITTIER, 7215 BRIGHT AVE., 10TH FLOOR, JANUARY 1, 1976 - 0920 PST
IWD0100 WHITTIER, 7215 BRIGHT AVE., 10TH FLOOR WEST

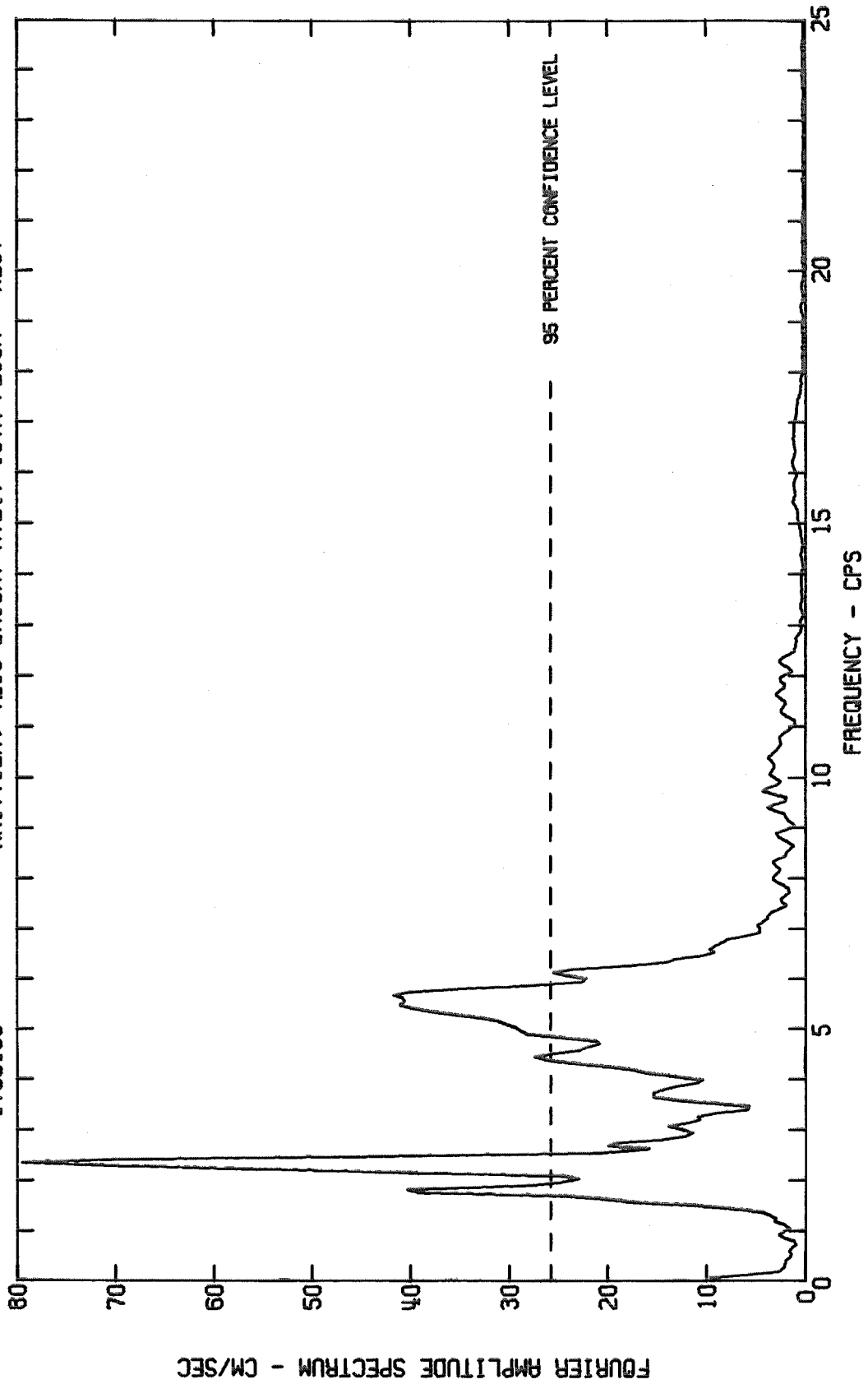


Fig. 25-a

FOURIER AMPLITUDE SPECTRUM OF ACCELERATION
WHITTIER, 7215 BRIGHT AVE., 10TH FLOOR, JANUARY 1, 1976 - 0920 PST
IV00100 WHITTIER, 7215 BRIGHT AVE., 10TH FLOOR WEST

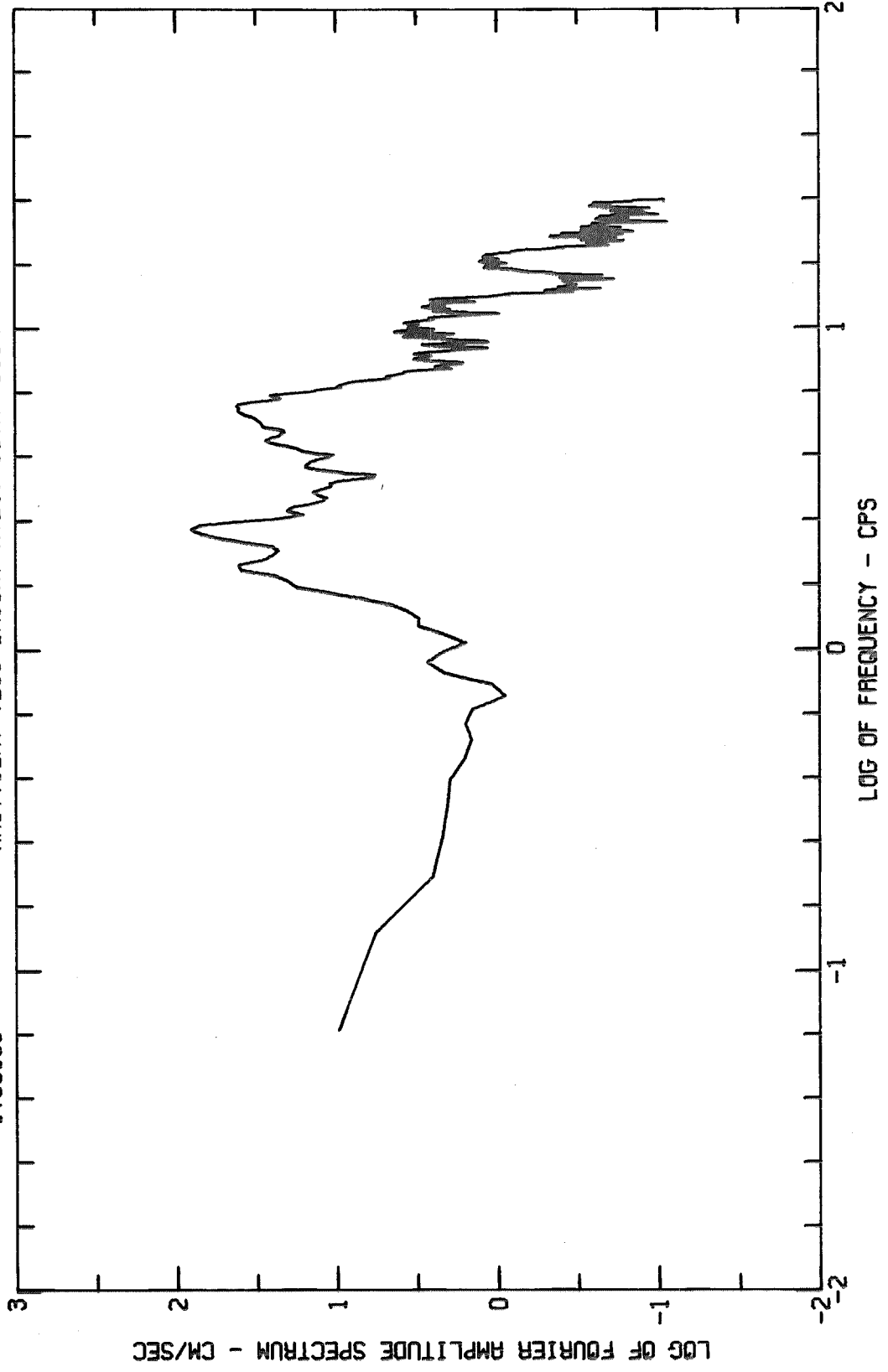


Fig. 25-b

FOURIER AMPLITUDE SPECTRUM OF ACCELERATION
WHITTIER, 7215 BRIGHT AVE., 10TH FLOOR, JANUARY 1, 1976 - 0920 PST
IV00100 WHITTIER, 7215 BRIGHT AVE., 10TH FLOOR NORTH

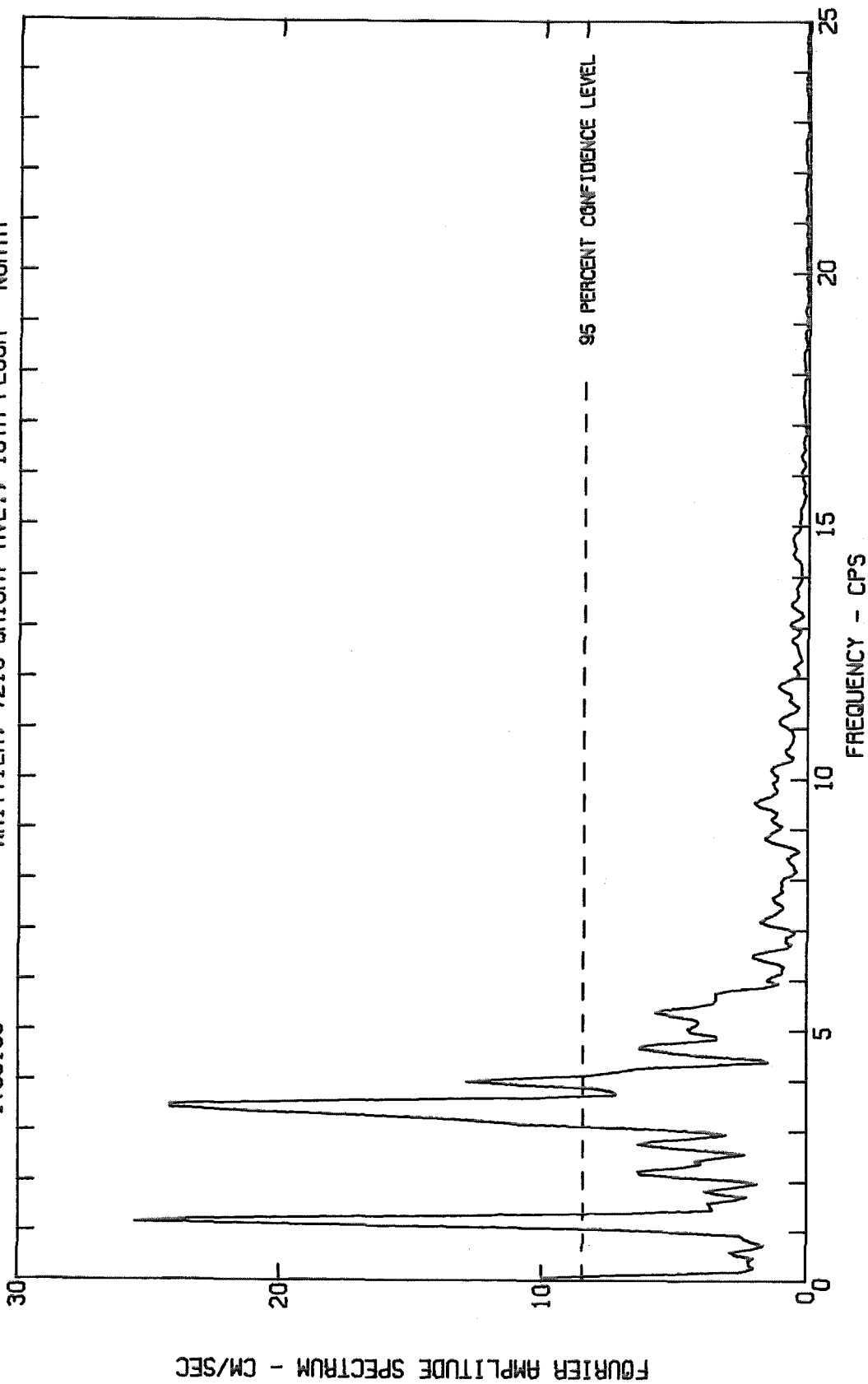


Fig. 26-a

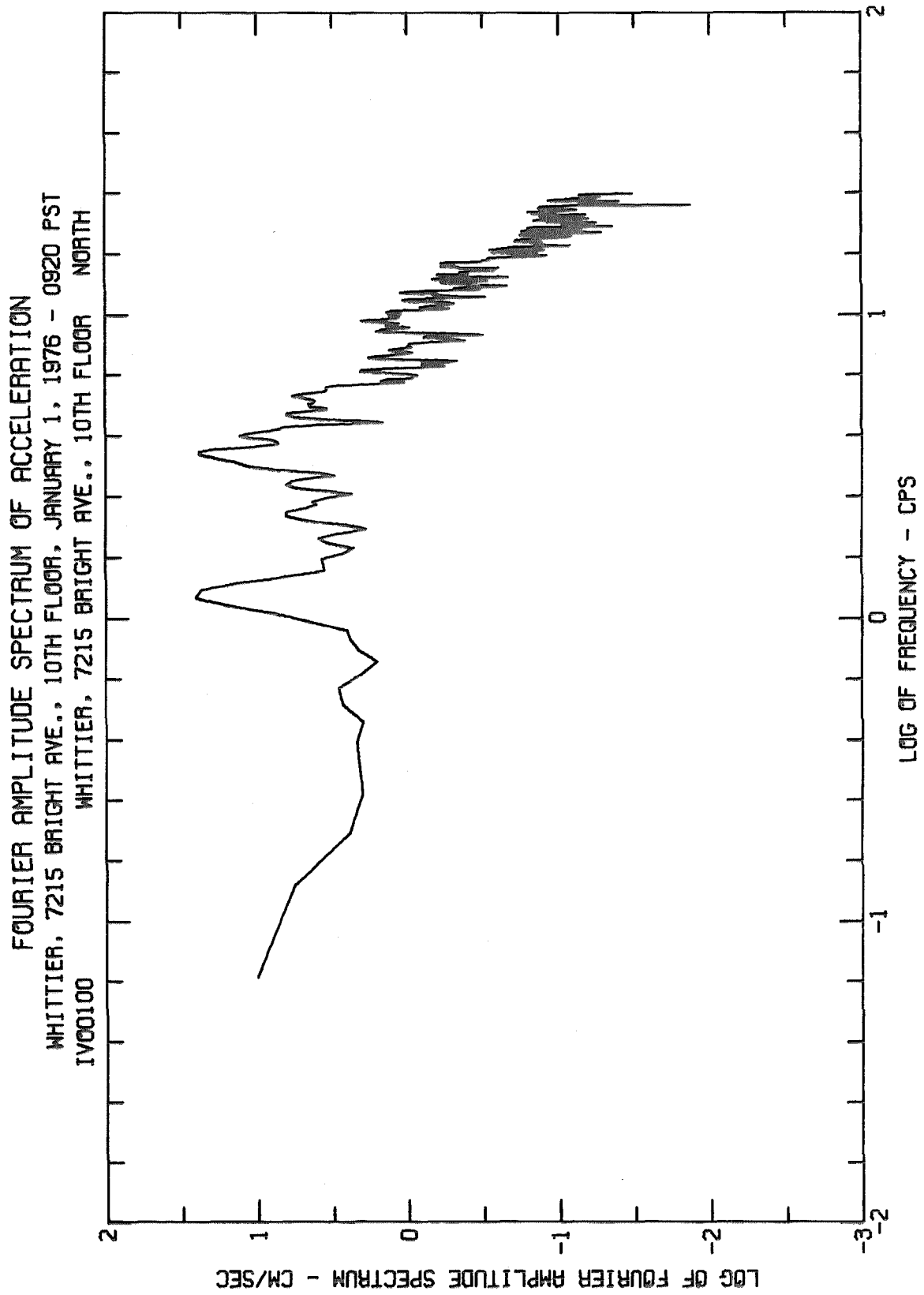


Fig. 26-b

FOURIER AMPLITUDE SPECTRUM OF ACCELERATION
WHITTIER, 7215 BRIGHT AVE., 10TH FLOOR, JANUARY 1, 1976 - 0920 PST
IV00100 WHITTIER, 7215 BRIGHT AVE., 10TH FLOOR DOWN

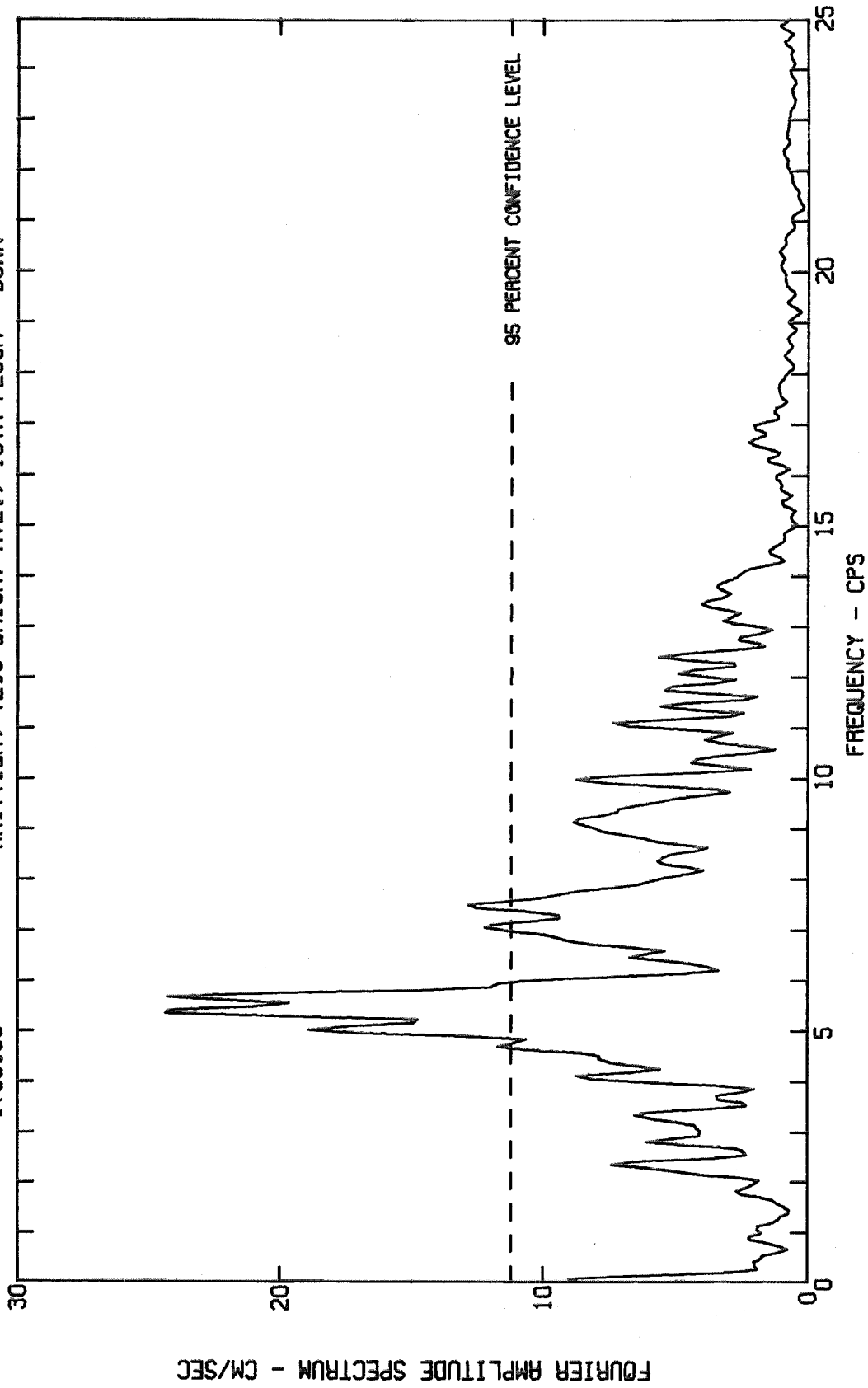


Fig. 27-a

FOURIER AMPLITUDE SPECTRUM OF ACCELERATION
WHITTIER, 7215 BRIGHT AVE., 10TH FLOOR, JANUARY 1, 1976 - 0920 PST
IV00100 WHITTIER, 7215 BRIGHT AVE., 10TH FLOOR DOWN

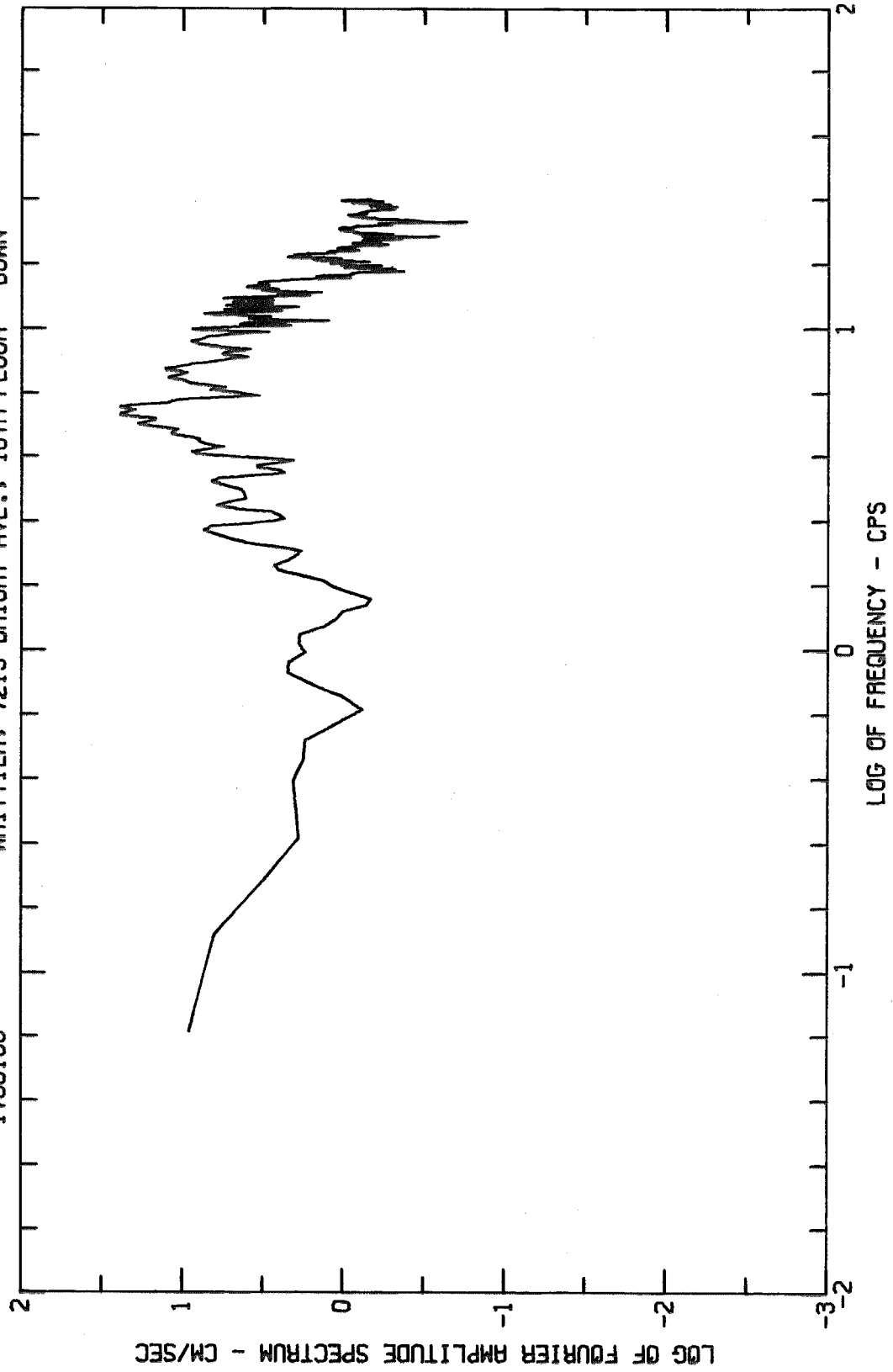


Fig. 27-b

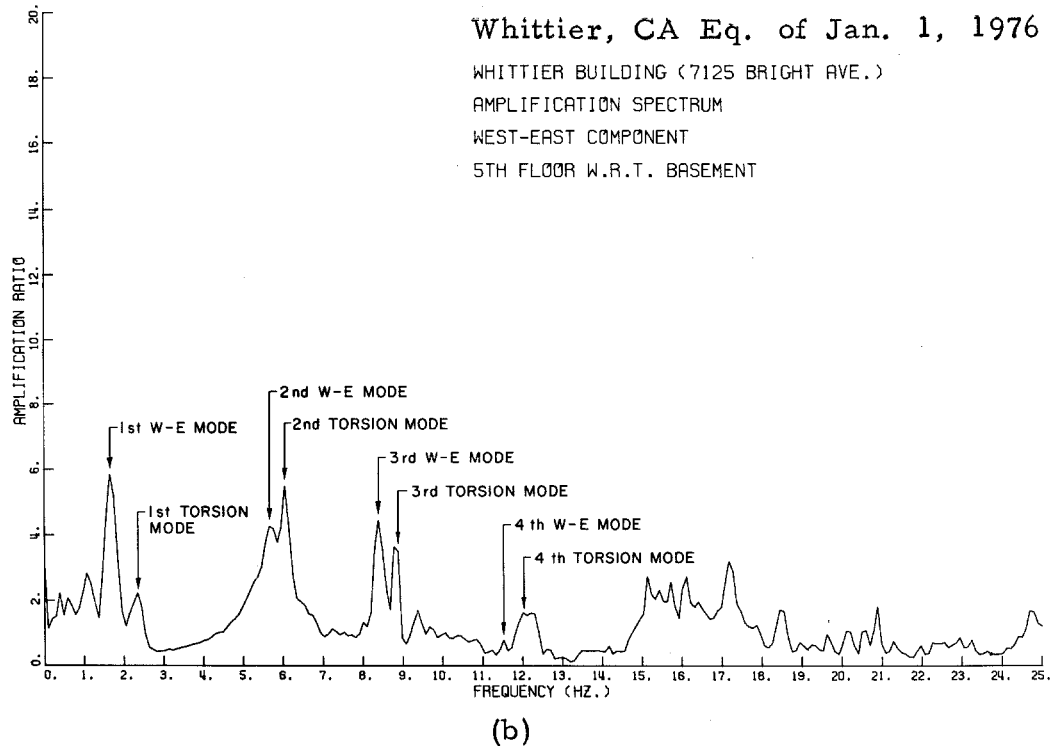
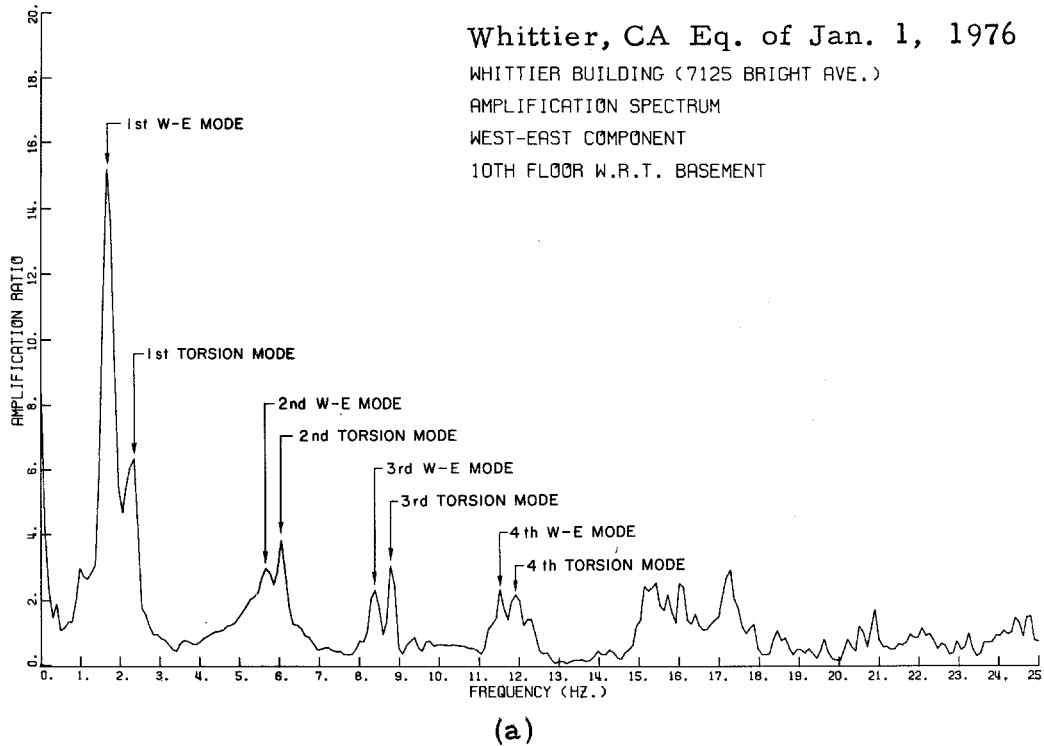


Fig. 28

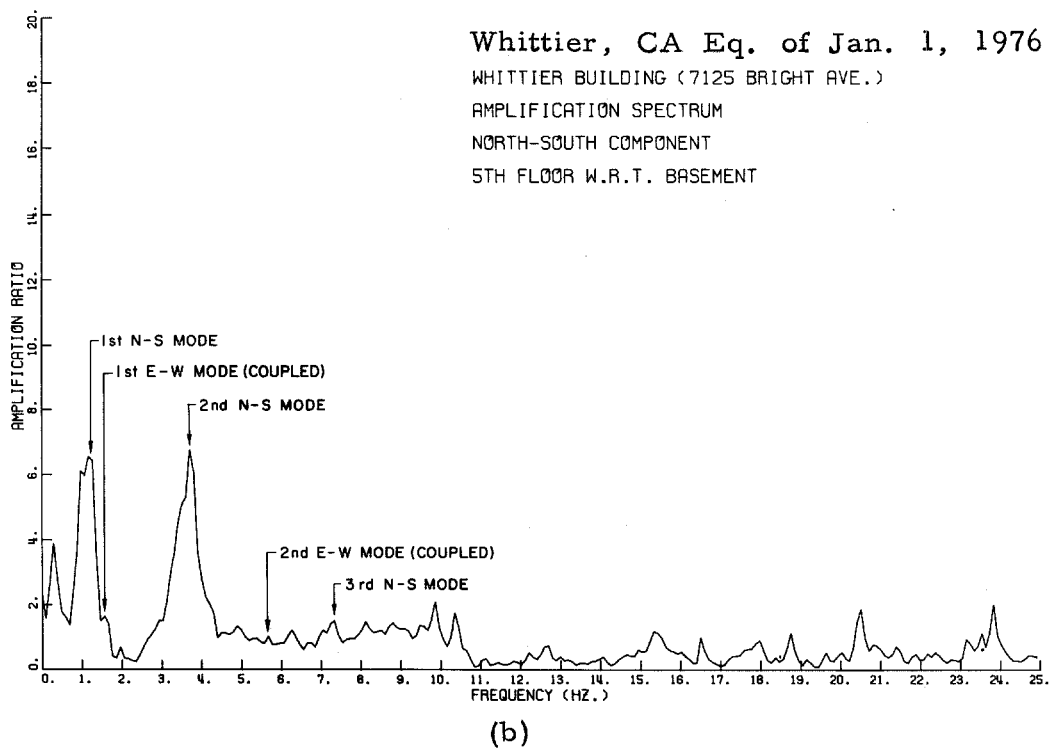
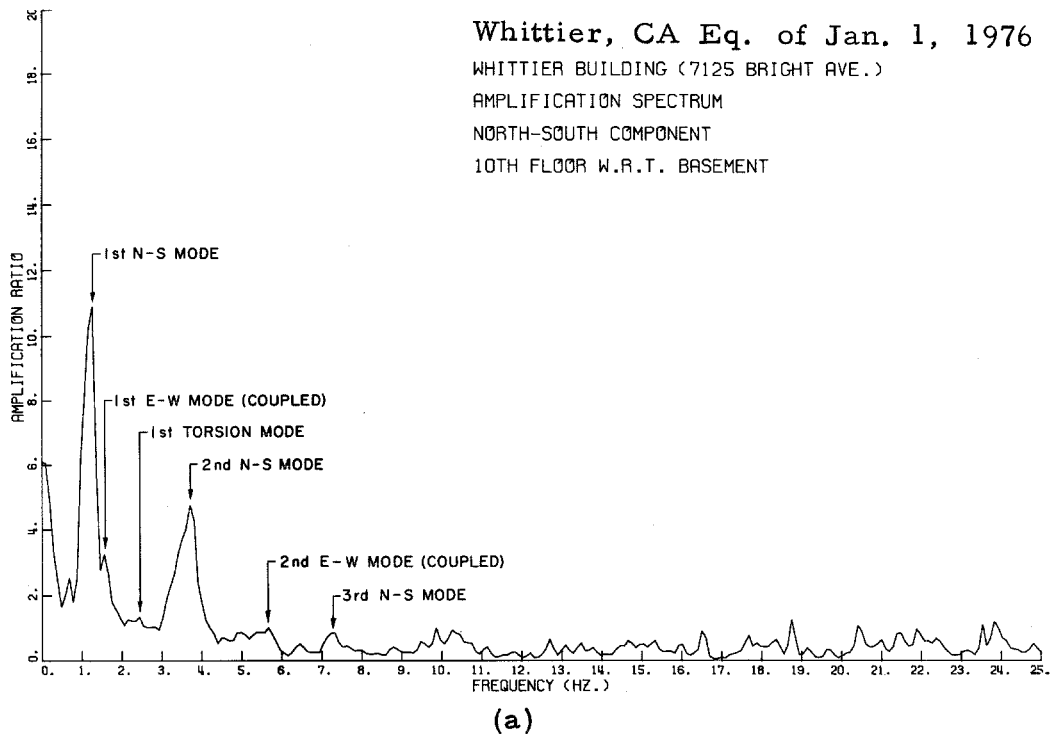


Fig. 29

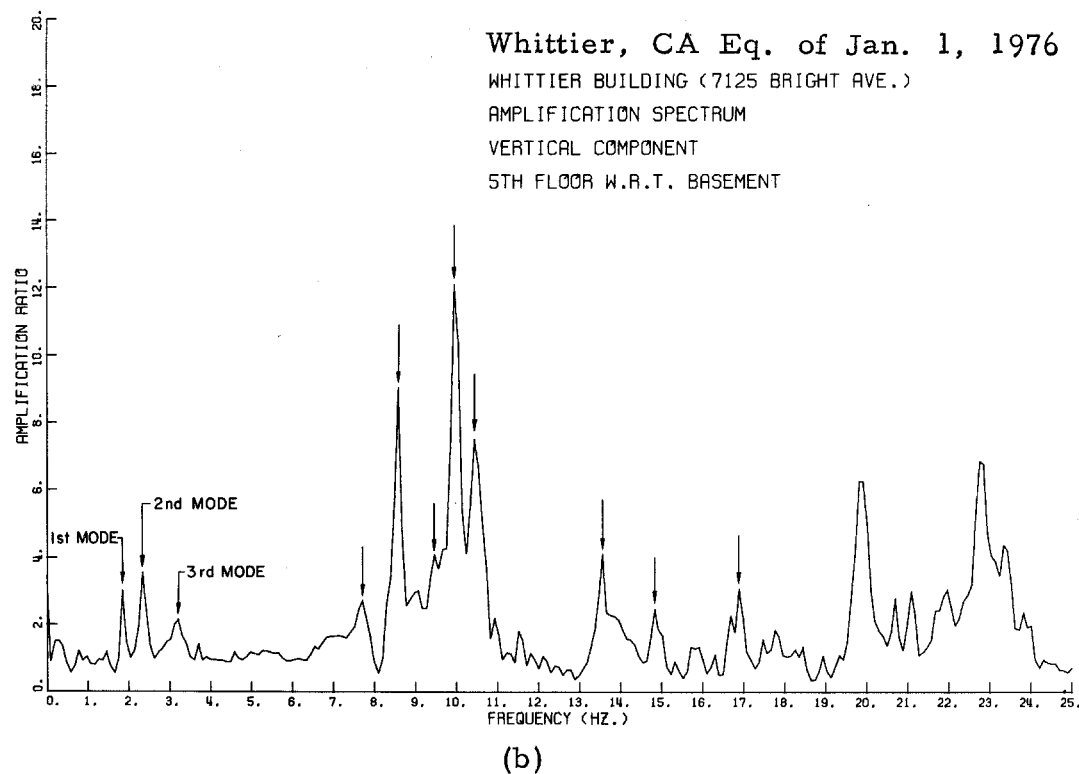
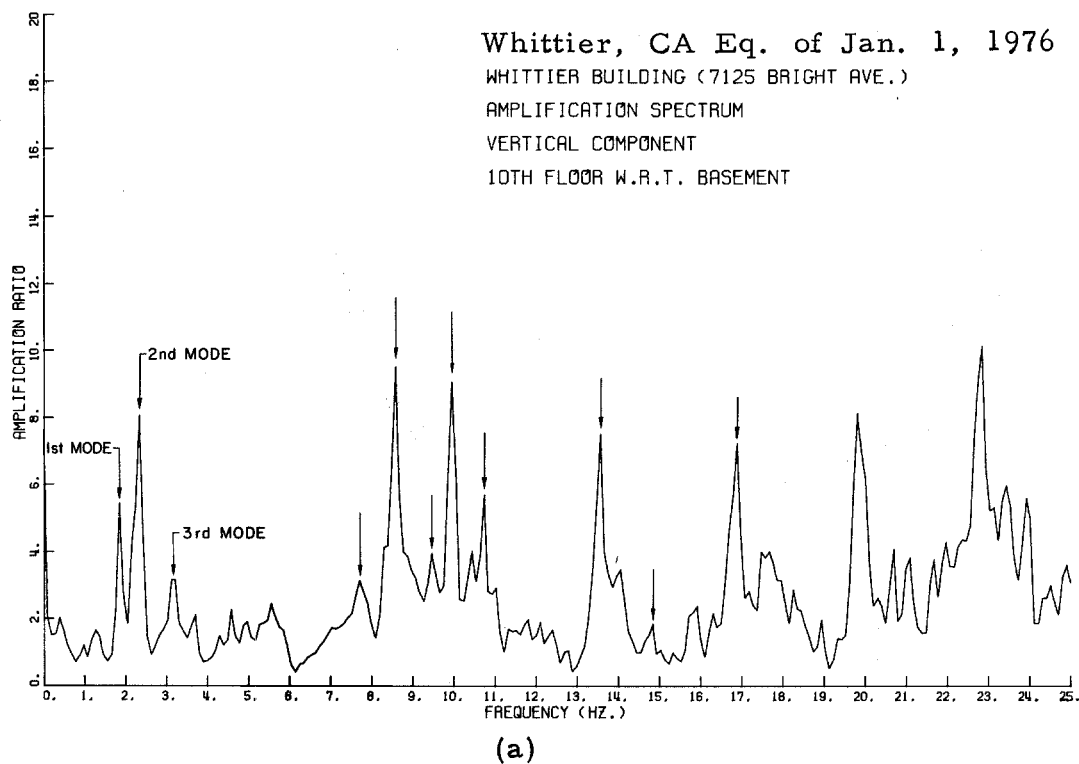
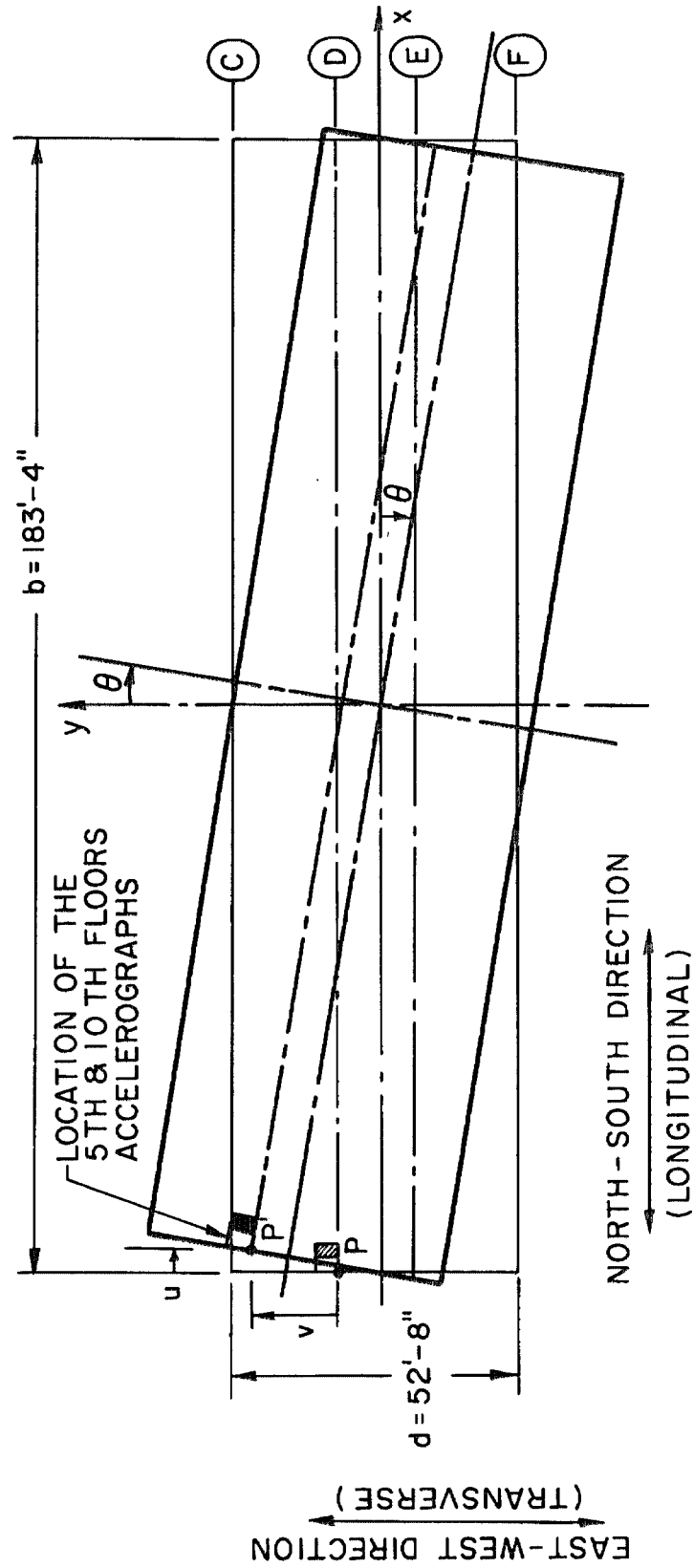


Fig. 30



TORSIONAL VIBRATION OF THE FOURTH THRU TENTH FLOORS

Fig. 31

ESTIMATED MODES OF VIBRATION FROM THE AMPLIFICATION SPECTRUM CURVES Whittier California Earthquake of 1 January, 1976 (Whittier Lutheran Towers)

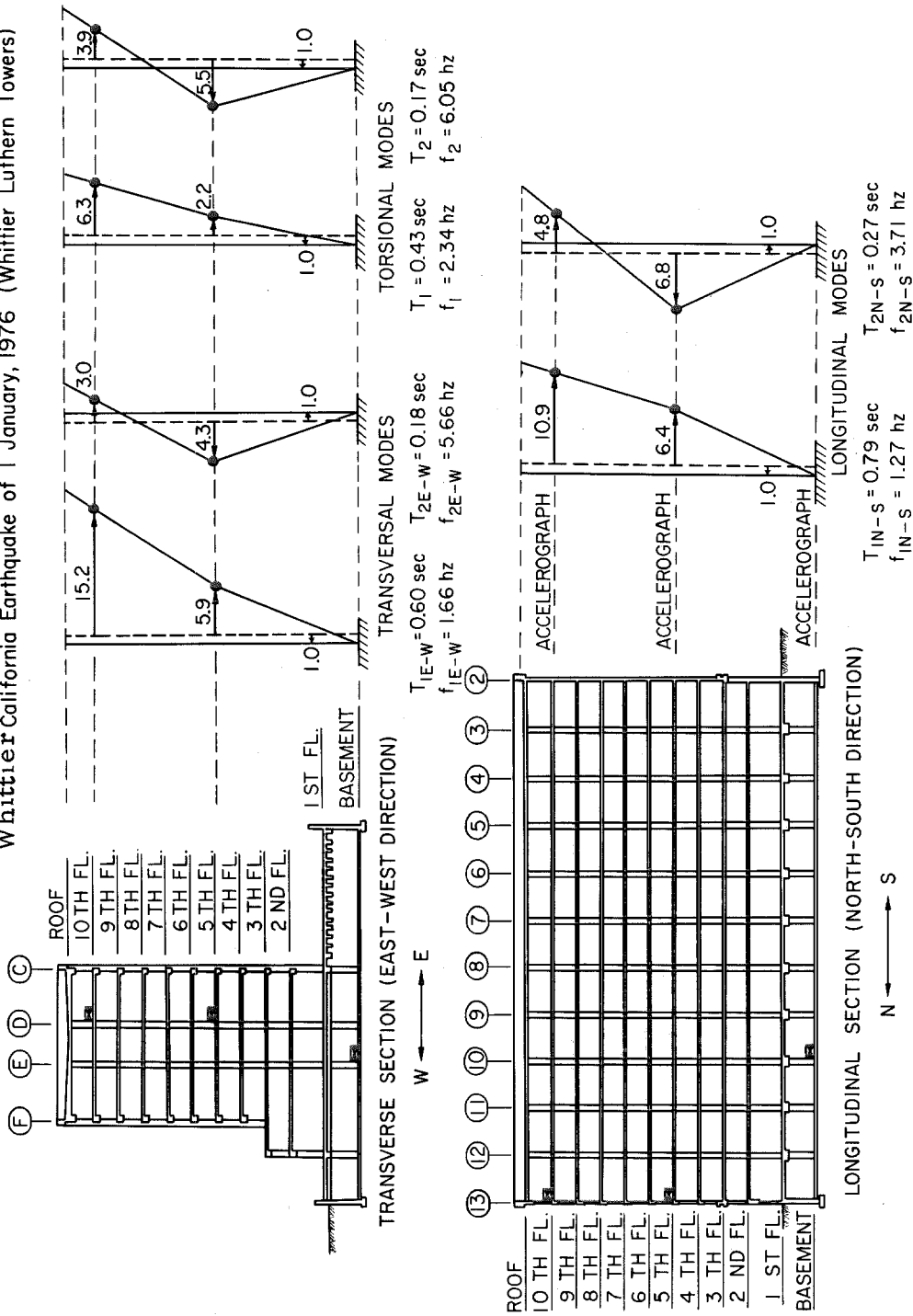


Fig. 32

TABLE 2

Observed Natural Frequencies and Modal Participation Factors
From the Fourier Amplitude Spectra and the Amplification Spectra
Whittier, California Earthquake of Jan. 1, 1976 (Whittier Building)
East-West Component

Fourier Amplitude Spectrum of Acceleration				Amplification Spectrum (Transfer Function)						Modal Identification		
10th Floor		5th Floor		Basement		10th Fl. w. r. t. Basement		5th Fl. w. r. t. Basement				
Frequency Hz	Amplitude cm/sec	Frequency Hz	Amplitude cm/sec	Frequency Hz	Amplitude cm/sec	Frequency Hz	Amplif. Ratio	Particip. Factor	Frequency Hz		Amplif. Ratio	Particip. Factor
-	-	-	-	-	-	0.98	2.98		1.07	2.84		1st E-W Mode 1st Torsion Mode
1.66	40.0	1.66	12.0	-	-	1.66	15.18	1.00	1.66	5.86	1.00	
2.34	80.0	2.34	26.0	-	-	2.34	6.35	1.00	2.34	2.24	1.00	
-	-	-	-	2.50	11.0							2nd E-W Mode 2nd Torsion Mode
2.81	20.0	-	-	2.81	16.0							
3.12	15.0	3.12	8.0	3.12	18.0							
3.82	15.0	3.82	12.0	3.82	20.0							3rd E-W Mode 3rd Torsion Mode
4.45	27.0	4.45	25.0	4.45	25.0							
-	-	-	-	5.30	18.0							
5.66	42.0	5.66	58.0	-	-	5.66	3.01	0.20	5.66	4.28	0.73	2nd E-W Mode 2nd Torsion Mode
6.05	26.0	6.05	36.0	-	-	6.05	3.85	0.61	6.05	5.50	2.46	
-	-	-	-	6.30	10.0							
-	-	-	-	6.80	9.0							3rd E-W Mode 3rd Torsion Mode
-	-	-	-	7.80	5.0							
-	-	-	-	-	-							
8.40	3.0	8.40	5.0	-	-	8.40	2.34	0.15	8.40	4.46	0.76	3rd E-W Mode 3rd Torsion Mode
8.79	4.0	8.79	4.0	-	-	8.79	3.09	0.49	8.79	3.65	1.63	

TABLE 4
Natural Frequencies of Translational and Torsional Vibrations
of a Ten-Story Reinforced Concrete Building
(Determined from the Building Response to Whittier, California
Earthquake of January 1, 1976, with Local Magnitude 4.2)

Translational Modes (Transverse and Longitudinal)							Torsional Modes		
East-West Direction				North-South Direction					
Mode Order	Frequency (Hz)	Frequency Ratio w.r.t. First Mode		Mode Order	Frequency (Hz)	Frequency Ratio w.r.t. First Mode	Mode Order	Frequency (Hz)	Frequency Ratio w.r.t. First Mode
First	1.66	1.00		First	1.27	1.00	First	2.34	1.00
Second	5.66	3.41		Second	3.71	2.92	Second	6.05	2.59
Third	8.40	5.06		Third	7.23	5.69	Third	8.79	3.76
Fourth	11.52	6.94					Fourth	12.01	5.13

CHAPTER III

CARBON CANYON DAM

III-I Description of the Structure

Most of the following descriptive information about Carbon Canyon Dam was obtained from a report by Morrison, Maley, Brady and Porcella (Ref. 1, 1977). Additional information was obtained from pertinent data sheets and engineering drawings of the dam which were provided by the Army Corps of Engineers, Los Angeles.

Carbon Canyon Dam is located across Carbon Canyon Creek in Orange County, California, approximately 7 Km (4.4 miles) east of Brea and 40 Km (25 miles) southeast of Los Angeles. The dam is a random earthfill structure 587 m (1,925 ft) long, with a crest width of 6 m (20 ft) and a maximum height of 31 m (100 ft) above the main streambed. Figure 33 shows a detailed embankment cross-section of the Carbon Canyon Dam. The crest of the dam continues across a saddle fill at the right abutment for an additional length of 210 m (688.5 ft). The dam contains over 1.1 million cubic meters of embankment material and has a reservoir capacity of 8.15×10^6 cubic meters (6,615 acre-feet) at maximum pool elevation.

The dam, constructed by the Army Corps of Engineers as a flood-control structure, was completed in 1961, and is part of the comprehensive plan for the Santa Ana River Basin in Orange County.

From the geological point of view, Carbon Canyon Dam is situated near the Southern boundary of the Puente Hills, a region of soft sedimentary Cenozoic rocks. The dominant geologic feature in

this region is the northwest trending Whittier fault zone that passes within 1.5 Km (0.95 miles) north of Carbon Canyon Dam. The dam rests on approximately 30 m (100 ft) of recent silt, sand and gravel. The valley floor is nearly flat, except for the steep-walled gully that contains the present stream channel. The abutments consist of Upper Pleistocene terrace deposits and the Pico and Repetto formations, chiefly siltstones and sandstones, that locally dip 30-40° to the southwest.

In 1968 a Teledyne RFT-250 accelerograph was installed on the crest of the dam in the standby generator house close to the spillway location (Fig. 34). This old accelerograph was not moved or replaced since installation until recently when three improved SMA-1 accelerographs equipped with WWVB radio time receivers were installed on and around the dam (June, 1975). The San Fernando earthquake of February 9, 1971 was recorded by the crest Teledyne RFT-250. Uncorrected and corrected accelerograms and the calculated velocity and displacement curves as well as the response spectra and Fourier spectra of the record can be found in Ref. 3.

Figure 34 shows the new accelerograph array at Carbon Canyon Dam. There are two accelerographs mounted on the right and left abutments of the dam to give some indication of the uniformity of conditions, and to provide a back-up in the event of instrument malfunction (Bolt and Hudson, 1975). In addition, there is one accelerograph on the central region of the dam crest to measure dam response. The three accelerographs have components oriented parallel to the longitudinal axis of the dam (N50°W).

III-2 Time Domain Analysis

The dam was about 7.4 Km south of the epicenter as shown in Fig. 1. The two abutment accelerographs were about 587 m (1,925 ft) apart and both seismograms from these stations show peak accelerations of 0.14 g (Table 1). The crest station recorded a slightly lower (0.12 g) peak acceleration. Figures 35-a, b and c show the uncorrected digitized accelerographs while Figs. 36 through 38 show the corrected accelerographs and the integrated velocity and displacement curves. The accelerographs were connected for simultaneous starting.

It can be seen from Figs. 35-a, b, Figs. 36-a, b and 37-a, b that the strong ground shaking began two seconds after the instruments triggered and lasted only about one second. This strong shaking was followed by comparatively small amplitude motion. However, the two horizontal components of the crest record (Figs. 38-a and b) show that the strong response of the dam lasted longer than one second.

Visual examination of the upstream/downstream crest record (Fig. 38-a) indicates that a relatively large number of vibrational modes contributed to the response of the dam in this direction. However, a period of about 0.6 secs (from 6 to 7 secs and from 8 to 11 secs on the velocity curve) seems to be the fundamental period of vibration. It did not dominate the response, but in the computed velocity curve of Fig. 38-a from about 6 to 8 secs and from about 3 to 7 secs, it is seen with higher modes superimposed on it. The horizontal component aligned with the longitudinal axis of the dam (N50°W), as seen in Fig. 38-b, also shows a significant contribution to the response from a large number of modes with apparent fundamental period of about 0.75 secs (see the integrated velocity curve of Fig. 38-b).

Finally, the accelerograms recorded on Carbon Canyon Dam during the San Fernando earthquake of 1971 (Ref. 3, Vol. II) indicate an apparent fundamental period in the upstream/downstream direction of about 0.6 secs and an apparent period in the longitudinal direction of the dam of about 0.75 secs. These accelerograms also show significant contributions from higher modes.

III-3 Frequency Domain Analysis

The response spectra calculated from the corrected data are shown in Figs. 39 through 47. For each component there are two figures (a and b); the first plot (Fig. 39-a, etc.) is that of the true relative velocity response spectrum while the second plot (Fig. 39-b, etc.) is that of the pseudo velocity response spectrum together with the relative displacement spectrum, and the pseudo acceleration spectrum in a tripartite logarithmic plot versus period. The Fourier spectra are shown in Figs. 48 through 56 on the logarithmic plot (Fig. 48-b, etc.) as well as on the linear spectrum plot (Fig. 48-a, etc.) on which the data lying above the 95 percent confidence level may be considered relevant to that degree.

Amplification spectra were computed to indicate the natural frequencies of the dam by separating the characteristics of the structure from those of the earthquake ground motion at both abutments. This enabled an estimate of the relative contribution of different modes and illustrated the correlation of the earthquake input motions at the two different abutments of the dam which are separated by canyon topography. The potential differences in the motion recorded at the

two abutments can be shown by the amplification spectrum curves of Figs. 57 and 58-a and b. In the upstream/downstream direction, the motion at the right abutment appears stronger than that at the left abutment as indicated by amplification spectra of Figs. 57-a and b, and, also, by examination of response spectra of Figs. 39-b and 42-b. The amplification pattern of the right abutment with respect to the left abutment shows significant effects are confined to frequency bands from 0 to 9 Hz and from 17 to 22 Hz (Fig. 57-a); several major peaks were found in these bands. The maximum amplification ratio is 9.5 at a frequency of 6.8 Hz. The left abutment amplification spectrum (Fig. 57-b) shows relatively slight magnification of the motion in the frequency band 9 to 16 Hz. The maximum amplification ratio is 5 at about 9.5 Hz. The large amplifications and reductions are consequences, as indicated by Wong and Jennings (1975), of such things as the effects of topography, the effect of dam-foundation interaction and the angle of incidence of the seismic waves.

Generally, the amplification of the right abutment with respect to the left abutment in the longitudinal direction (N50°W) is smaller than the amplification in the upstream/downstream direction (S40°W) as shown by Fig. 58-a. Several relatively smaller peaks are shown (in Fig. 58-a) in the low frequency range as well as the high frequency range; the latter shows two strong peaks at frequencies 17.5 Hz and 19.0 Hz. The amplification spectrum of the vertical component (Fig. 58-b) shows a very high peak at a frequency of 4.5 Hz.

By tabulating all the possible peaks and the associated frequencies of both the Fourier amplitude spectra and the amplification spectra

for the crest and the two abutments, it is possible to detect some of the natural frequencies of the dam. Tables 5 and 6 show those spectral peaks in the frequency range 0 to 4 Hz; they also show the peaks of the Fourier amplitude spectrum of the crest (only) record recovered from the San Fernando earthquake of 1971. Examination of these tables indicates that the fundamental frequency in the upstream/downstream direction is 1.56 Hz (0.64 secs period), while in the longitudinal direction the fundamental frequency is 1.37 Hz (0.73 secs period). The values of these fundamental frequencies agree with those obtained from the analysis of accelerograms. Tables 5 and 6 indicate, also, that the two earthquakes (Whittier earthquake, 1976 and San Fernando earthquake, 1971) shook the dam at essentially the same resonant frequencies.

To estimate the shear wave velocity within the dam material from the observed resonant frequencies and to check the values of the resonant frequencies corresponding to peak values of the amplification spectra, a two-dimensional shear beam theory is used. The natural frequencies determined by this theory are given by

$$\omega_{n,r} = \frac{v_s}{h} \left[\beta_n^2 + \left(\frac{r\pi h}{l} \right)^2 \right]^{\frac{1}{2}}, \quad n, r = 1, 2, 3, \dots \quad (1)$$

where v_s is the shear wave velocity within the dam, h is the height of the dam, l is the length of the dam and β_n , $n = 1, 2, 3, \dots$ are the roots of the Bessel function of zero order of the first kind, $J_0(\beta_n)$, [e.g., $\beta_1 = 2.4048$, $\beta_2 = 5.5201$, $\beta_3 = 8.653$, etc.].

For this 2-D theory of a triangular wedge in a rectangular canyon, the trapezoidal canyon of Carbon Canyon Dam (Fig. 34) is represented by an equivalent rectangle of length l equal to the average of the crest length (1,925 ft) and the length of the base of the trapezoidal section (1,000 ft), i.e., $l = 1462.5$ ft. Substituting values of $h = 0.5$ (81.5 + 103.5) = 92.5 ft and of $\omega_{1,1} = 2\pi$ (1.56) rad/sec (natural frequency in the upstream/downstream direction) and $l = 1462.5$ ft, in Eq. 1, gives a value for v_s equal to 375.7 ft/sec. Shear wave velocities for homogeneous compacted fill dams can vary over a wide range of values depending on the nature of the material. Martin (1965) indicates that for hydraulic fill dams and for dams constructed of compacted silty clay, values of v_s between 200-400 ft/sec seem appropriate; for compacted sandy clays values of v_s between 400-800 ft/sec would be of the right order, while for well graded alluvial material with some binder, and compacted gravelly clays, values between 800-1200 ft/sec seem appropriate. Thus the estimated value of $v_s = 375.7$ ft/sec of Carbon Canyon Dam seems reasonable for a random fill earth dam.

The values of higher frequencies ($> f_{1,1}$) were computed by substituting the value of $v_s = 375.7$ ft/sec in Eq. (1); these computed natural frequencies are listed in Table 7 where they have also been compared with those observed from the amplification spectra. It is important to note that the frequency resolution used for obtaining these amplification spectrum curves was 0.0977 Hz since the average duration of the records is about 12 seconds. Table 7 shows that the difference between any two adjacent computed frequencies increases

monotonically with the frequency order. The fact that several observed resonant frequencies were compared only with the symmetric computed frequencies can be explained by the fact that the location of the crest accelerograph was at the central part of the crest. The non-appearance of the second and third symmetric (observed) natural frequencies can be explained by the small frequency resolution (0.0977 Hz) in the Fourier transform computer subroutines, and by the small difference between any two adjacent frequencies.

In general, values of the observed resonant frequencies vary slightly from those predicted by the 2-D shear beam theory as seen from Table 7.

REFERENCES

1. Morrison, P., Maley, R., Brady, G. and Porcella, R., "Earthquake Recordings on and Near Dams", USCOLD, Report by the Committee on Earthquakes, Panel on Instrumental Recordings at Dams, 1977.
2. Corps of Engineers, Los Angeles, California, 1957, General Design for Carbon Canyon Dam and Channel: pp 1-2, two figures, one table.
3. Earthquake Engineering Research Laboratory, California Institute of Technology, Strong Motion Earthquake Accelerograms:
 - Vol. I, Uncorrected Accelerograms, Part N
 - Vol. II, Corrected Acceleration, Velocity and Displacement, Part N
 - Vol. III, Response Spectra, Part N
 - Vol. IV, Fourier Spectra, Part N
4. Bolt, B.A. and Hudson, D.E., "Seismic Instrumentation of Dams", Journal of the Geotechnical Engineering Division, ASCE, GT11, November 1975.
5. Wong, H.L. and Jennings, P.C., "Effects of Canyon Topography on Strong Ground Motion", Bulletin of the Seismological Society of America, Vol. 65, No. 5, pp 1239-1257, October 1975.
6. Martin, G.R., "The Response of Earth Dams to Earthquakes", Ph.D. Thesis, 1965, Civil Engineering Department, University of California, Berkeley.

CARBON CANYON DAM, CALIFORNIA
EMBANKMENT CROSS SECTION

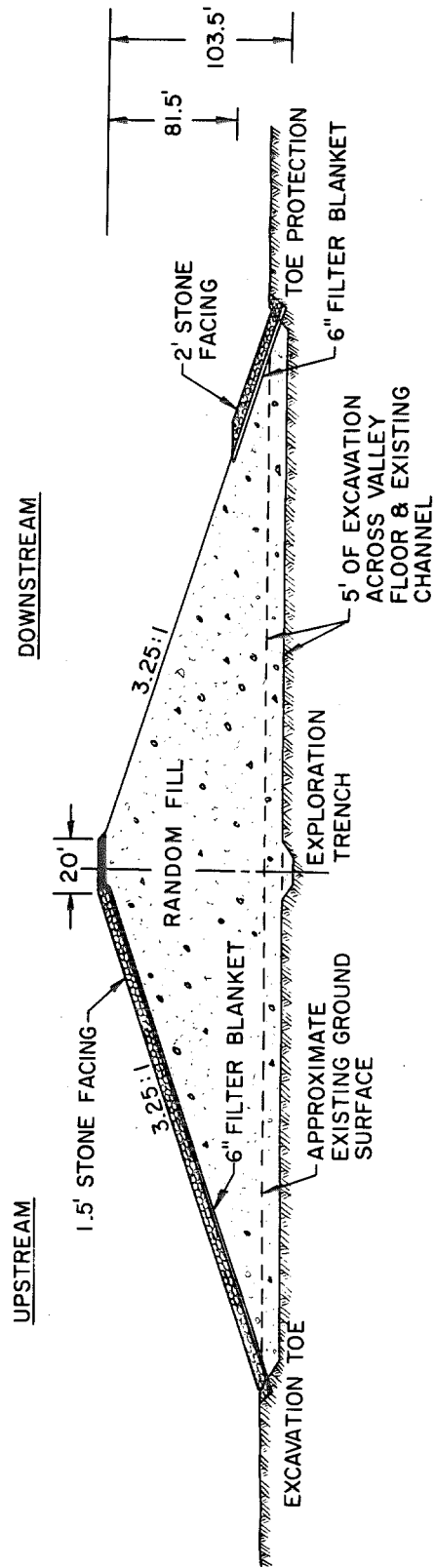


Fig. 33

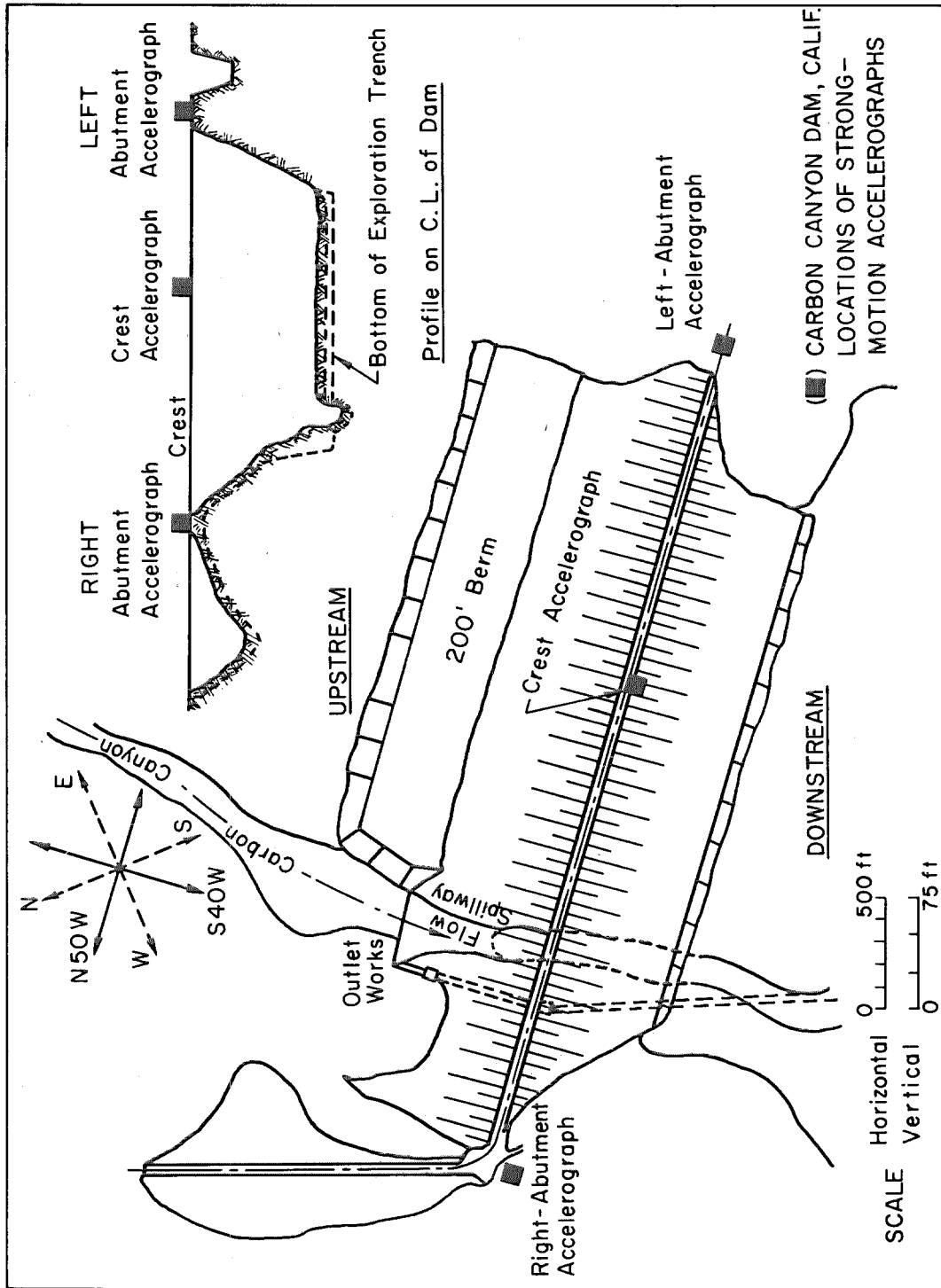


Fig. 34

CARBON CANYON DAM, RIGHT ABUTMENT E/Q OF JAN 1 1976

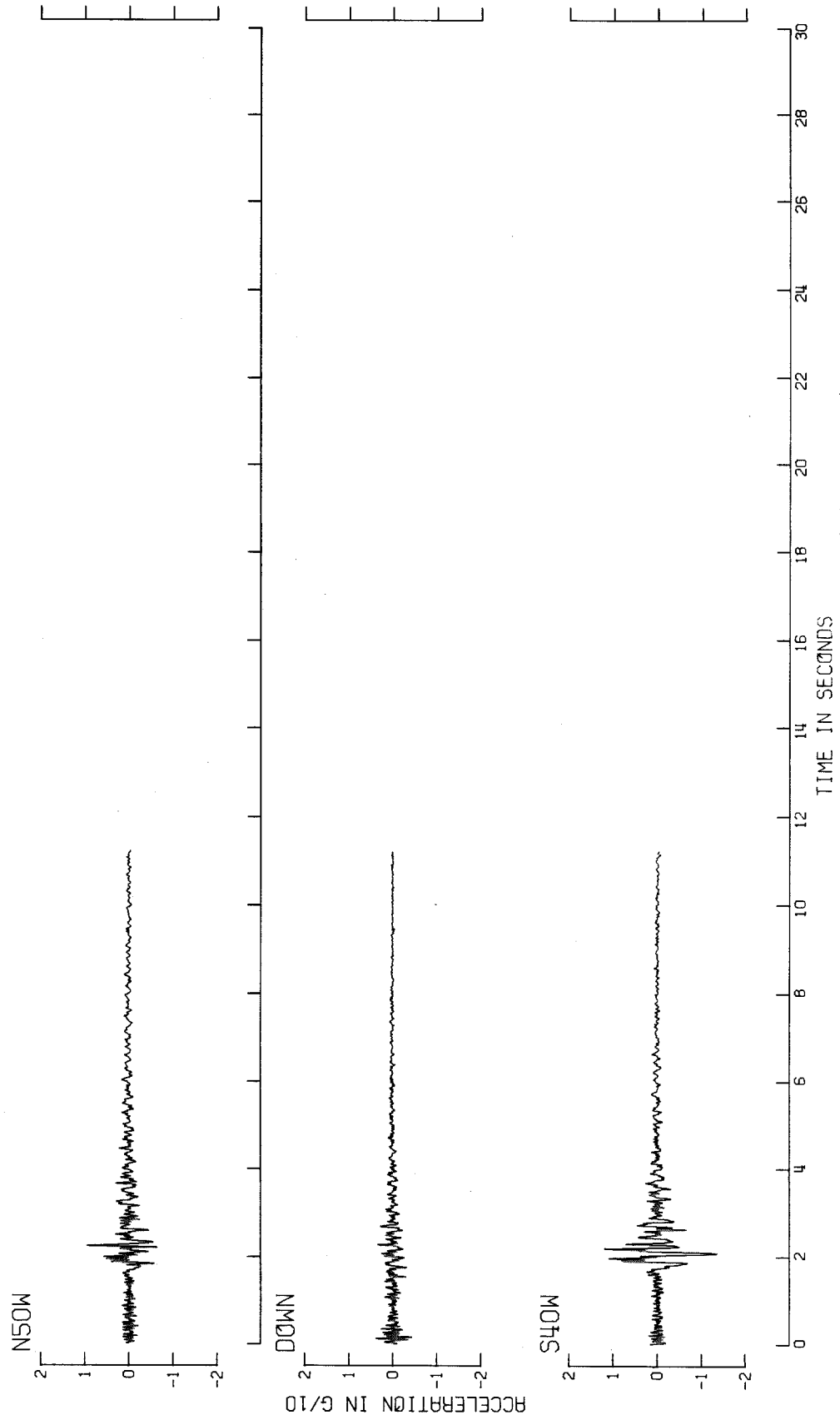


Fig. 35-a Uncorrected Accelerograms (Right Abutment)

CARBON CANYON DAM, LEFT ABUTMENT, JAN 1 1976 0920 PST

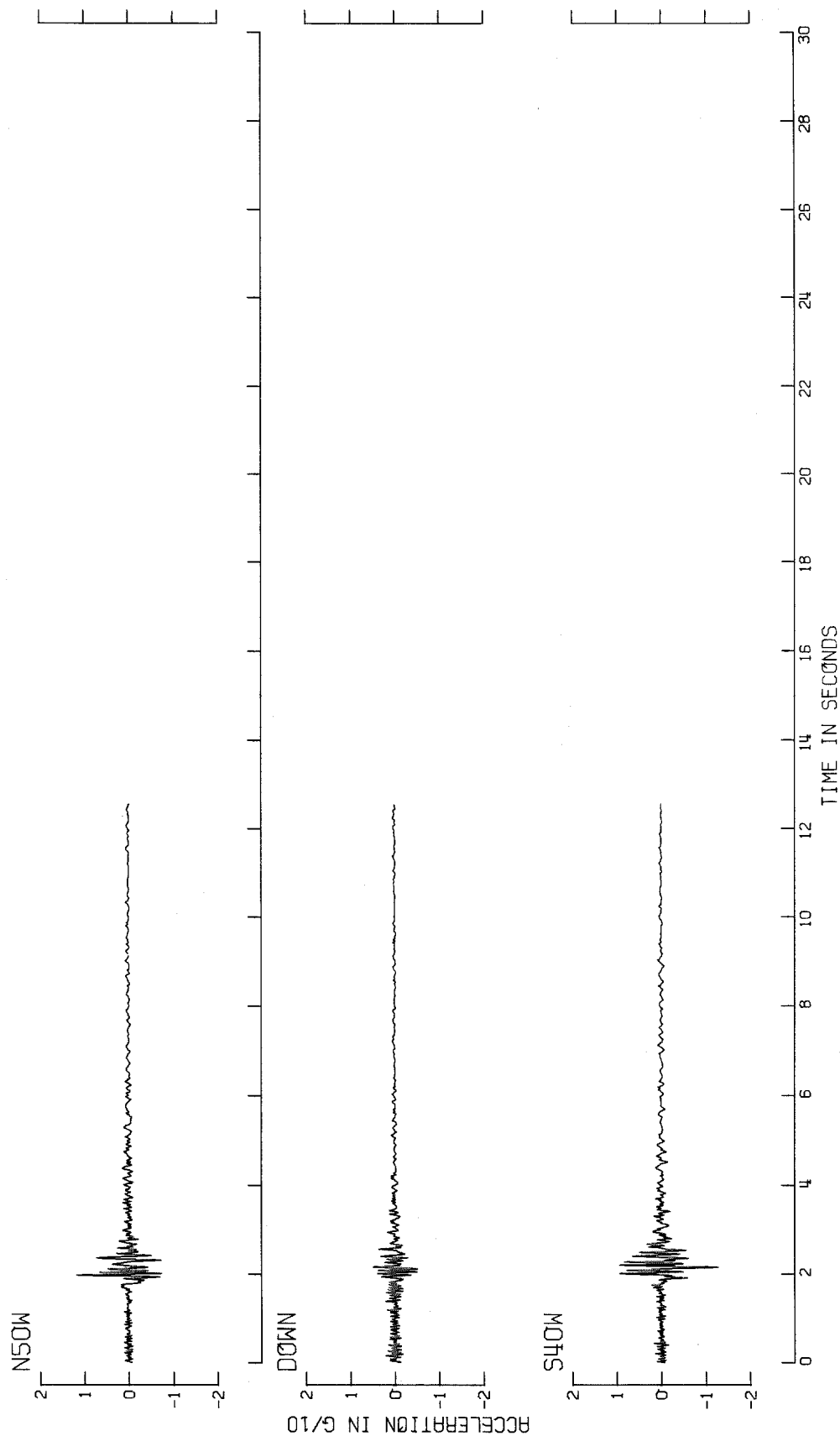


Fig. 35-b Uncorrected Accelerograms (Left Abutment)

CARBON CANYON DAM, CREST, E/Q OF JAN 1 1976 0920 PST

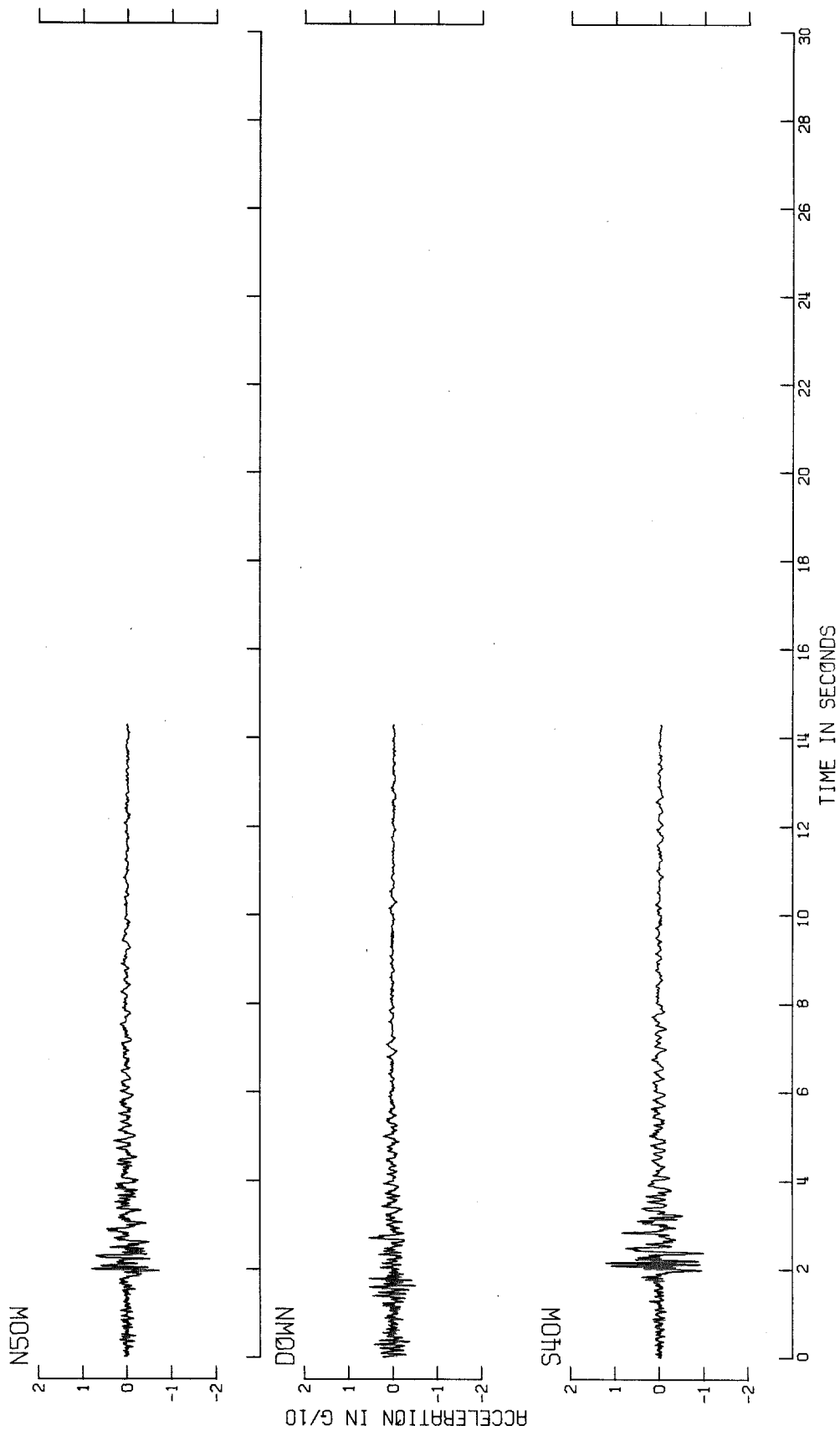


Fig. 35-c Uncorrected Accelerograms (Crest)

CARBON CANYON DAM, RIGHT ABUTMENT, JAN 1 1976-0920 PST
 IN03400 CARBON CANYON DAM, RIGHT ABUTMENT COMPSHOW

PEAK VALUES : ACCEL = 124.3 CM/SEC/SEC VELOCITY = 3.9 CM/SEC DISPL = 1.7 CM

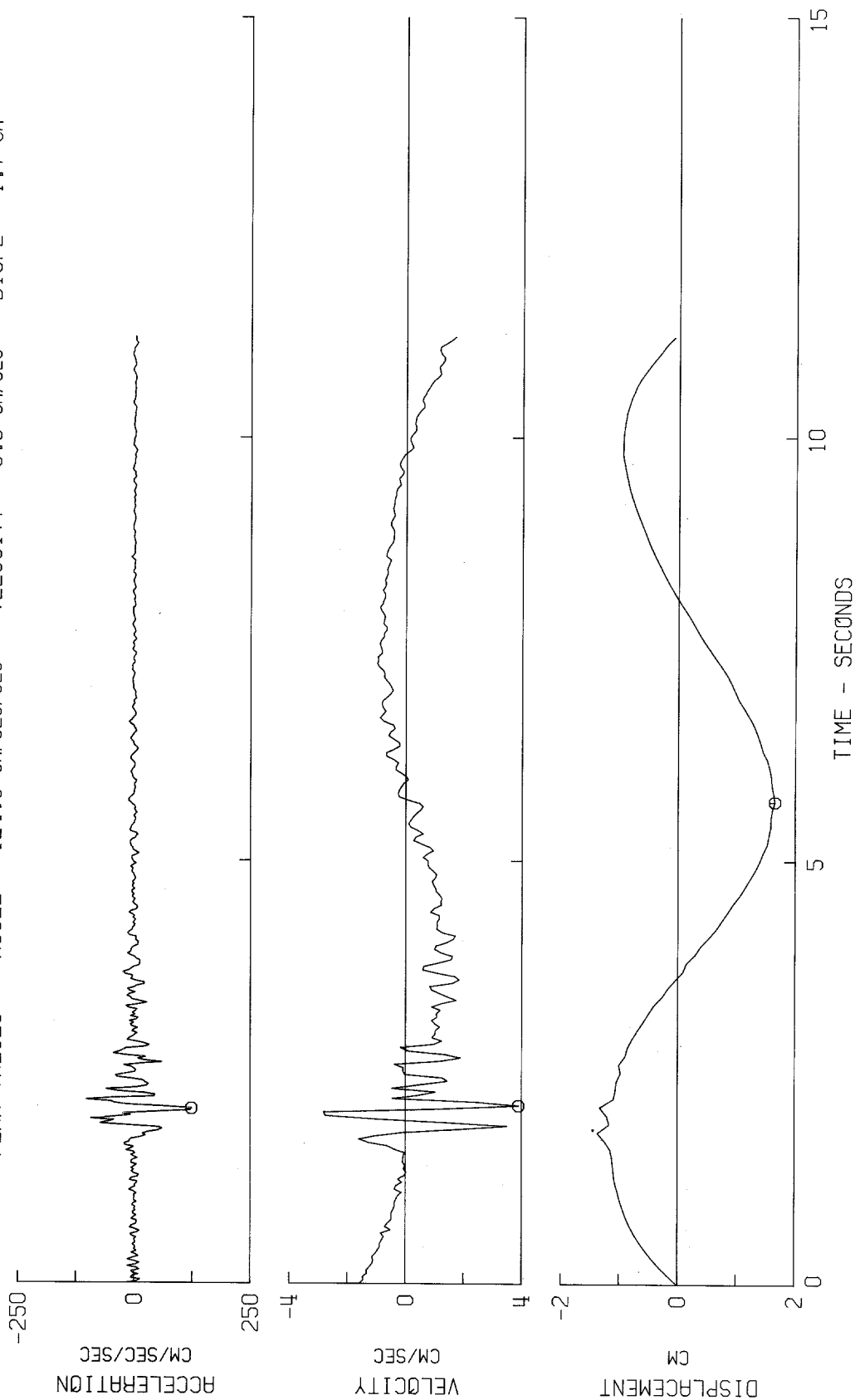


Fig. 36-a

CARBON CANYON DAM, RIGHT ABUTMENT, JAN 1 1976-0920 PST
 IN03400 CARBON CANYON DAM, RIGHT ABUTMENT COMP50W
 ○ PEAK VALUES : ACCEL = -70.8 CM/SEC/SEC VELOCITY = 2.7 CM/SEC DISPL = 1.7 CM

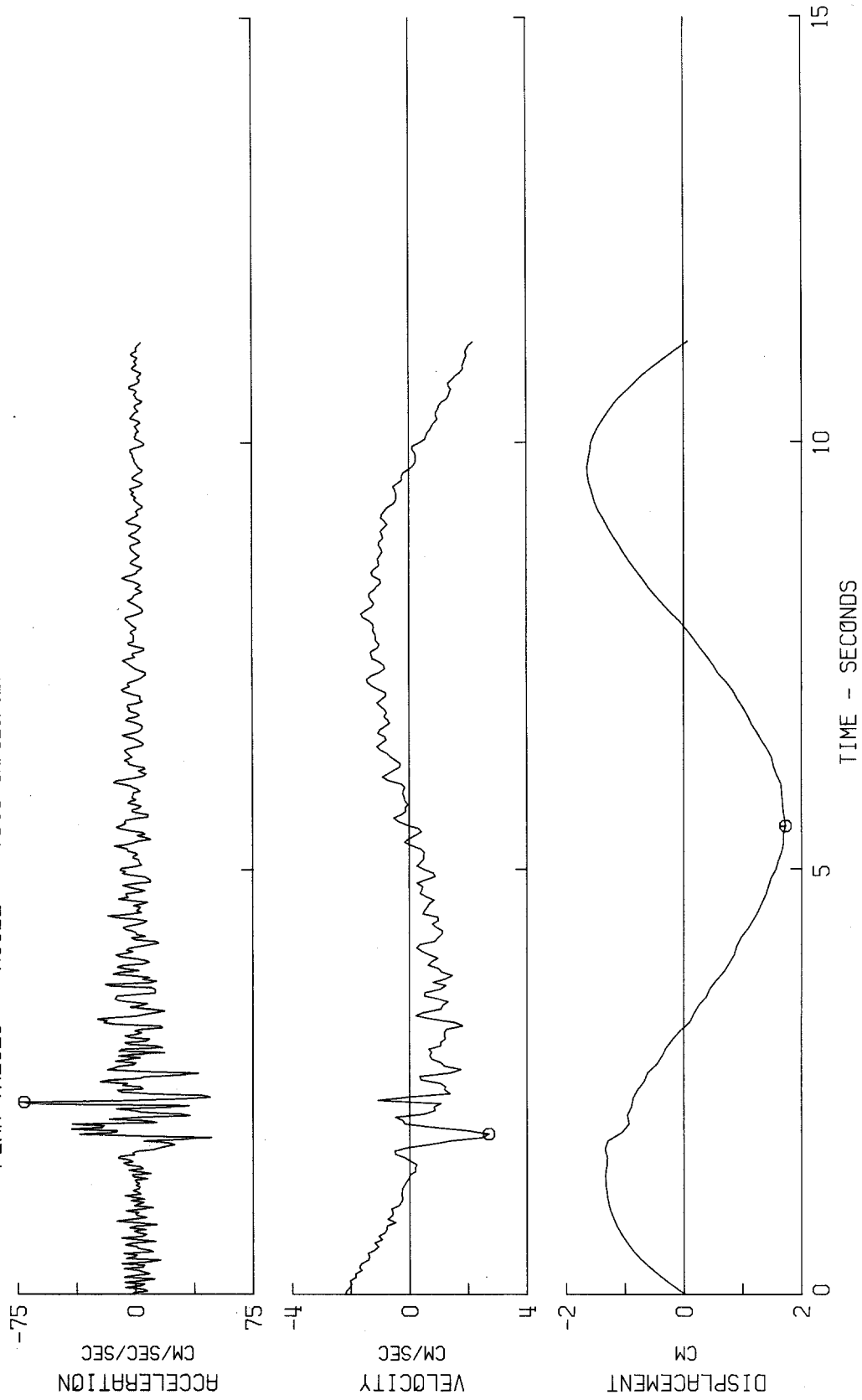
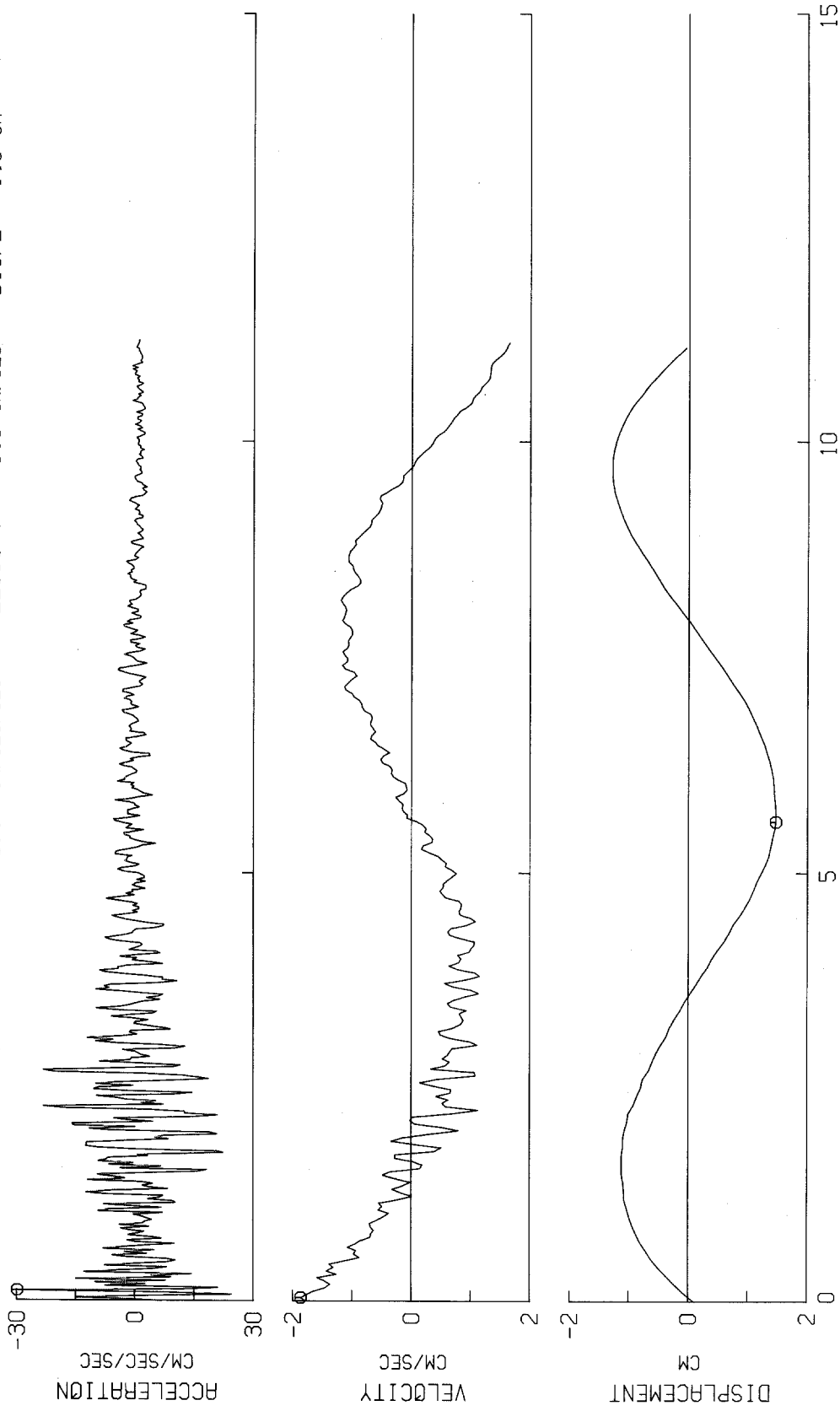


Fig. 36-b

CARBON CANYON DAM, RIGHT ABUTMENT, JAN 1 1976-0920 PST
IN03400 CARBON CANYON DAM, RIGHT ABUTMENT COMPDOWN

Ø PEAK VALUES : ACCEL = -29.7 CM/SEC/SEC VELOCITY = -1.9 CM/SEC DISPL = 1.5 CM



TIME - SECONDS

Fig. 36-c

CARBON CANYON DAM, LEFT ABUTMENT, JAN 1 1976-0920 PST
IN03200
CARBON CANYON DAM, LEFT ABUTMENT COMPS40W
PEAK VALUES : ACCEL = 115.9 CM/SEC/SEC VELOCITY = 2.0 CM/SEC DISPL = 0.8 CM

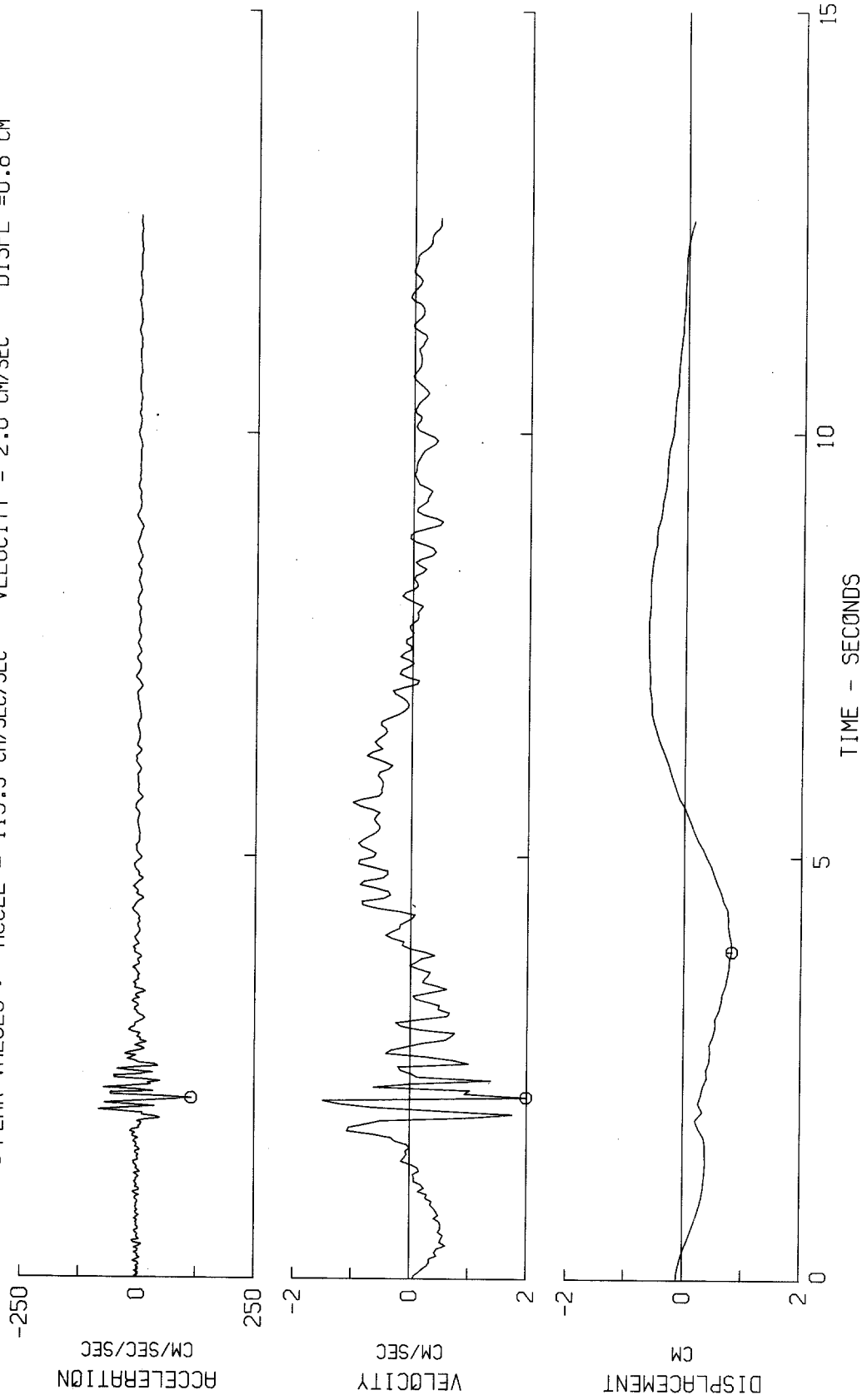


Fig. 37-a

CARBON CANYON DAM, LEFT ABUTMENT, JAN 1 1976-0920 PST
 IN03200
 CARBON CANYON DAM, LEFT ABUTMENT COMP50W
 @ PEAK VALUES : ACCEL = -91.0 CM/SEC/SEC VELOCITY = 1.5 CM/SEC DISPL = 0.7 CM

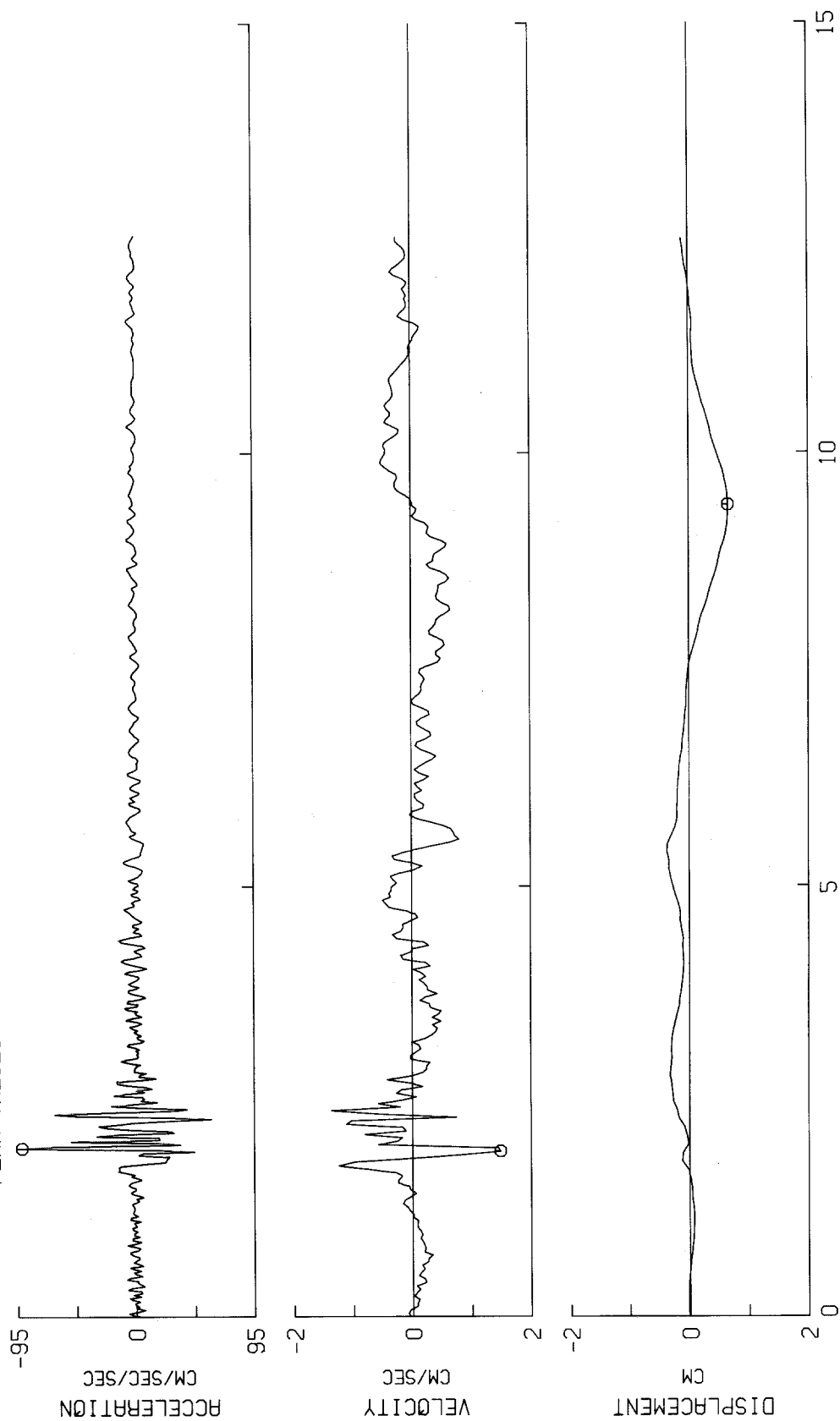


Fig. 37-b

CARBON CANYON DAM, LEFT ABUTMENT, JAN 1 1976-0920 PST
IN03200
CARBON CANYON DAM, LEFT ABUTMENT COMPDOWN
○ PEAK VALUES : ACCEL = 40.4 CM/SEC/SEC VELOCITY = 0.9 CM/SEC DISPL = 0.6 CM

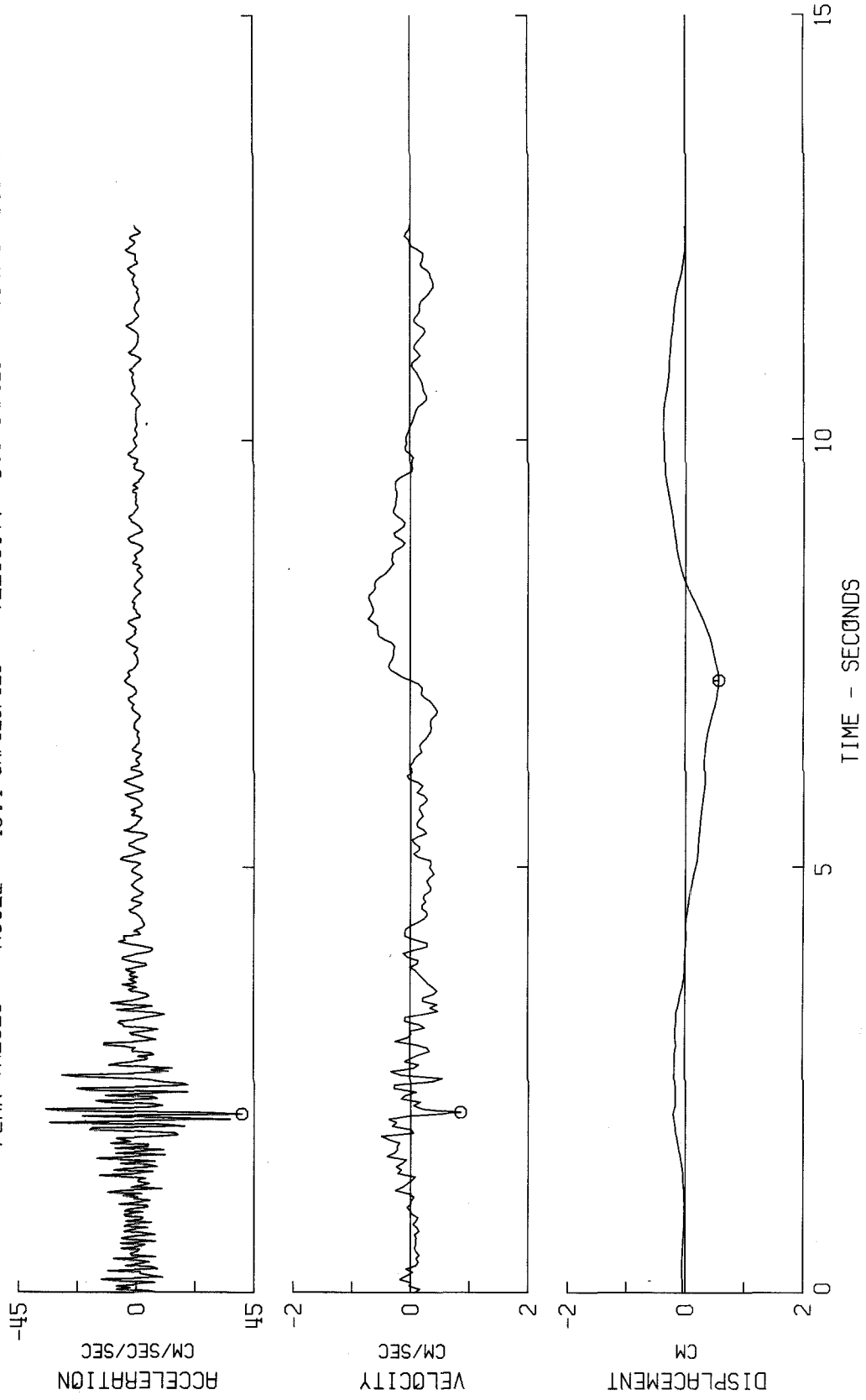


Fig. 37-c

CARBON CANYON DAM, CREST, JAN 1 1976-0920 PST
 IN03300 CARBON CANYON DAM, CREST COMPS40W
 PEAK VALUES : ACCEL = -97.5 CM/SEC/SEC VELOCITY = 3.5 CM/SEC DISPL = -2.8 CM

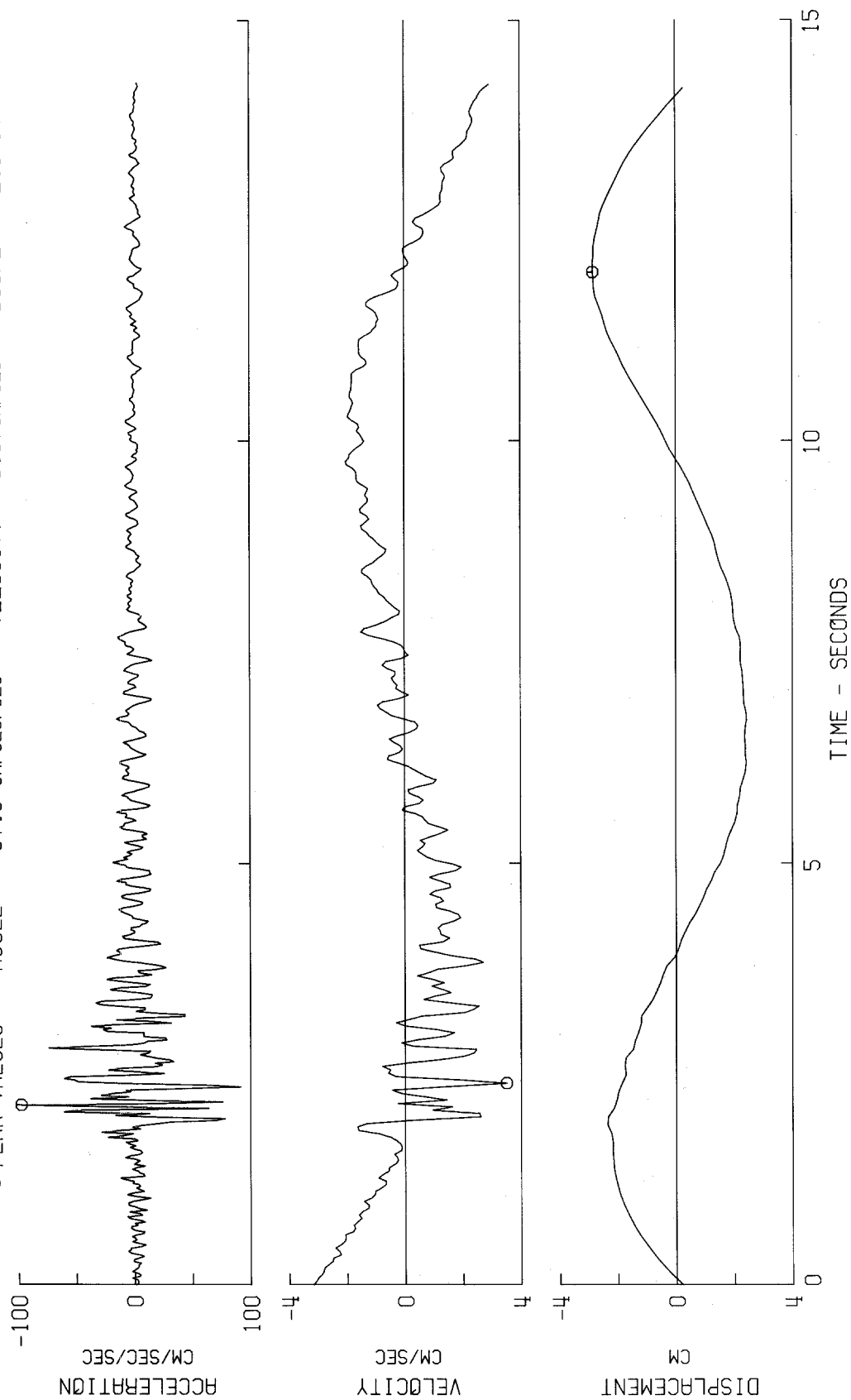


Fig. 38-a

CARBON CANYON DAM, CREST, JAN 1 1976-0920 PST
 IN03300 CARBON CANYON DAM, CREST COMP50W
 o PEAK VALUES : ACCEL = -62.9 CM/SEC/SEC VELOCITY = -3.6 CM/SEC DISPL = 3.4 CM

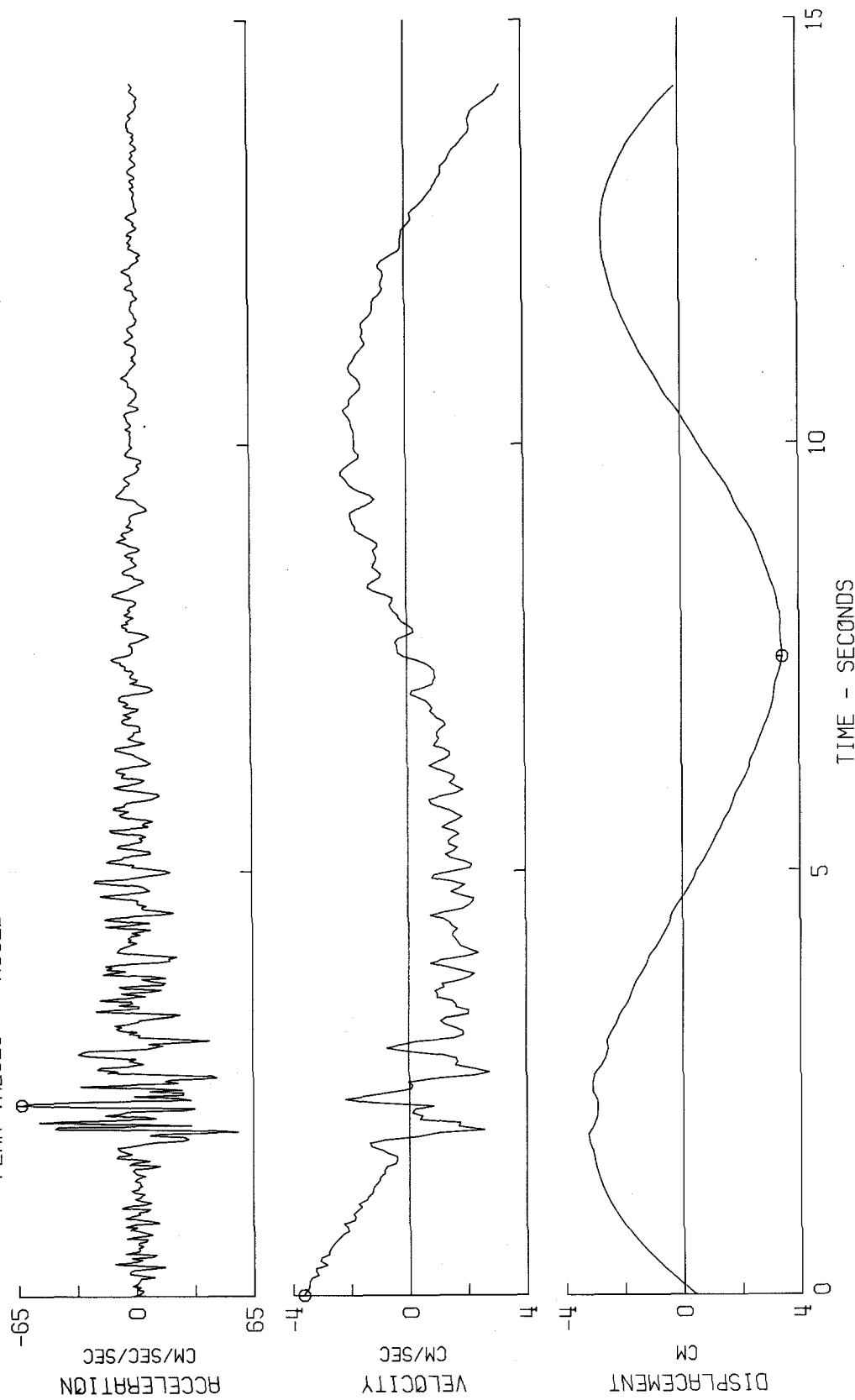


Fig. 38-b

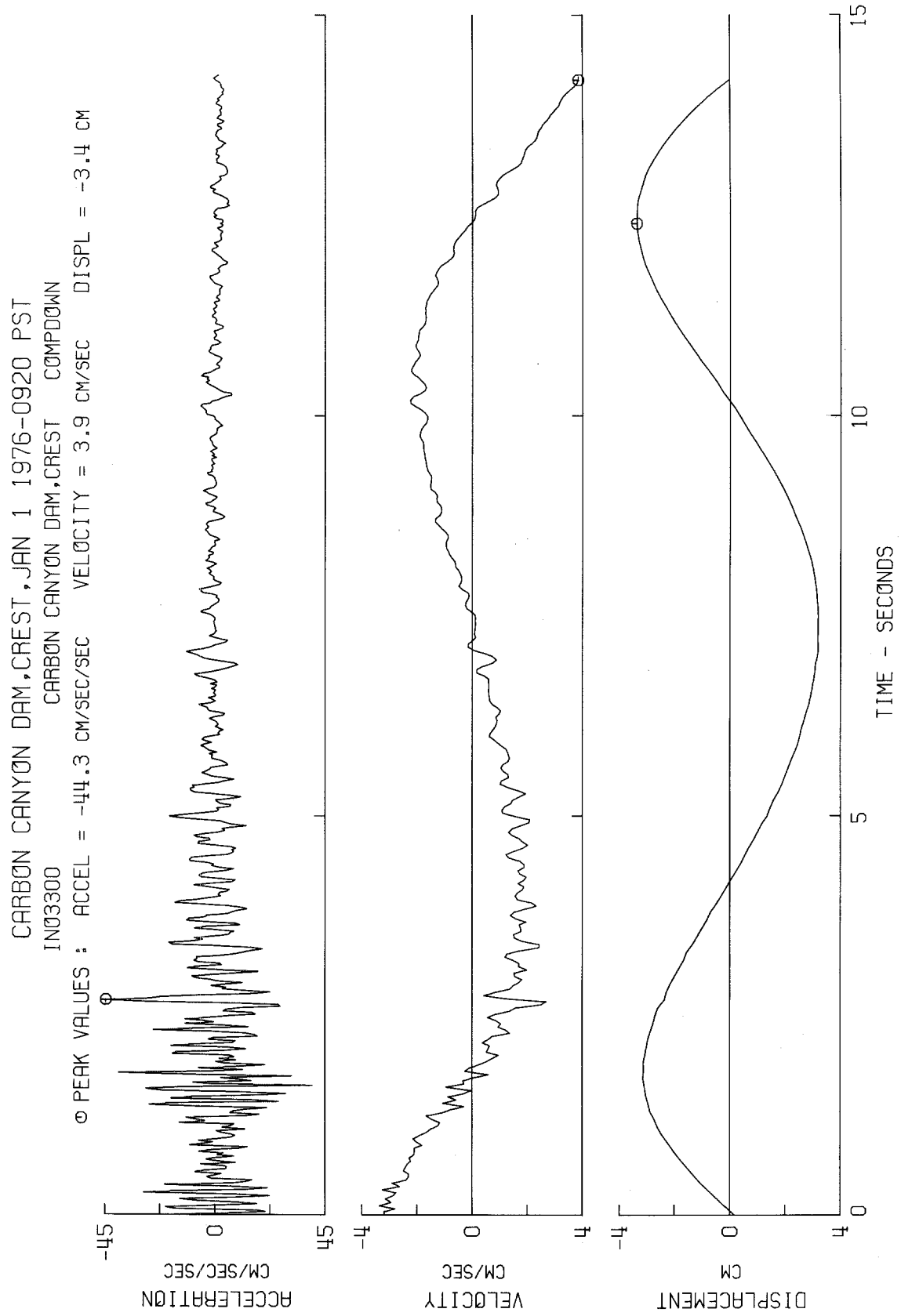


Fig. 38-c

RELATIVE VELOCITY RESPONSE SPECTRUM
CARBON CANYON DAM, RIGHT ABUTMENT, JAN 1 1976-0920 PST
IIN03400 CARBON CANYON DAM, RIGHT ABUTMENT COMPS40W
DAMPING VALUES ARE 0, 2, 5, 10 AND 20 PERCENT OF CRITICAL

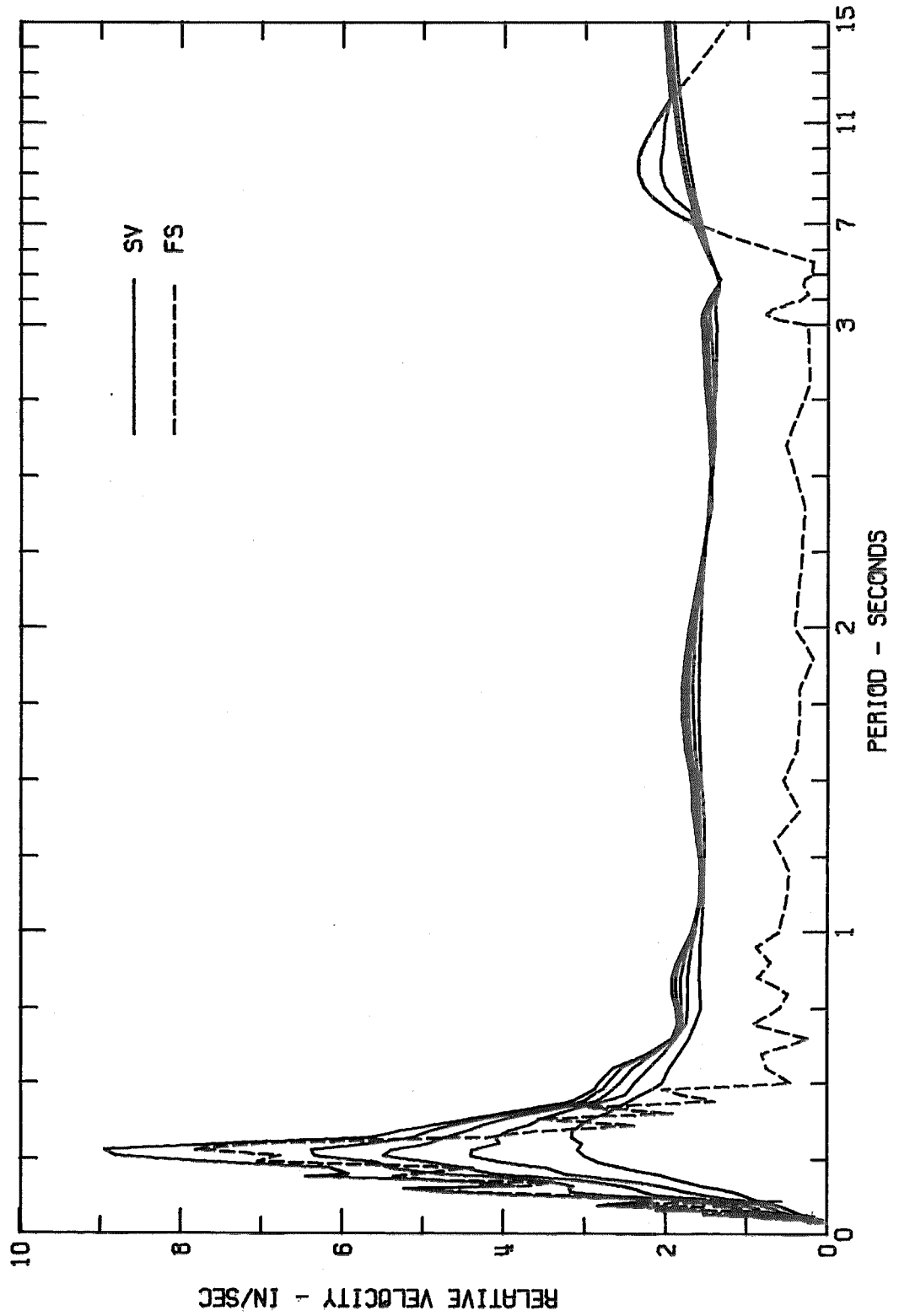


Fig. 39-a

RESPONSE SPECTRUM

CARBON CANYON DAM, RIGHT ABUTMENT, JAN 1 1976-0920 PST

IIN03400

CARBON CANYON DAM, RIGHT ABUTMENT COMPS40W

DAMPING VALUES ARE 0, 2, 5, 10 AND 20 PERCENT OF CRITICAL

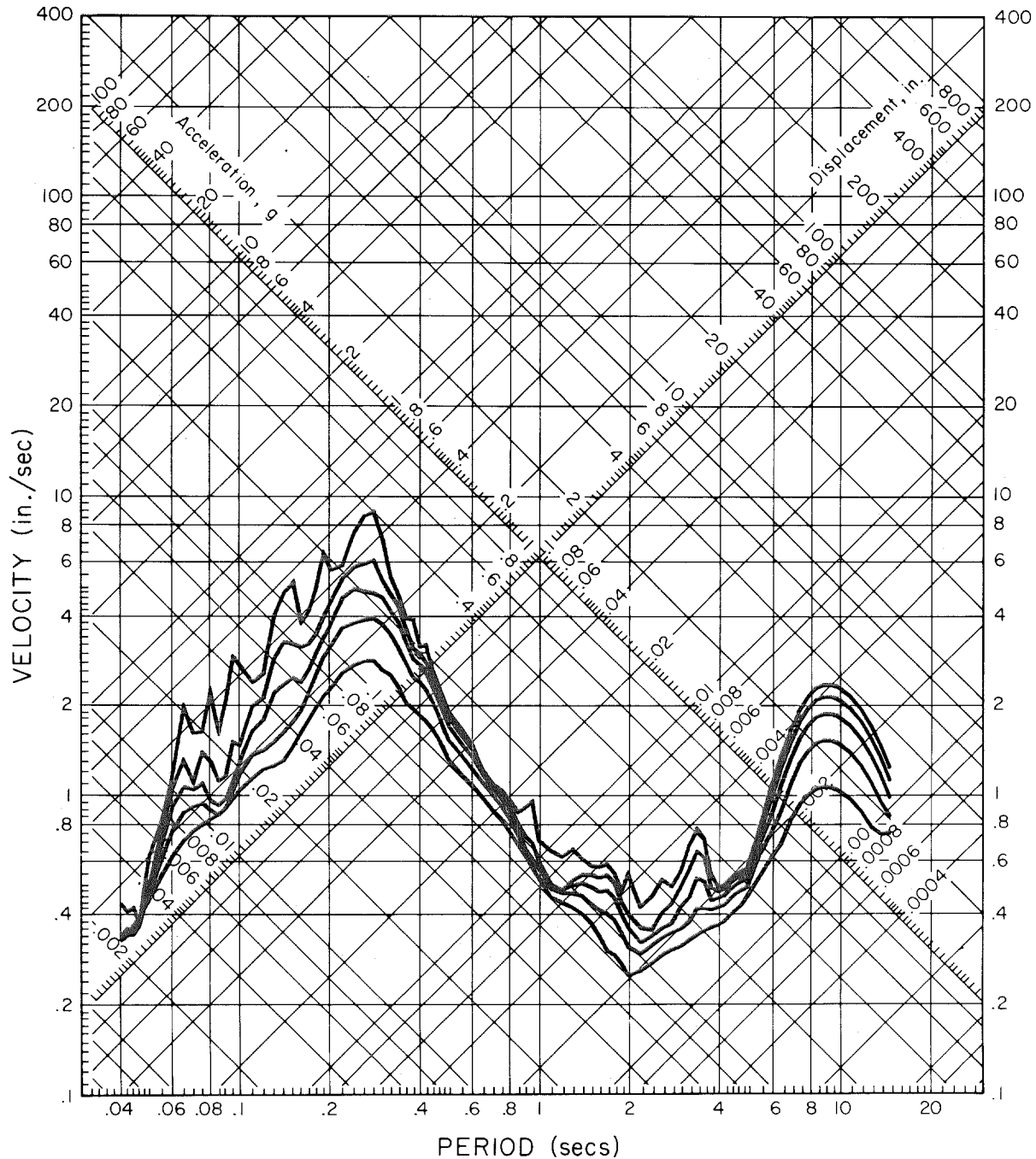


Fig. 39-b

RELATIVE VELOCITY RESPONSE SPECTRUM
CARBON CANYON DAM, RIGHT ABUTMENT, JAN 1 1976-0920 PST
IIN03400 CARBON CANYON DAM, RIGHT ABUTMENT COMPANION
DAMPING VALUES ARE 0, 2, 5, 10 AND 20 PERCENT OF CRITICAL

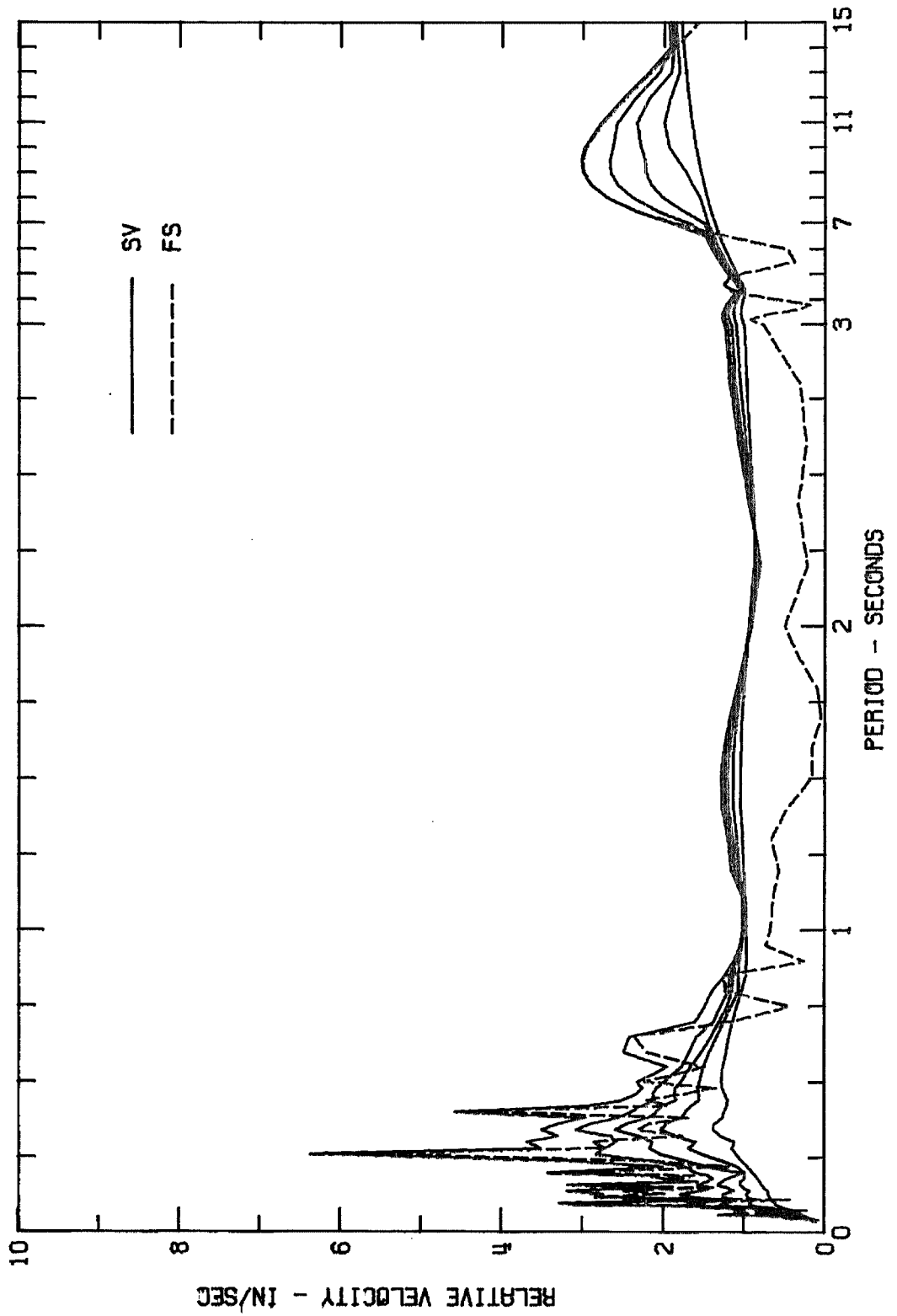


Fig. 40-a

RESPONSE SPECTRUM

CARBON CANYON DAM, RIGHT ABUTMENT, JAN 1 1976-0920 PST

IIN03400

CARBON CANYON DAM, RIGHT ABUTMENT COMPNSOW

DAMPING VALUES ARE 0, 2, 5, 10 AND 20 PERCENT OF CRITICAL

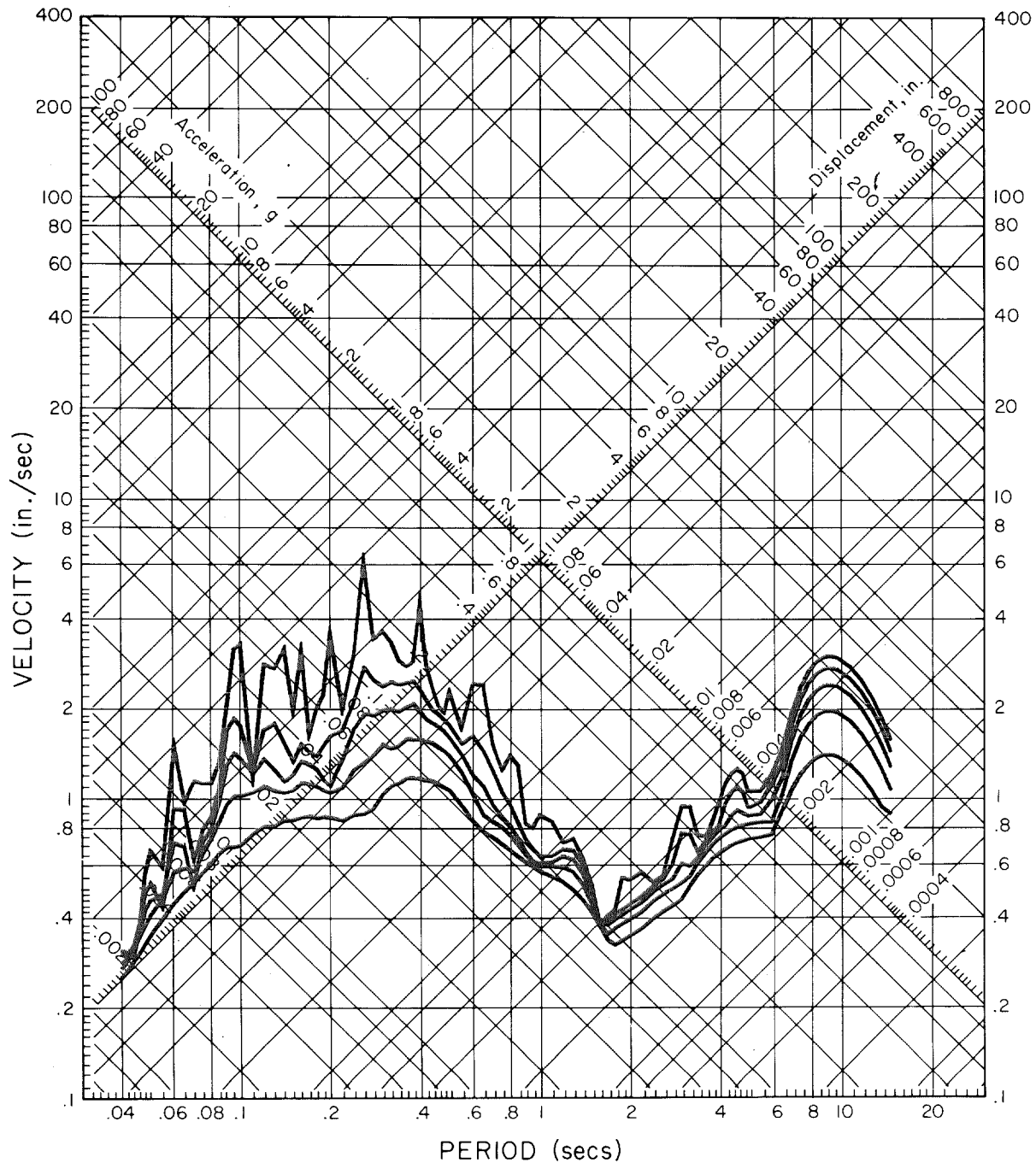


Fig. 40-b

RELATIVE VELOCITY RESPONSE SPECTRUM
 CARBON CANYON DAM, RIGHT ABUTMENT, JAN 1 1976-0920 PST
 IIN03400 CARBON CANYON DAM, RIGHT ABUTMENT COMPDOWN
 DAMPING VALUES ARE 0, 2, 5, 10 AND 20 PERCENT OF CRITICAL

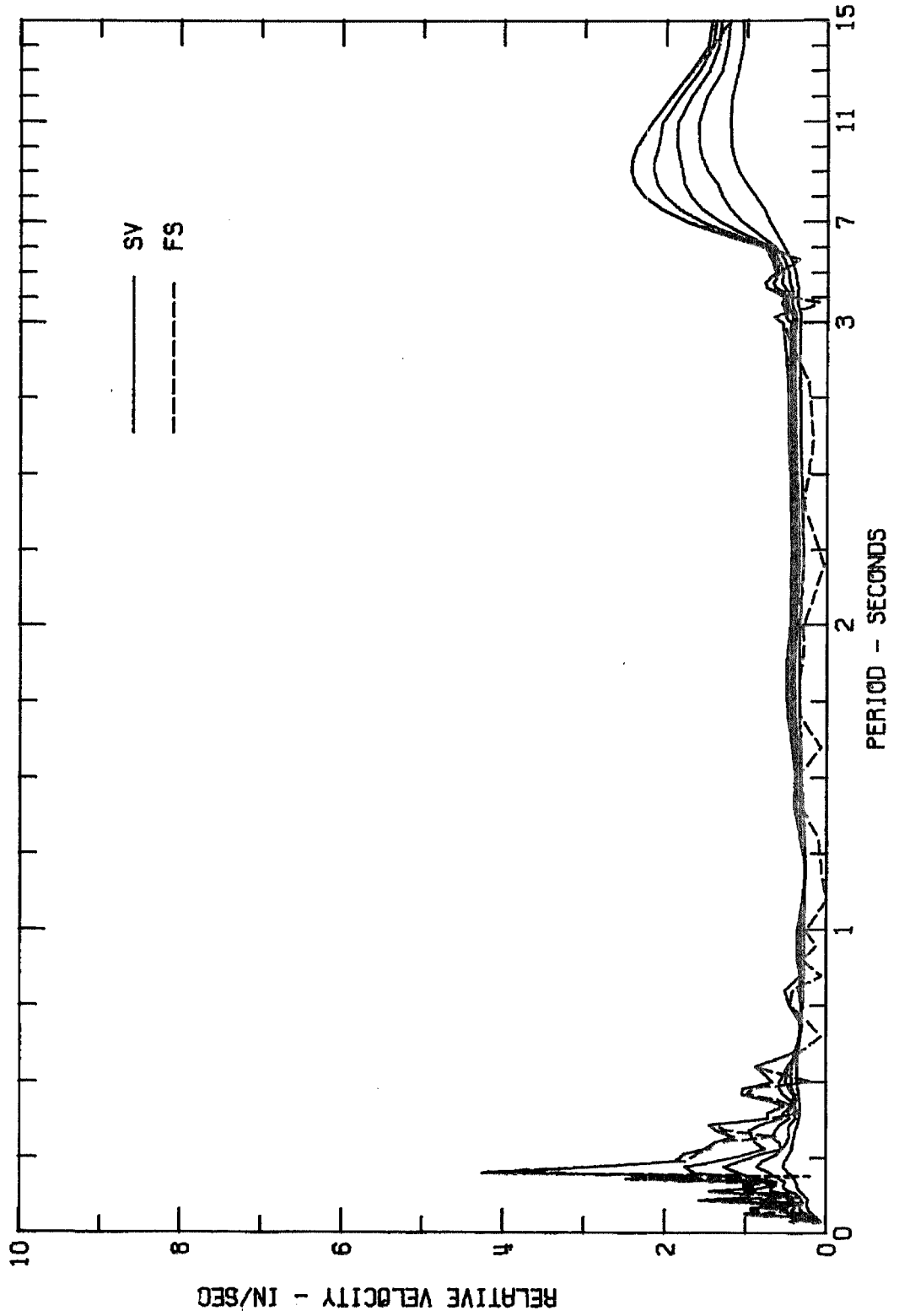


Fig. 41-a

RESPONSE SPECTRUM

CARBON CANYON DAM, RIGHT ABUTMENT, JAN 1 1976-0920 PST

IIN03400

CARBON CANYON DAM, RIGHT ABUTMENT COMDOWN

DAMPING VALUES ARE 0, 2, 5, 10 AND 20 PERCENT OF CRITICAL

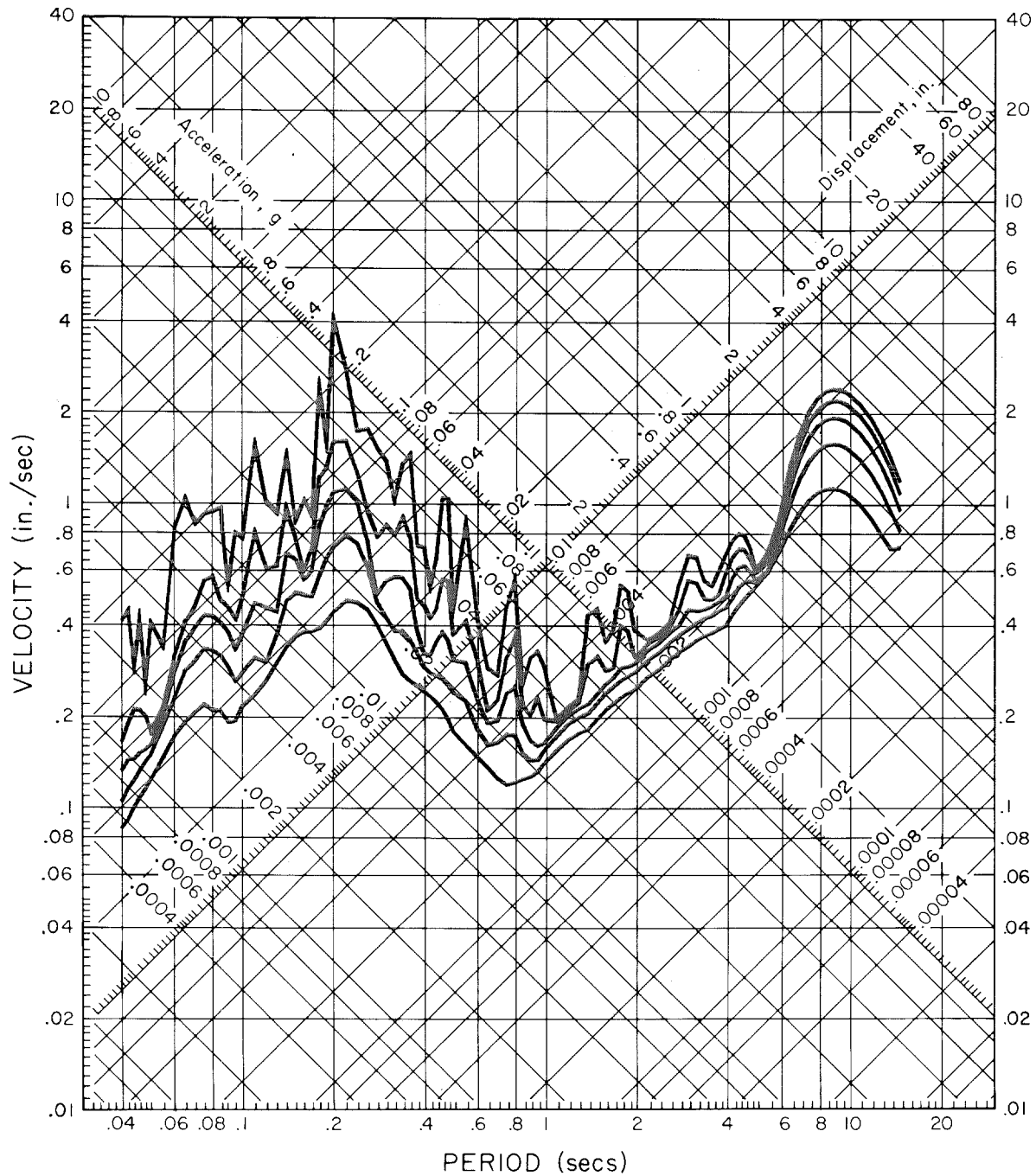


Fig. 41-b

RELATIVE VELOCITY RESPONSE SPECTRUM
CARBON CANYON DAM, LEFT ABUTMENT, JAN 1 1976-0920 PST
IIN03200 CARBON CANYON DAM, LEFT ABUTMENT COMPS40W
DAMPING VALUES ARE 0, 2, 5, 10 AND 20 PERCENT OF CRITICAL

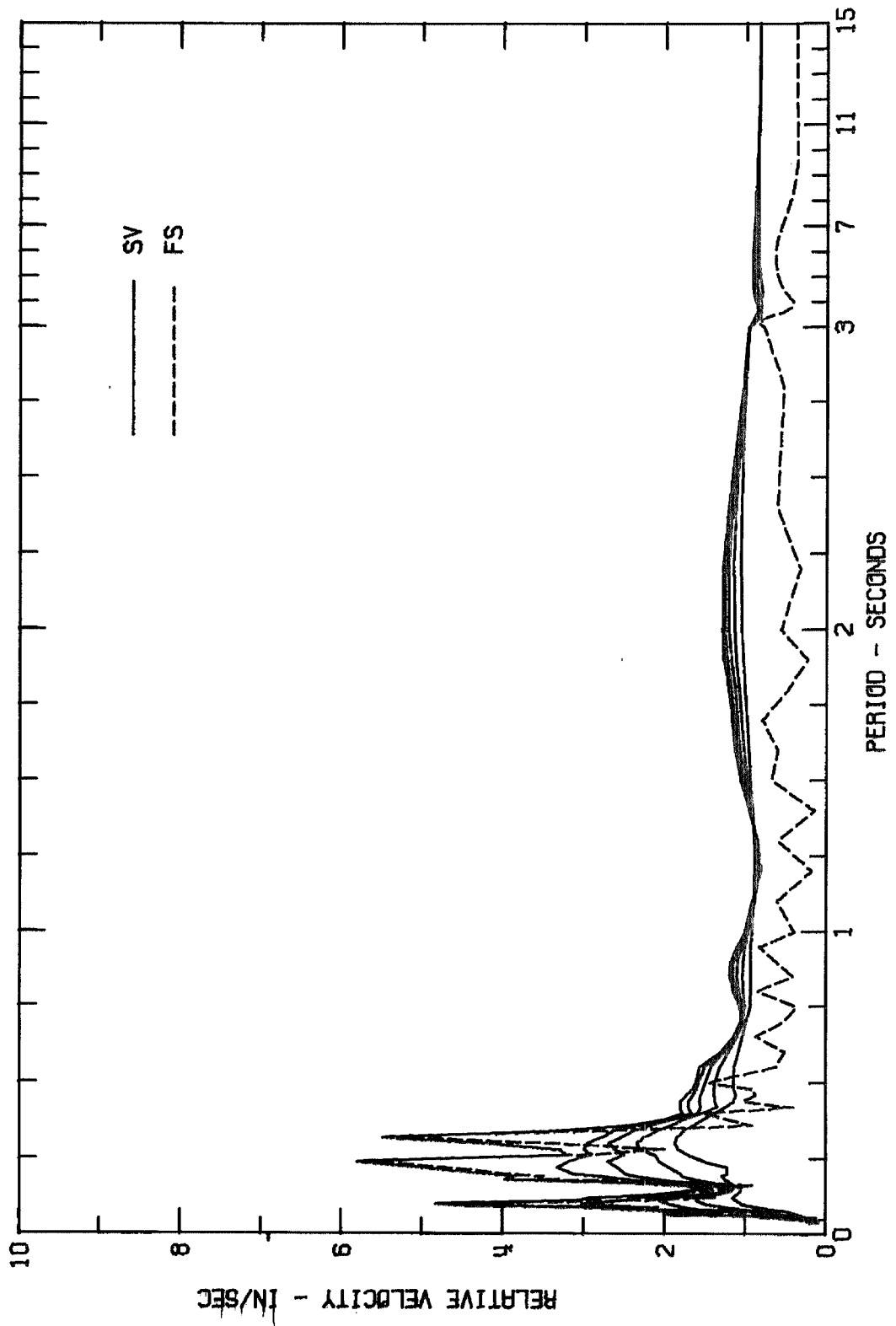


Fig. 42-a

RESPONSE SPECTRUM

CARBON CANYON DAM, LEFT ABUTMENT, JAN 1 1976-0920 PST

11N03200

CARBON CANYON DAM, LEFT ABUTMENT COMPS40W

DAMPING VALUES ARE 0, 2, 5, 10 AND 20 PERCENT OF CRITICAL

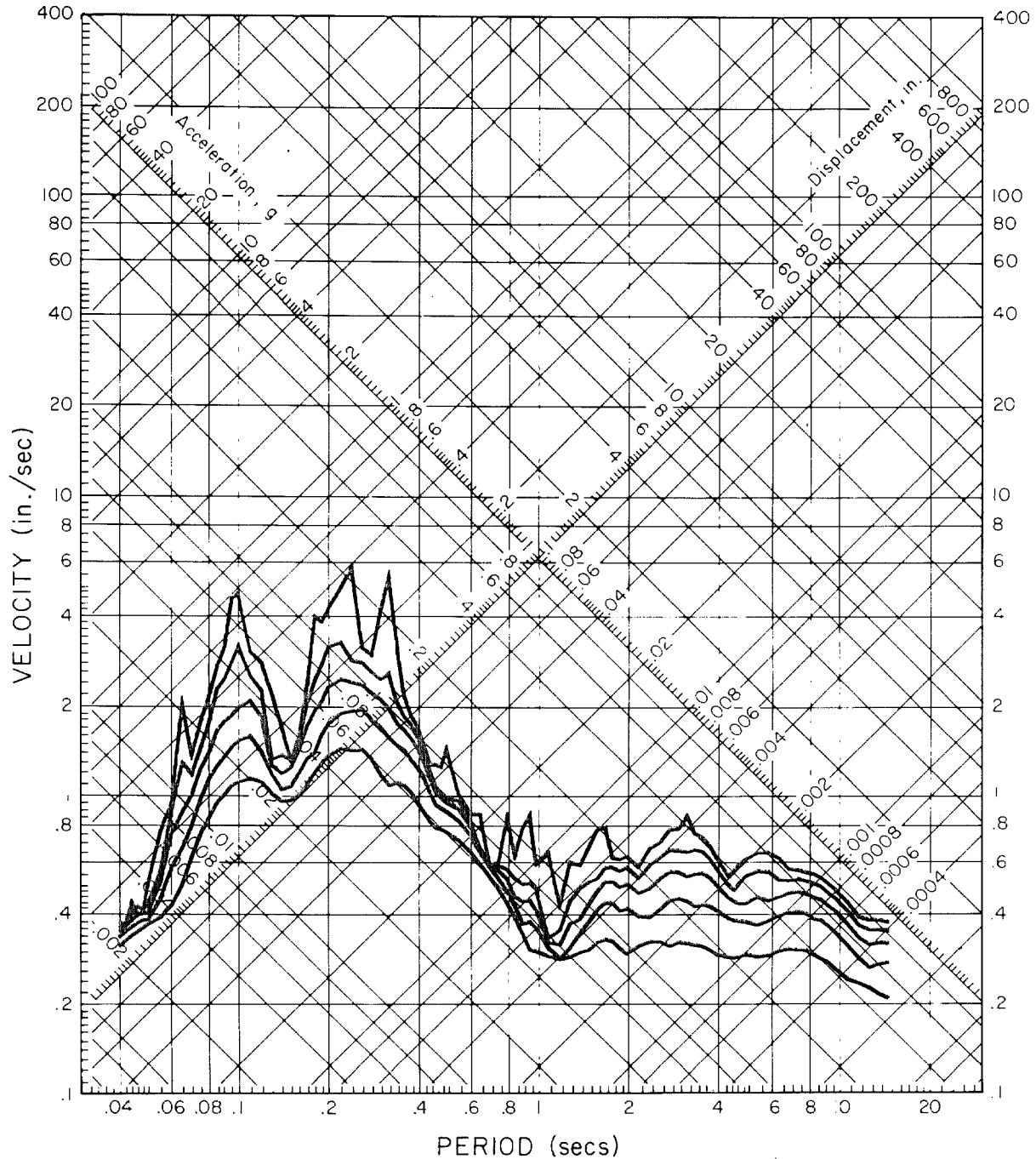


Fig. 42-b

RELATIVE VELOCITY RESPONSE SPECTRUM
CARBON CANYON DAM, LEFT ABUTMENT, JAN 1 1976-0920 PST
IING3200 CARBON CANYON DAM, LEFT ABUTMENT COMPANSON
DAMPING VALUES ARE 0, 2, 5, 10 AND 20 PERCENT OF CRITICAL

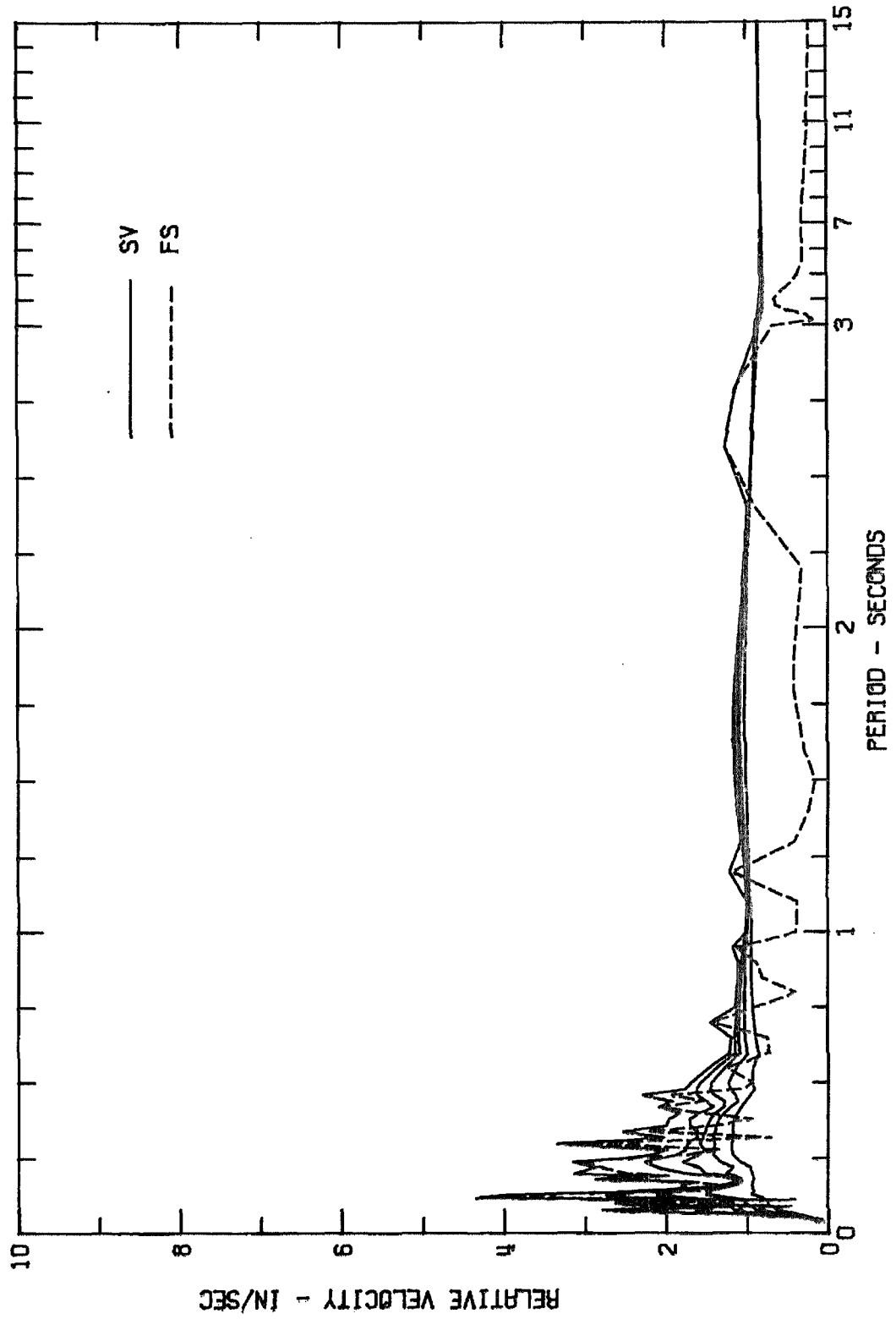


Fig. 43-a

RESPONSE SPECTRUM

CARBON CANYON DAM, LEFT ABUTMENT, JAN 1 1976-0920 PST

11N03200

CARBON CANYON DAM, LEFT ABUTMENT COMPNSOW

DAMPING VALUES ARE 0, 2, 5, 10 AND 20 PERCENT OF CRITICAL

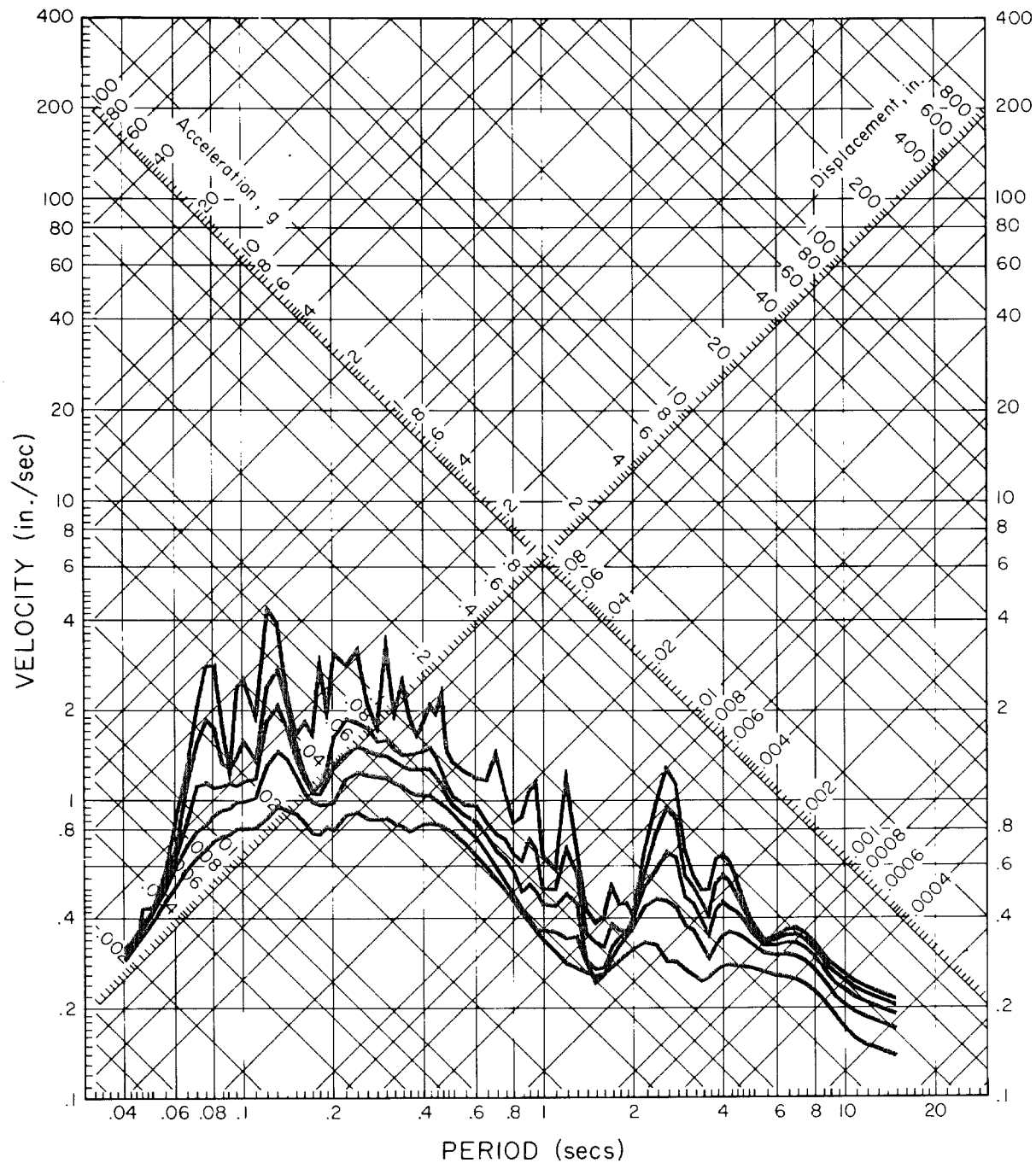


Fig. 43-b

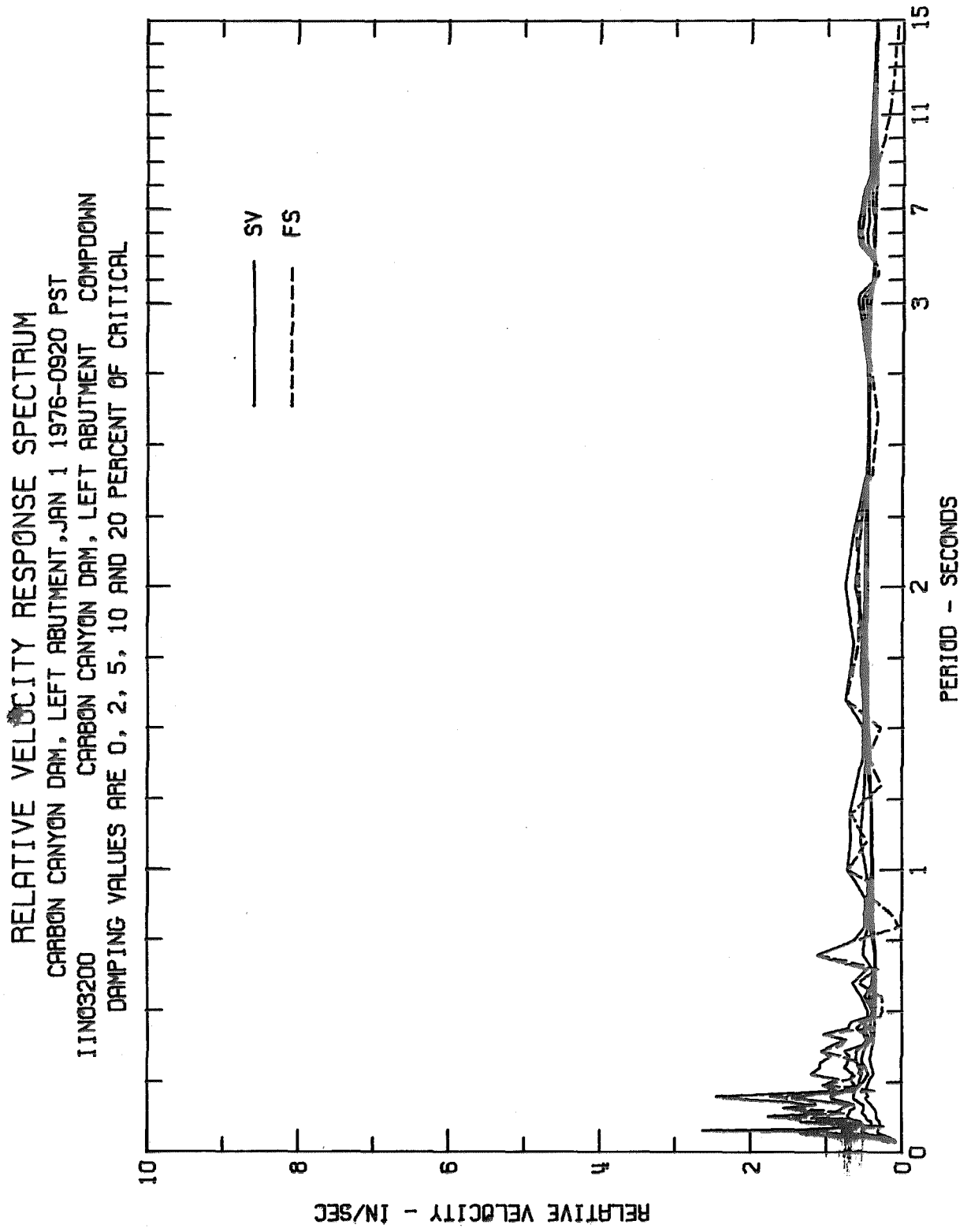


Fig. 44-a

RESPONSE SPECTRUM

CARBON CANYON DAM, LEFT ABUTMENT, JAN 1 1976-0920 PST

IIN03200

CARBON CANYON DAM, LEFT ABUTMENT COMPDOWN

DAMPING VALUES ARE 0, 2, 5, 10 AND 20 PERCENT OF CRITICAL

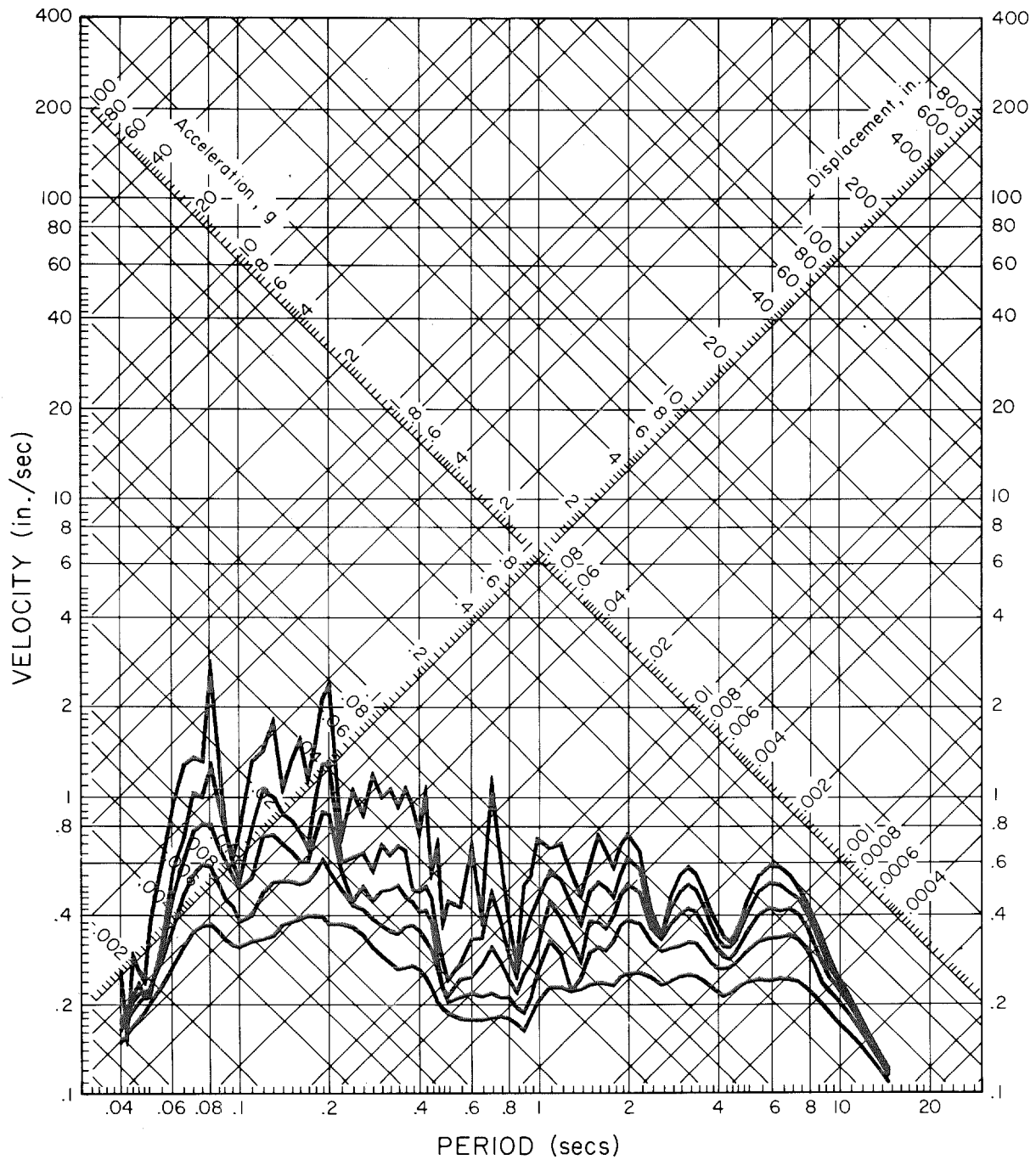


Fig. 44-b

RELATIVE VELOCITY RESPONSE SPECTRUM
CARBON CANYON DAM, CREST, JAN 1 1976-0920 PST
IIN03300 CARBON CANYON DAM, CREST COMPS40W
DAMPING VALUES ARE 0, 2, 5, 10 AND 20 PERCENT OF CRITICAL

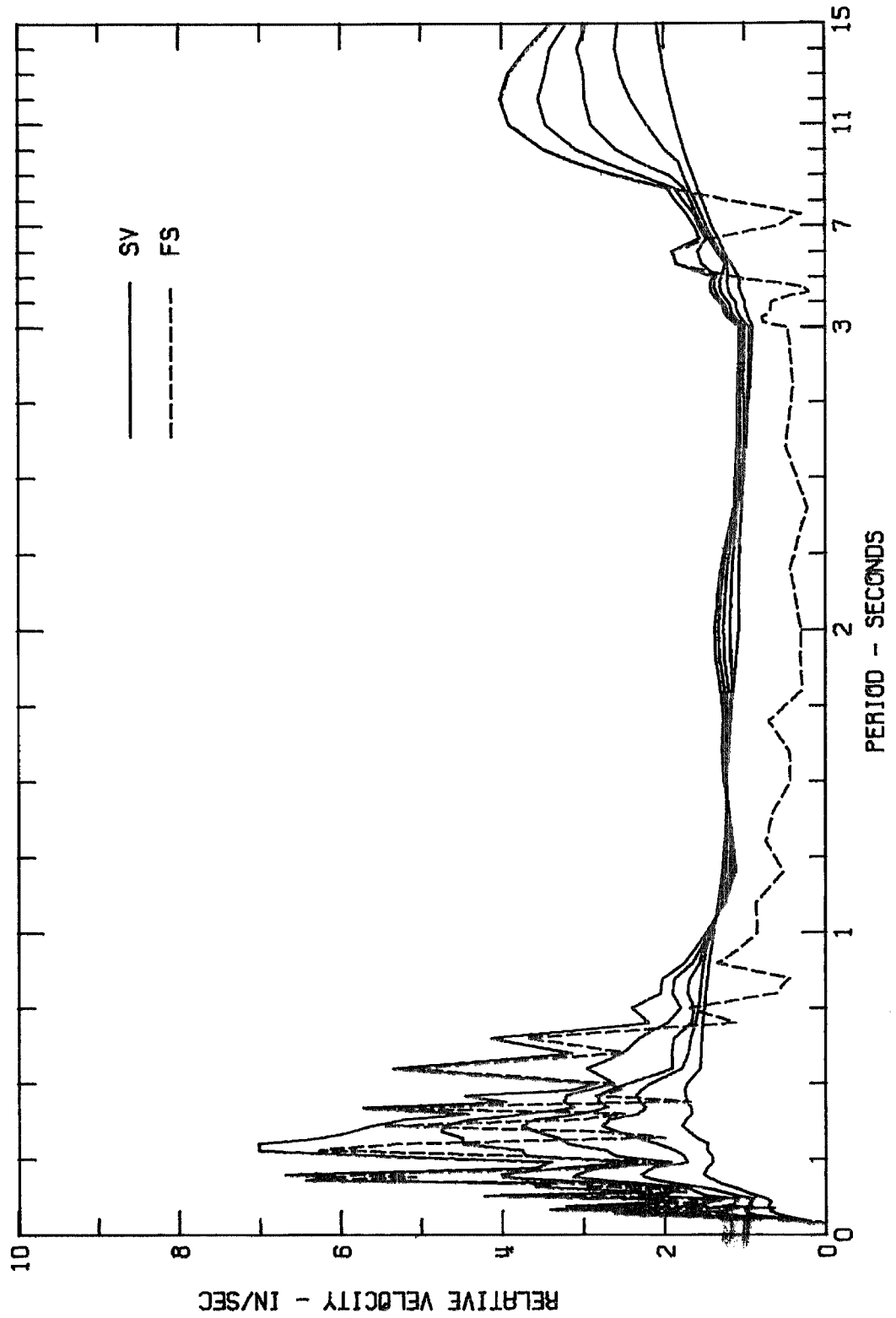


Fig. 45-a

RESPONSE SPECTRUM

CARBON CANYON DAM, CREST, JAN 1 1976-0920 PST

IIN03300

CARBON CANYON DAM, CREST COMPS40W

DAMPING VALUES ARE 0, 2, 5, 10 AND 20 PERCENT OF CRITICAL

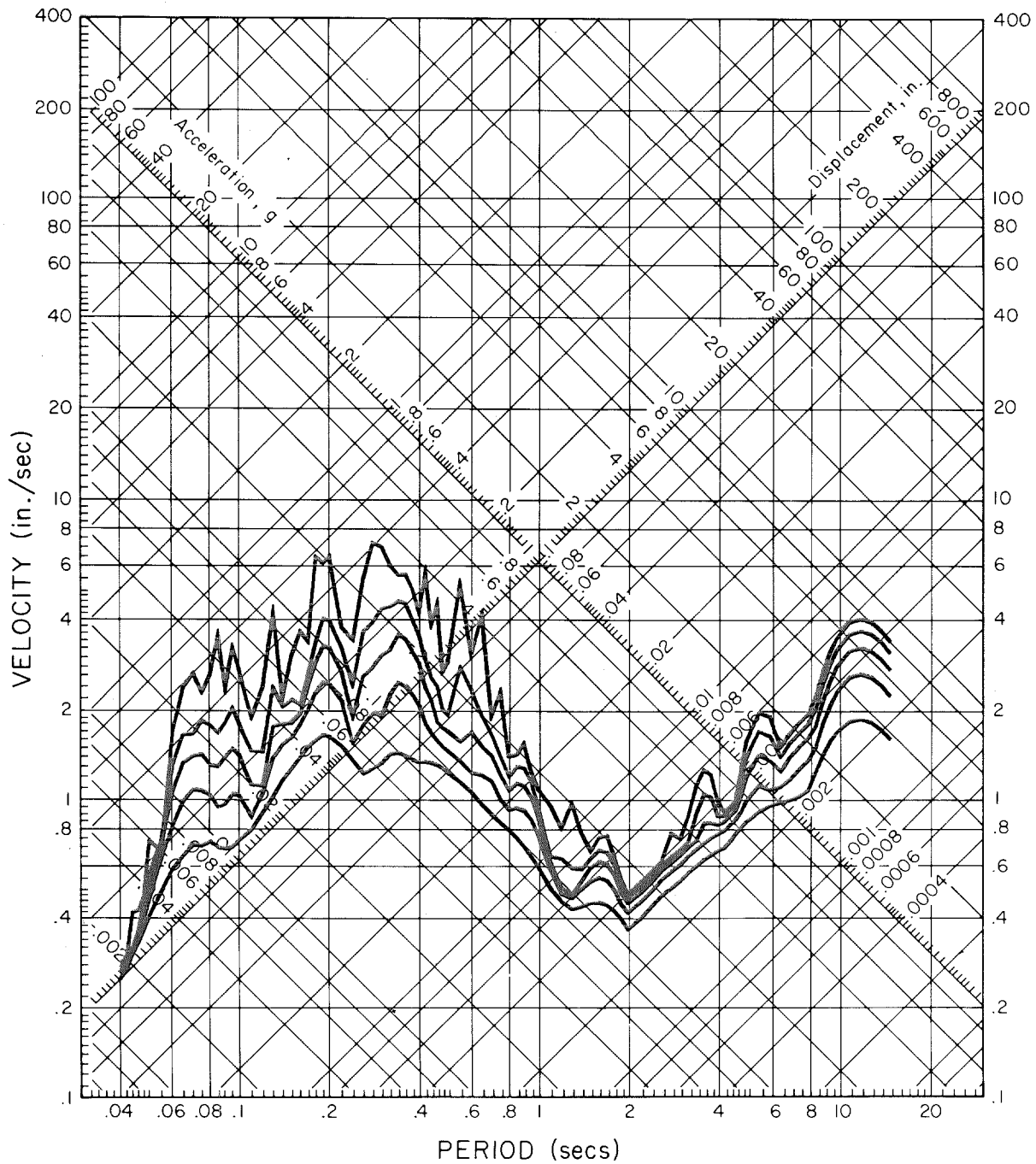


Fig. 45-b

RELATIVE VELOCITY RESPONSE SPECTRUM
CARBON CANYON DAM, CREST, JAN 1 1976-0920 PST
IIN03300 CARBON CANYON DAM, CREST COMPNSOW
DAMPING VALUES ARE 0, 2, 5, 10 AND 20 PERCENT OF CRITICAL

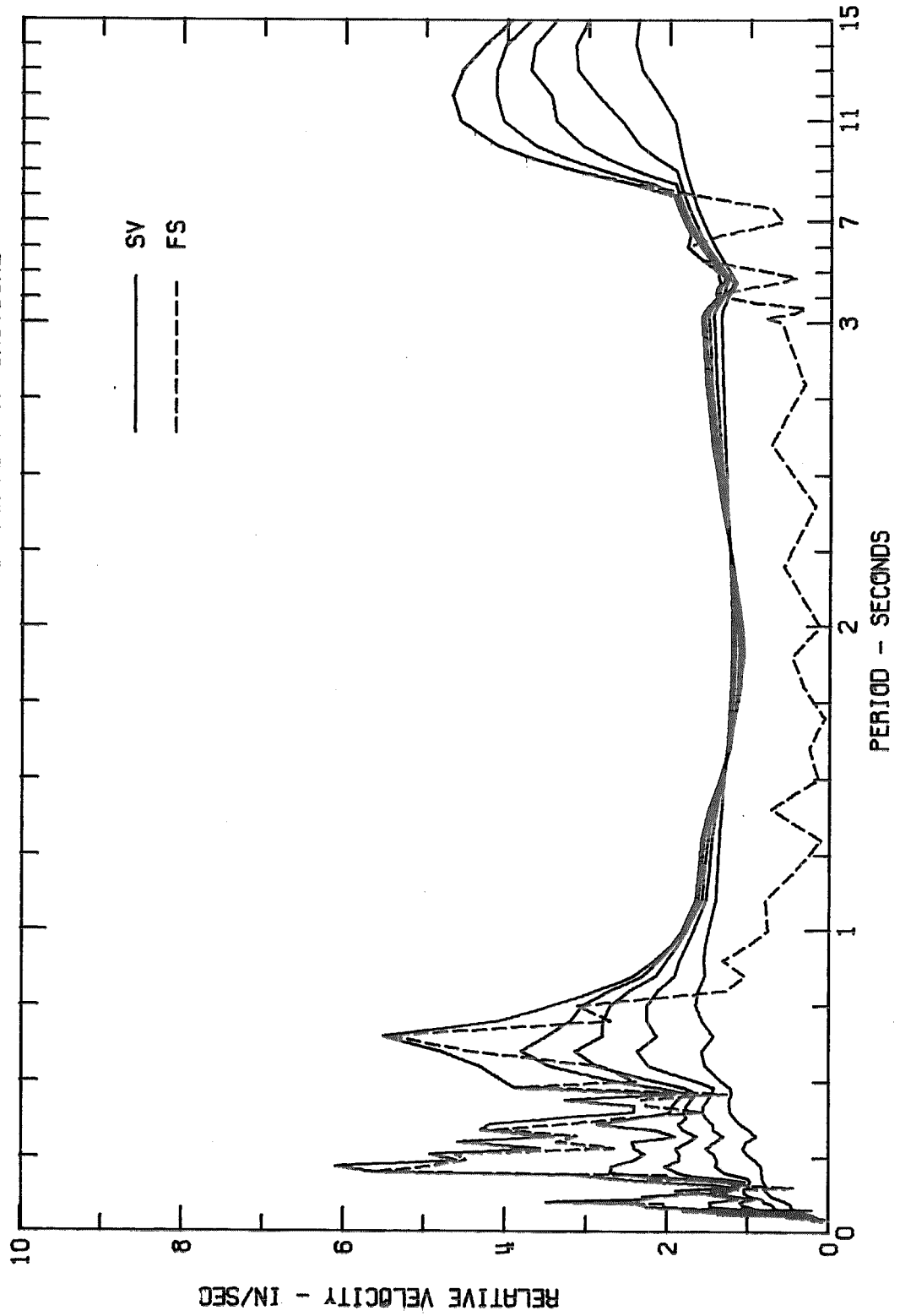


Fig. 46-a

RESPONSE SPECTRUM

CARBON CANYON DAM, CREST, JAN 1 1976-0920 PST

IIN03300

CARBON CANYON DAM, CREST COMPNSOW

DAMPING VALUES ARE 0, 2, 5, 10 AND 20 PERCENT OF CRITICAL

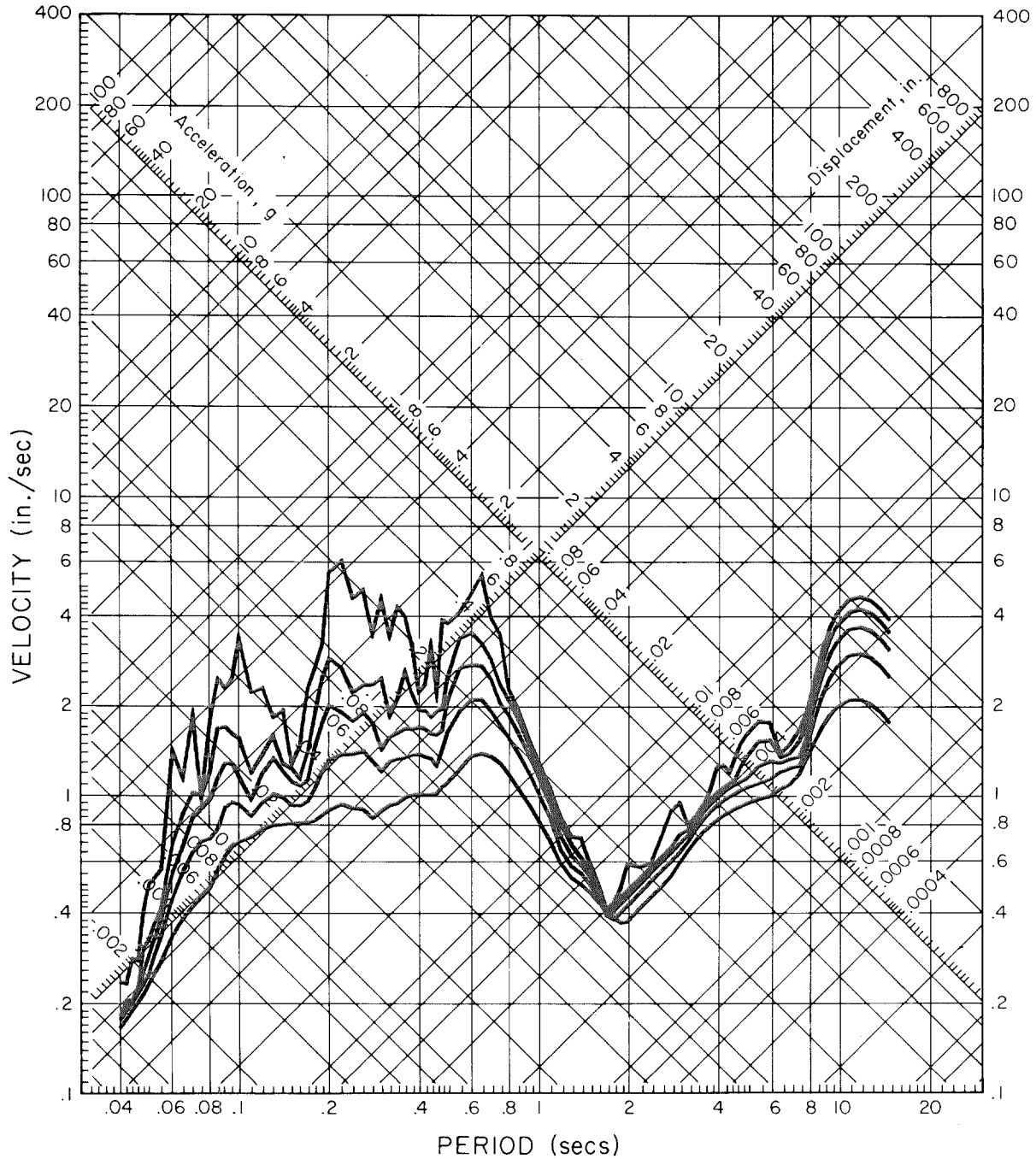


Fig. 46-b

RELATIVE VELOCITY RESPONSE SPECTRUM
CARBON CANYON DAM, CREST, JAN 1 1976-0920 PST
IIN03300 CARBON CANYON DAM, CREST COMDOWN
DAMPING VALUES ARE 0, 2, 5, 10 AND 20 PERCENT OF CRITICAL

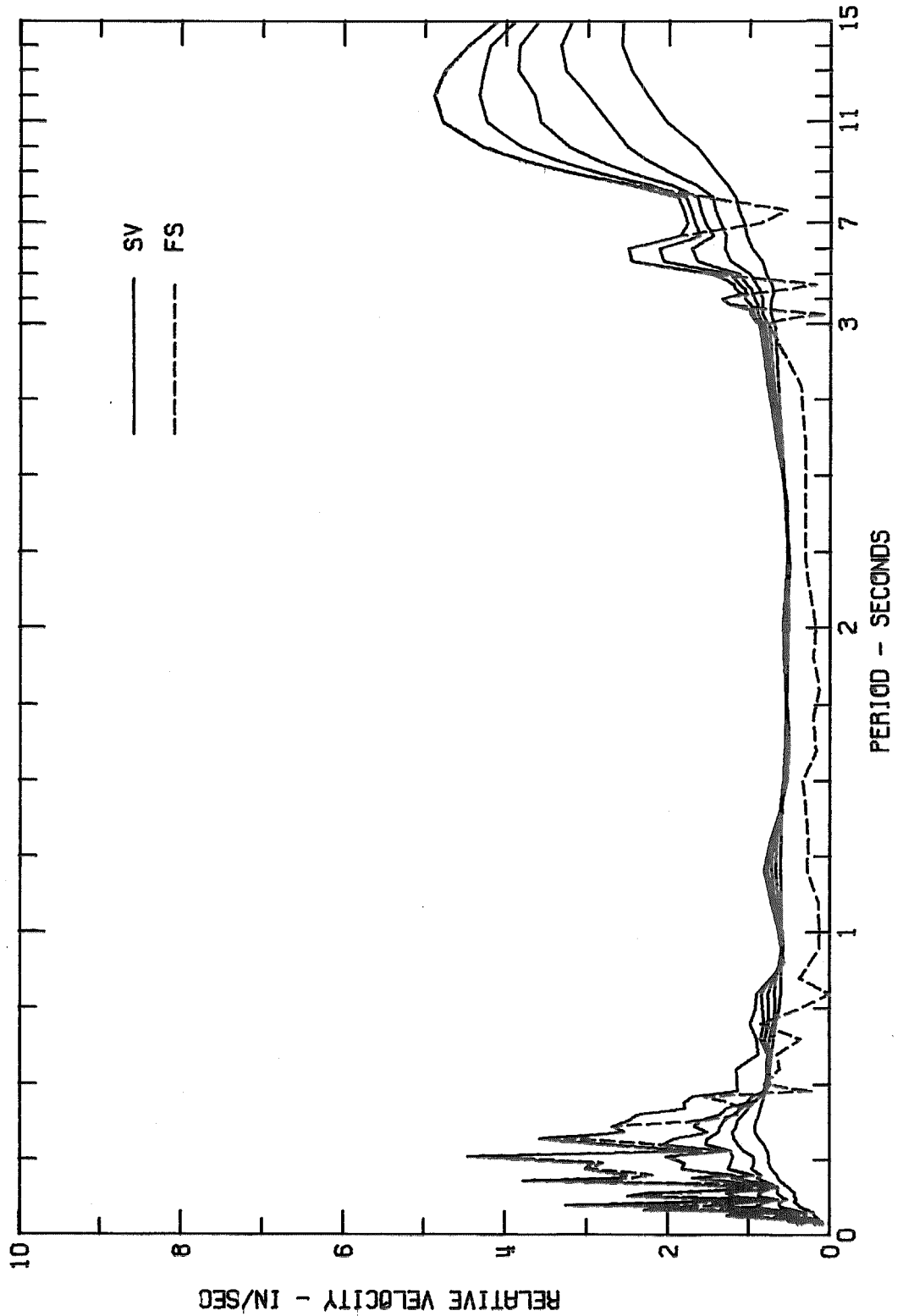


Fig. 47-a

RESPONSE SPECTRUM

CARBON CANYON DAM, CREST, JAN 1 1976-0920 PST

IIN03300

CARBON CANYON DAM, CREST COMDOWN

DAMPING VALUES ARE 0, 2, 5, 10 AND 20 PERCENT OF CRITICAL

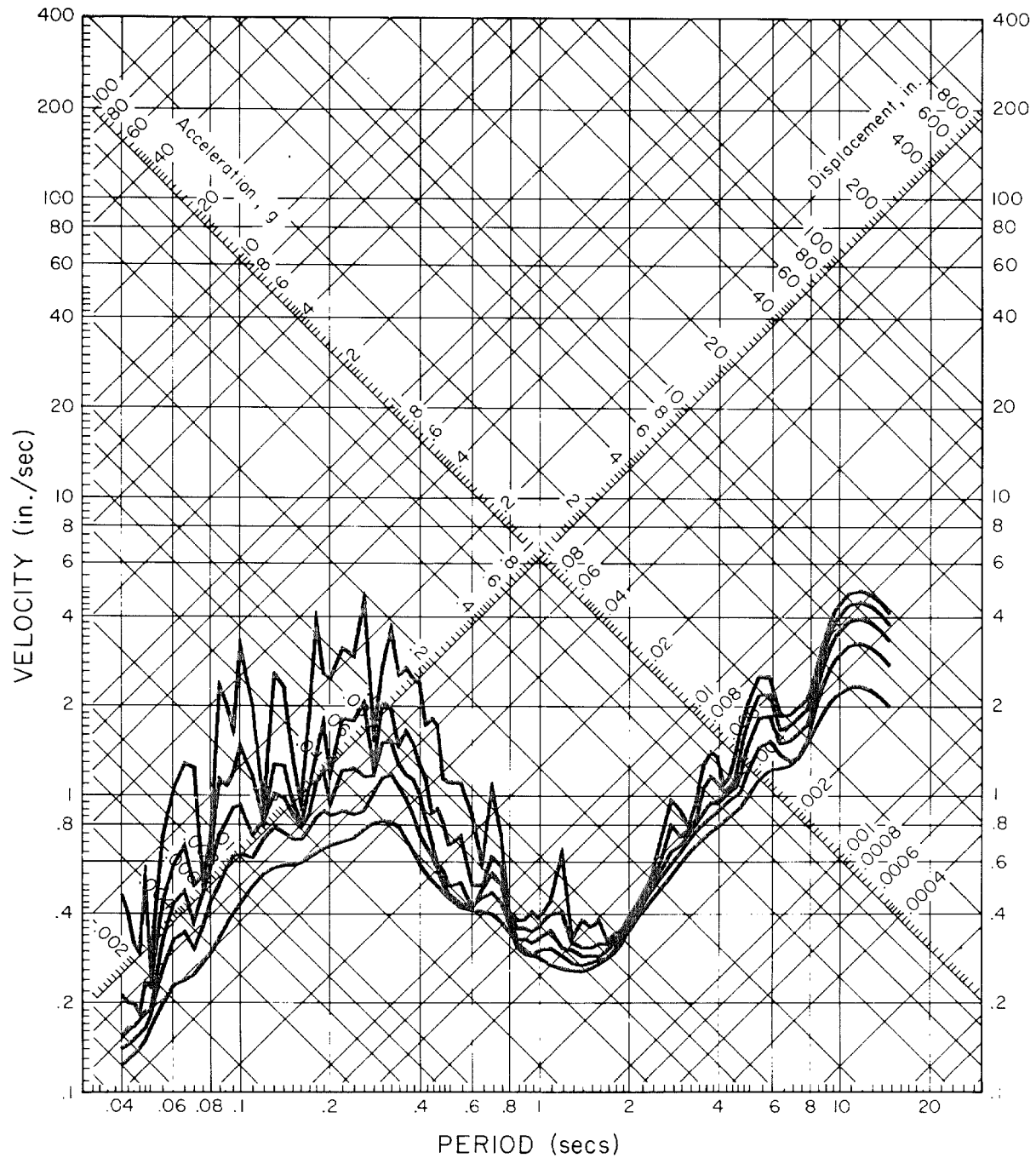


Fig. 47-b

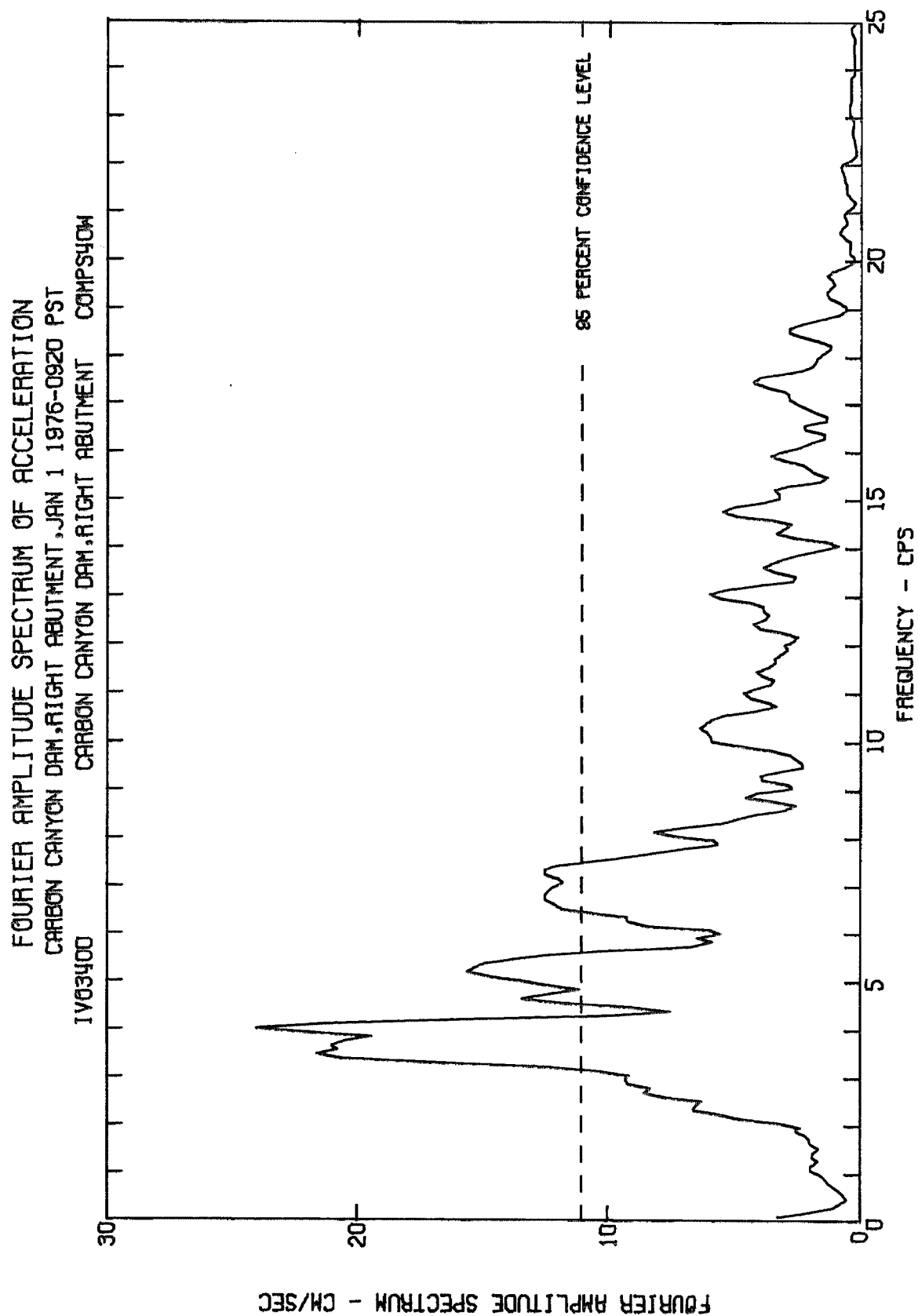


Fig. 48-a

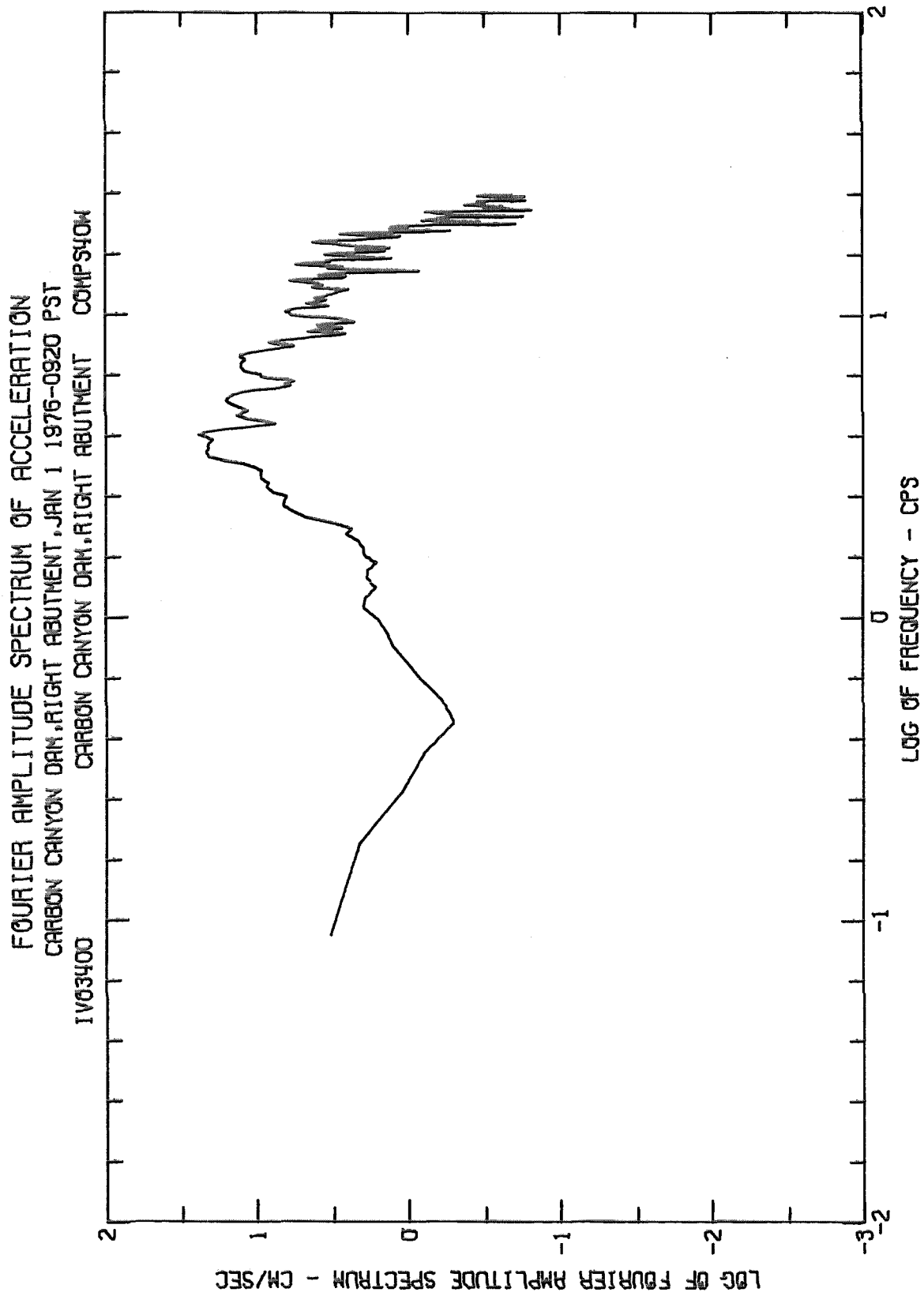


Fig. 48-b

FOURIER AMPLITUDE SPECTRUM OF ACCELERATION
CARBON CANYON DAM, RIGHT ABUTMENT, JAN 1 1976-0920 PST
IV03400 CARBON CANYON DAM, RIGHT ABUTMENT COMPNSOW

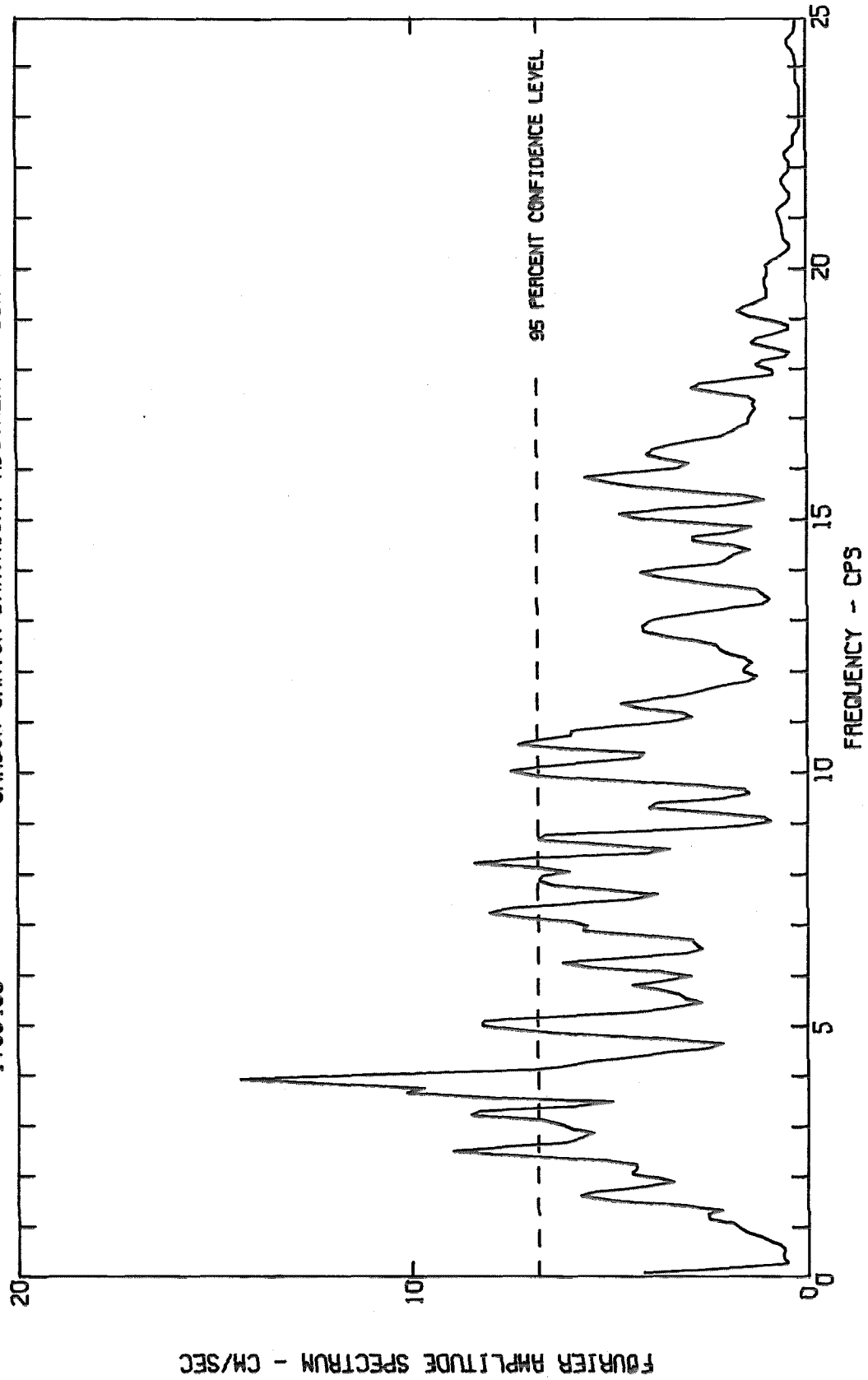


Fig. 49-a

FOURIER AMPLITUDE SPECTRUM OF ACCELERATION
CARBON CANYON DAM, RIGHT ABUTMENT, JAN 1 1976-0920 PST
1V03400 CARBON CANYON DAM, RIGHT ABUTMENT COMP50W

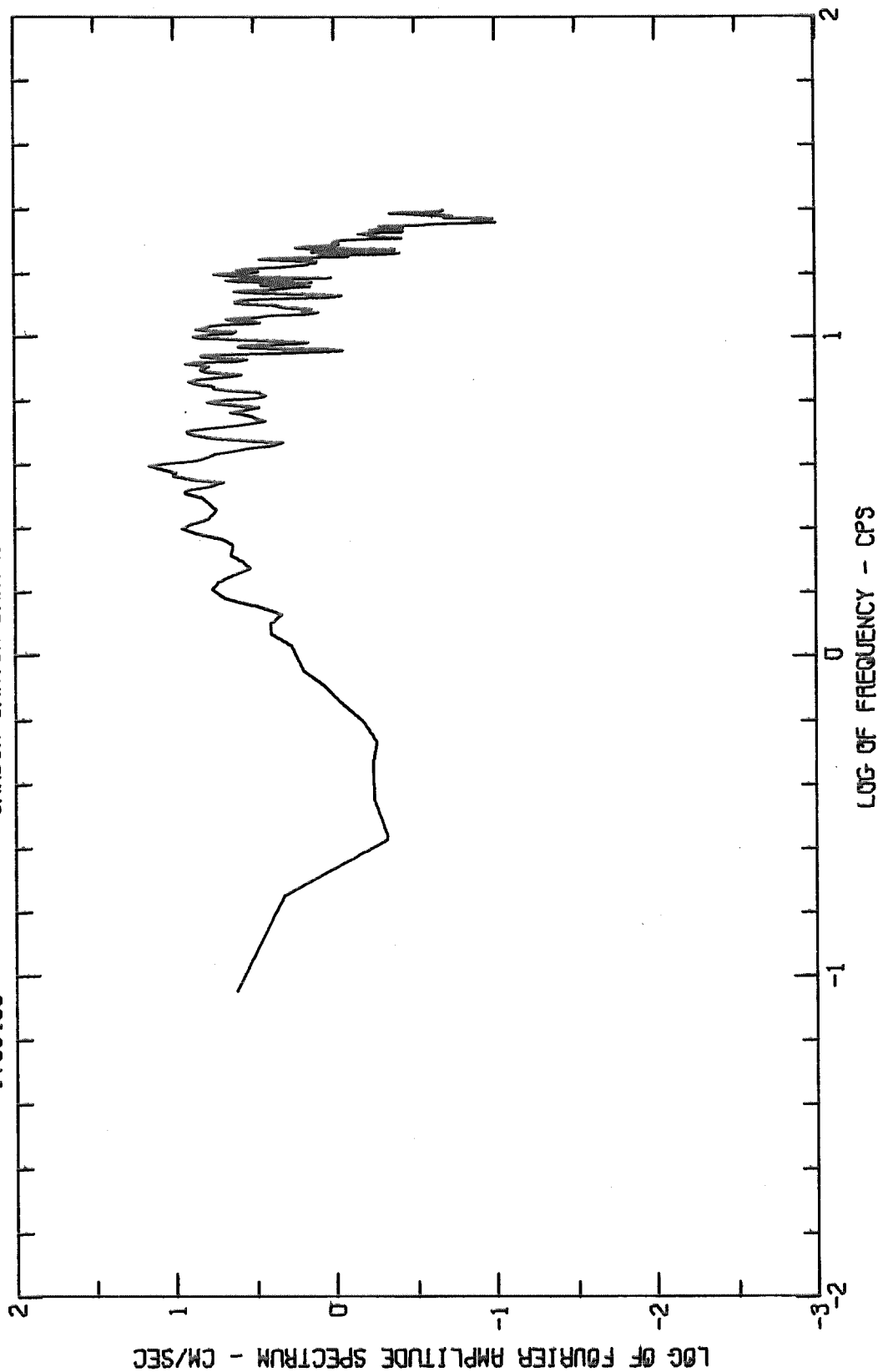


Fig. 49-b

FOURIER AMPLITUDE SPECTRUM OF ACCELERATION
CARBON CANYON DAM, RIGHT ABUTMENT, JAN 1 1976-0920 PST
CARBON CANYON DAM, RIGHT ABUTMENT COMPOUND

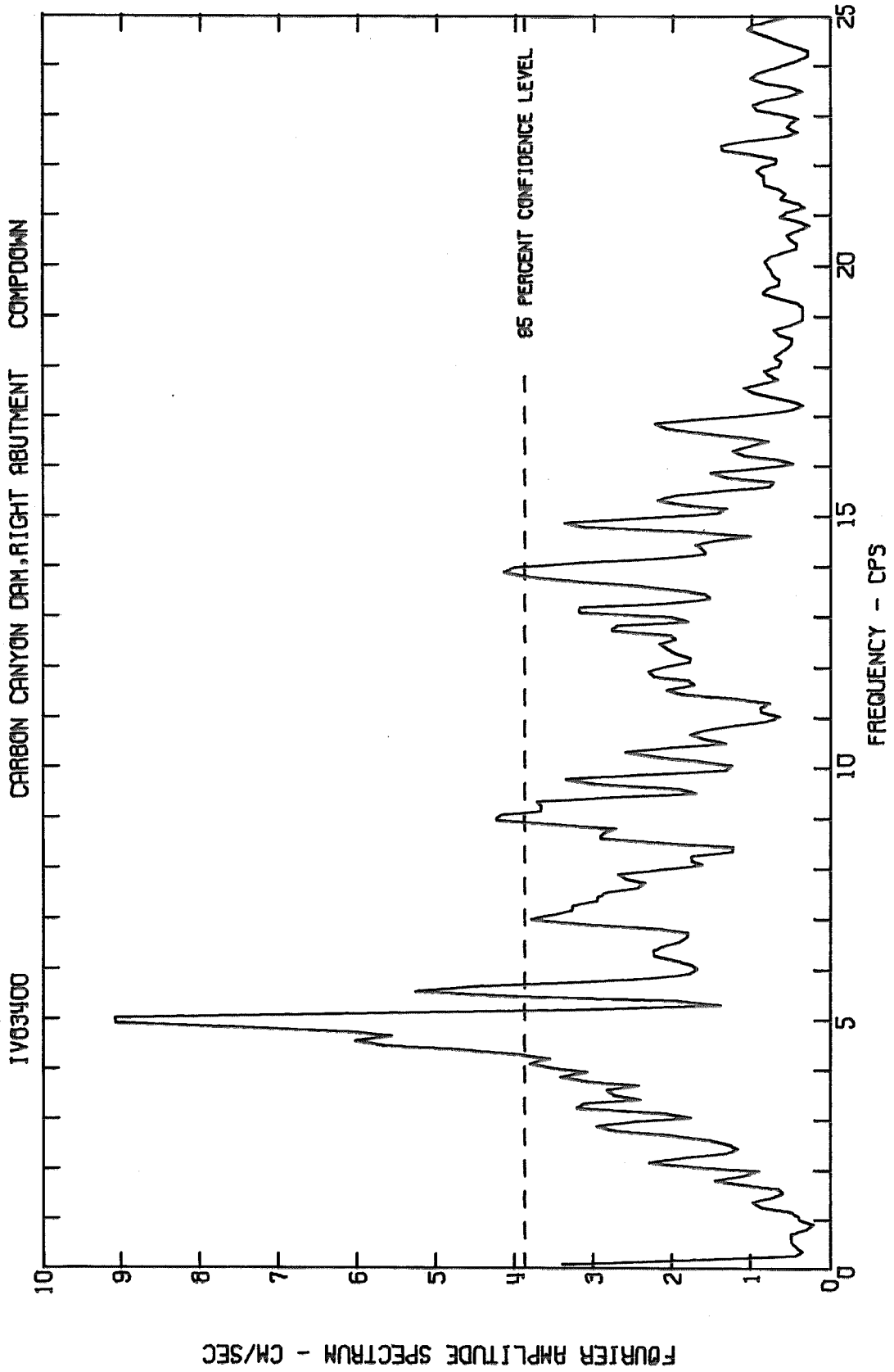


Fig. 50-a

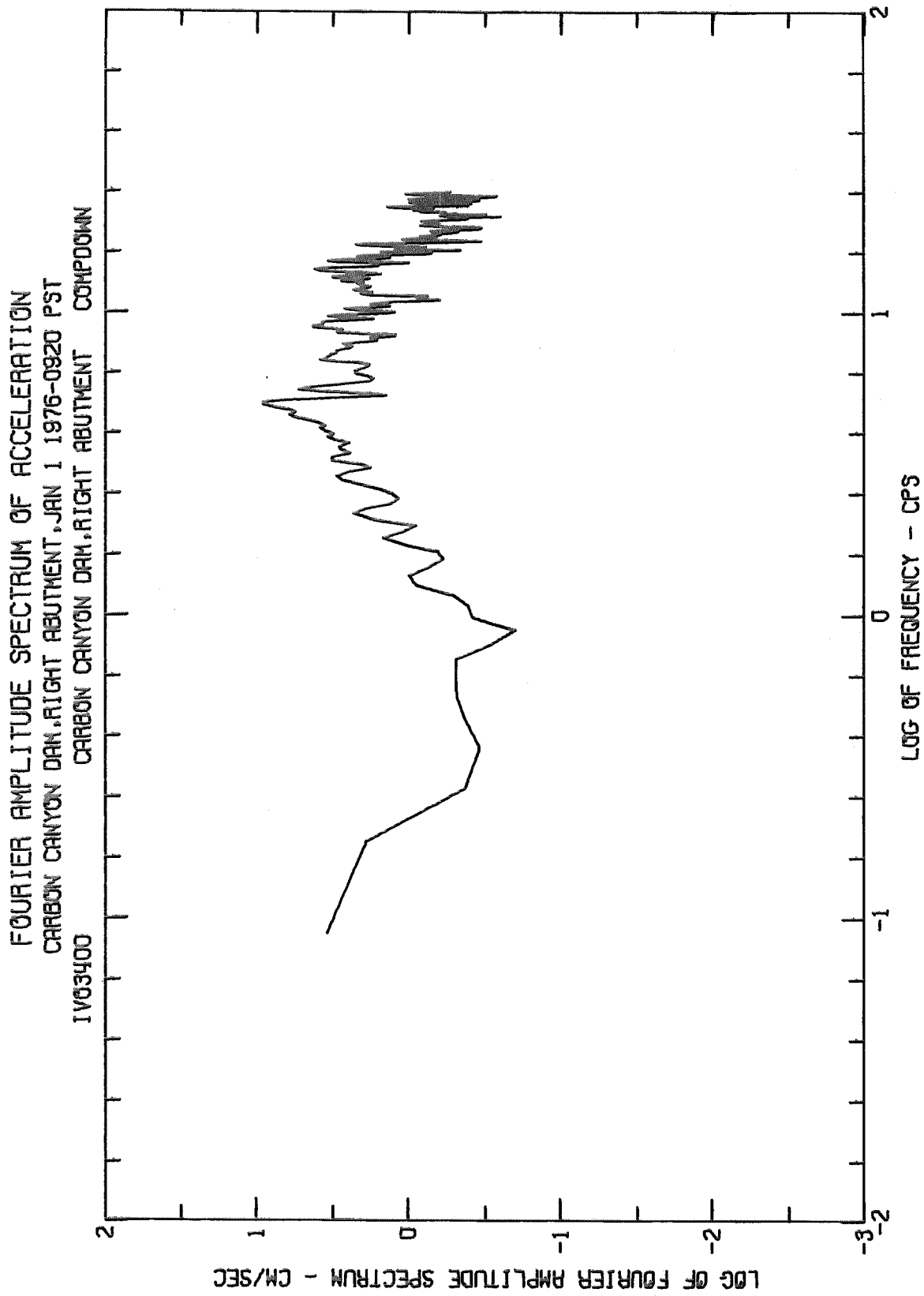


Fig. 50-b

FOURIER AMPLITUDE SPECTRUM OF ACCELERATION
CARBON CANYON DAM, LEFT ABUTMENT, JAN 1 1976-0920 PST
1V03200 CARBON CANYON DAM, LEFT ABUTMENT COMPS40W

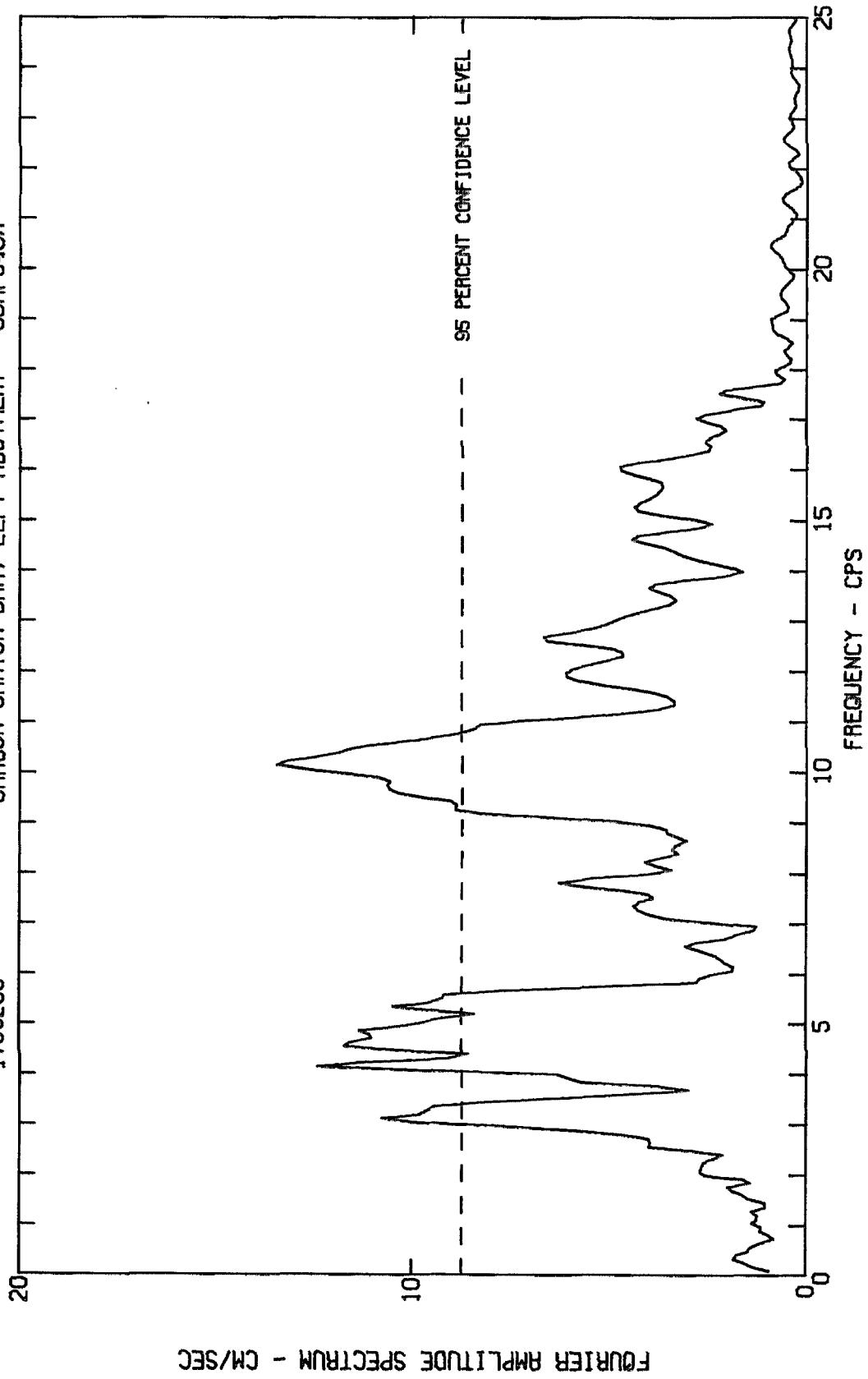


Fig. 51-a

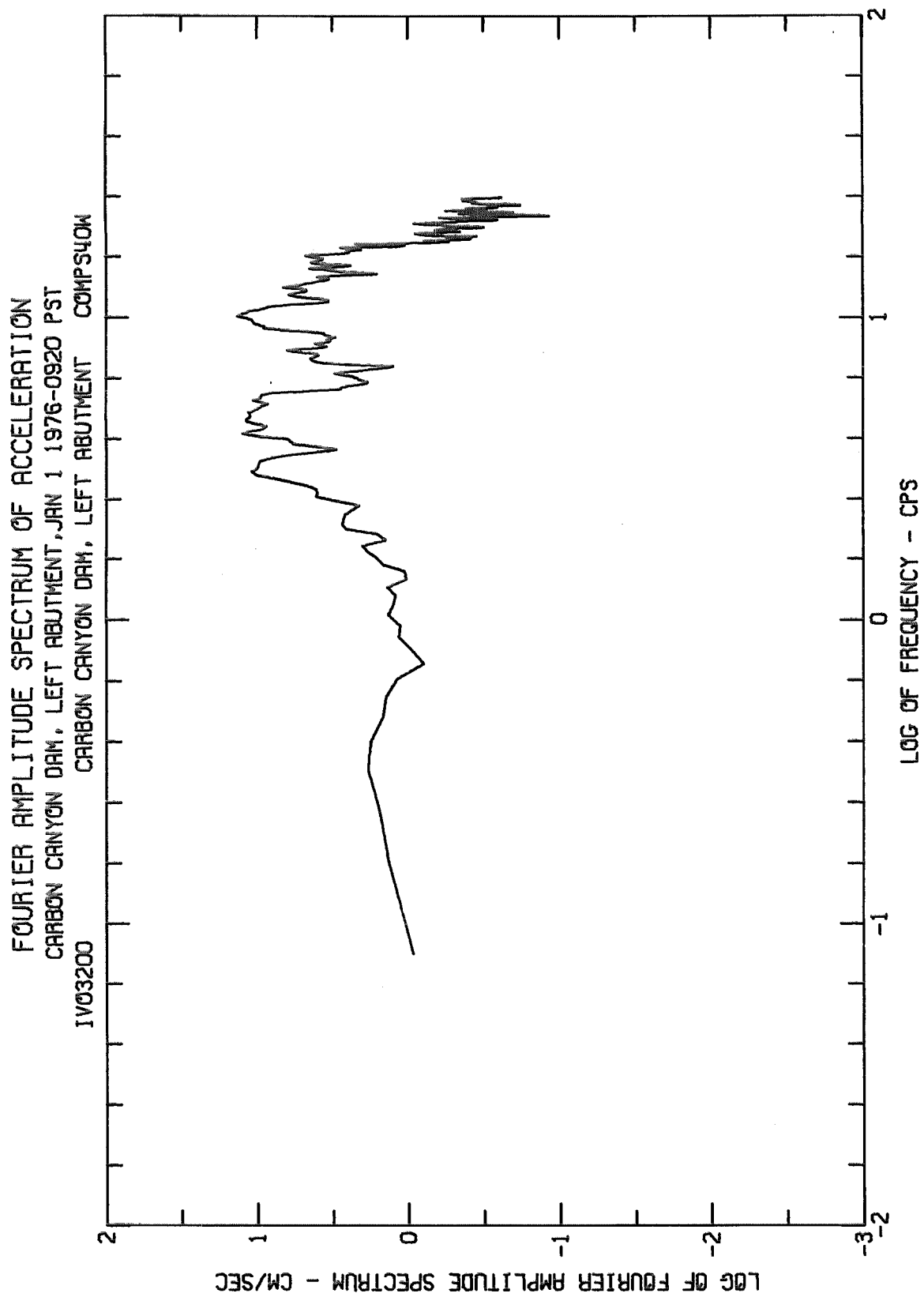


Fig. 51-b

FOURIER AMPLITUDE SPECTRUM OF ACCELERATION
CARBON CANYON DAM, LEFT ABUTMENT, JAN 1 1976-0920 PST
IV03200 CARBON CANYON DAM, LEFT ABUTMENT COMPN50W

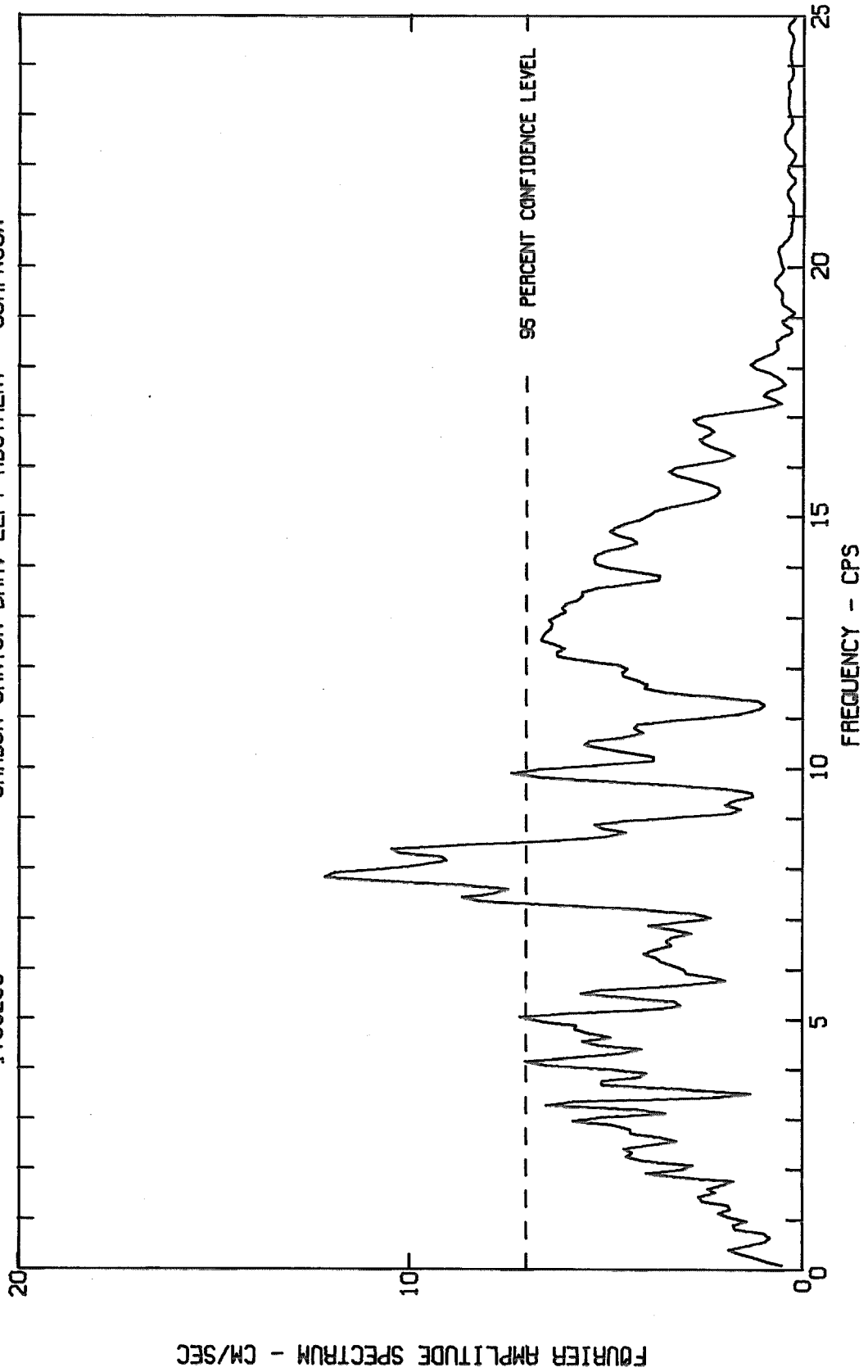


Fig. 52-a

FOURIER AMPLITUDE SPECTRUM OF ACCELERATION
CARBON CANYON DAM, LEFT ABUTMENT, JAN 1 1976-0920 PST
IV03200 CARBON CANYON DAM, LEFT ABUTMENT COMPNSOW

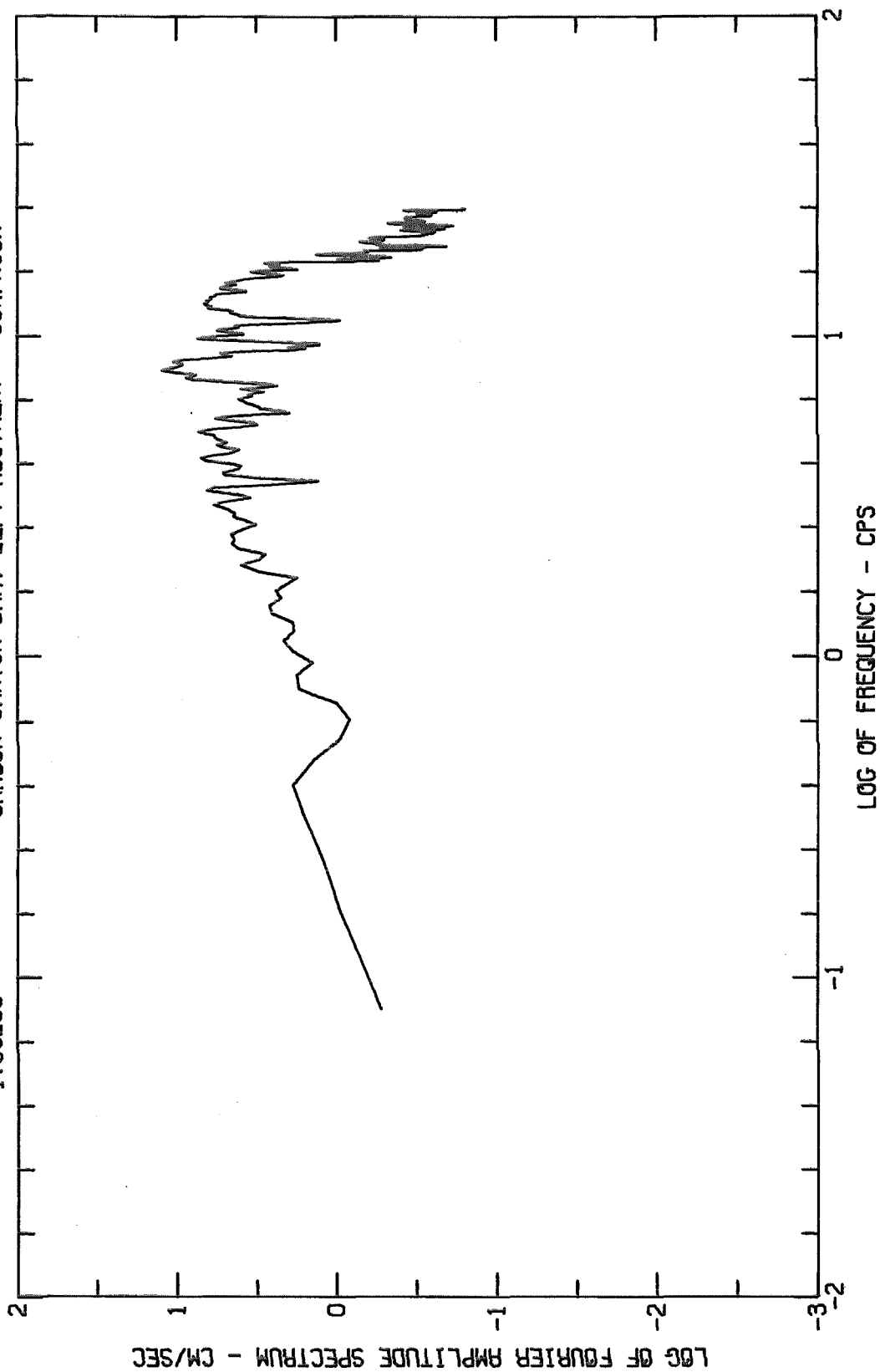


Fig. 52-b

FOURIER AMPLITUDE SPECTRUM OF ACCELERATION
CARBON CANYON DAM, LEFT ABUTMENT, JAN 1 1976-0920 PST
IV03200 CARBON CANYON DAM, LEFT ABUTMENT COMPDOWN

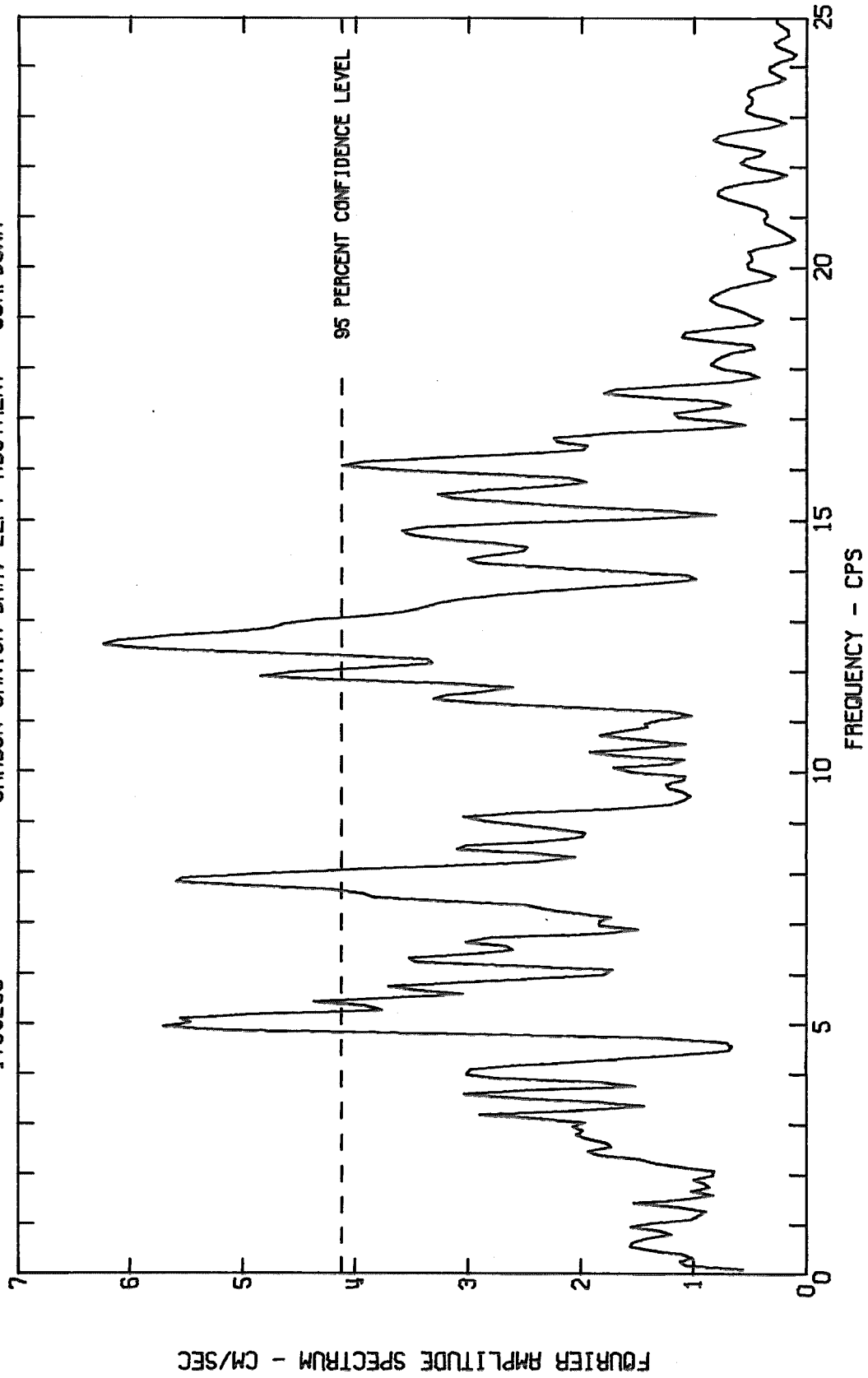


Fig. 53-a

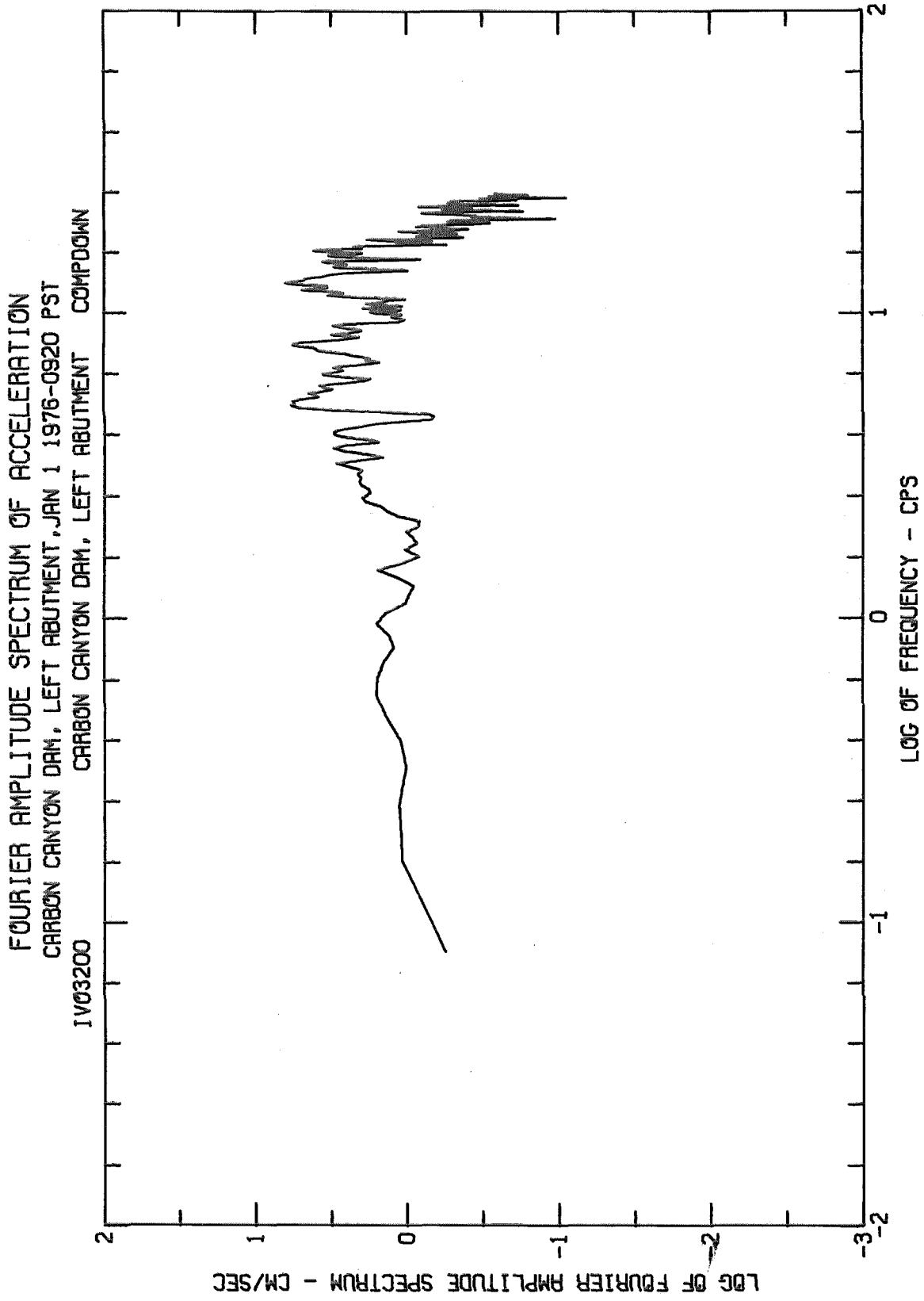


Fig. 53-b

FOURIER AMPLITUDE SPECTRUM OF ACCELERATION
CARBON CANYON DAM, CREST, JAN 1 1976-0920 PST
IV03300 CARBON CANYON DAM, CREST COMPS40W

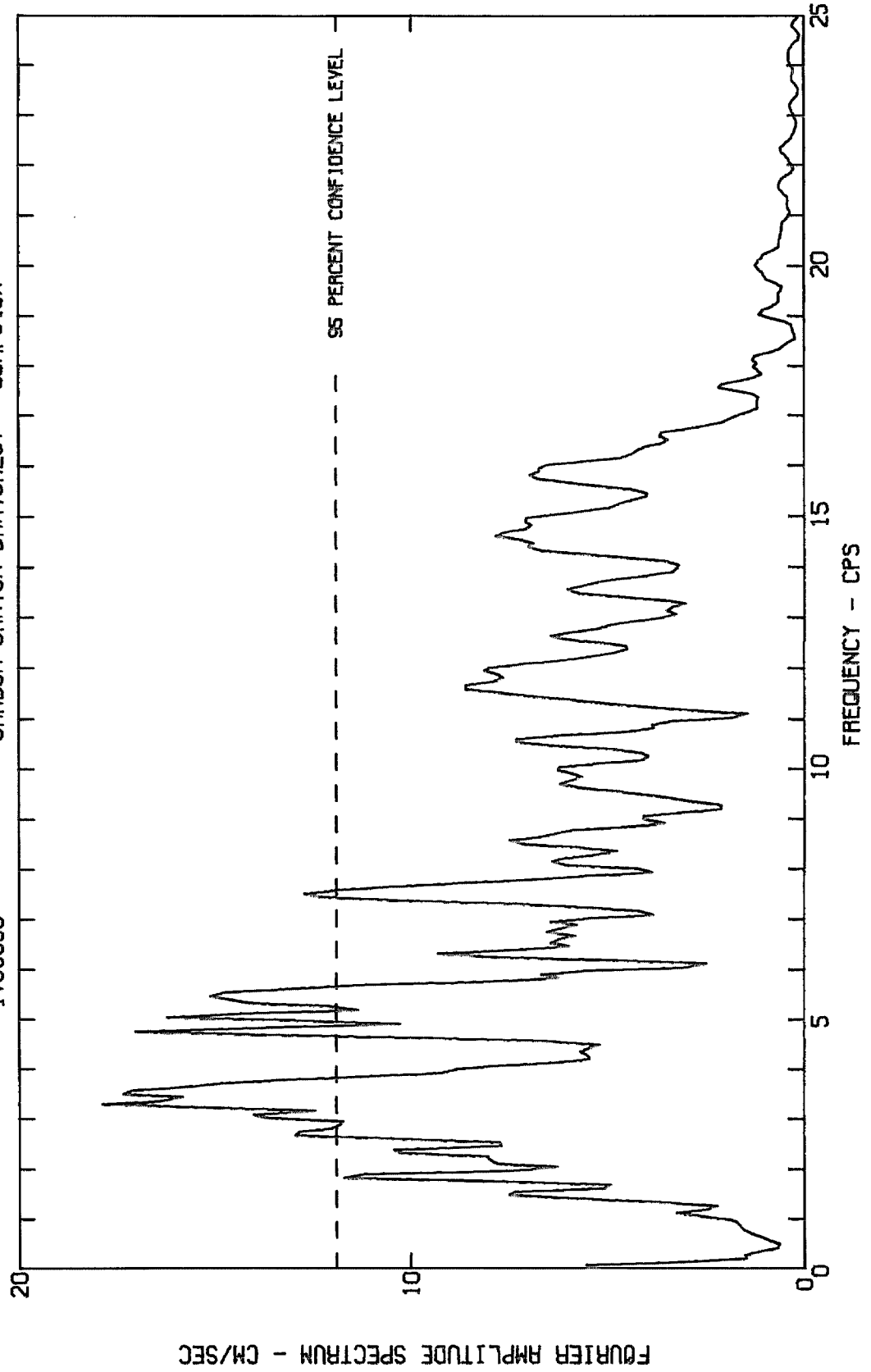
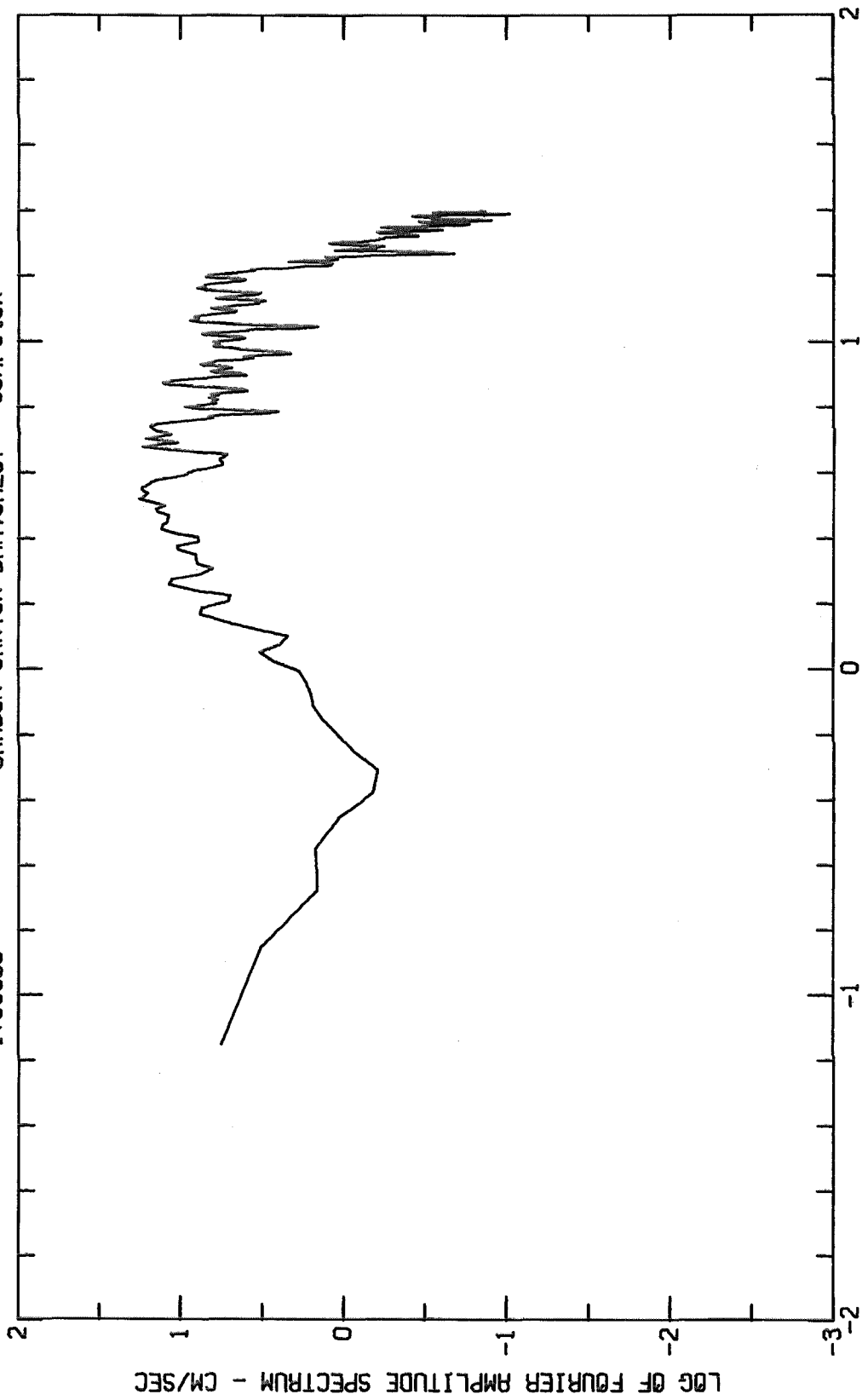


Fig. 54-a

FOURIER AMPLITUDE SPECTRUM OF ACCELERATION
CARBON CANYON DAM, CREST, JAN 1 1976-0920 PST
1V03300 CARBON CANYON DAM, CREST COMPS40W



LOG OF FREQUENCY - CPS

Fig. 54-b

FOURIER AMPLITUDE SPECTRUM OF ACCELERATION
CARBON CANYON DAM, CREST, JAN 1 1976-0920 PST
1V03300 CARBON CANYON DAM, CREST COMPNS0W

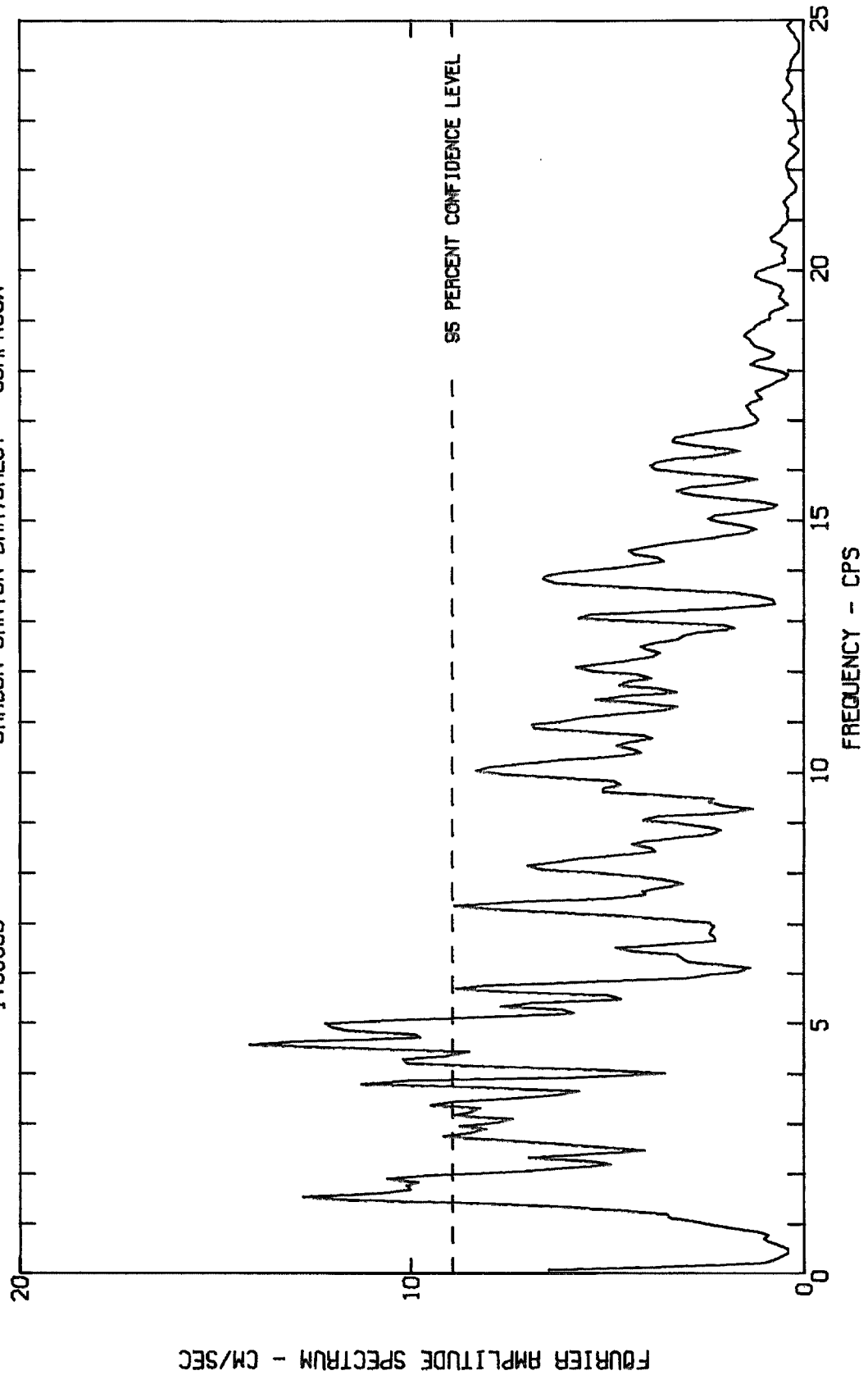
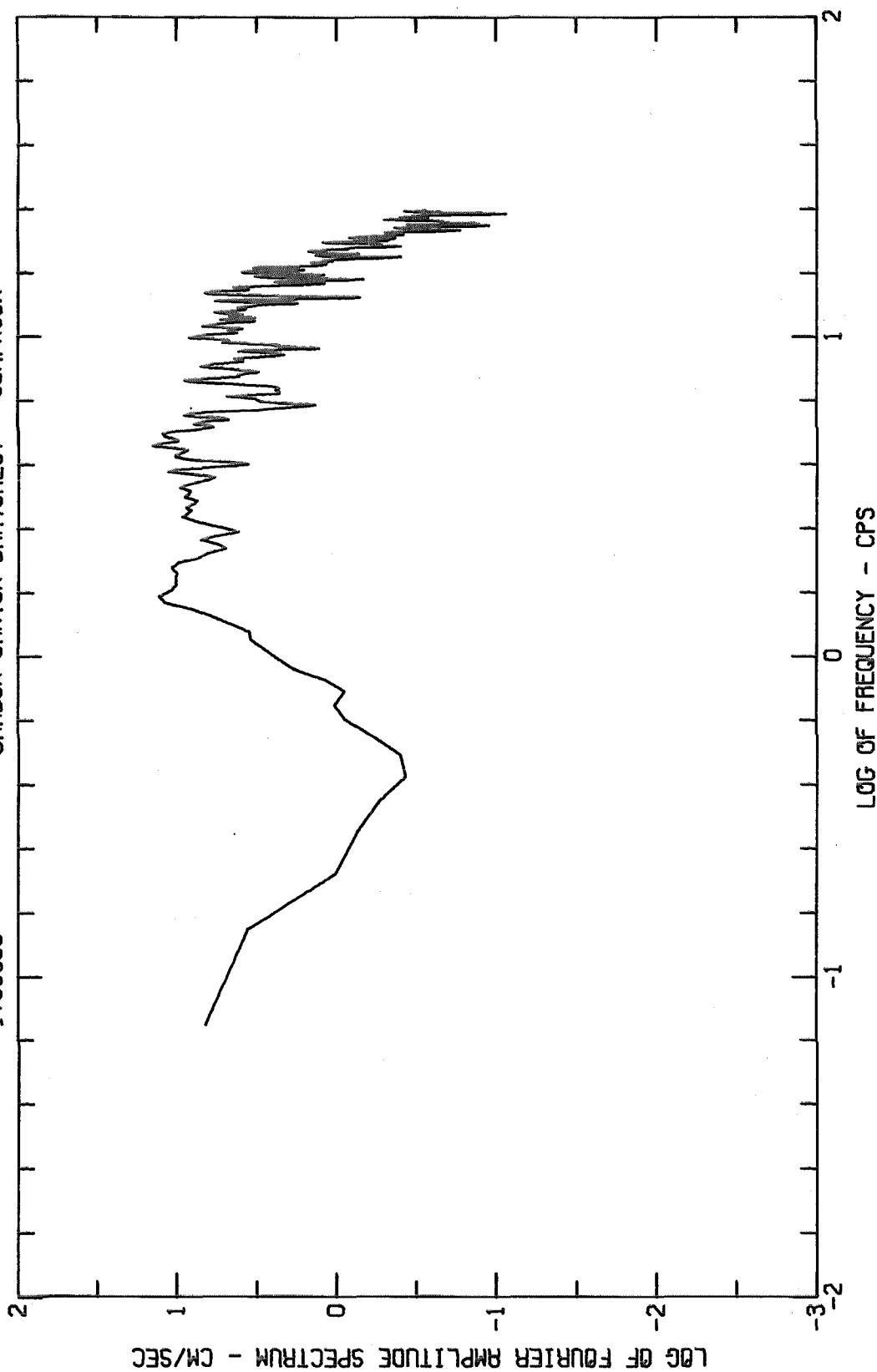


Fig. 55-a

FOURIER AMPLITUDE SPECTRUM OF ACCELERATION
CARBON CANYON DAM, CREST, JAN 1 1976-0920 PST
IV03300 CARBON CANYON DAM, CREST COMPNSOW



LOG OF FREQUENCY - CPS

Fig. 55-b

FOURIER AMPLITUDE SPECTRUM OF ACCELERATION
CARBON CANYON DAM, CREST, JAN 1 1976-0920 PST
1V03300 CARBON CANYON DAM, CREST COMDOWN

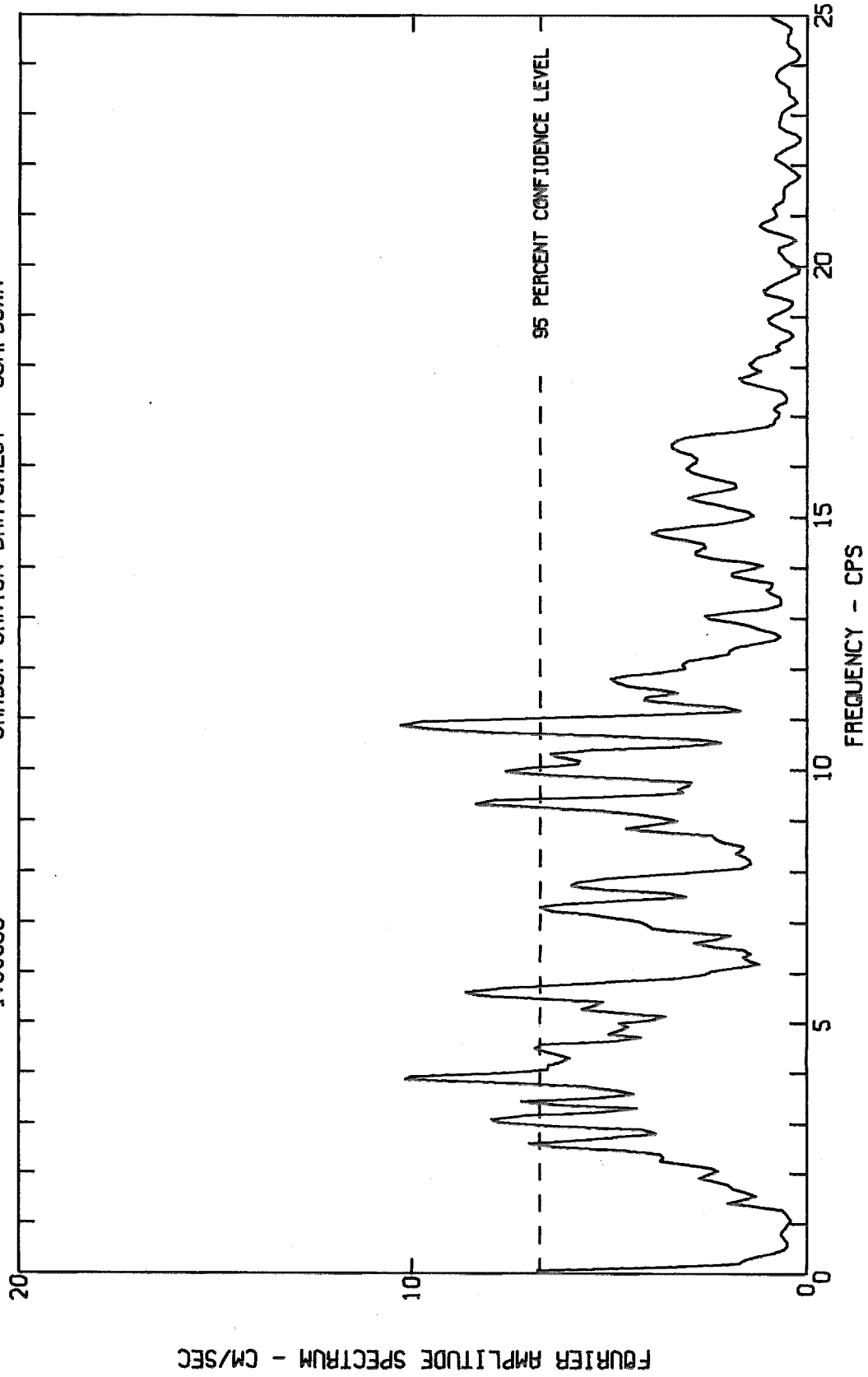
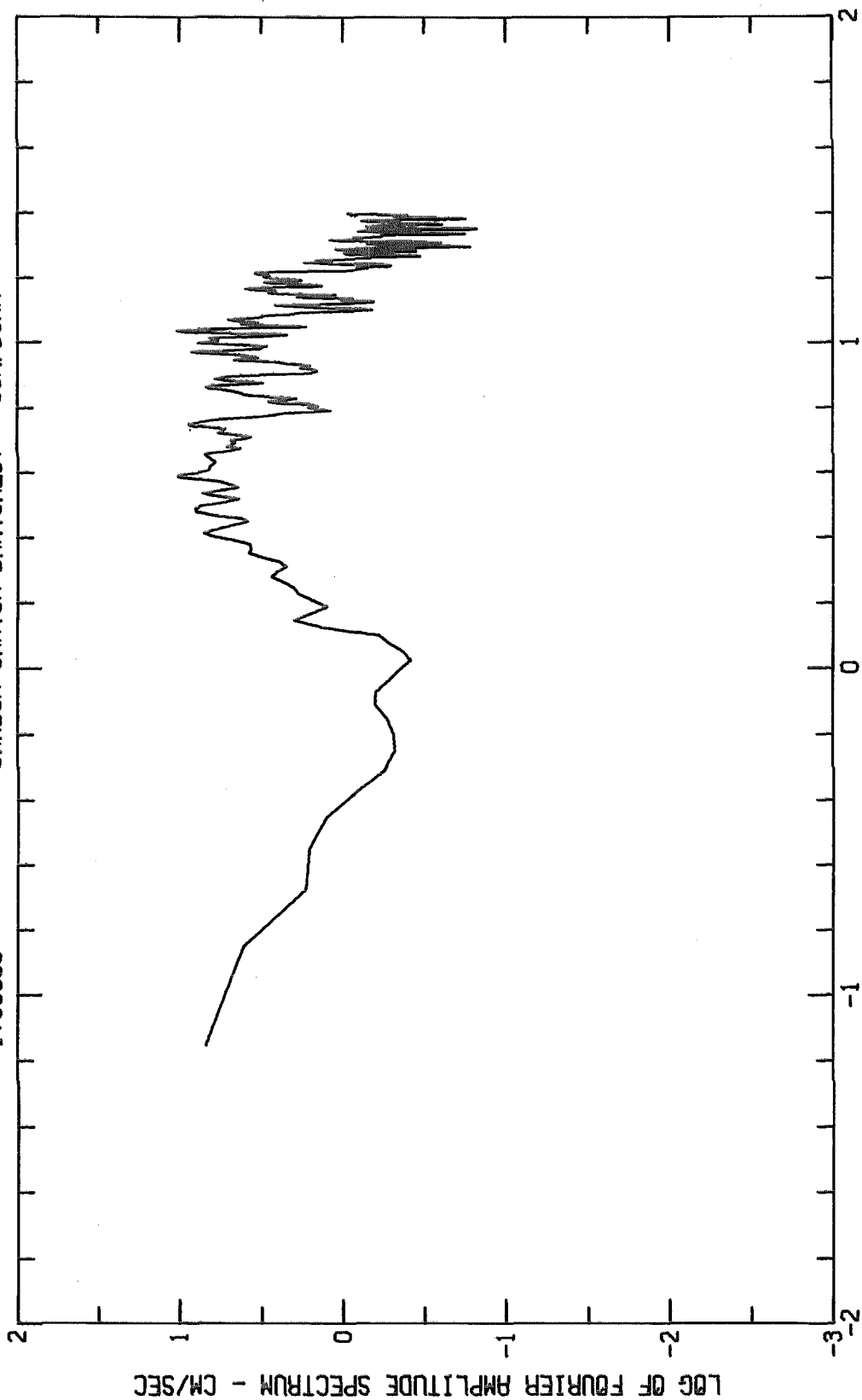


Fig. 56-a

FOURIER AMPLITUDE SPECTRUM OF ACCELERATION
CARBON CANYON DAM, CREST, JAN 1 1976-0920 PST
IV03300 CARBON CANYON DAM, CREST COMPDOWN



LOG OF FREQUENCY - CPS
Fig. 56-b

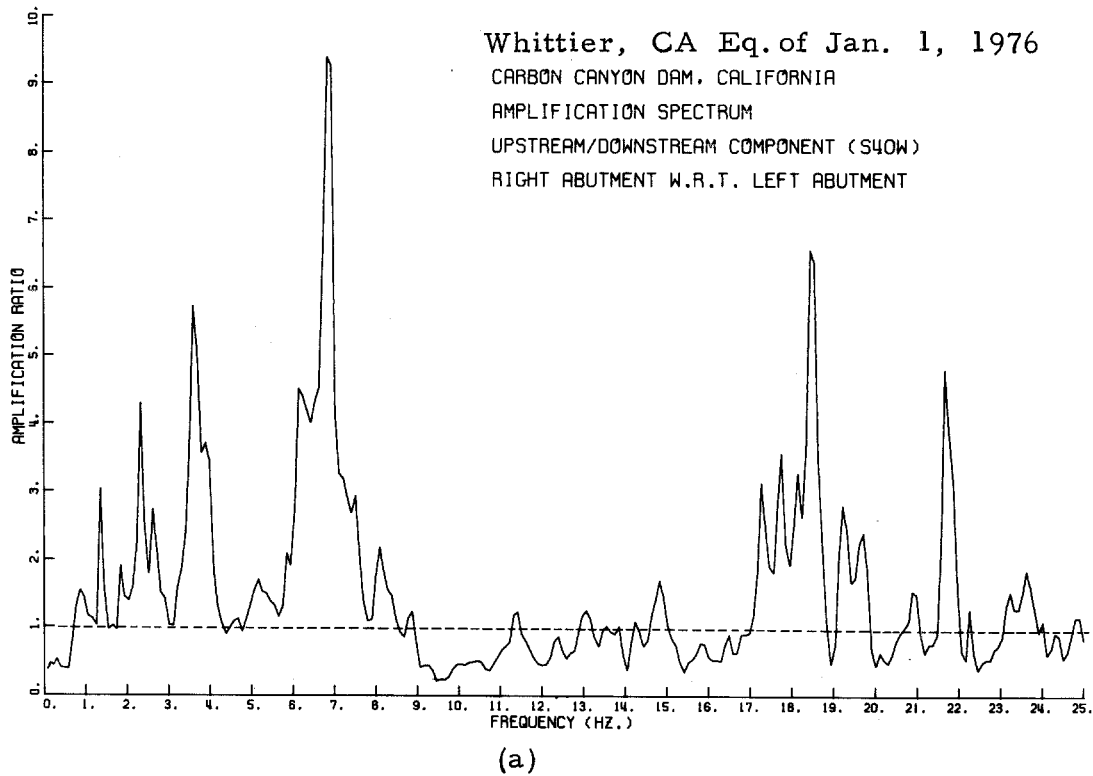
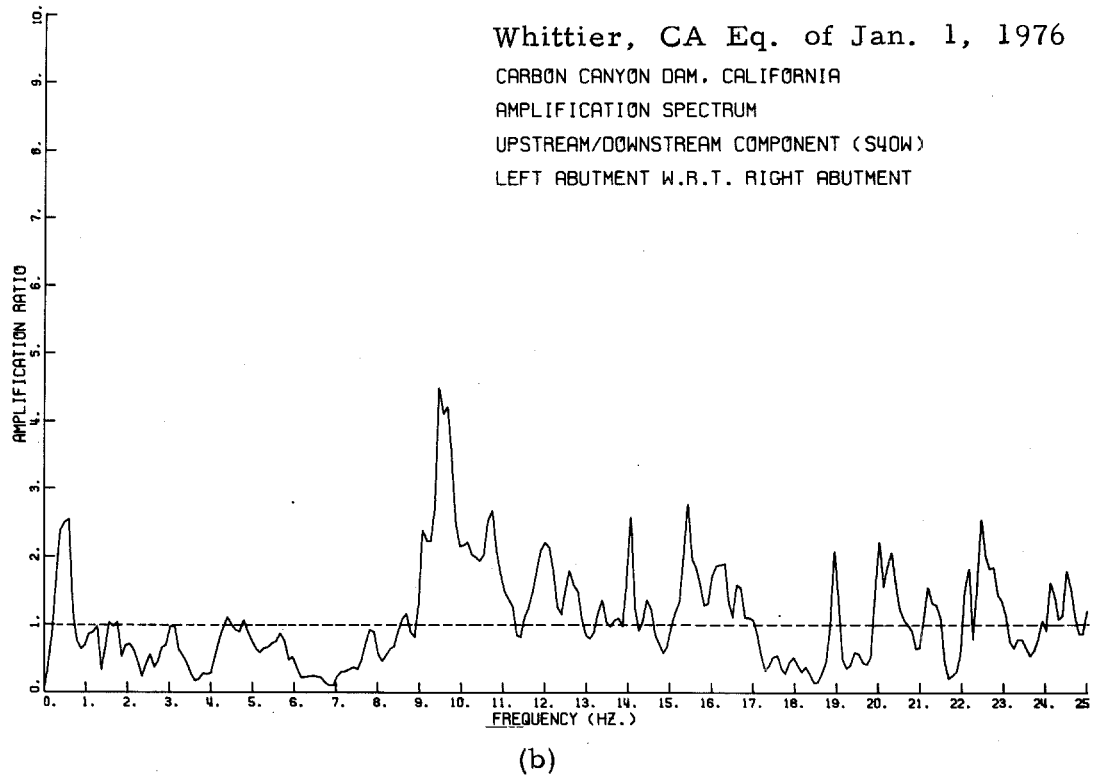


Fig. 57

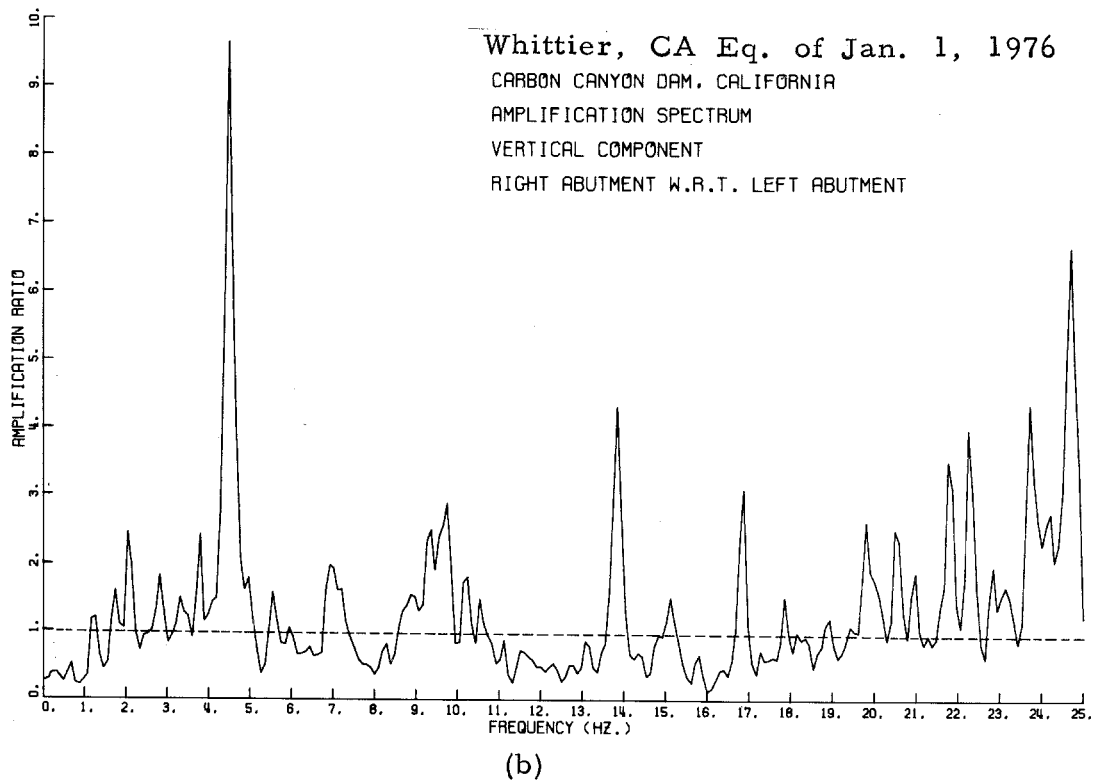
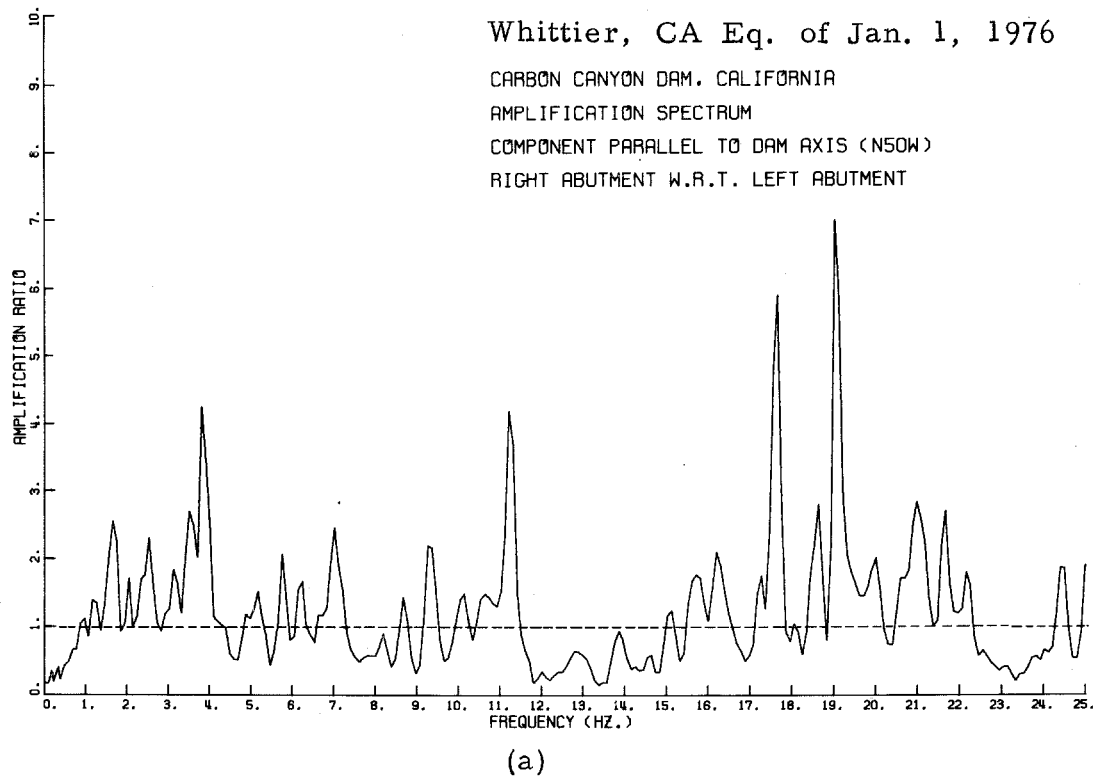


Fig. 58

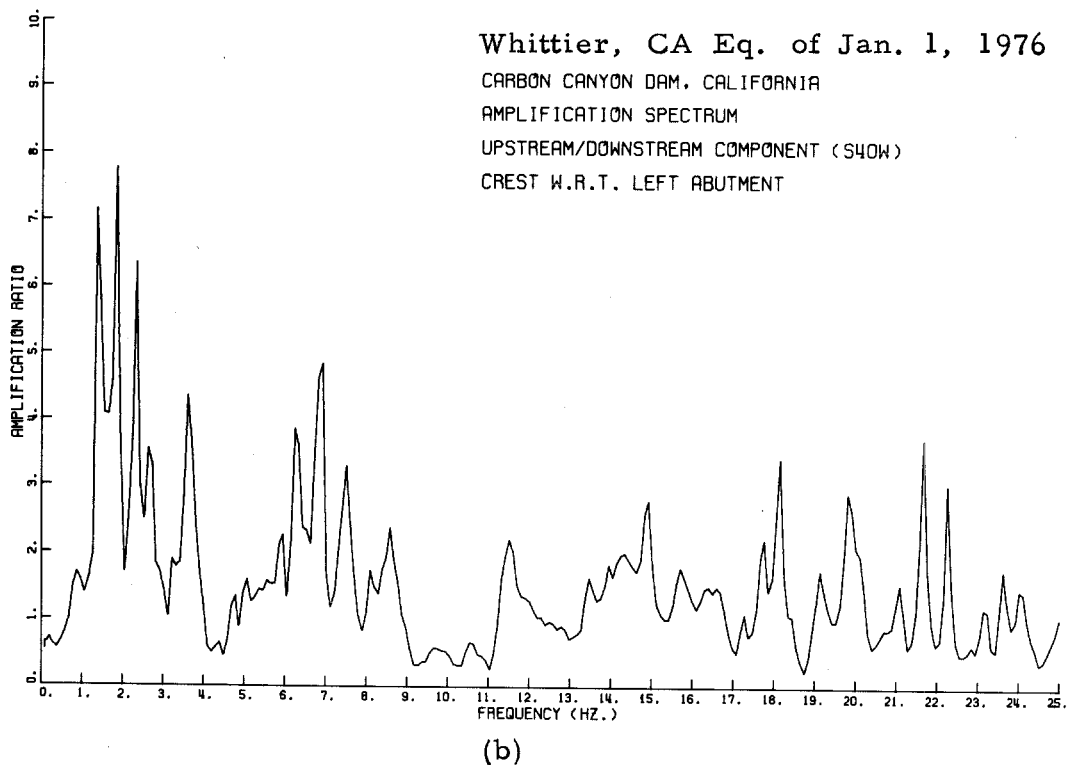
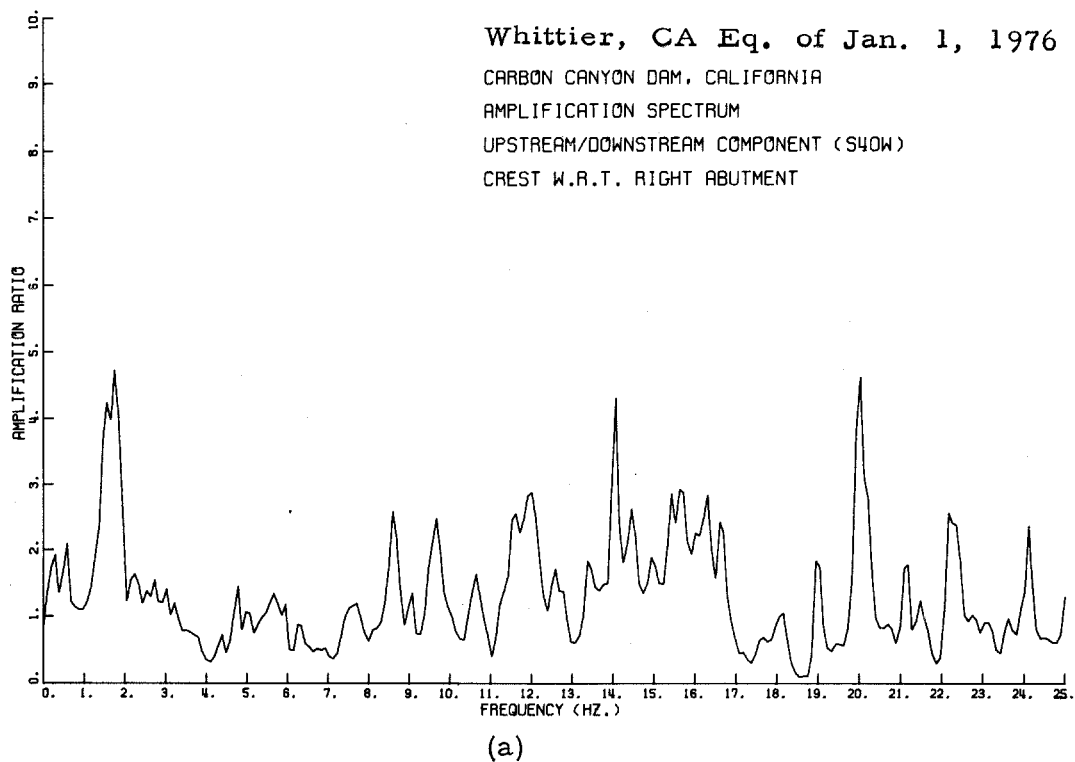


Fig. 59

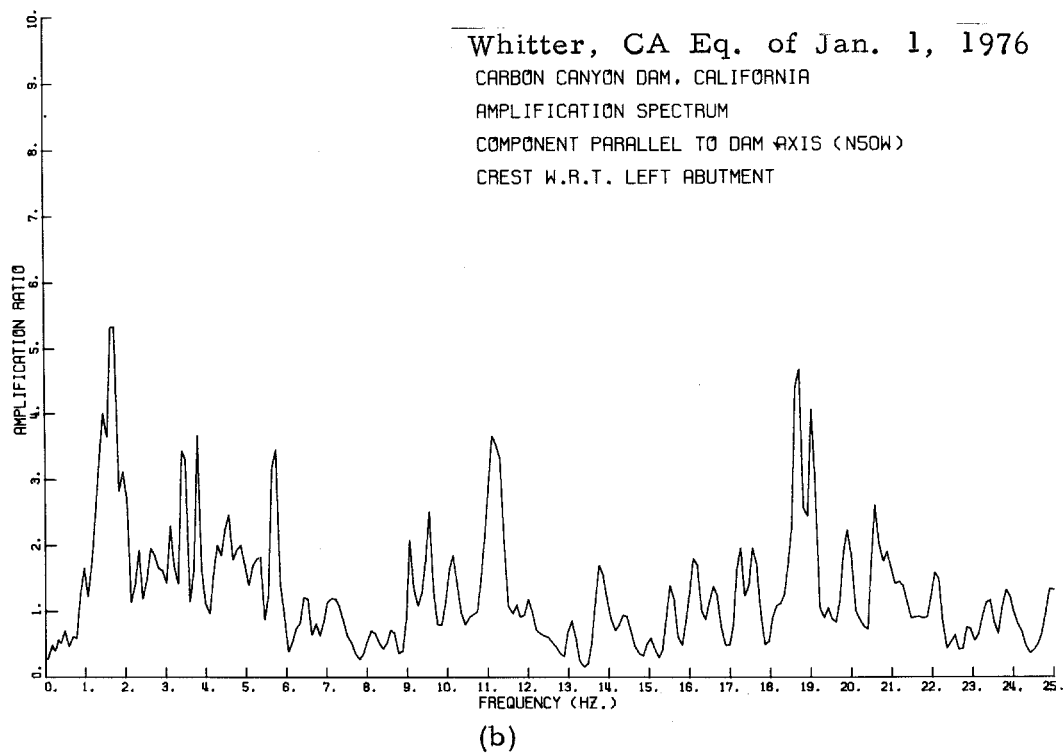
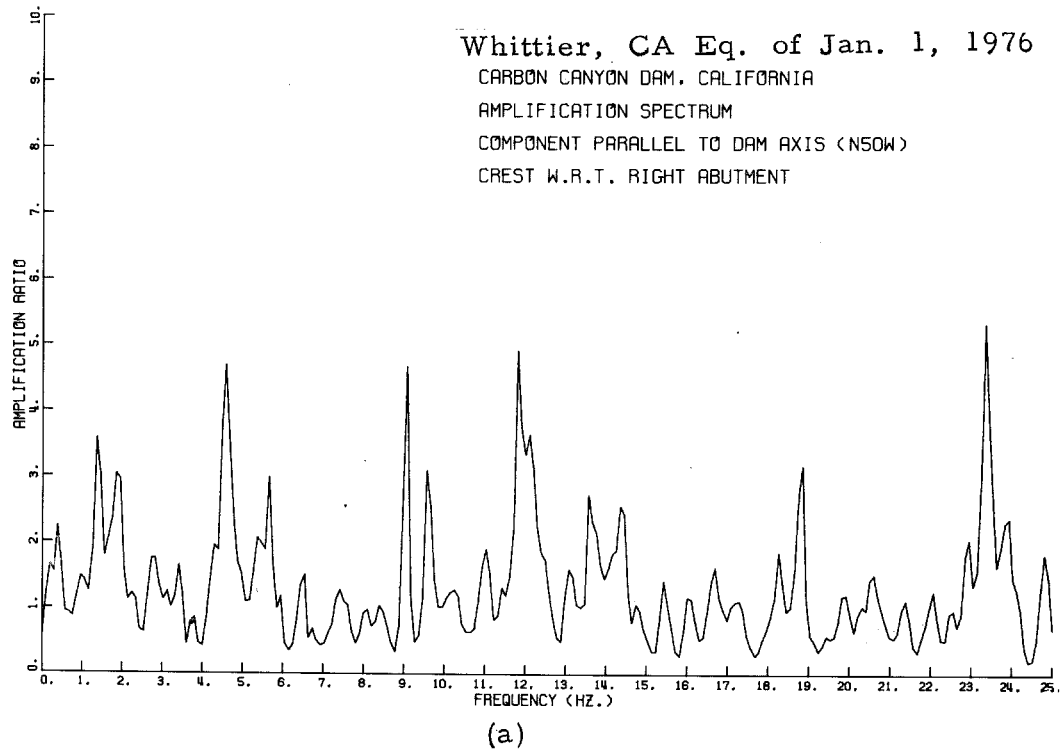
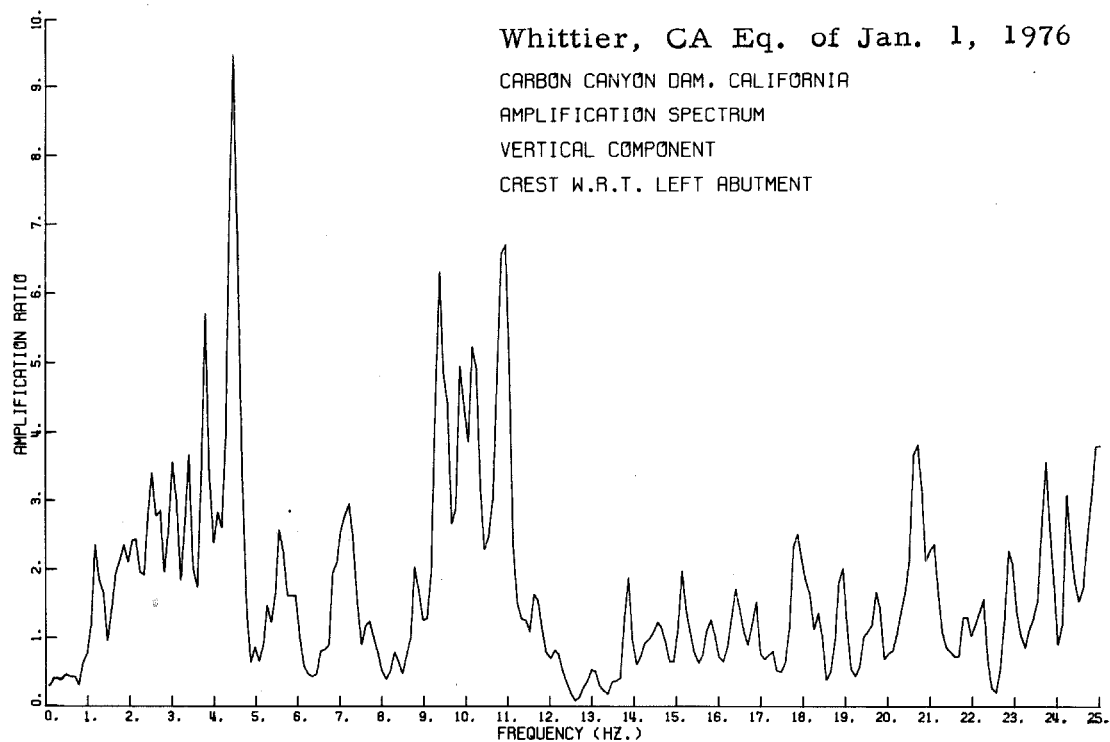
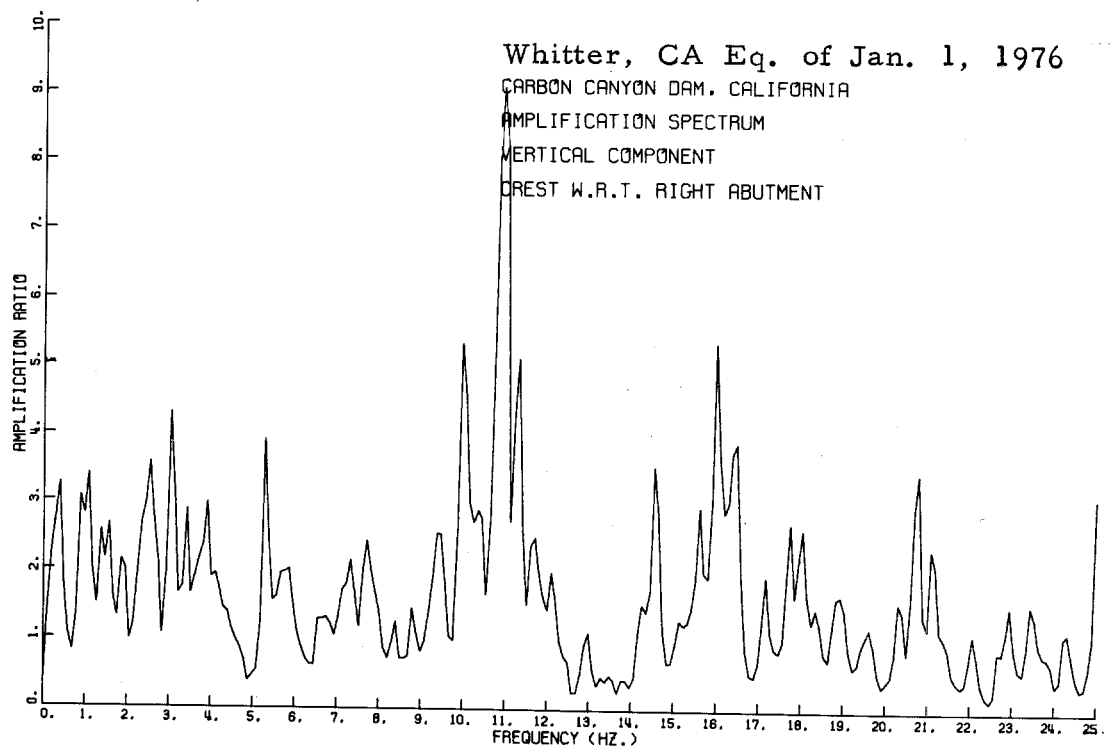


Fig. 60



(b)



(a)

Fig. 61

TABLE 5

Fourier Amplitude Spectrum of Acceleration						Amplification Spectrum						Modal Identification					
Right Abut. Whittier, 1976		Left Abut. Whittier, 1976		Crest Whittier, 1976		Crest S.F. 1971		Crest w.r.t. Right Abut.		Crest w.r.t. Left Abut.			Left Abut. w.r.t. Right Abut.		Right Abut. w.r.t. Left Abut.		
Freq. Hz	Amplit. cm/sec	Freq. Hz	Amplit. cm/sec	Freq. Hz	Amplit. cm/sec	Freq. Hz	Amplit. cm/sec	Freq. Hz	Ampl. Ratio	Freq. Hz	Ampl. Ratio		Freq. Hz	Ampl. Ratio	Freq. Hz	Ampl. Ratio	
2.3	6			1.56	8	1.37	13	1.56	4.2	1.37	7.2	1.37	3.0	1.37	3.0	Interference from 1st long. Mode First Mode Second Mode Third Mode Fourth Mode Fifth Mode Sixth Mode Seventh Mode Eighth Mode Ninth Mode Tenth Mode	
				1.86	12	1.75	15	1.76	4.7	1.56	4		1.86	1.9	1.86		1.9
				2.0	7.5	2.0	29	2.25	1.6	2.25							
2.75 3.0	9 10			2.34	10	2.34	28	2.63	1.3	2.34	6.4	2.34	4.3	2.34	4.3	Sixth Mode Seventh Mode Eighth Mode Ninth Mode	
				2.75	13	2.75	20	2.73	1.55	2.63	3.56		2.63	2.74	2.63		2.74
		3.0	11	3.0	13	3.0	34	3.0	1.3	3.0	1.2		3.0		3.0		1.2
3.3 3.5	22 21			3.3	18	3.2	55	3.2	1.2	3.2	1.9	3.2		3.2		Tenth Mode	
				3.5	17	3.3	32	3.2	1.2	3.2							
3.7	21			3.75	27	3.75	27	3.61	4.4	3.61	4.4	3.61	5.7	3.61	5.7		
4.0	25	4.1	13	4.0	8	4.0	78						3.7	3.91	3.7		

TABLE 6

Observed Natural Frequencies from the Fourier Amplitude Spectra and the Amplification Spectra
Whittier, California Earthquake of Jan. 1, 1976, Carbon Canyon Dam
Component Parallel to Dam Axis (N50° W)

Fourier Amplitude Spectrum of Acceleration						Amplification Spectrum						Modal Identification				
Right Abut. Whittier, 1976		Left Abut. Whittier, 1976		Crest Whittier, 1976		Crest S.F. 1971		Crest w.r.t. Right Abut.		Crest w.r.t. Left Abut.			Left Abut. w.r.t. Right Abut.		Right Abut. w.r.t. Left Abut.	
Freq. Hz	Amplit. cm/sec	Freq. Hz	Amplit. cm/sec	Freq. Hz	Amplit. cm/sec	Freq. Hz	Amplit. cm/sec	Freq. Hz	Ampl. Ratio	Freq. Hz	Ampl. Ratio		Freq. Hz	Ampl. Ratio	Freq. Hz	Ampl. Ratio
1.66	6			1.37 1.47	9 12	1.37 1.47	21 12	1.37	3.6	1.47	4.0			1.66	2.6	First Mode Second Mode
2.05	4.5			1.75 1.86	10 11	1.75 1.86	17 17	1.86	3.0	1.76	5.3					Third Mode Fourth Mode
2.5	9	1.9	3.5							1.95	3.1			2.05	1.7	Fifth Mode
		2.2	4	2.3	7	2.3	38	2.3	1.3	2.3	1.9			2.5	2.3	Sixth Mode
				2.8 3.15	9 9	2.64 3.15	44 40	2.8 3.15	1.8 1.3	2.64 3.15	1.96 2.3			3.15	1.8	Seventh Mode Eighth Mode Ninth Mode
3.2	8	3.0 3.2	6 7	3.2 3.4	9 10	3.45	37	3.4	1.66	3.4	3.4			3.6	2.7	Tenth Mode

TABLE 7

Comparison Between Observed Resonant Frequencies
and Those Computed by 2-D Shear Beam Theory
Whittier, California Earthquake of Jan. 1, 1976
Carbon Canyon Dam
Upstream/Downstream Direction (S40°W)

Computed Natural Frequencies [Equation (1)]			Difference Between Two Adjacent Frequencies (Hz)	Observed Natural Frequencies (Hz)	Remarks
Symmetric	Antisymmetric				
$f_{n,r}$	Hz	$f_{n,r}$	Hz		
$f_{1,1}$	1.56*	$f_{1,2}$	1.58	1.56	* only observed Computed
$f_{1,3}$	1.60	$f_{1,4}$	1.64	-	"
$f_{1,5}$	1.68			-	"
$f_{1,7}$	1.80	$f_{1,6}$	1.73		"
$f_{1,9}$	1.94	$f_{1,8}$	1.86	1.76	"
$f_{1,11}$	2.10	$f_{1,10}$	2.02	1.86	"
$f_{1,13}$	2.28	$f_{1,12}$	2.19	2.25	"
$f_{1,15}$	2.47	$f_{1,14}$	2.38	2.34	"
$f_{1,17}$	2.68	$f_{1,16}$	2.58	2.63	"
$f_{1,19}$	2.89	$f_{1,18}$	2.78	2.73	"
$f_{1,21}$	3.11	$f_{1,20}$	3.00	3.00	"
$f_{1,23}$	3.34	$f_{1,22}$	3.22	3.20	"
$f_{2,1}$	3.57	$f_{1,24}$	3.45	-	"
				3.61	"

CHAPTER IV

BREA DAM

IV-1 Description of the Structure

The descriptive information presented in this report was mainly obtained from pertinent data sheets and engineering drawings which were provided by the Army Corps of Engineers, Los Angeles Operations Branch.

Brea Dam, located 32 Km (20 miles) southeast of downtown Los Angeles, was constructed by the Army Corps of Engineers as a flood-control structure across Brea Creek in Orange County California (approximately 15 Km (9.4 miles) east of Brea). The dam, completed in the late 1940's and early 1950's, is part of the comprehensive plan for the Santa Ana River Basin in Orange County.

Principal features of the dam are a zoned earthfill embankment, outlet works and an overflow concrete spillway; Figure 62 shows a detailed embankment cross section. The dam's crest is approximately 538 m (1,765 ft) in length; the effective length of the dam (perpendicular to the flow) is about 213.5 m (700 ft) beyond which the crest continues at the right abutment for an additional length of about 324.5 m (1,065 ft), as shown by Fig. 63. The crest has a height, above the original stream bed, of 26.5 m (87 ft) and a maximum height (including the excavation trench at the center line of the cross section of Fig. 62) of 32.6 m (107 ft); the crest width is 6.1 m (20 ft). The central impervious core is composed of graded material obtained from the core trench excavation and other borrow pits; the shell is constructed of random material obtained

from spillway excavations as well as selected excavation from abutments, foundations and outlet works. The maximum capacity of the reservoir is 5,660 acre-feet at spillway design surcharge level. The direction of the longitudinal axis of the dam is $S40^{\circ}W$, while the upstream/downstream direction is $N50^{\circ}W$ (Fig. 63).

Three SMA-1 accelerographs were installed on the dam and in the immediate vicinity of the dam in June 1975. Figure 63 shows the locations of these three strong-motion accelerographs. One is at the center of the crest of the dam to measure dam response, a second is mounted on the dam's left abutment to record earthquake motion in the foundation, and the third one is placed at an appropriate site (downstream) to also record input earthquake ground motion. During the Whittier earthquake of January 1, 1976 the crest and downstream instruments provided records, but the left abutment accelerograph was inoperative. The dam was about 9.3 Km southeast of the epicenter.

IV-2 Time Domain Analysis

The three accelerographs on and around Brea Dam were not interconnected for simultaneous starting, but a comparison of S-wave minus trigger intervals indicates that the crest and downstream instruments triggered within 0.3 seconds of one another, as shown in Table 1. The crest accelerograph recorded a maximum peak acceleration of 0.12 g (Vol. I) along the axis of the dam ($S40^{\circ}W$). The downstream accelerograph recorded a maximum acceleration of 0.09 g in the upstream/downstream direction ($N50^{\circ}W$); the maximum

peak acceleration in the $S40^{\circ}W$ direction was only 0.06 g (50% less than the value recorded at the crest in the same direction).

The crest record, on 70-mm film, was about 15 seconds long and the downstream record was about 13 seconds. In digitizing and processing these records, only about 6 seconds of the crest record (where the significant shaking occurred) was used, while the whole 13 seconds of the downstream record was used. The uncorrected (raw) digitized data of the two records are shown in Figs. 64-a and b. The corrected acceleration and the computed velocity and displacement are shown in Figs. 65-a through 66-c.

The computed velocity curve from the crest accelerogram in the upstream/downstream direction (Fig. 66-a) shows that, during the first two seconds of the record, the dam responded in its fundamental mode with an apparent period of about 0.36 seconds (2.8 Hz); this was followed by a mixture of different higher mode responses. In the direction parallel to the longitudinal axis of the dam ($S40^{\circ}W$), the computed velocity curve transverse to the crest (Fig. 66-b) shows an apparent fundamental period of about 0.38 seconds (2.63 Hz). The vertical component (Fig. 66-c) would indicate a period of about 0.34 seconds (2.97 Hz) for the vertical fundamental period.

IV-3 Frequency Domain Analysis

The response spectrum curves (linear and logarithmic plots) of the two records are shown in Figs. 67 through 72; the Fourier amplitude spectrum curves (linear and logarithmic) are shown in Figs. 73 through 78. Amplification spectra of the dam were computed for the three components by dividing the Fourier amplitude

spectrum of the acceleration recorded on the crest by the spectrum of the motion recorded by the downstream accelerograph (see Figs. 79 and 80). Tables 8 and 9 show the resonant frequencies associated with the peaks of both the Fourier amplitude spectra (of the crest and downstream records) and the amplification spectra for the two horizontal components. In the upstream/downstream direction ($N50^{\circ}W$) Table 8 indicates that the fundamental frequency is 2.73 Hz, while at the same time Table 9 indicates the same frequency for the fundamental mode in the longitudinal direction ($S40^{\circ}W$). The two Tables (8 and 9) also show amplification ratios of 3.4 and 2.3 at frequencies 0.78 and 1.56 Hz for the $N50^{\circ}W$ component and ratios of 3.34 and 4.98 at frequencies 0.78 and 1.56 Hz for the $S40^{\circ}W$ component. But since there are no peaks in the Fourier spectra of the crest records corresponding to these frequencies, it was decided not to consider them structural frequencies. Presumably, they are due to very low values of the Fourier spectra of the downstream record at these frequencies. It is important to note that due to the short duration of the crest record (about 6 seconds) the frequency resolution of all the Fourier as well as amplification spectra was 0.1953 Hz, which definitely reduced the accuracy of the computed spectra.

The two-dimensional tapered shear-beam theory (frequency equation, Eq. 1, in Chapter III) was used to check the values of the resonant frequencies corresponding to peak values of the amplification spectrum in the upstream/downstream direction and to estimate the shear wave velocity of the dam material. Owing to its irregular

nature, the reservoir was represented by an equivalent rectangle of length l equal to 600 ft and of average height h equal to 97 ft. Substituting values of $f_{1,1} = 2.73$ Hz, $l = 600$ ft and $h = 97$ ft in Eq. 1 (Chapter III) gives a value of $v_s = 677$ ft/sec. Shear wave velocities for dams constructed with central impervious cores of graded material can vary over a wide range (between 400-1200 ft/sec) depending on the nature of the material. Substituting a value of $v_s = 677$ ft/sec in the frequency equation (Eq. 1 of Chapter III) gives estimated natural frequencies (of the higher modes) of the dam. Table 10 illustrates a comparison between observed resonant frequencies and estimated values computed by Eq. 1. The comparison is confined to the symmetric modes of vibration since the crest accelerograph was located at the center of the crest (Fig. 63).

BREA DAM, CALIFORNIA
EMBANKMENT CROSS SECTION

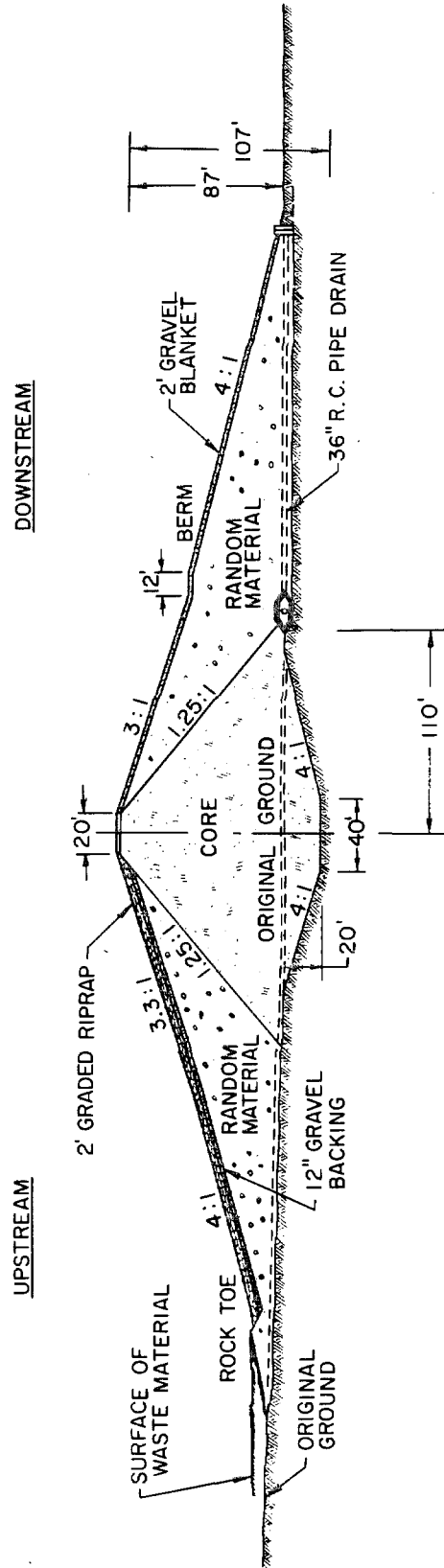


Fig. 62

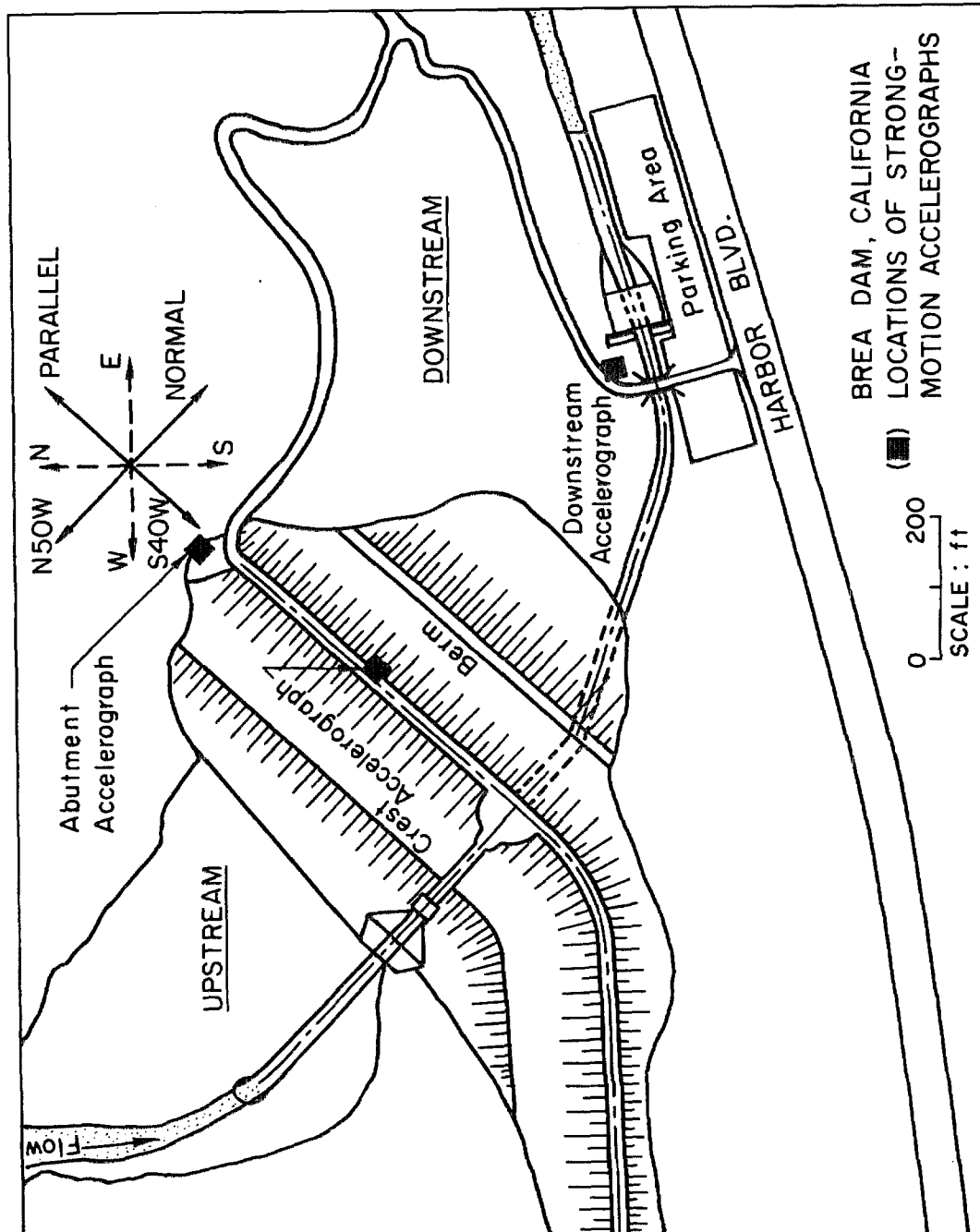


Fig. 63

BREA DAM, DOWN STREAM, E/Q OF 1 JAN 1976 0920 PST

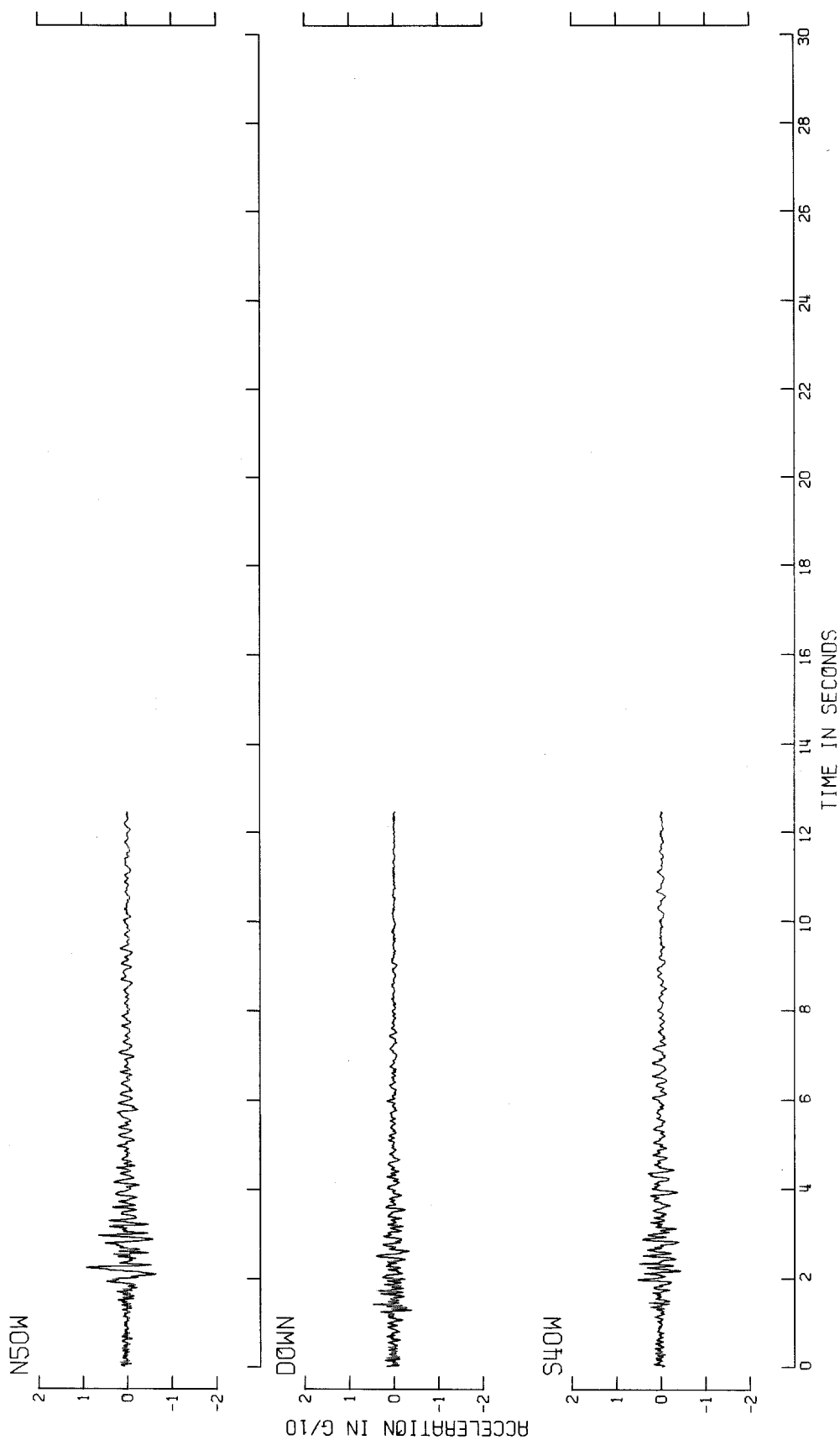


Fig. 64-a Uncorrected Accelerograms (Downstream)

BREA DAM, CREST, E/O OF JAN 1 1976 0920 PST

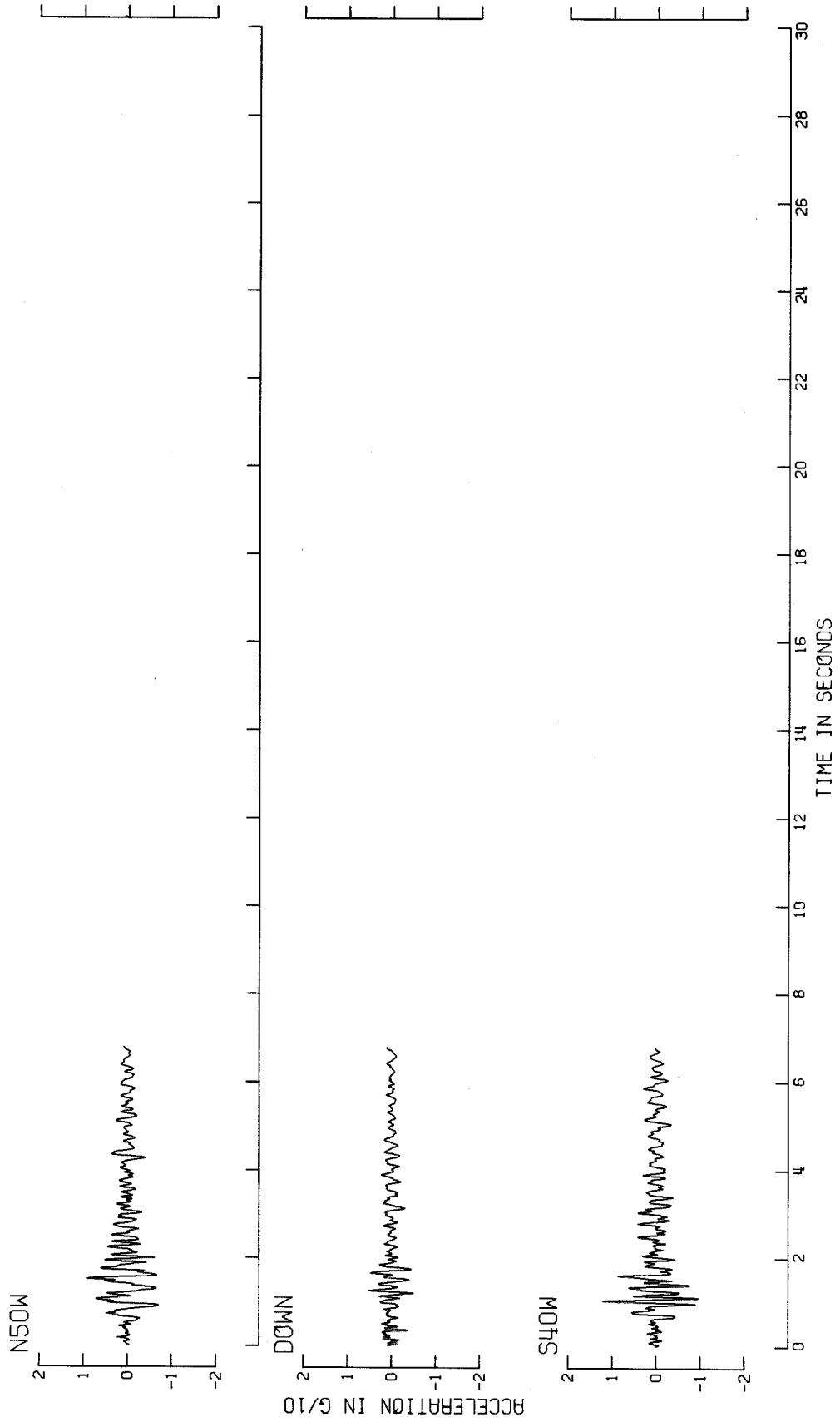


Fig. 64-b Uncorrected Accelerograms (Crest)

BREA DAM, DOWNSTREAM, JAN 1 1976-0920 PST
 IN03700 BREA DAM, DOWNSTREAM COMP50W

PEAK VALUES : ACCEL = -82.7 CM/SEC/SEC VELOCITY = 2.8 CM/SEC DISPL = -.9 CM

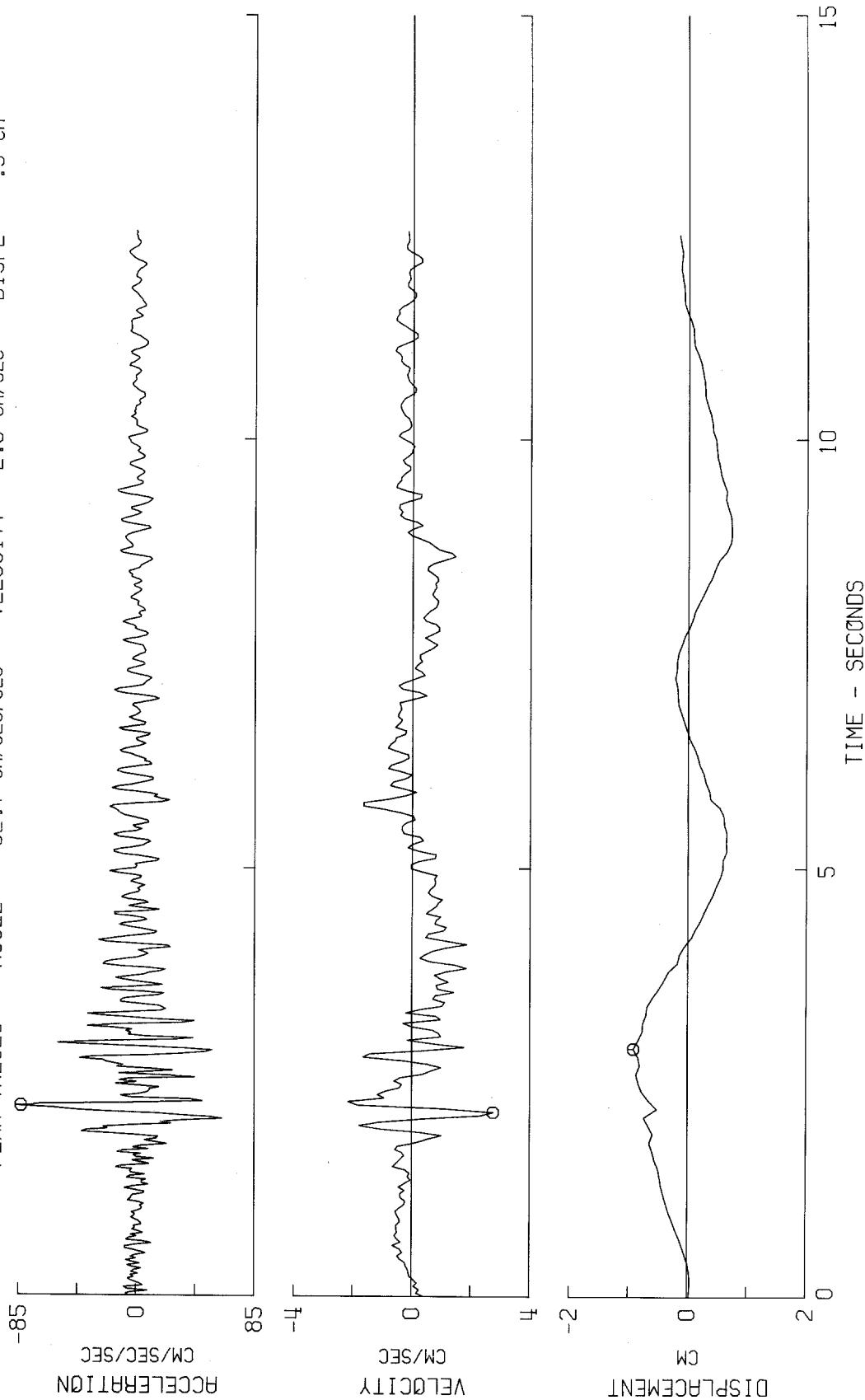


Fig. 65-a

BREA DAM, DOWNSTREAM, JAN 1 1976-0920 PST
IN03700 BREA DAM, DOWNSTREAM COMPS40W
PEAK VALUES : ACCEL = -43.2 CM/SEC/SEC VELOCITY = 1.9 CM/SEC DISPL = -.9 CM

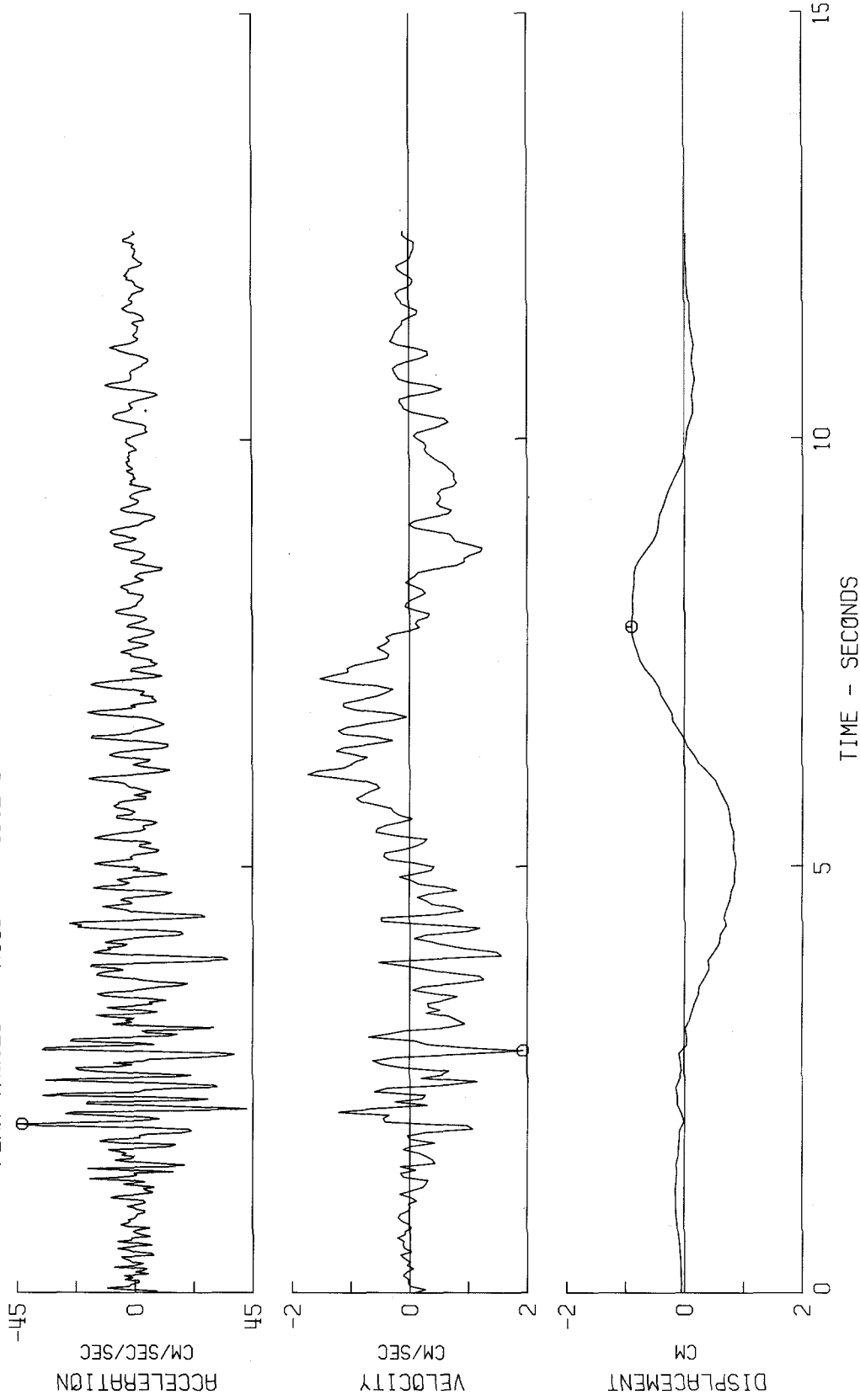
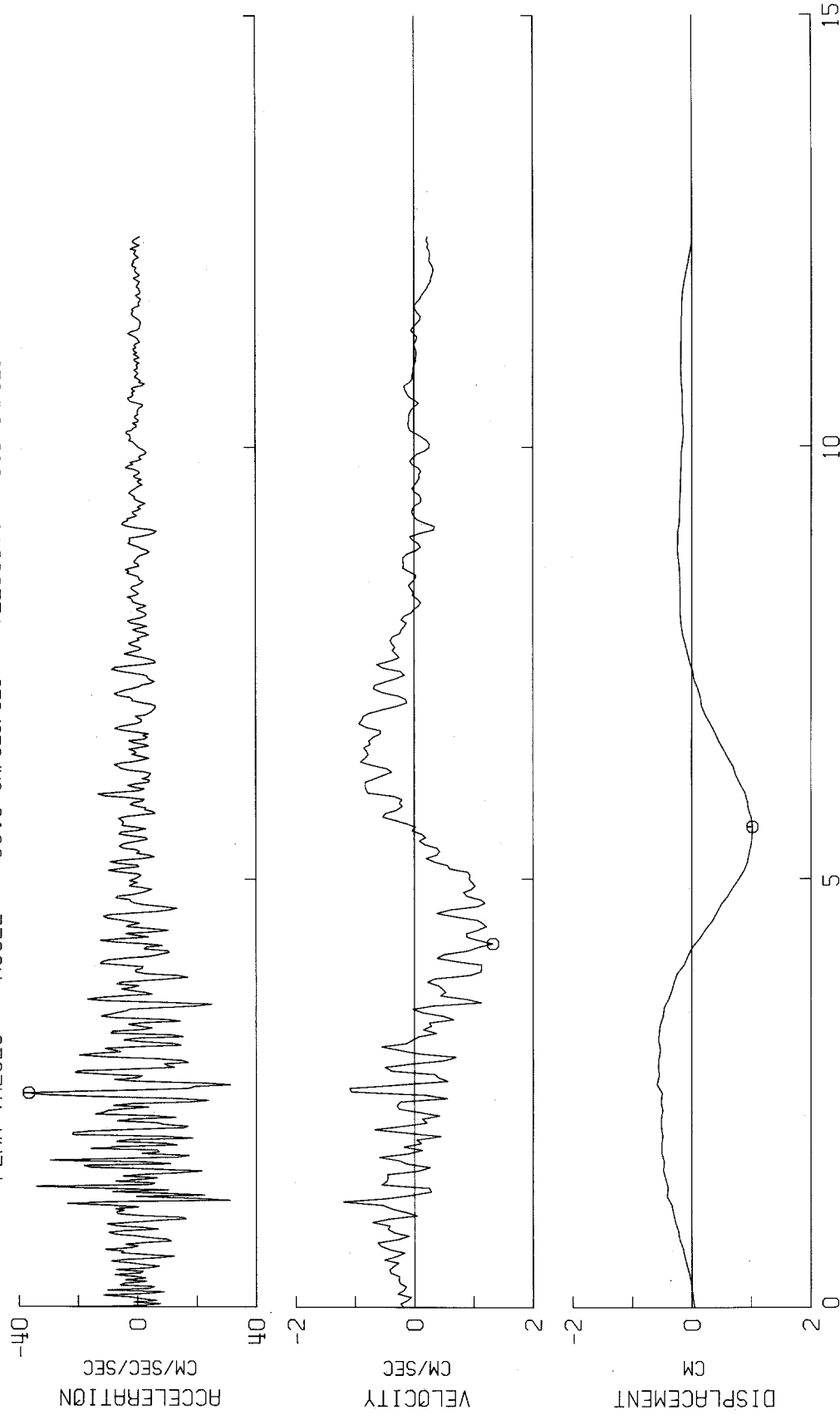


Fig. 65-b

BREA DAM, DOWNSTREAM, JAN 1 1976-0920 PST
IN03700 BREA DAM, DOWNSTREAM COMPDOWN

○ PEAK VALUES : ACCEL = -36.5 CM/SEC/SEC VELOCITY = 1.3 CM/SEC DISPL = 1.0 CM

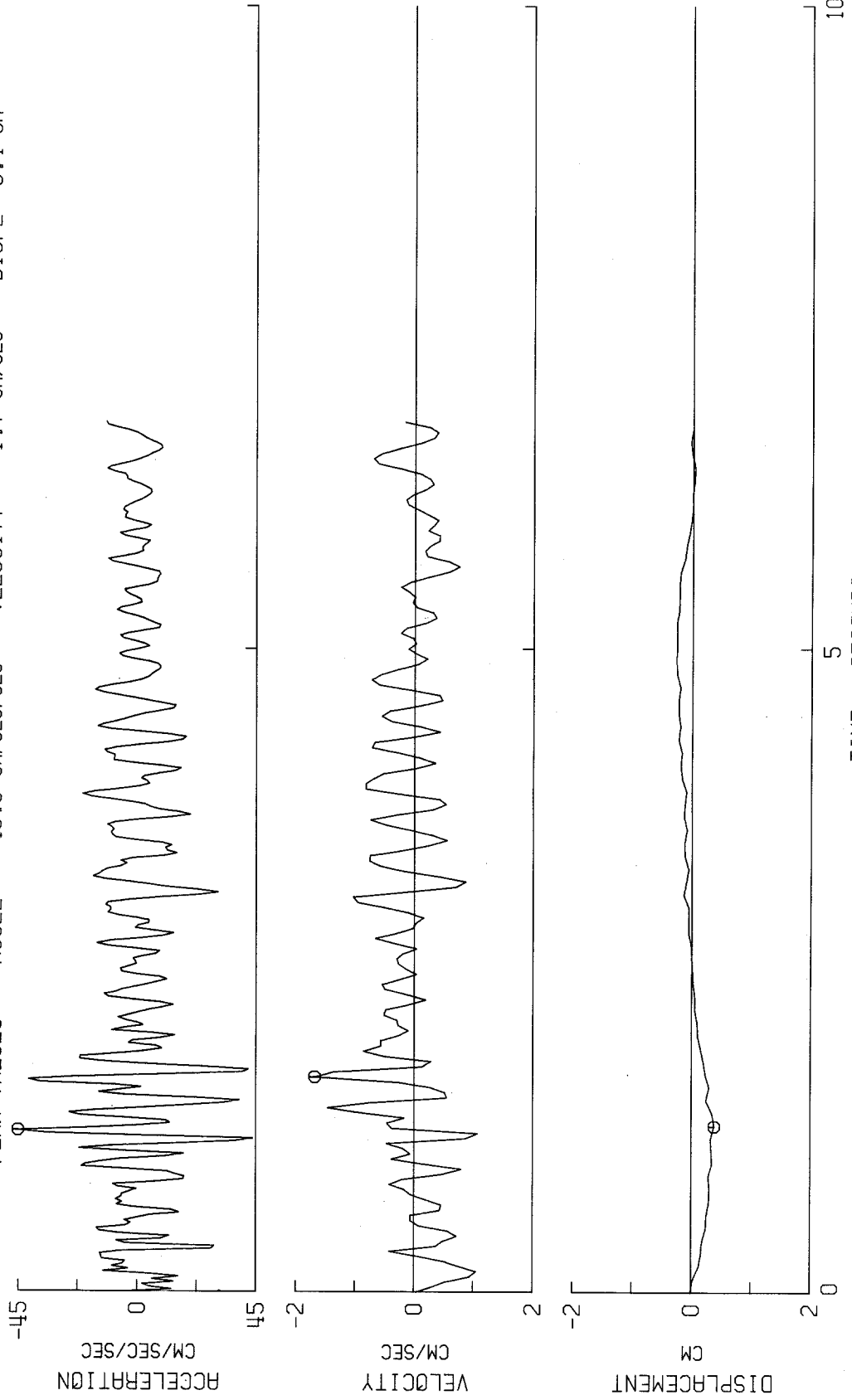


TIME - SECONDS

Fig. 65-c

Pages 155 and 156 are missing.

BREA DAM, CREST, JAN 1 1976-0920 PST
IN03600 BREA DAM, CREST COMPDOWN
PEAK VALUES : ACCEL = -45.0 CM/SEC/SEC VELOCITY = -1.7 CM/SEC DISPL = 0.4 CM



TIME - SECONDS

Fig. 66-c

RELATIVE VELOCITY RESPONSE SPECTRUM
BREAR DAM, DOWNSTREAM, JAN 1 1976-0920 PST
IIN03700 BREAR DAM, DOWNSTREAM COMPNS0W
DAMPING VALUES ARE 0, 2, 5, 10 AND 20 PERCENT OF CRITICAL

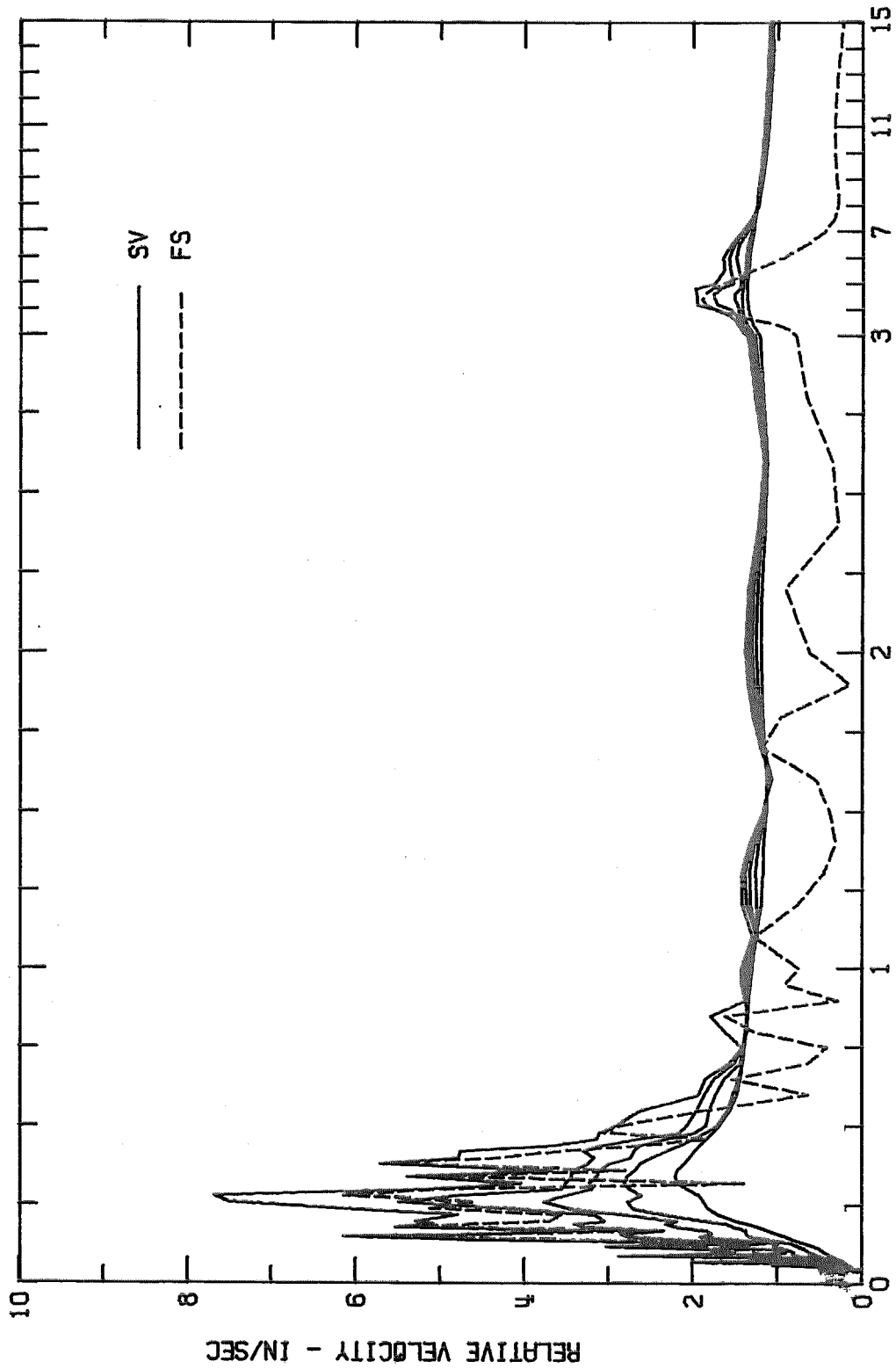


Fig. 67-a

RESPONSE SPECTRUM

BREA DAM, DOWNSTREAM, JAN 1 1976-0920 PST

IIN03700

BREA DAM, DOWNSTREAM COMPNSOW

DAMPING VALUES ARE 0, 2, 5, 10 AND 20 PERCENT OF CRITICAL

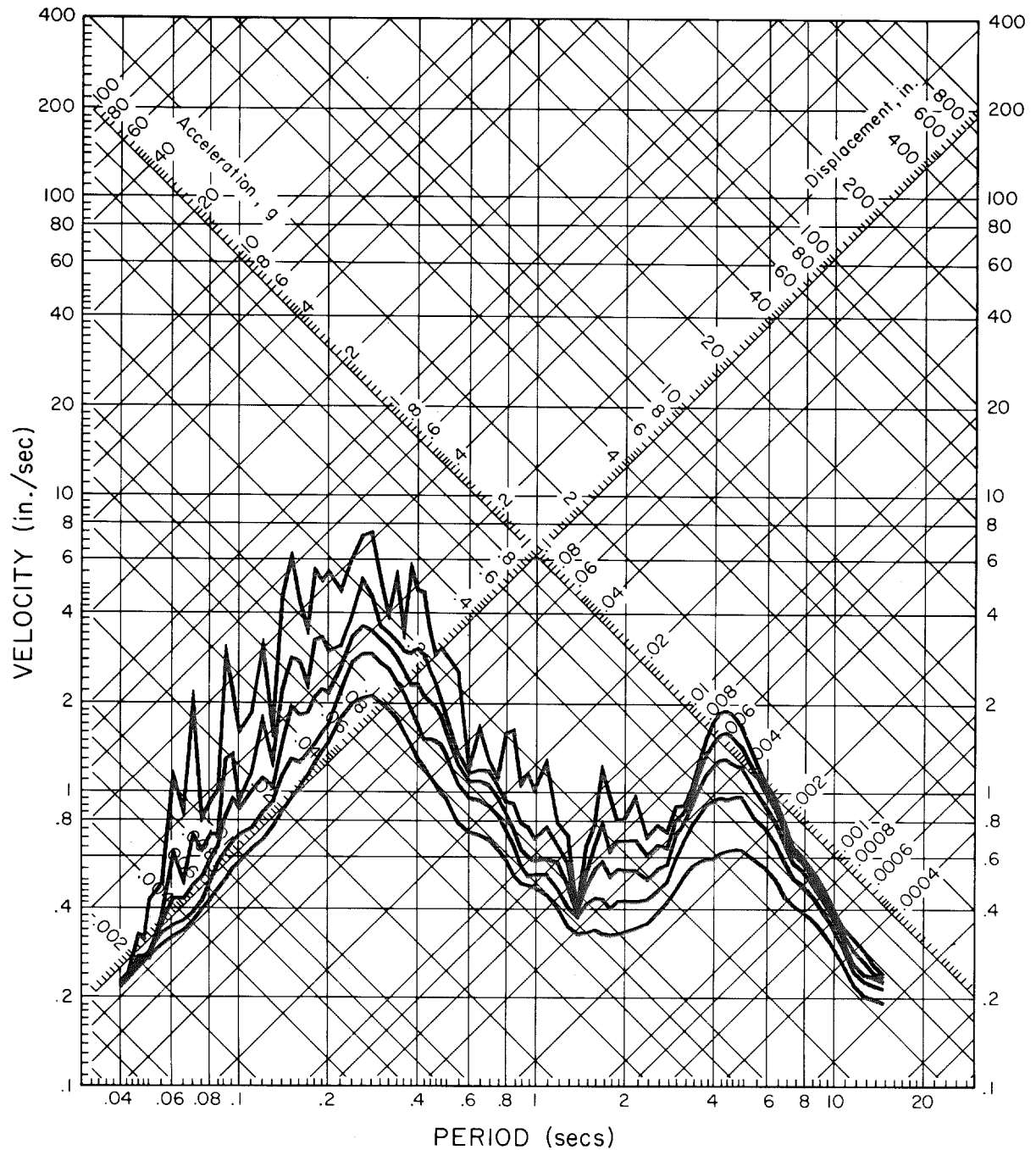


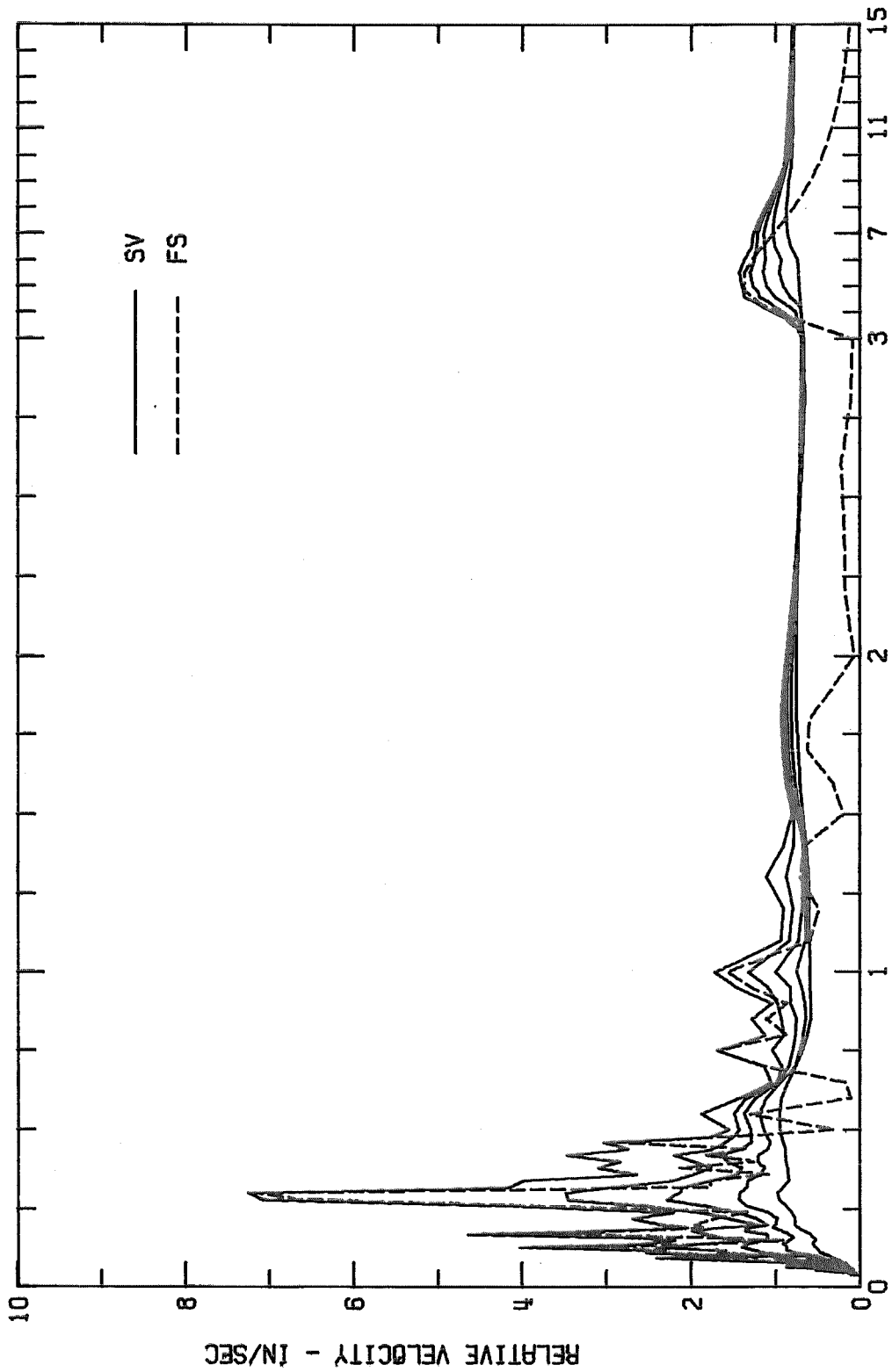
Fig. 67-b

RELATIVE VELOCITY RESPONSE SPECTRUM

BREA DAM, DOWNSTREAM, JAN 1 1976-0920 PST

IING3700 BREA DAM, DOWNSTREAM COMPS40W

DAMPING VALUES ARE 0, 2, 5, 10 AND 20 PERCENT OF CRITICAL



PERIOD - SECONDS

Fig. 68-a

RESPONSE SPECTRUM

BREA DAM, DOWNSTREAM, JAN 1 1976-0920 PST

IIN03700

BREA DAM, DOWNSTREAM COMPS40W

DAMPING VALUES ARE 0, 2, 5, 10 AND 20 PERCENT OF CRITICAL

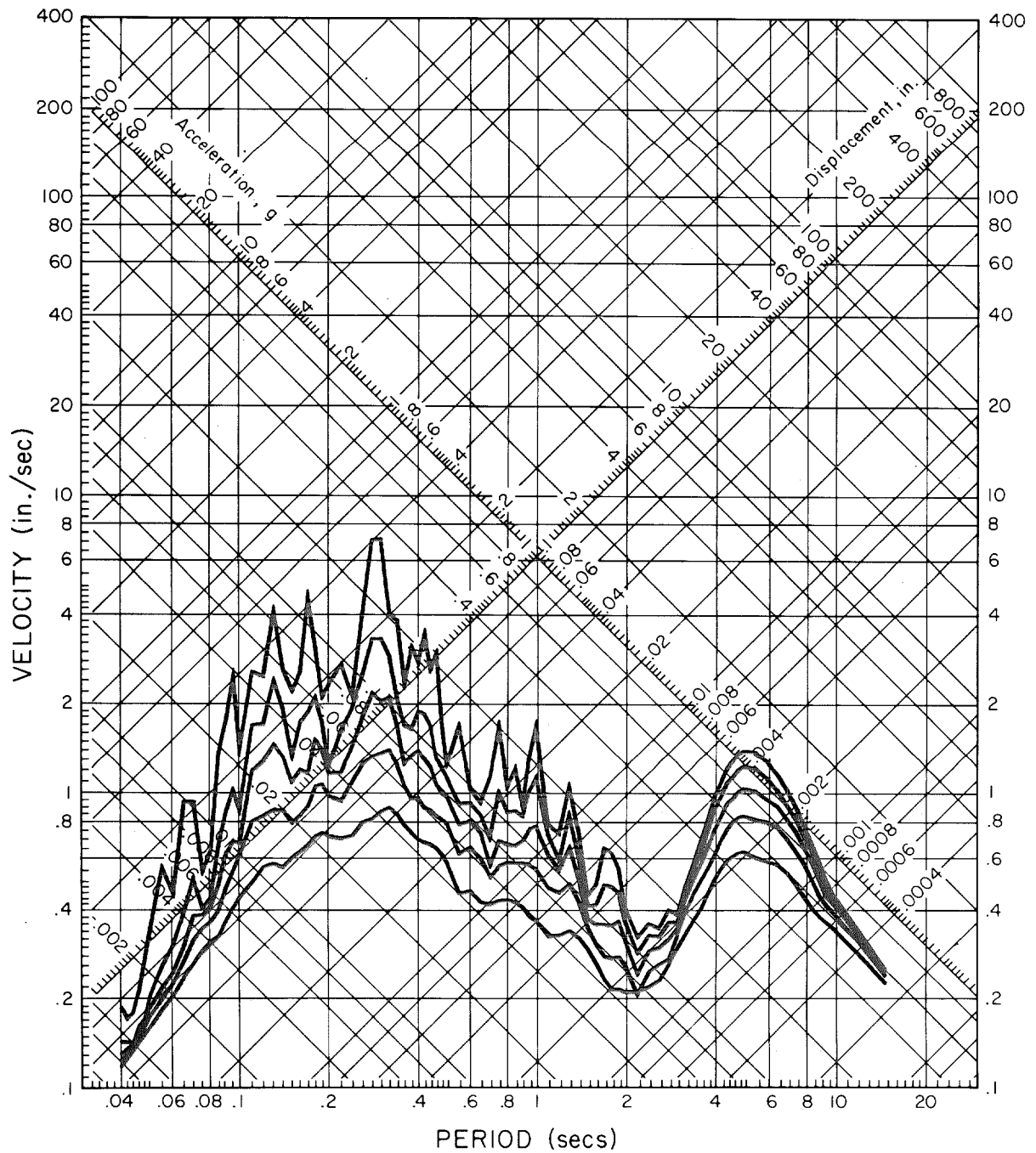


Fig. 68-b

RELATIVE VELOCITY RESPONSE SPECTRUM

BREA DAM, DOWNSTREAM, JAN 1 1976-0920 PST

IING3700 BREA DAM, DOWNSTREAM COMPDOWN

DAMPING VALUES ARE 0, 2, 5, 10 AND 20 PERCENT OF CRITICAL

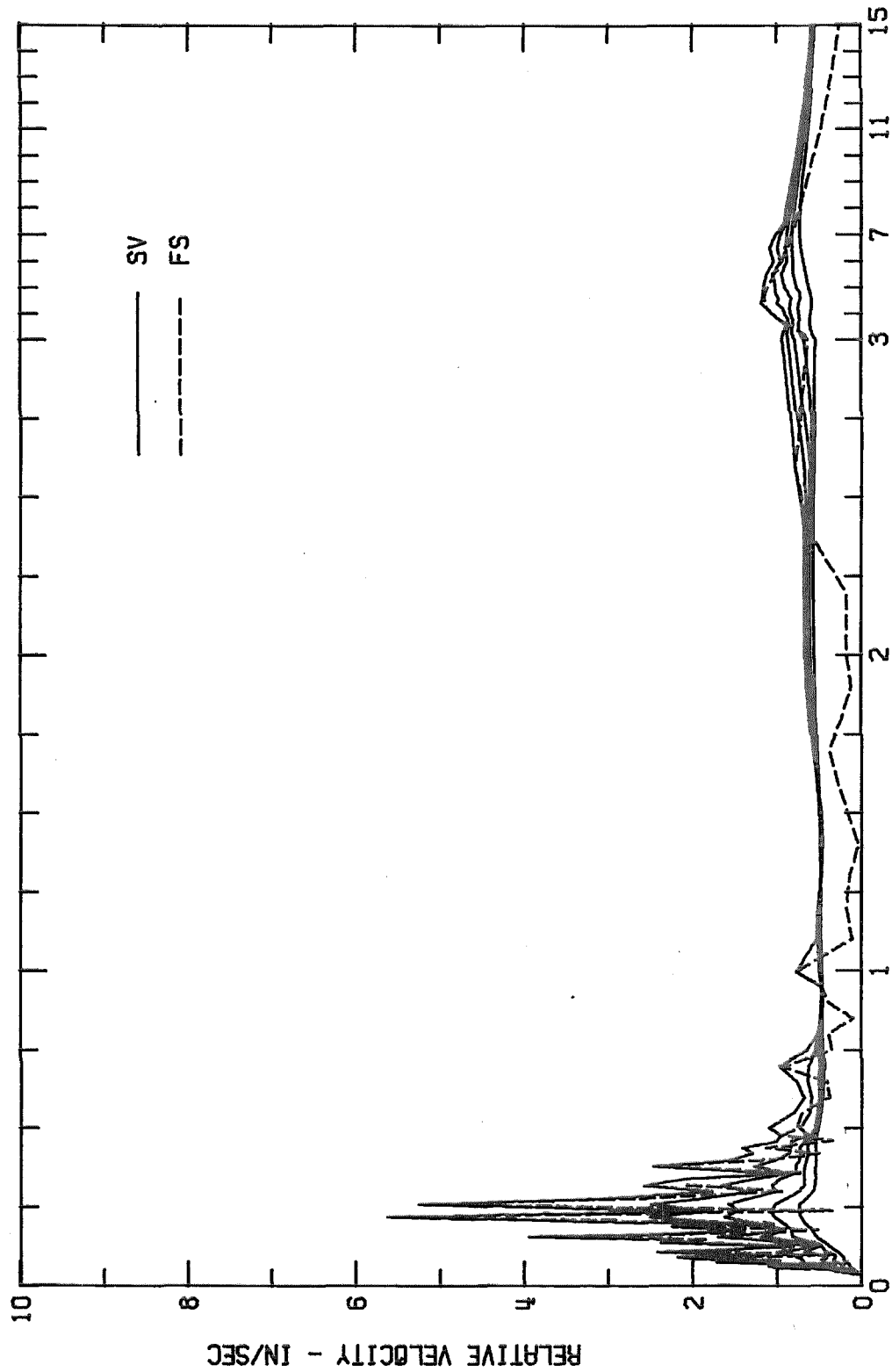


Fig. 69-a

RESPONSE SPECTRUM

BREA DAM, DOWNSTREAM, JAN 1 1976-0920 PST

IIN03700

BREA DAM, DOWNSTREAM COMDOWN

DAMPING VALUES ARE 0, 2, 5, 10 AND 20 PERCENT OF CRITICAL

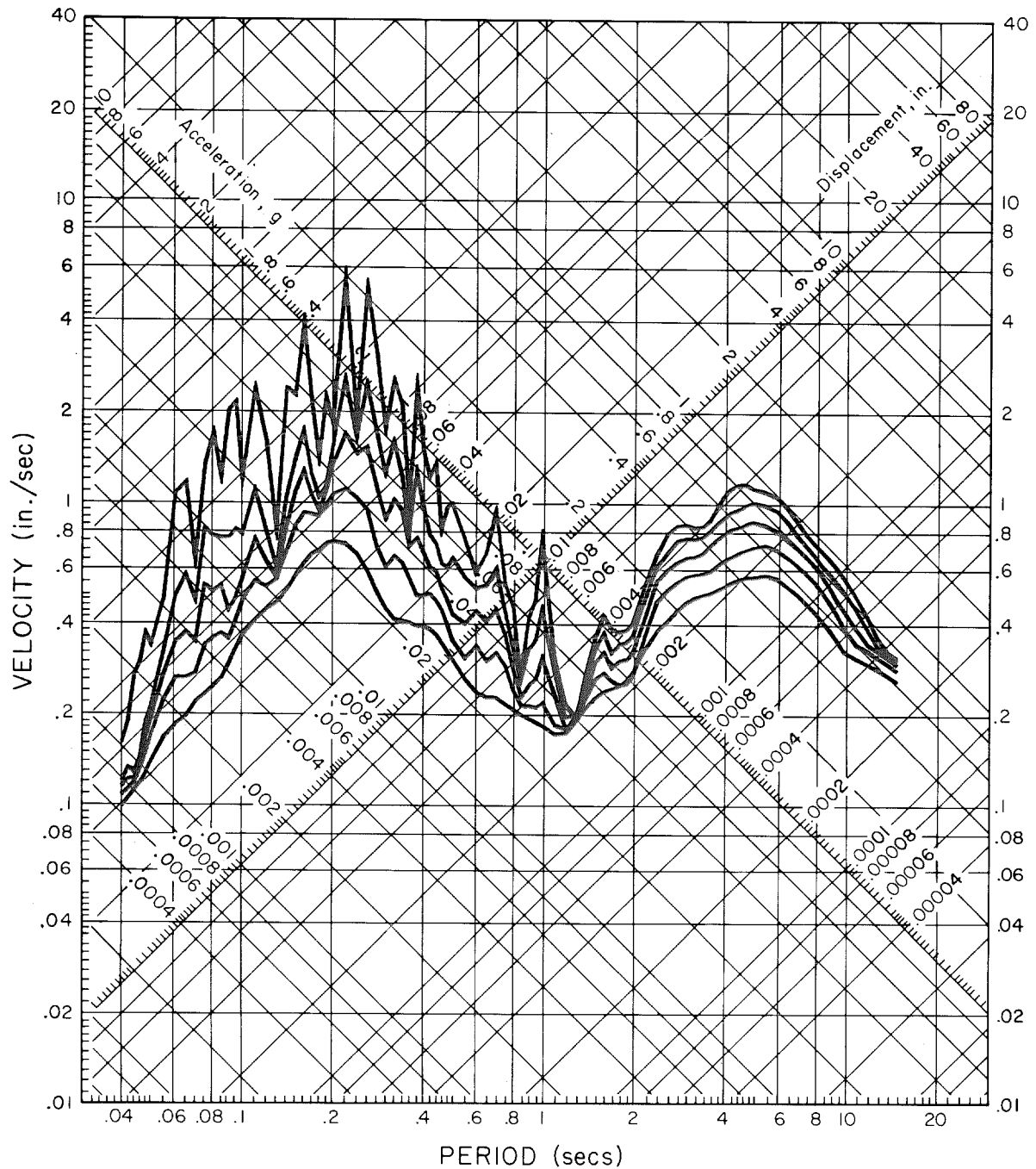


Fig. 69-b

RELATIVE VELOCITY RESPONSE SPECTRUM

BREA DAM, CREST, JAN 1 1976-0920 PST

11N03600 BREA DAM, CREST COMPNS0W

DAMPING VALUES ARE 0, 2, 5, 10 AND 20 PERCENT OF CRITICAL

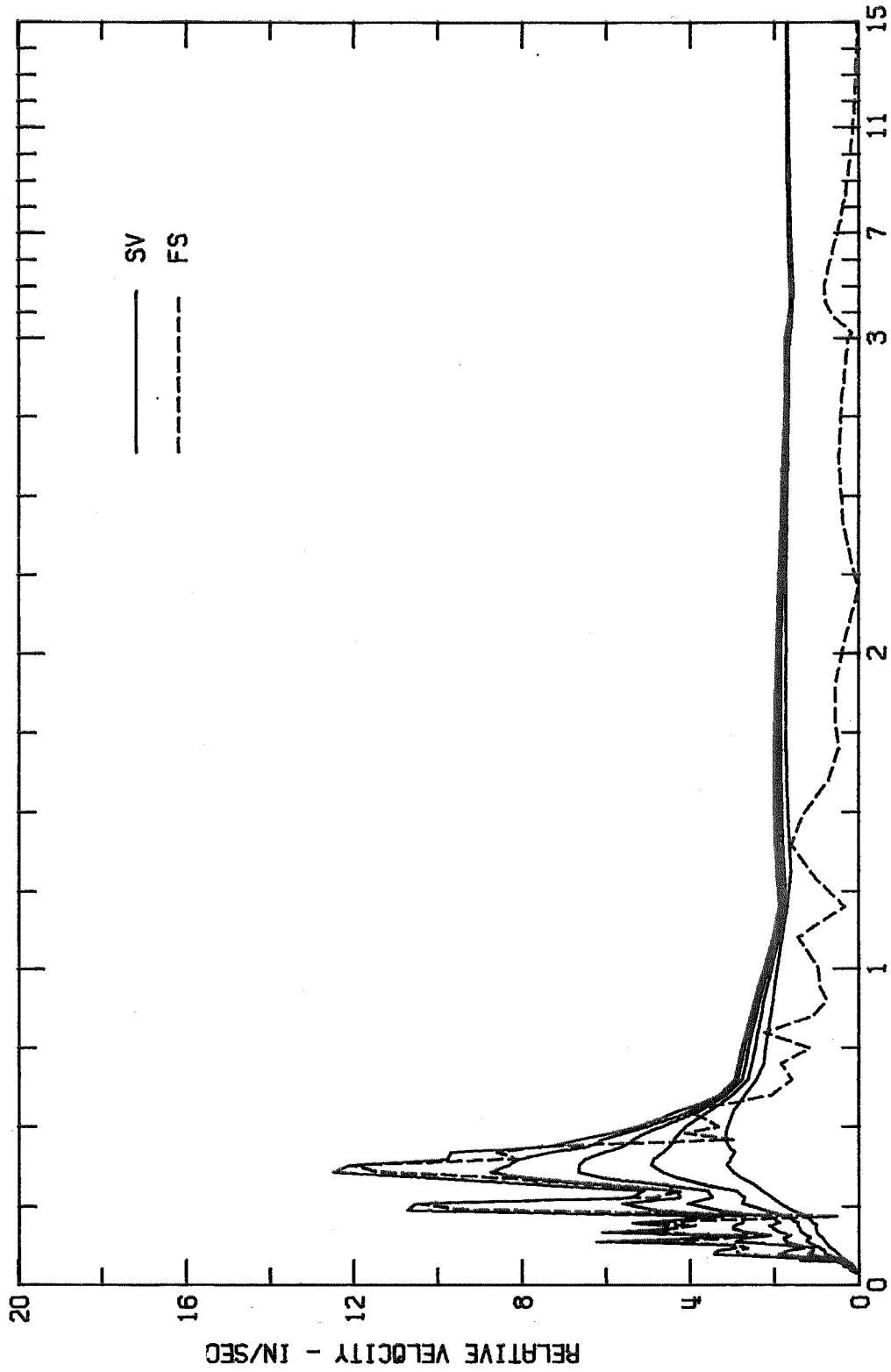


Fig. 70-a

RESPONSE SPECTRUM

BREA DAM,CREST,JAN 1 1976-0920 PST

IIN03600

BREA DAM,CREST COMPNSOW

DAMPING VALUES ARE 0, 2, 5, 10 AND 20 PERCENT OF CRITICAL

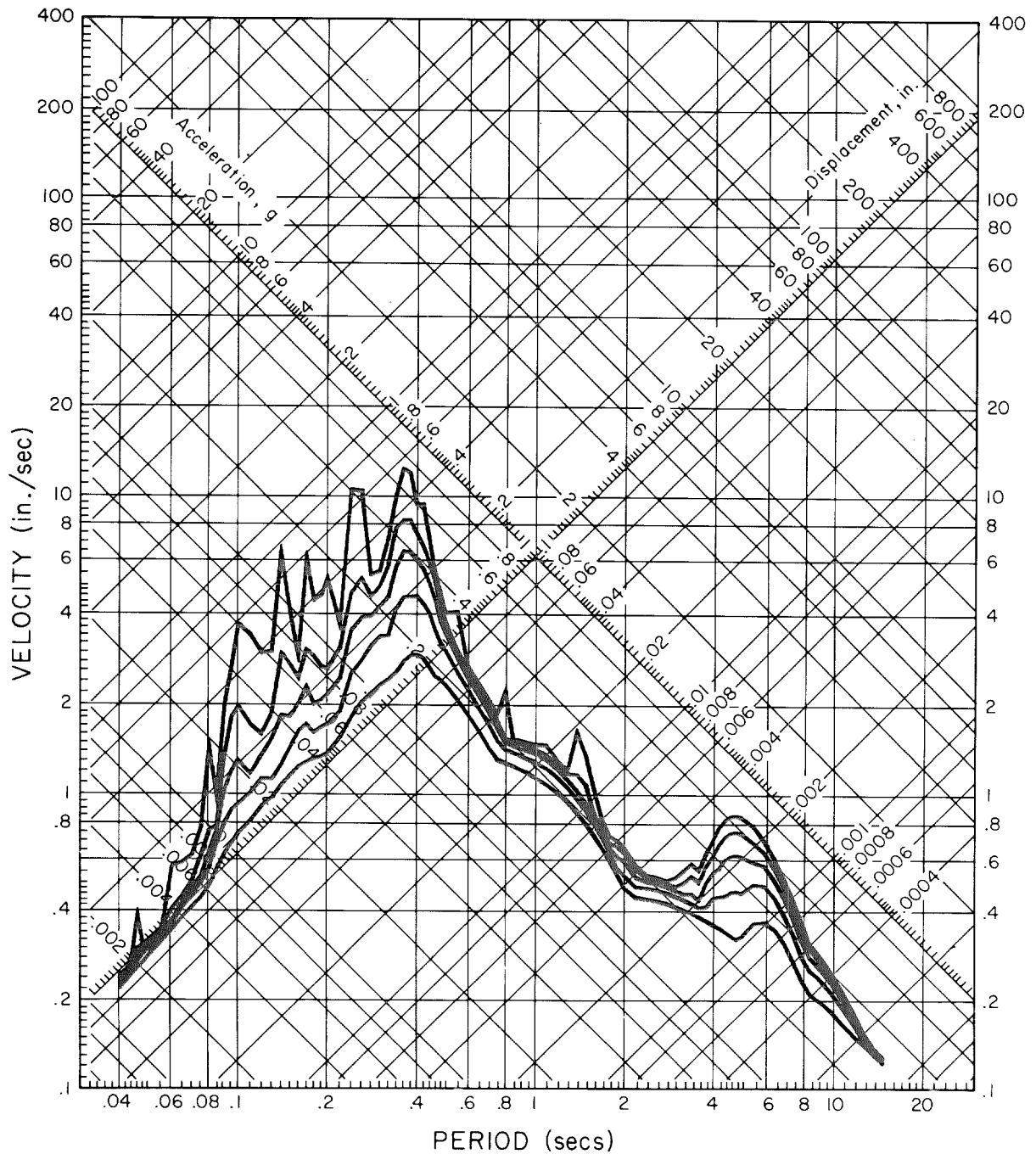


Fig. 70-b

RELATIVE VELOCITY RESPONSE SPECTRUM

BREA DAM, CREST, JAN 1 1976-0920 PST

IIN03600 BREA DAM, CREST COMPS40W

DAMPING VALUES ARE 0, 2, 5, 10 AND 20 PERCENT OF CRITICAL

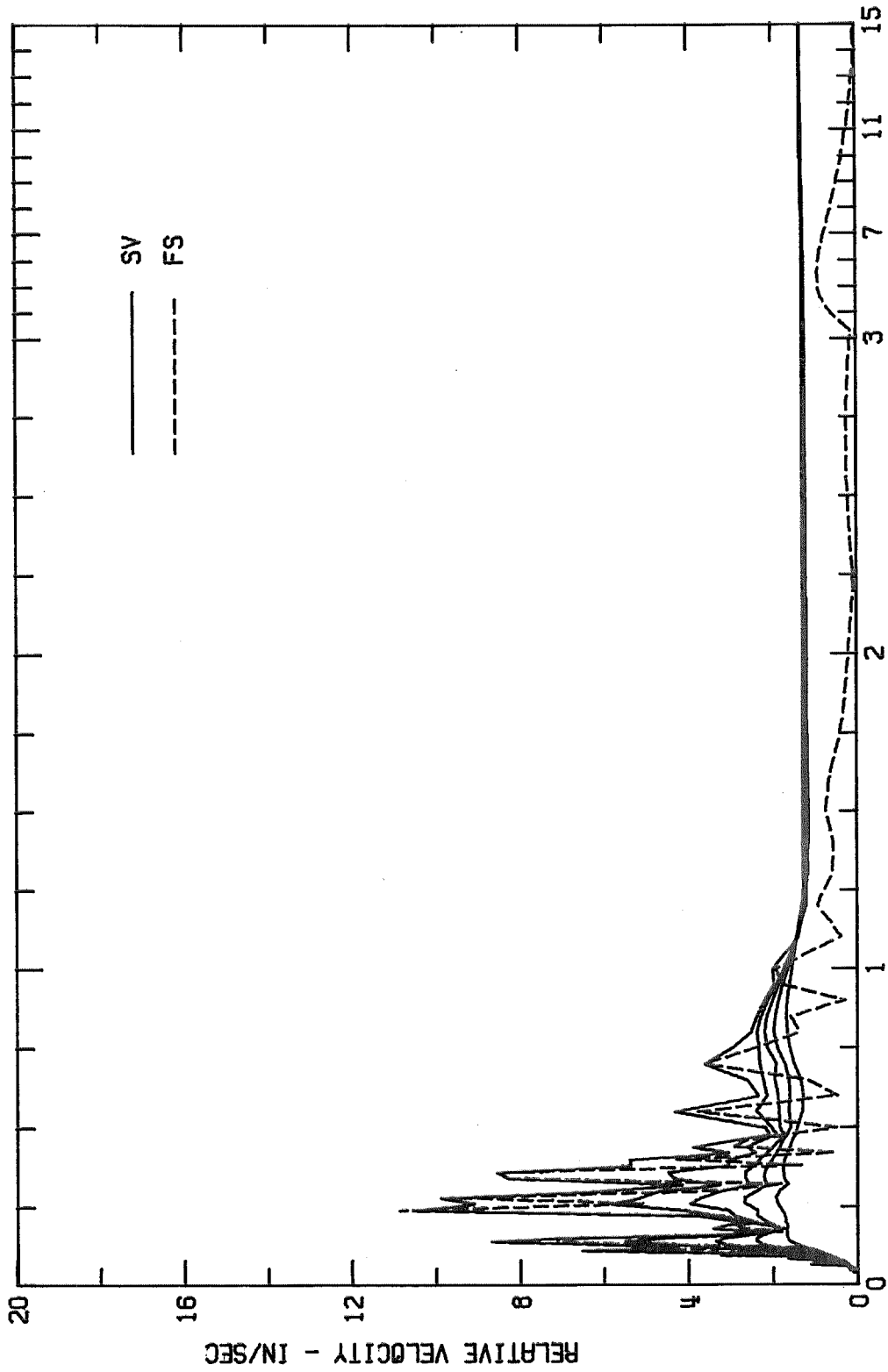


Fig. 71-a

RESPONSE SPECTRUM

BREA DAM, CREST, JAN 1 1976-0920 PST

IIN03600

BREA DAM, CREST COMPS40W

DAMPING VALUES ARE 0, 2, 5, 10 AND 20 PERCENT OF CRITICAL

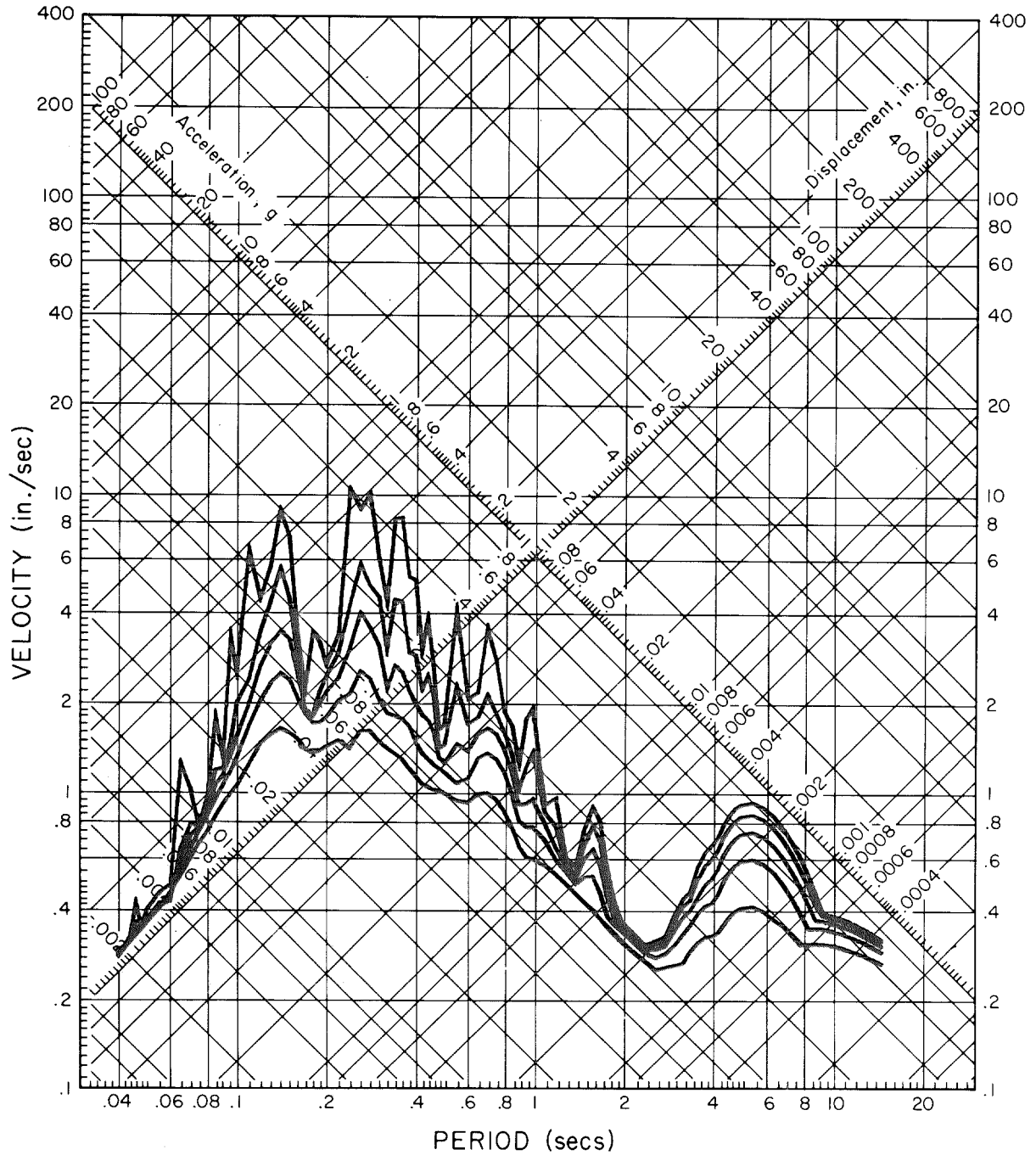


Fig. 71-b

RELATIVE VELOCITY RESPONSE SPECTRUM

BREA DAM, CREST, JAN 1 1976-0920 PST

IIN03600 BREA DAM, CREST COMDOWN

DAMPING VALUES ARE 0, 2, 5, 10 AND 20 PERCENT OF CRITICAL

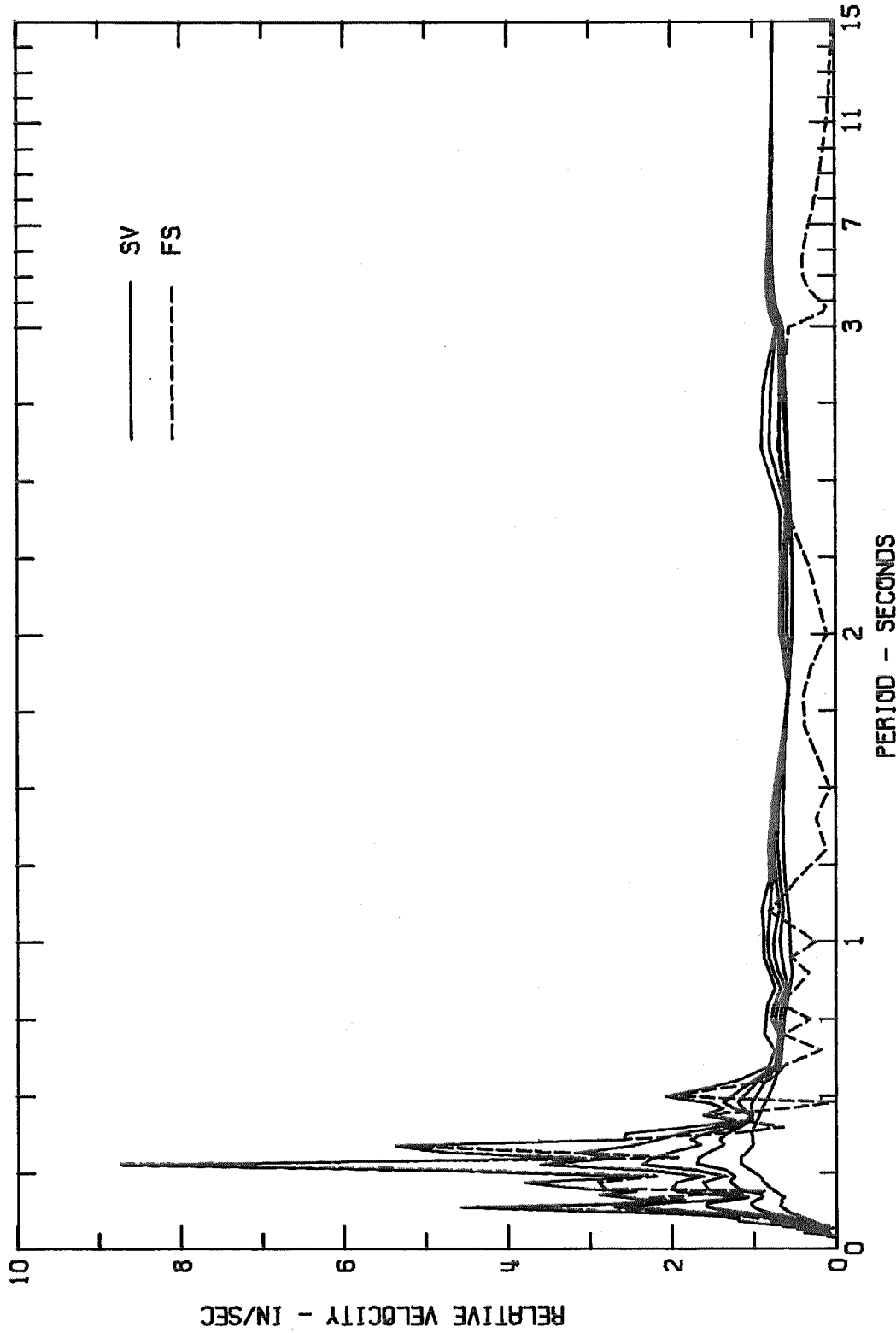


Fig. 72-a

RESPONSE SPECTRUM

FOURIER AMPLITUDE SPECTRUM OF ACCELERATION
BREAR DAM, DOWNSTREAM, JAN 1 1976-0920 PST
IV03700 BREAR DAM, DOWNSTREAM COMPANSON

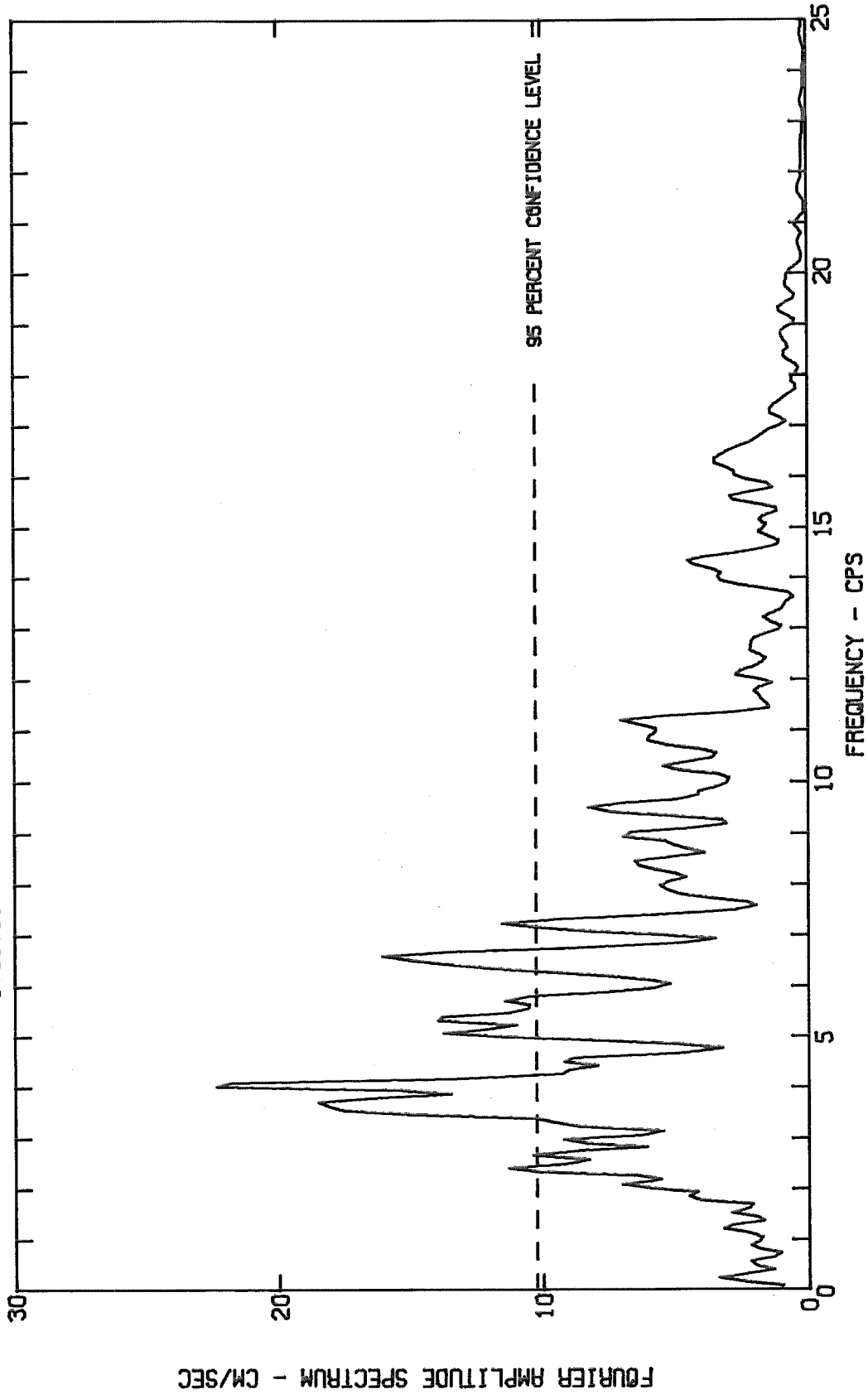
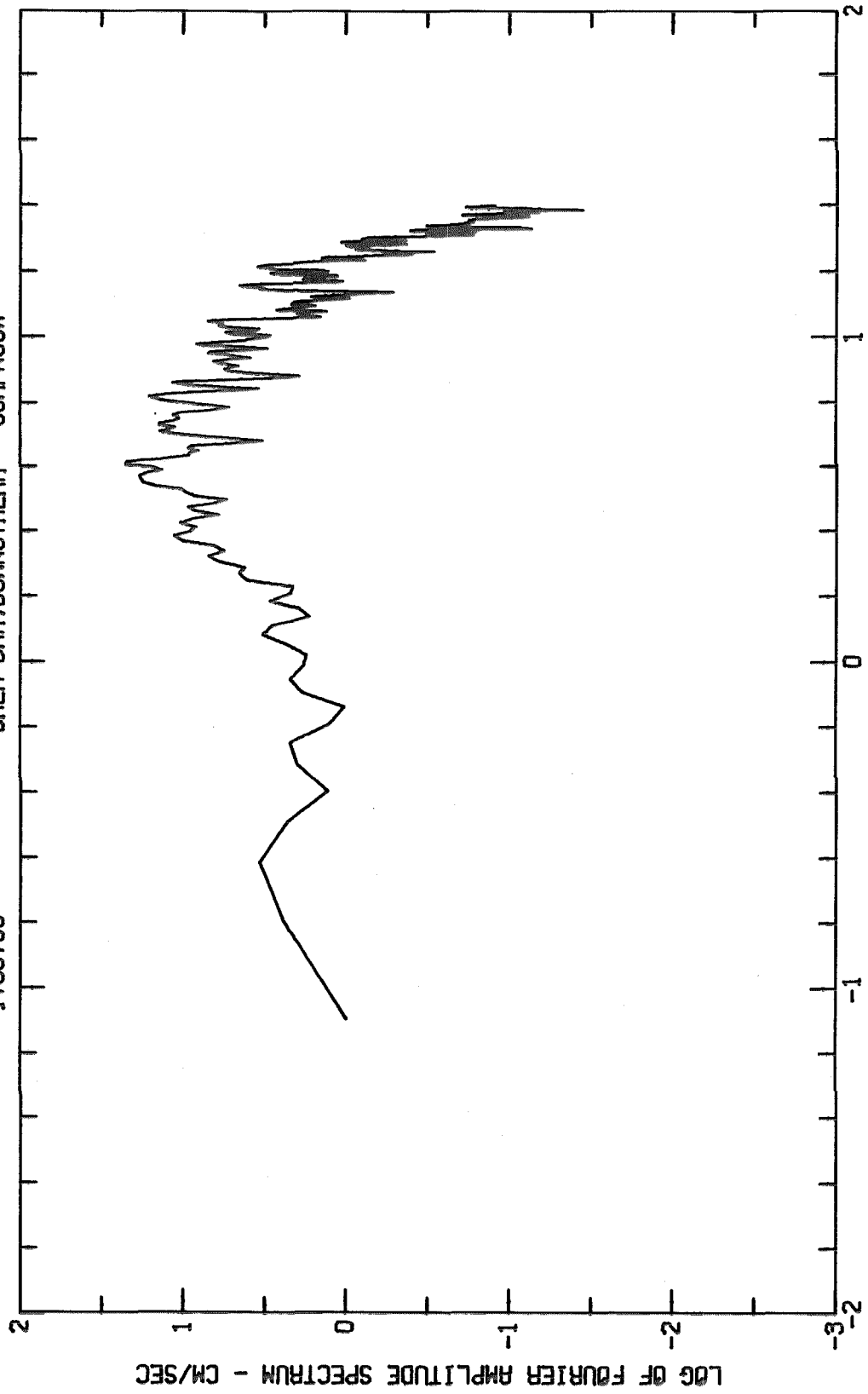


Fig. 73-a

FOURIER AMPLITUDE SPECTRUM OF ACCELERATION
BRAE DAM, DOWNSTREAM, JAN 1 1976-0920 PST
1V03700 BRAE DAM, DOWNSTREAM COMPNSOH



LOG OF FREQUENCY - CPS

Fig. 73-b

FOURIER AMPLITUDE SPECTRUM OF ACCELERATION
BRAER DAM, DOWNSTREAM, JAN 1 1976-0920 PST
1V03700 BRAER DAM, DOWNSTREAM COMPS40W

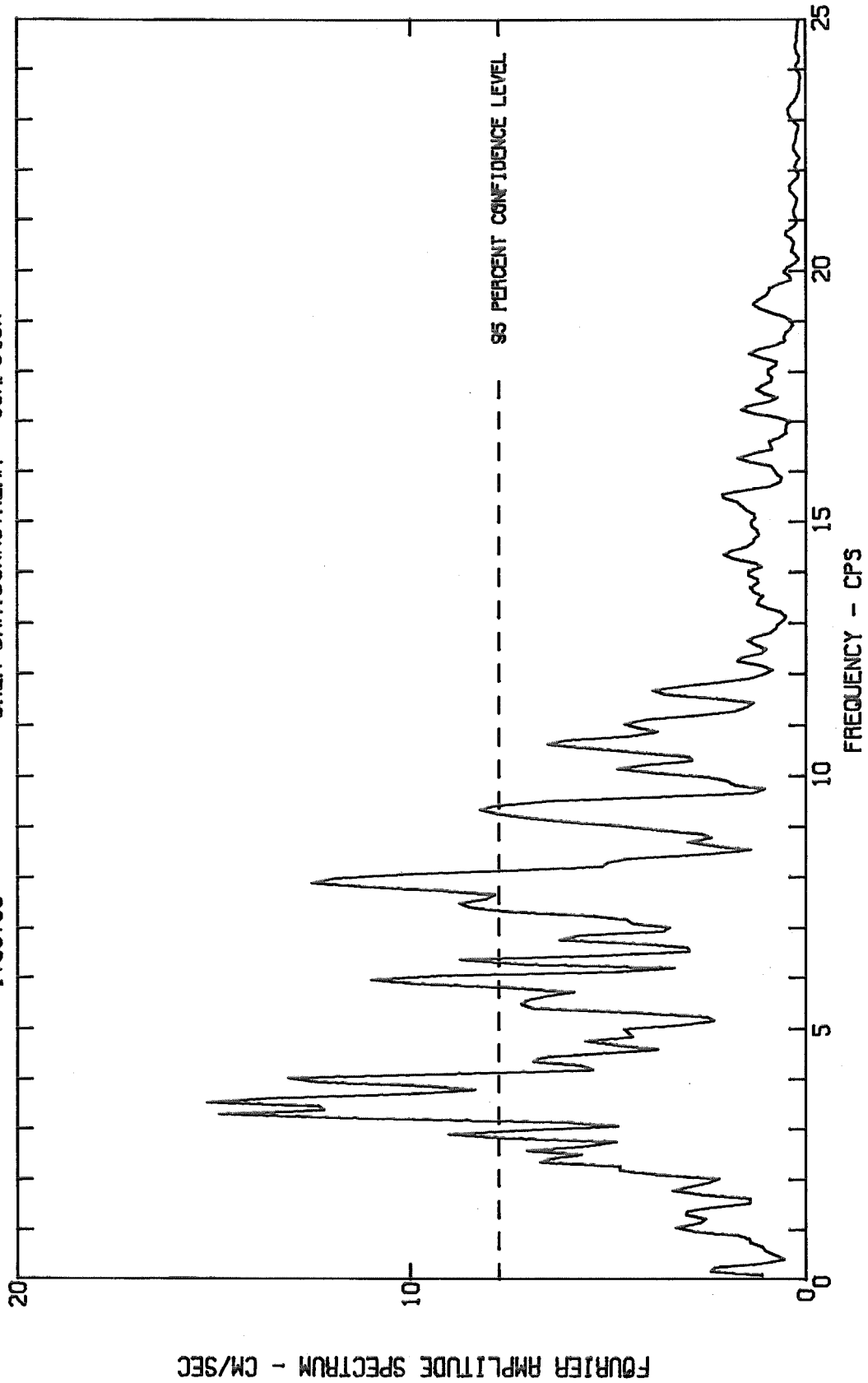
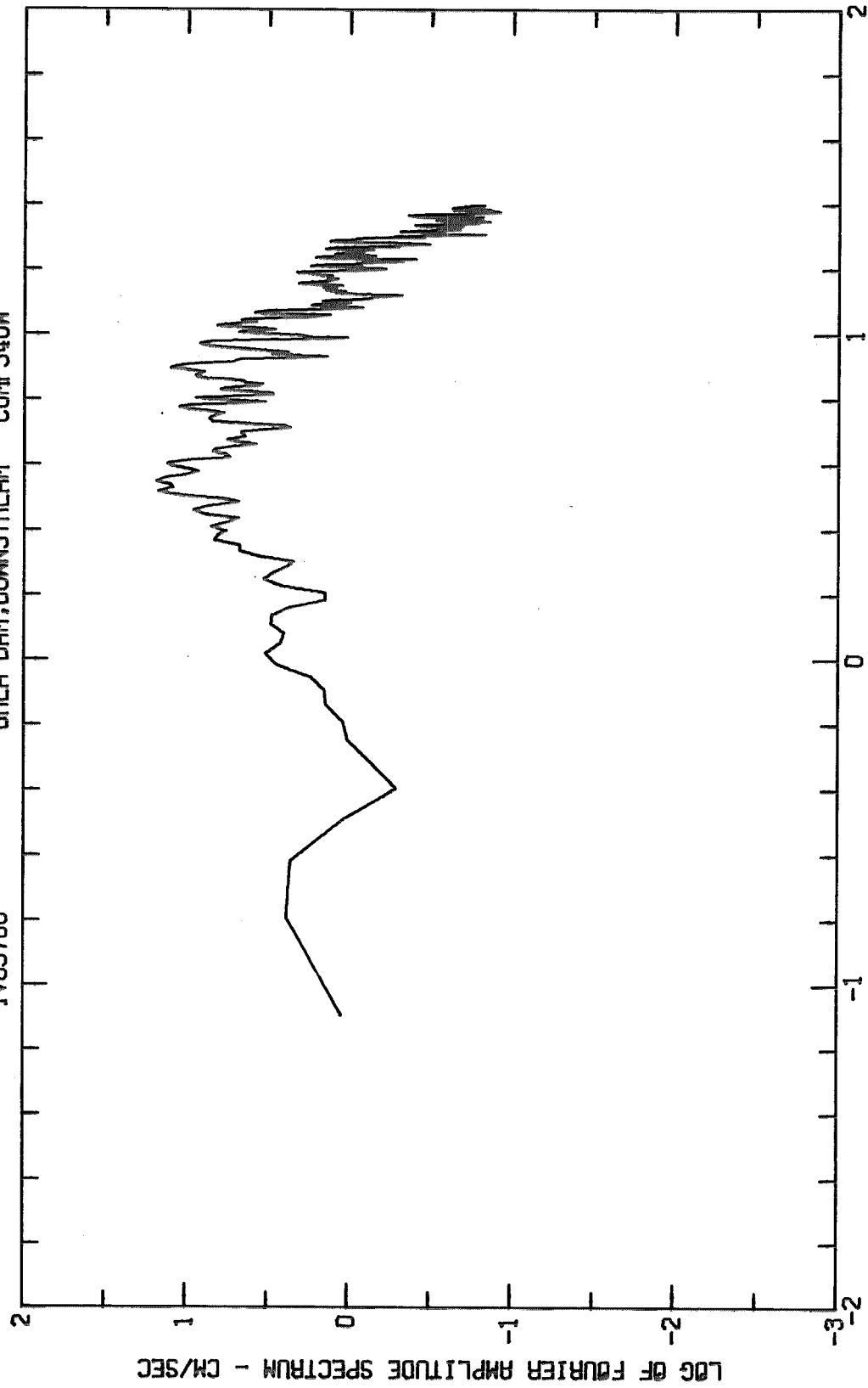


Fig. 74-a

FOURIER AMPLITUDE SPECTRUM OF ACCELERATION
BREAR DAM, DOWNSTREAM, JAN 1 1976-0920 PST
IV03700 BREAR DAM, DOWNSTREAM COMPSHOW



LOG OF FREQUENCY - CPS
Fig. 74-b

FOURIER AMPLITUDE SPECTRUM OF ACCELERATION
BREAR DAM, DOWNSTREAM, JAN 1 1976-0920 PST
1V03700 BREAR DAM, DOWNSTREAM COMPOUND

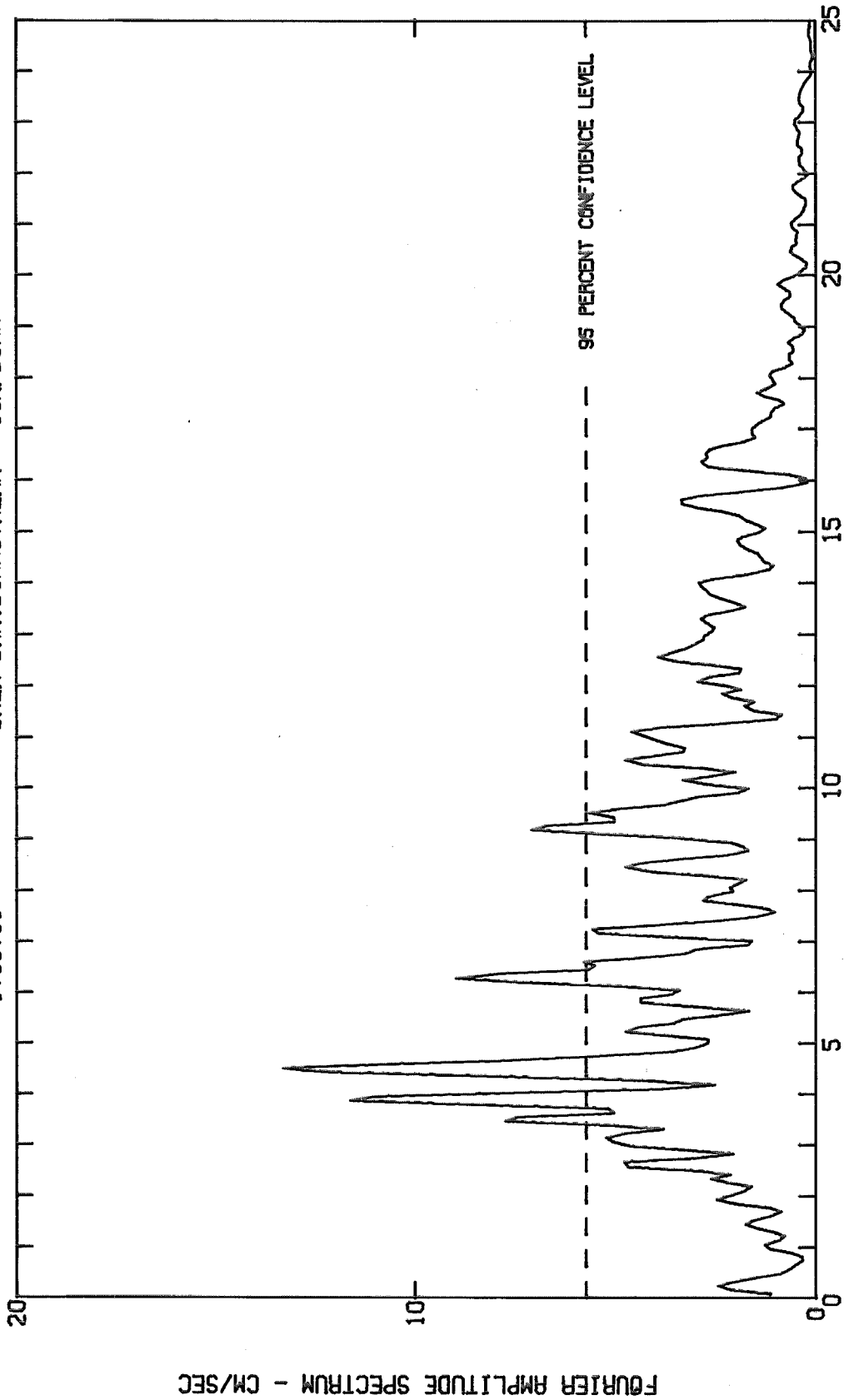
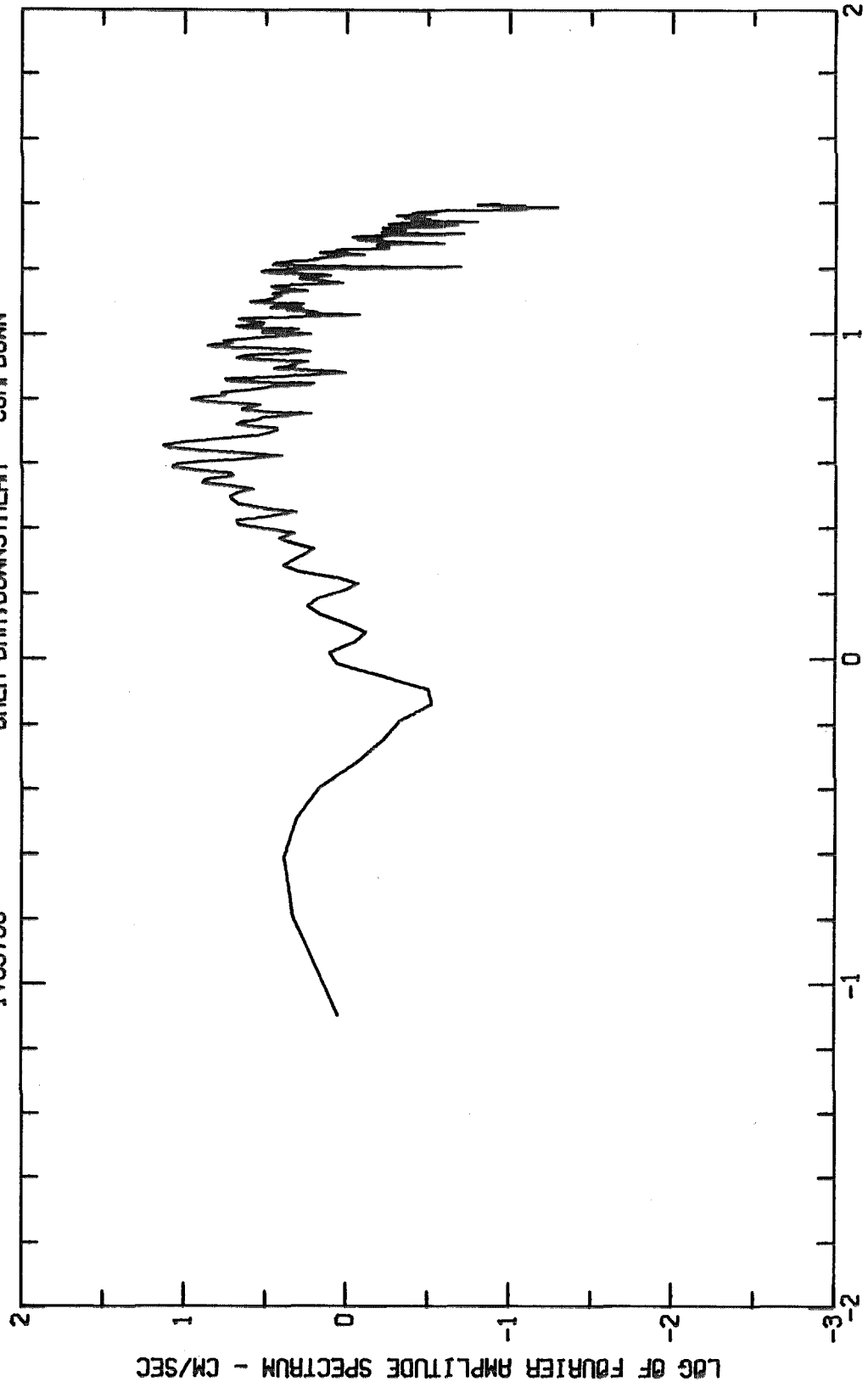


Fig. 75-a

FOURIER AMPLITUDE SPECTRUM OF ACCELERATION
BREAR DAM, DOWNSTREAM, JAN 1 1976-0920 PST
IV03700 BREAR DAM, DOWNSTREAM COMPOUND



LOG OF FREQUENCY - CPS

Fig. 75-b

FOURIER AMPLITUDE SPECTRUM OF ACCELERATION

BREA DAM, CREST, JAN 1 1976-0920 PST

IV03600 BREA DAM, CREST COMPNS04

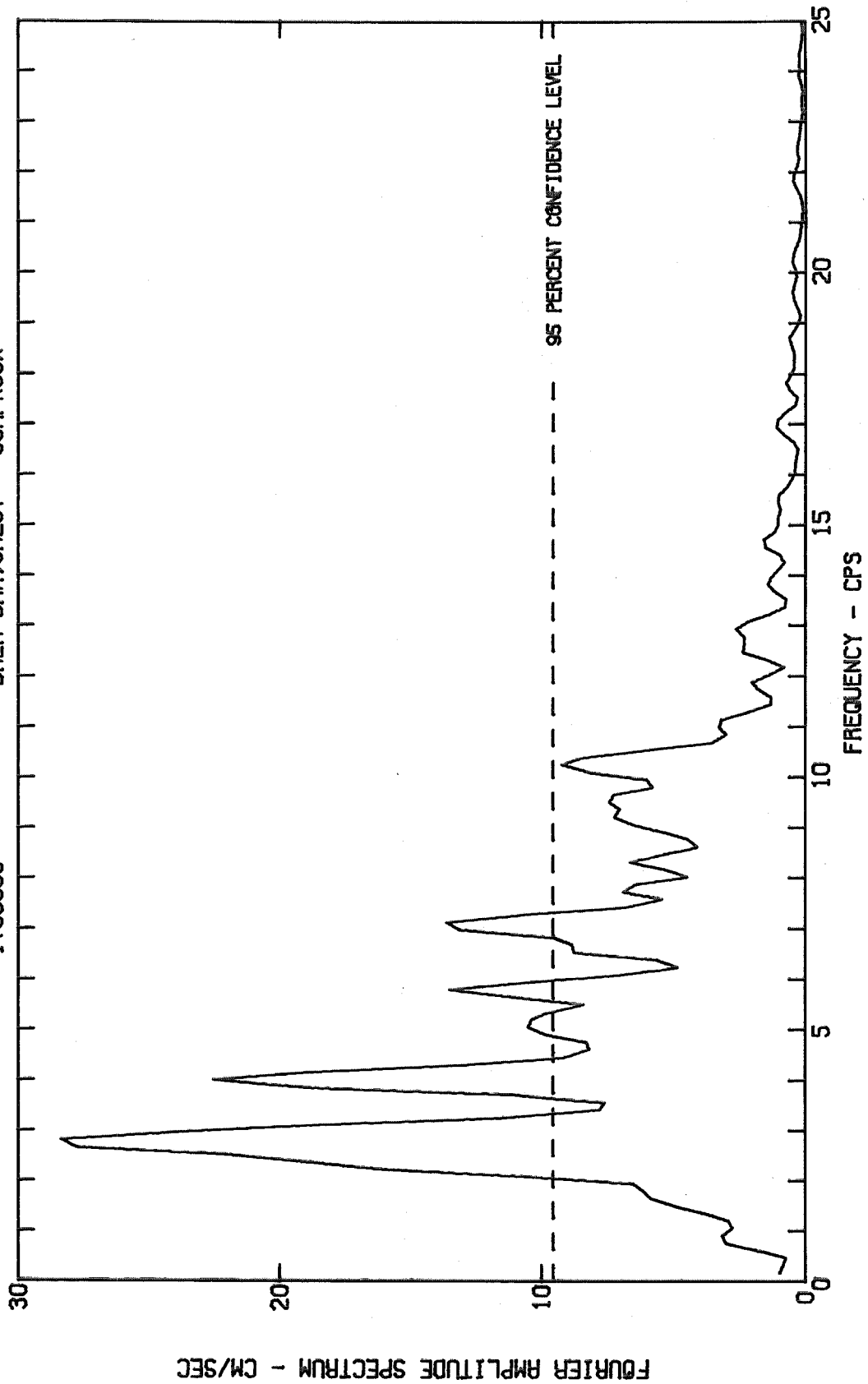


Fig. 76-a

FOURIER AMPLITUDE SPECTRUM OF ACCELERATION
BRAER DAM, CREST, JAN 1 1976-0920 PST
IV03600 BRAER DAM, CREST COMPNS0W

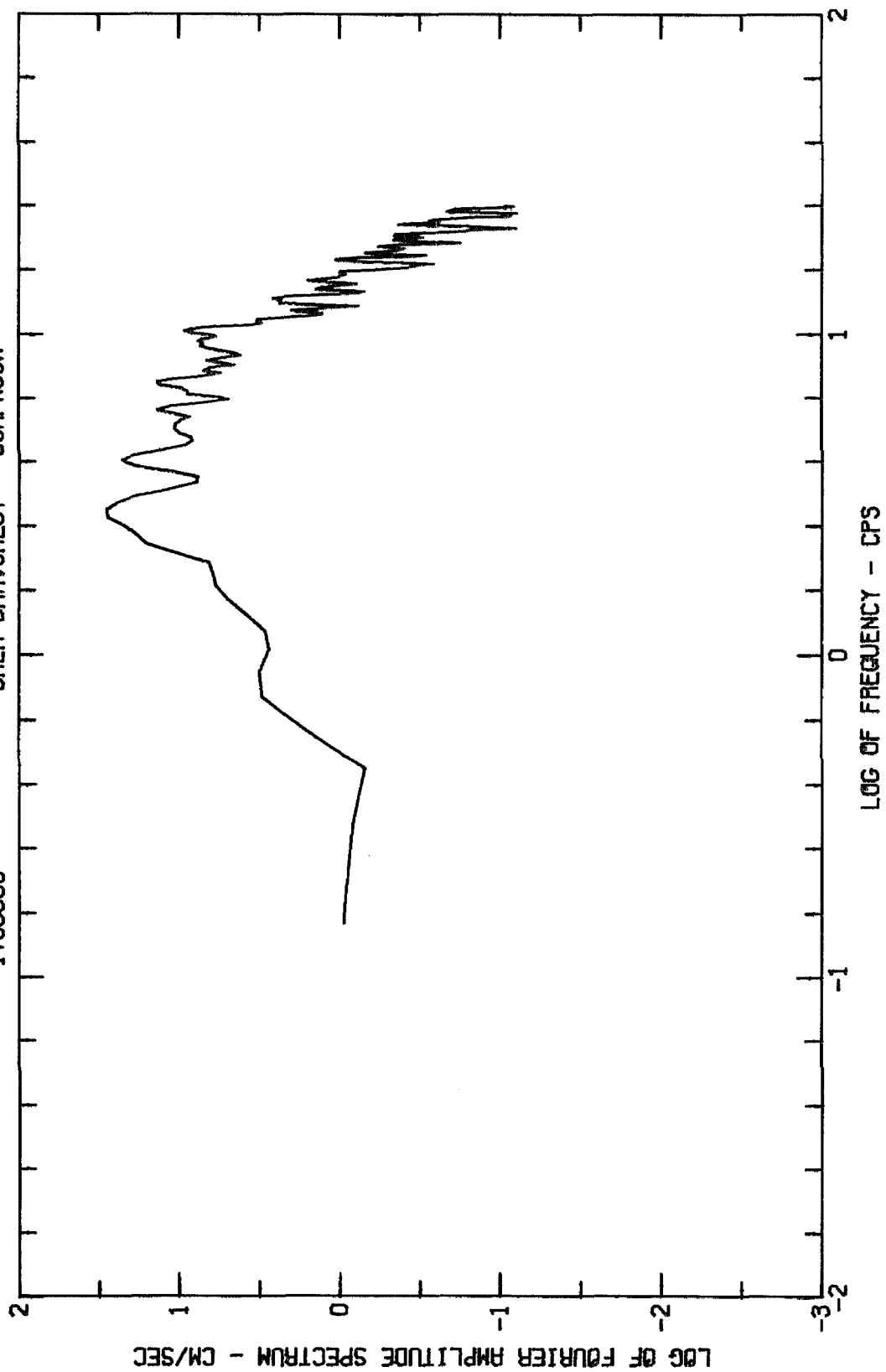


Fig. 76-b

FOURIER AMPLITUDE SPECTRUM OF ACCELERATION

BREA DAM, CREST, JAN 1 1976-0920 PST

IV03600 BREA DAM, CREST COMPSLOW

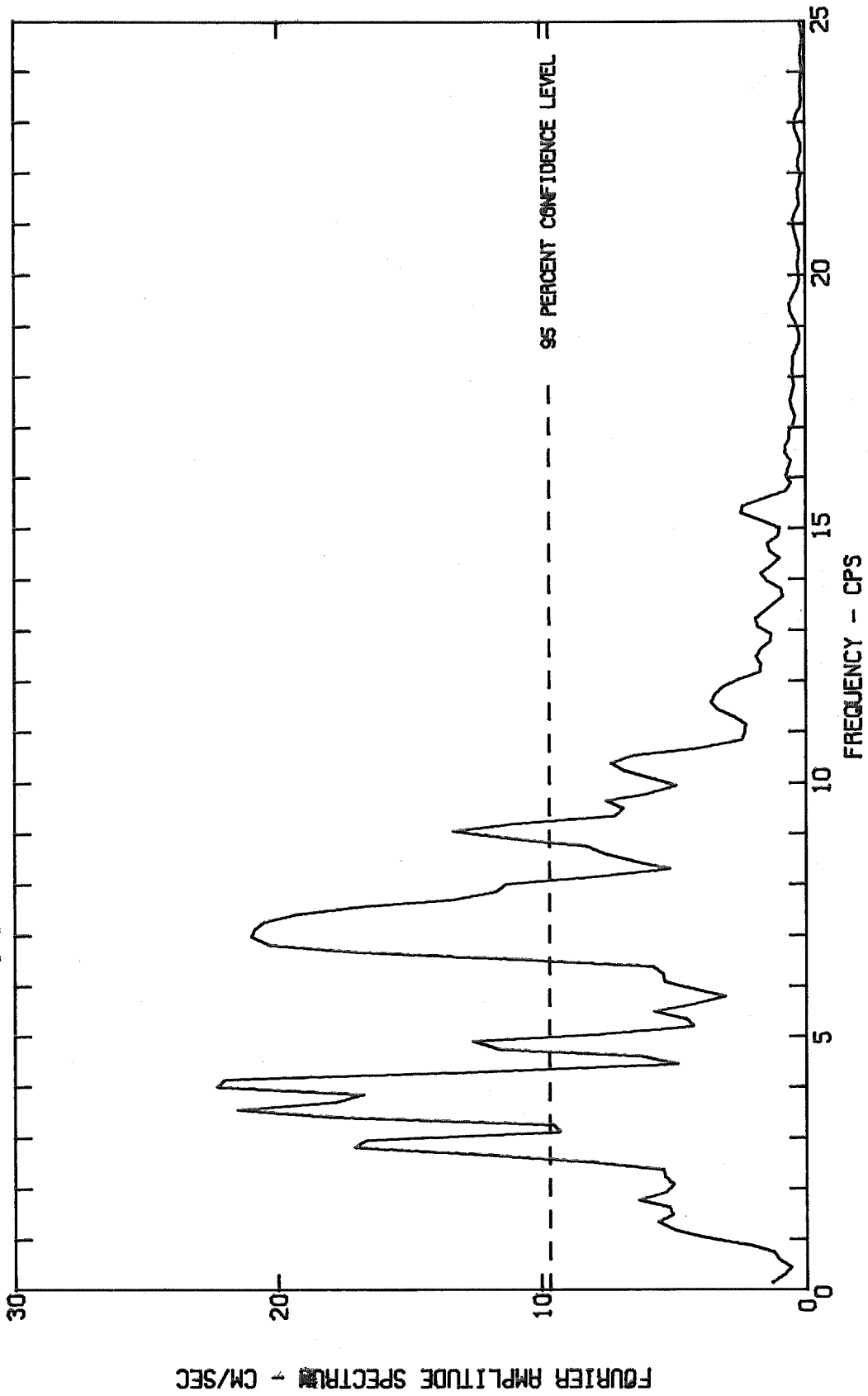
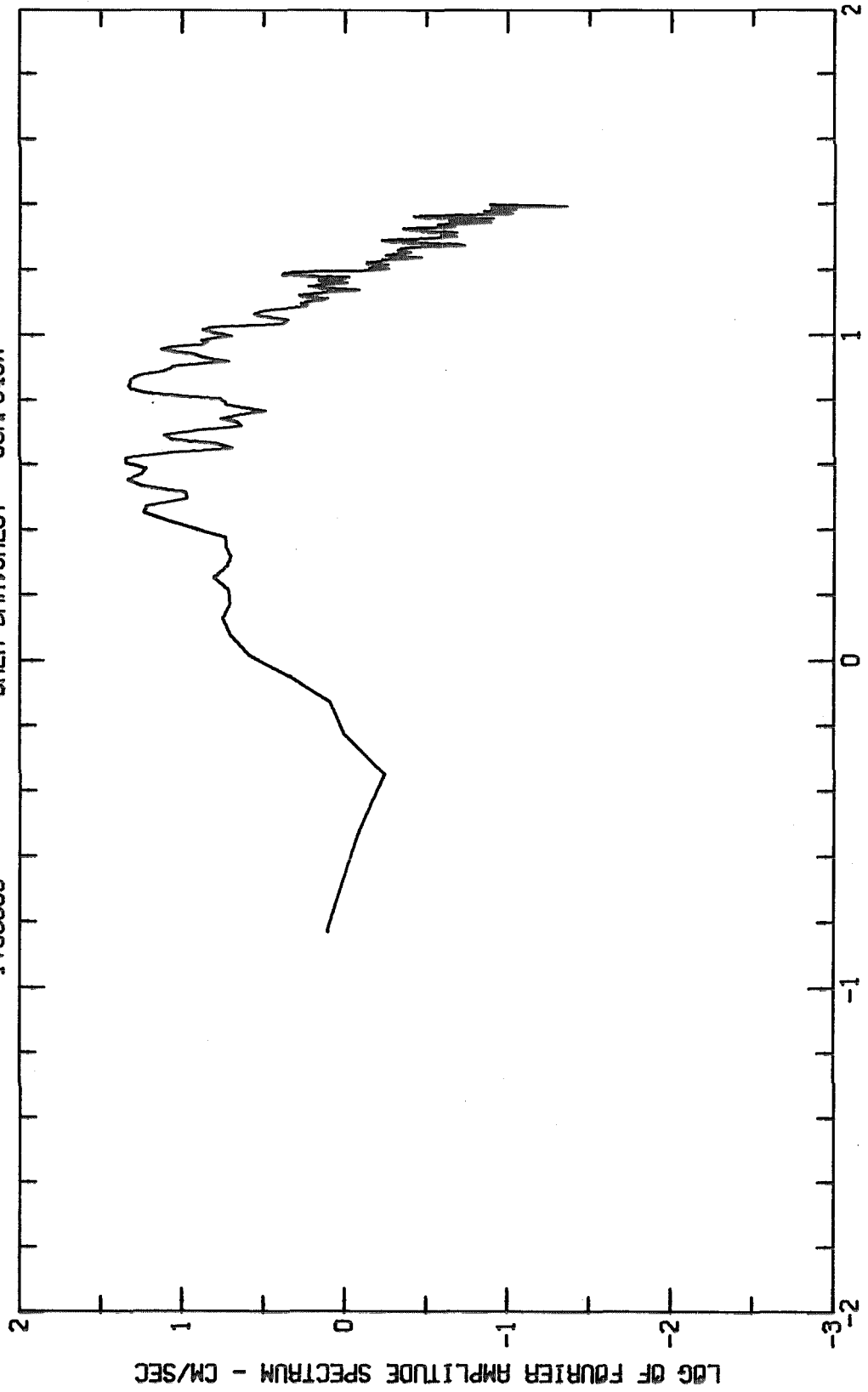


Fig. 77-a

FOURIER AMPLITUDE SPECTRUM OF ACCELERATION
BREAR DAM, CREST, JAN 1 1976-0920 PST
IV03600 BREAR DAM, CREST COMPS40H

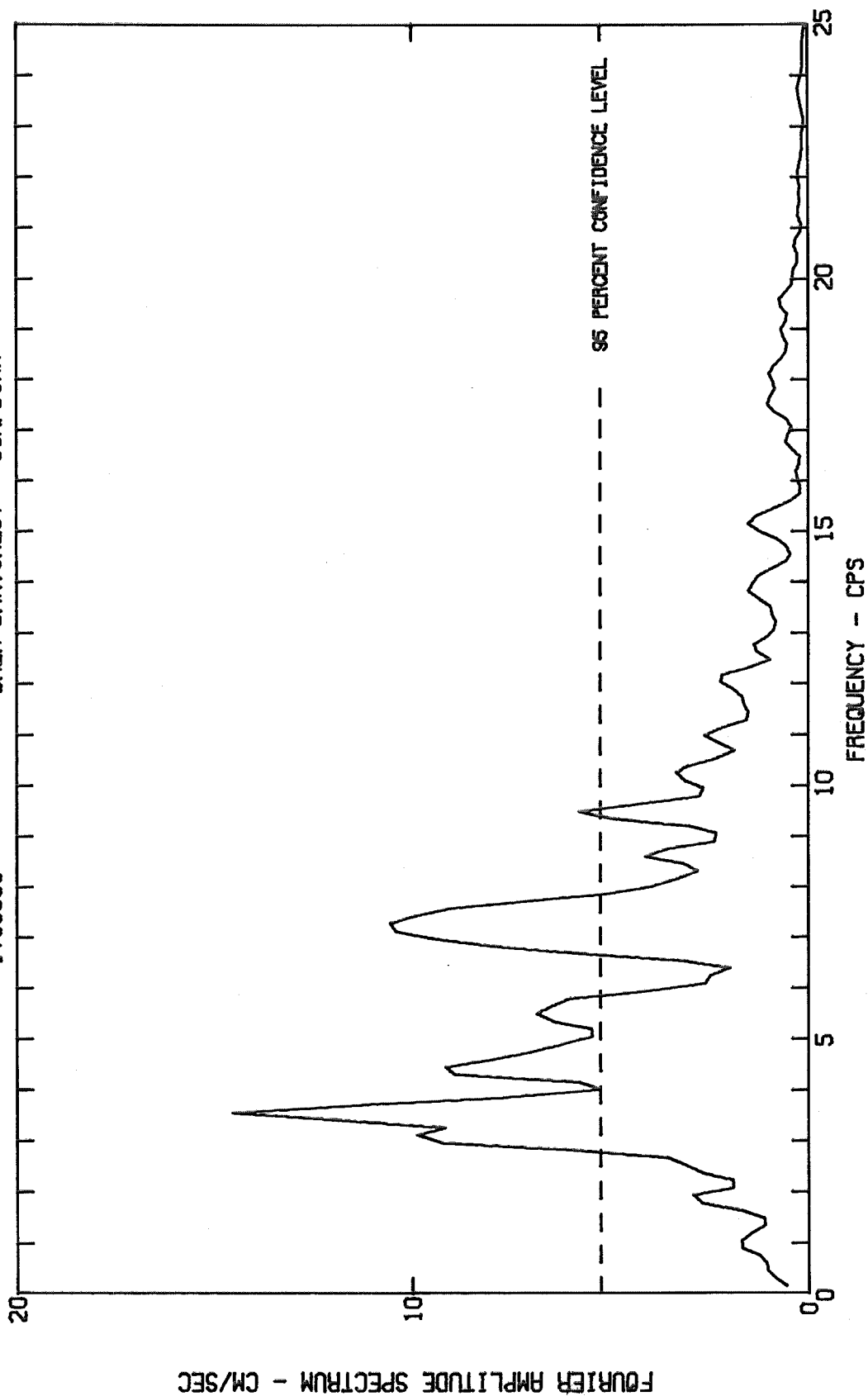


LOG OF FREQUENCY - CPS
Fig. 77-b

FOURIER AMPLITUDE SPECTRUM OF ACCELERATION

BREA DAM, CREST, JAN 1 1976-0920 PST

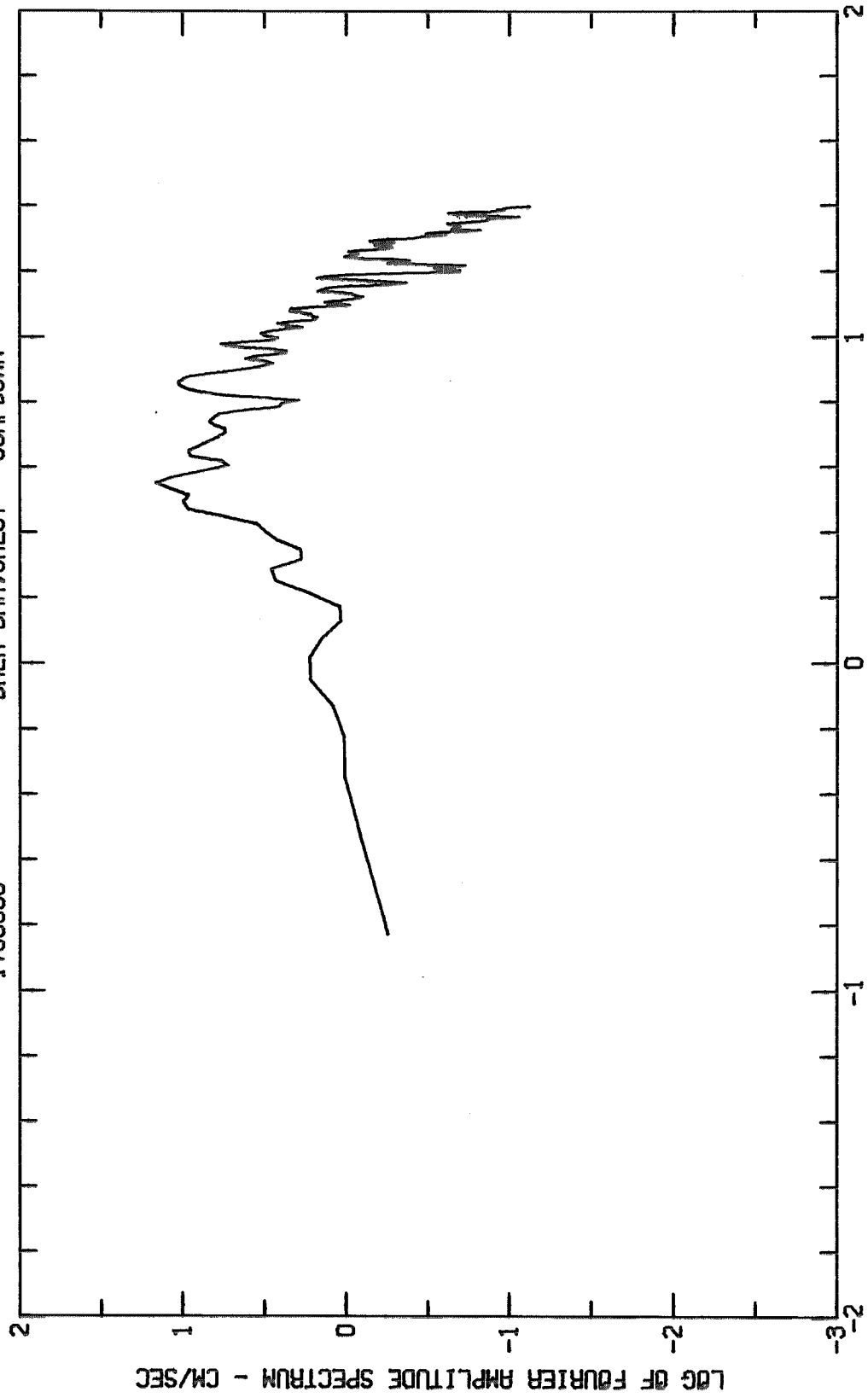
IV03600 BREA DAM, CREST COMPDOWN



FREQUENCY - CPS

Fig. 78-a

FOURIER AMPLITUDE SPECTRUM OF ACCELERATION
BREA DAM, CREST, JAN 1 1976-0920 PST
1V03600 BREA DAM, CREST COMPDOWN



LOG OF FREQUENCY - CPS
Fig. 78-b

Whittier, California Earthquake of Jan. 1, 1976
BREA DAM, CALIFORNIA
AMPLIFICATION SPECTRUM
UPSTREAM/DOWNSTREAM COMPONENT (N50W)
CREST W.R.T. DOWNSTREAM

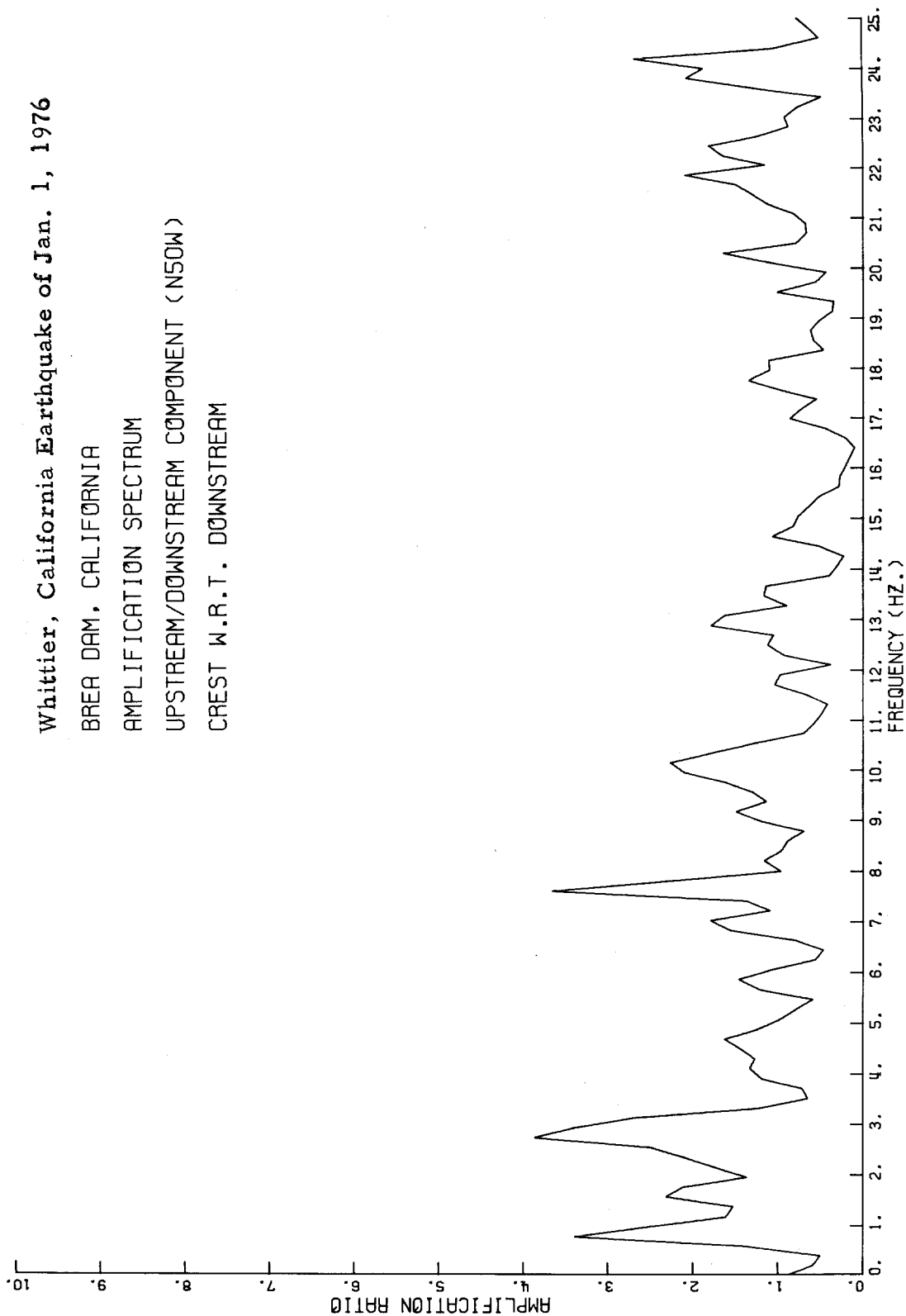


Fig. 79

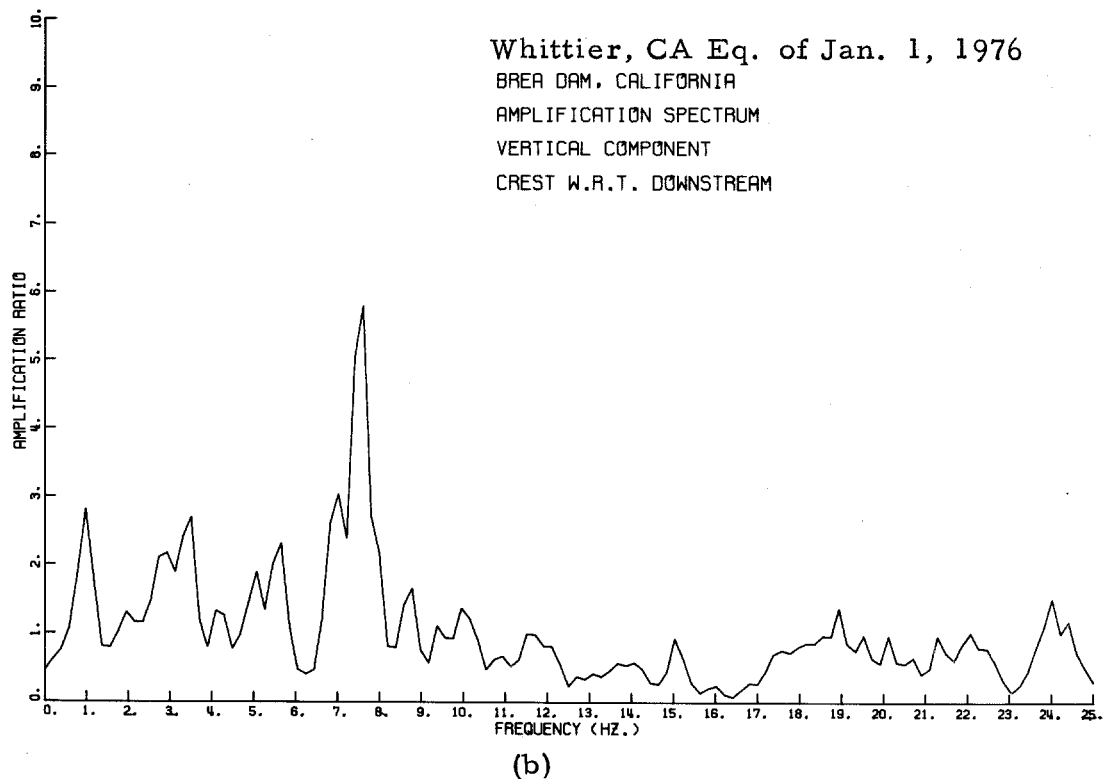
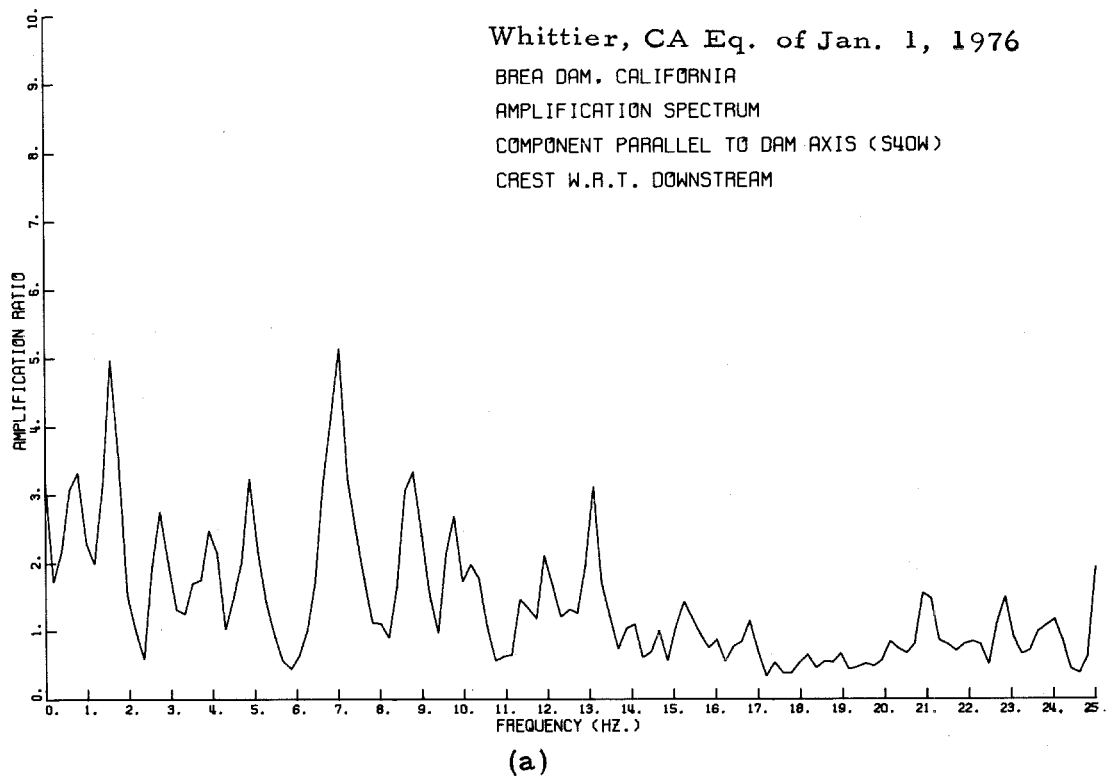


Fig. 80

TABLE 8

Observed Natural Frequencies From the Fourier Amplitude Spectra
and the Amplification Spectrum
Whittier, California Earthquake of Jan. 1, 1976
Brea Dam
Upstream/Downstream Direction (N50°W)

Fourier Amplitude Spectrum of Acceleration (Crest)		Fourier Amplitude Spectrum of Acceleration (Downstream)		Amplification Spectrum of the Crest		Modal Identification
Frequency Hz	Amplitude cm/sec	Frequency Hz	Amplitude cm/sec	Frequency Hz	Amplification Ratio	
-	-	-	-	0.78	3.40	First Mode
-	-	-	-	1.56	2.30	
-	-	2.0	7.0	-	-	
-	-	2.3	11.0	-	-	
-	-	2.6	10.0	-	-	Second Mode?
2.75	28.0	-	-	2.73	3.87	
-	-	3.0	9.0	-	-	
-	-	3.6	19.0	-	-	
-	-	3.95	23.0	-	-	Third Mode?
4.10	22.0	-	-	4.10	1.34	
-	-	4.45	9.0	-	-	
-	-	-	-	4.69	1.63	
-	-	5.0	13.0	-	-	Fourth Mode?
5.15	12.0	-	-	-	-	
-	-	5.3	13.0	-	-	
-	-	5.7	11.0	-	-	
5.85	13.0	-	-	5.86	1.47	Fifth Mode?
-	-	6.5	16.0	-	-	
7.10	13.0	-	-	7.03	1.80	
-	-	7.25	11.0	-	-	
7.65	8.0	-	-	7.62	3.66	Sixth Mode?
-	-	7.95	5.0	-	-	
8.20	8.0	-	-	8.20	1.17	
-	-	8.35	6.0	-	-	
-	-	8.95	6.5	-	-	Seventh Mode?
9.10	8.0	-	-	9.10	1.50	
9.40	8.0	-	-	-	-	
-	-	9.55	7.5	-	-	
10.20	10.0	-	-	10.16	2.26	Ninth Mode?

TABLE 9

Observed Natural Frequencies From the Fourier Amplitude Spectra
and the Amplification Spectrum
Whittier, California Earthquake of Jan. 1, 1976
Brea Dam
Longitudinal Component (S40° W)

Fourier Amplitude Spectrum of Acceleration (Crest)		Fourier Amplitude Spectrum of Acceleration (Downstream)		Amplification Spectrum of the Crest		Modal Identification
Frequency Hz	Amplitude cm/sec	Frequency Hz	Amplitude cm/sec	Frequency Hz	Amplification Ratio	
-	-	-	-	0.78	3.34	First Mode
-	-	1.10	3	-	-	
-	-	1.30	3	-	-	
-	-	-	-	1.56	4.98	
-	-	1.85	3	-	-	Second Mode? Third Mode?
-	-	2.40	7	-	-	
-	-	2.60	7	-	-	
2.75	18	-	-	2.73	2.75	
-	-	2.90	9	-	-	Fourth Mode?
-	-	3.20	15	-	-	
3.55	22	3.55	16	3.55	1.73	
3.90	22	-	-	3.91	2.47	
-	-	4.00	13	-	-	Fifth Mode?
-	-	4.40	6	-	-	
4.88	12	-	-	4.88	3.25	
-	-	4.95	5	-	-	
5.45	5	5.45	7.5	-	-	Sixth Mode?
-	-	5.95	11.5	-	-	
-	-	6.30	9	-	-	
-	-	6.80	6	-	-	
7.03	21	-	-	7.03	5.14	Seventh Mode? Eighth Mode?
-	-	7.50	9	-	-	
-	-	7.90	13	-	-	
-	-	-	-	8.79	3.35	
9.00	12	-	-	-	-	Seventh Mode? Eighth Mode?
-	-	9.20	9	-	-	
9.70	8	-	-	9.77	2.68	
10.20	8	10.10	5	10.16	1.99	

TABLE 10
Comparison Between Observed Resonant Frequencies
and Those Computed by 2-D Shear Beam Theory
Whittier, California Earthquake of Jan. 1, 1976
Brea Dam
Upstream/Downstream Direction (N50° W)

Computed Natural Frequencies (Equation 1)				Difference Between Two Adjacent Frequencies (Hz)	Observed Natural Frequencies (Hz)	Remarks
Symmetric		Antisymmetric				
$f_{n, r}$	Hz	$f_{n, r}$	Hz			
$f_{1, 1}$	2.73*	$f_{1, 2}$	2.91	0.18	2.73	* only observed Computed
$f_{1, 3}$	3.18	$f_{1, 4}$	3.51	0.27 0.33	-	" "
$f_{1, 5}$	3.90	$f_{1, 6}$	4.33	0.39 0.43	4.10	" "
$f_{1, 7}$	4.79	$f_{1, 8}$	5.27	0.46 0.48	4.69	" "
$f_{1, 9}$	5.76	$f_{1, 10}, f_{2, 2}$	6.27	0.49	5.86	"
$f_{2, 1}$	6.18			0.42 0.09	-	" "
$f_{2, 3}$	6.39	$f_{2, 4}$	6.56	0.12 0.27	-	" "
$f_{1, 11}, f_{2, 5}$	6.79	$f_{2, 6}$	7.04	0.23 0.25	-	" "
		$f_{1, 12}$	7.31	0.27		"
$f_{2, 7}$	7.33	$f_{2, 8}$	7.65		7.03	" "
$f_{1, 13}$	7.84	$f_{2, 10}$ $f_{1, 14}$	8.37 8.38		7.62	"
$f_{2, 9}$	8.00				8.20	" "
$f_{2, 11}$	8.76	$f_{2, 12}$	9.18		-	"
$f_{1, 15}$	8.91				9.10	"

CHAPTER V

DIEMER FILTRATION PLANT

V-I Description of the Structure

The Robert B. Diemer Filtration Plant is located approximately 8 Km (5 miles) east of Brea and 41 Km (25.6 miles) southeast of Downtown Los Angeles. This water treatment facility receives water, purifies it, and then channels it for distribution to the Metropolitan Water District of Southern California (which also owns the plant). The facility consists of a group of settling basins, clarifiers, filters, a control building, a wash water tank and a large underground reservoir at the south end of the site. Figure 81 shows the Diemer Plant site and some of the surrounding topography. The original site was a plateau sloping down in all four directions (as shown in Fig. 81, where contours indicate an approximation of the existing grades).

The underground reservoir, which is 220 m (721 ft) by 91.8 m (301 ft) in plan dimensions (with two truncated corners as shown in Fig. 81), and about 6.8 m (22.3 ft) in vertical dimension, has a 35.6 cm (14 in) thick reinforced concrete roof slab supported on R.C. columns 50.8 cm (20 in) in diameter and 6.1 m (20 ft) on centers each way; the columns have drop slabs which are 2.1 m (7 ft) square and 50.8 cm (20 in) thick. The reservoir's reinforced concrete walls vary in thickness from 36 cm (1' - 2") to 51 cm (1' - 8"). Figure 82 shows structural details of the reservoir floor-plan. The reservoir is covered by filled ground about 0.6 m (2 ft) in thickness

on which there is 3.8 cm (1.5 in) asphalt and concrete pavement used as a parking area. There is a 2.5 m (8 ft) diameter bypass pipe from the inlet structure to the outlet structure of the reservoir; the pipe is mortar-lined, welded steel pipe (Fig. 82). The longitudinal direction of the reservoir is N79°W, and the transverse (short-side) direction is N11°E.

The headhouse (i.e., the control or administration building) is a three-story reinforced concrete structure with an influent conduit (12 in thick) passing through its basement as shown in Fig. 83. The building consists of chemical feeders, a main control room, the main supply and storage rooms, a laboratory, the main switchboard, and a machine shop.

As part of the reservoir structural improvement program, new shear walls (with openings) are proposed to increase the lateral resistance of the reservoir. This structural modification consists of building three new shear walls (1.12 m or 3' - 8" thick) in the transverse direction (short side or N11°E) and one new shear wall (46 cm or 18" thick) in the longitudinal direction. In addition, one new continuous wall block surrounding the interior of the reservoir walls is proposed. Figure 82, showing the plan of the reservoir, illustrates these suggested structural modifications.

There were two strong-motion accelerographs (SMA-1) located in the vicinity of the Diemer Water Treatment Plant site during the Whittier California earthquake of January 1, 1976. The site was about 8.9 Km (5.6 miles) from the epicenter. One accelerograph had been installed at the access structure on the roof of the reservoir.

The other accelerograph was on the sub-basement floor of the head-house (administration or control building) in the tunnel access room. The floor of this room is cement, 15.2 cm (6 in) thick and at an elevation of 247 m (810 ft). Figure 81 shows the plan of the Diemer Filtration plant with the location of the two accelerographs.

V-2 Time Domain Analysis

The eleven accelerograms recovered from the Whittier earthquake of Jan. 1, 1976 recorded peak accelerations of 10% g or greater except for the two instruments at the Diemer Filtration Plant. The reservoir instrument recorded a peak acceleration value of 7% g while the peak ground acceleration at the sub-basement level of the head-house was 2% g. The two accelerographs were about 275 m (900 ft) apart.

The digitized and uncorrected accelerograms recovered from the sub-basement and reservoir are shown in Figs. 84-a and 84-b, while Figs. 85 and 86 show the corrected accelerograms and the computed velocities and displacements.

The roof of the reservoir experienced stronger motion in the transverse direction (N11°E) than in the longitudinal direction, as shown by Figs. 84-b and 86-a and b. The accelerogram of the transverse component (N11°E) at the reservoir showed that the structure responded primarily to its fundamental mode of vibration with an apparent period of about 0.27 seconds (this is seen clearly from the integrated velocity curve of Fig. 86-a). The maximum peak-to-peak amplitude of the velocity curve of the N11°E component is 4 cm/sec; thus, if one assumes that the velocity is a sine wave

(i. e., $v(t) = 2 \sin \frac{2\pi}{T}t$, $T = 0.27$ secs) then the resulting displacement is $\frac{T}{\pi} \cos \frac{2\pi}{T}t$ with maximum displacement amplitude of $\frac{T}{\pi} = 0.1$ cm. In the longitudinal direction (S79°E) the reservoir responded in a manner related to its fundamental as well as to other higher modes of vibration (see Fig. 86-b) with an apparent fundamental period of about 0.25 seconds. The recorded vertical motion (Fig. 86-c) shows a dominant single peak of about 0.1 seconds. It is seen that the roof of the reservoir vibrated relatively strongly in the N11°E direction and these, presumably, were horizontal beam-type vibrations with the roof slab spanning from one end of the reservoir to the other. Such vibrations are not apparent with other direction (Fig. 86-b).

V-3 Frequency Domain Analysis

The response spectrum curves and the Fourier amplitude spectrum curves for the headhouse sub-basement and for the reservoir records are shown in Figs. 87 through 98. The relative velocity response spectrum (Fig. 90-a) and the response spectrum (Fig. 90-b) of the transverse component (N11°E) of the reservoir showed a single dominant peak at about 0.27 secs, which is clearly the fundamental period of vibration in that direction. In addition, the Fourier amplitude spectrum of acceleration (Fig. 96-a) of this transverse component is dominated by a single peak at frequency 2.7 Hz ($T = 0.27$ secs) whose amplitude is greater than five times those of the four next strongest peaks, occurring at 5.5, 6.5, 7.85 and 12.5 Hz. The longitudinal component (S79°E) does not show such a strong peak (Fig. 97-a); as would be expected from the proportions of the slab, no significant bending vibrations occurred in this direction.

Since the locations of the two strong-motion instruments were 900 ft apart, the characteristics of ground motion at each station may be different. For instance, during the 1971 San Fernando earthquake, the motions recorded by instruments located in Millikan Library, at one end of the campus of California Institute of Technology, differed greatly from those at the Caltech Athenaeum located at the other end. Bearing this in mind, in order to approximate the natural frequencies of the reservoir in three directions, the amplification spectra were computed by dividing the Fourier transform of the reservoir's accelerations by those of the headhouse sub-basements's accelerations. This should separate (to some extent) the characteristics of the reservoir from those of the earthquake ground motion and will enable an estimate of the relative contribution of different modes of vibration. The amplification spectrum curves for the three components are shown in Figs. 99-a, b and 100. Now, tabulating all the possible peaks and the associated frequencies of both the Fourier amplitude spectra and the amplification spectra for the two stations enables one to detect some of the natural frequencies of the reservoir (see Tables 11 and 12). It can be seen from Table 11 that the fundamental frequency of the reservoir in the transverse direction is 3.7 Hz, while in the longitudinal direction it is difficult to decide whether 4.0, 4.8 or 6.15 Hz is the natural frequency. Actually, the peak at 6.15 Hz dominated, suggesting that this is probably the natural frequency in this direction.

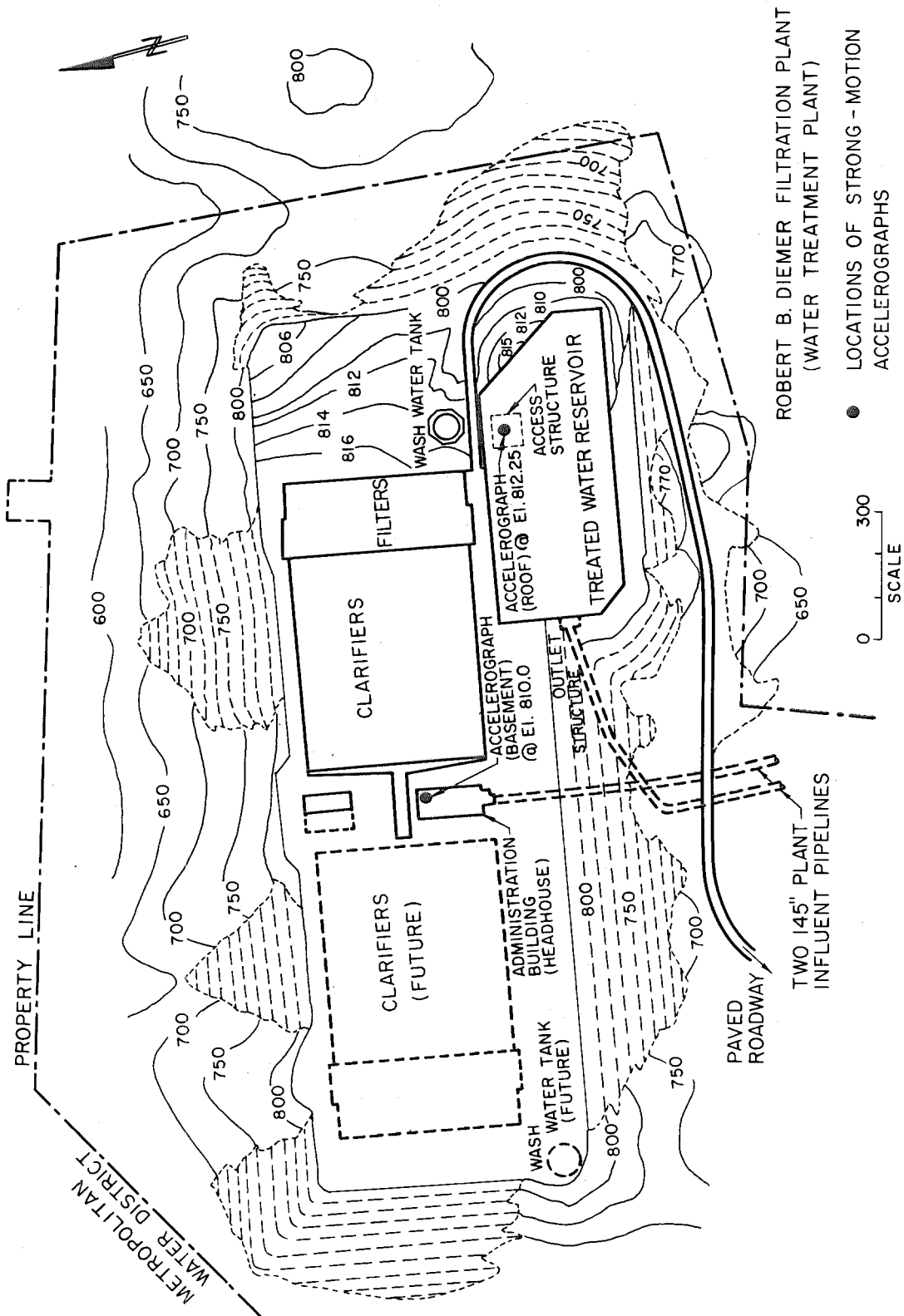
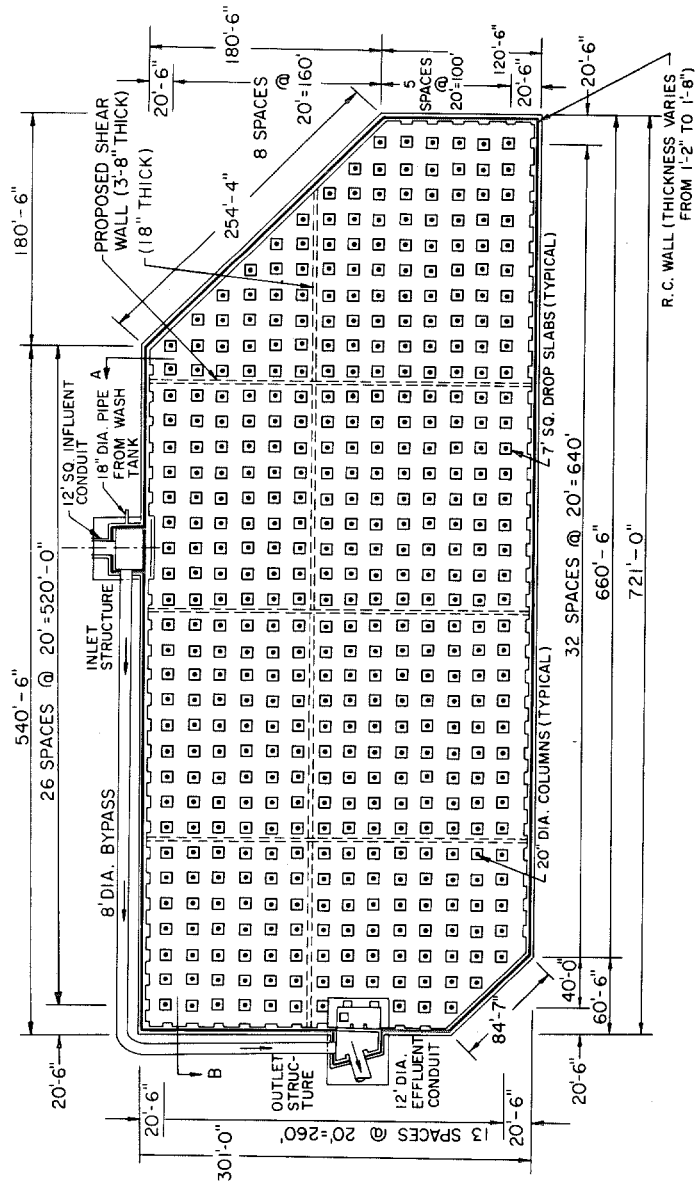
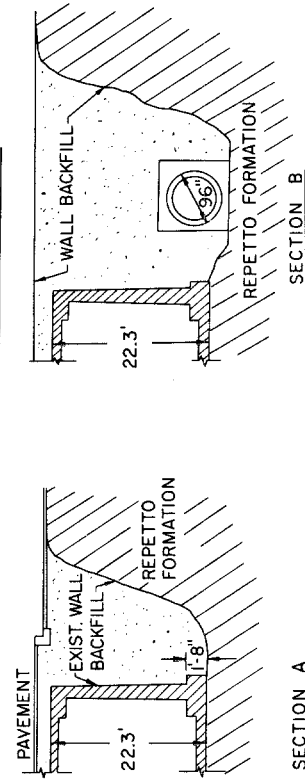


Fig. 81

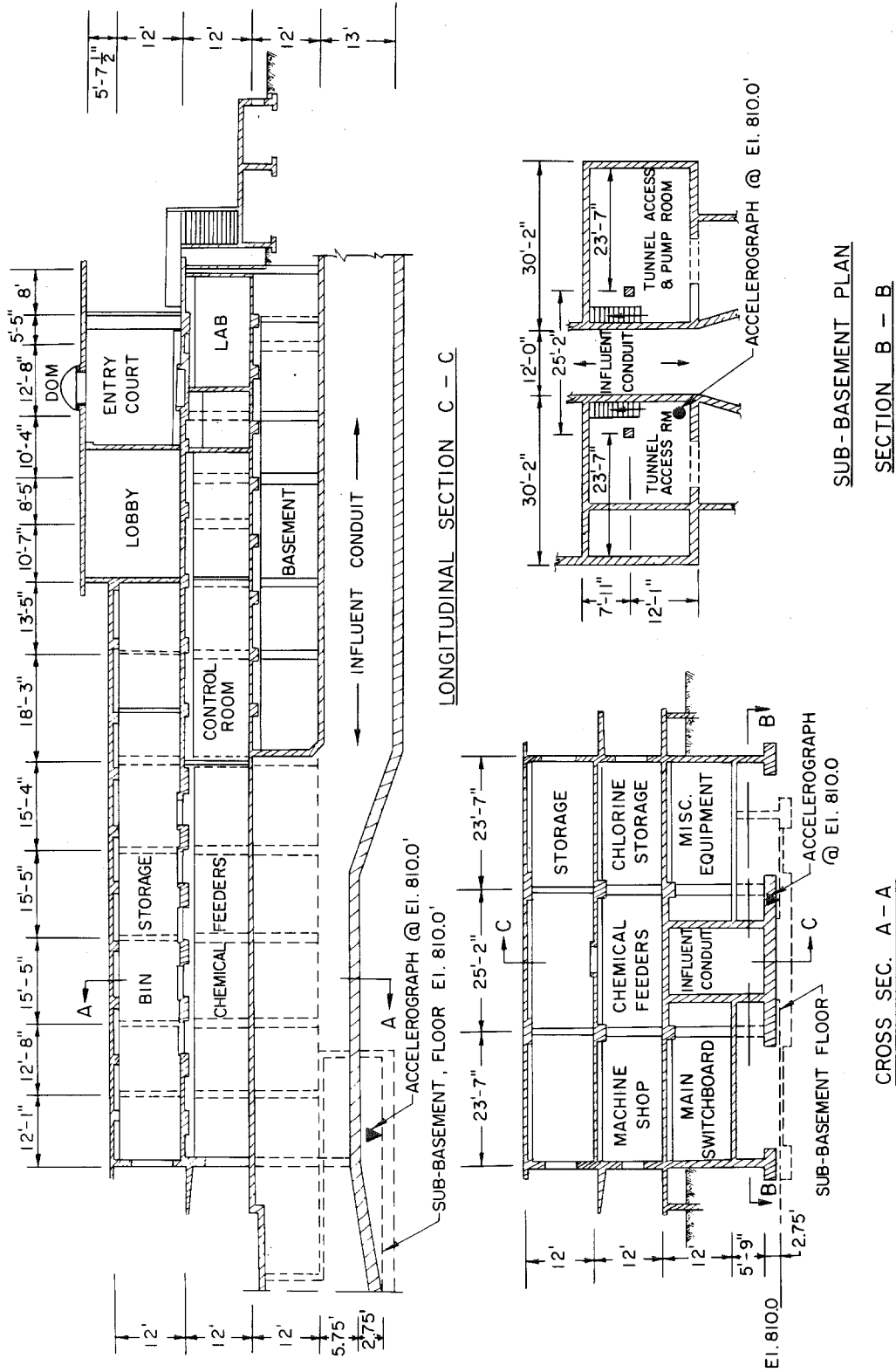


RESERVOIR FLOOR PLAN



STRUCTURAL DETAILS OF THE RESERVOIR (ROBERT B. DIEMER FILTRATION PLANT)

Fig. 82



STRUCTURAL DETAILS OF THE HEADHOUSE (R.B. DIEMER FILTRATION PLANT)

Fig. 83

DIEMER FILTER PLANT, ADMINISTRATION BLDG., JAN 1 1976

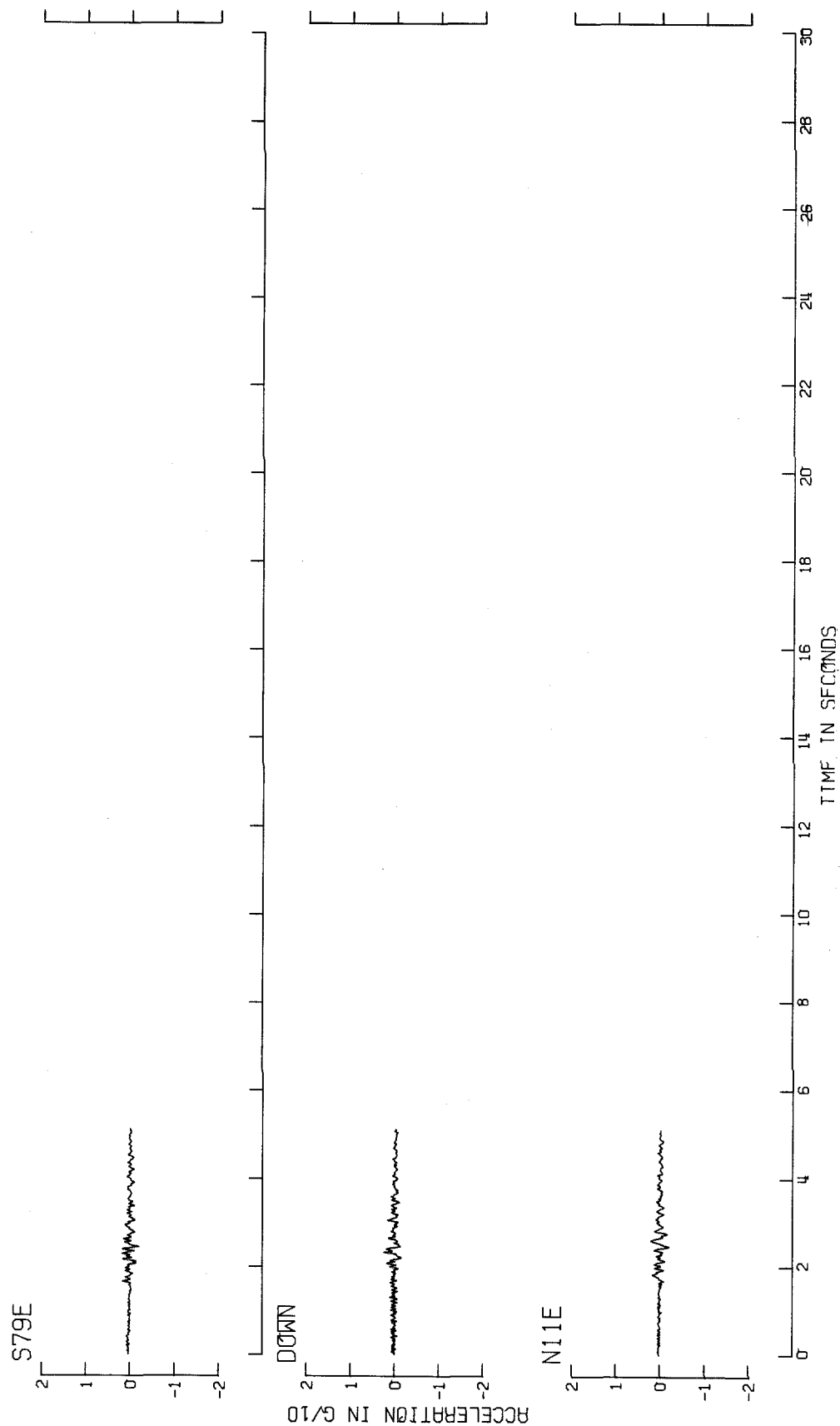


Fig. 84-a Uncorrected Accelerograms (Administration Building)

DIEMER FILTER PLANT, RESERVOIR, JAN 1 1976 0920 PST

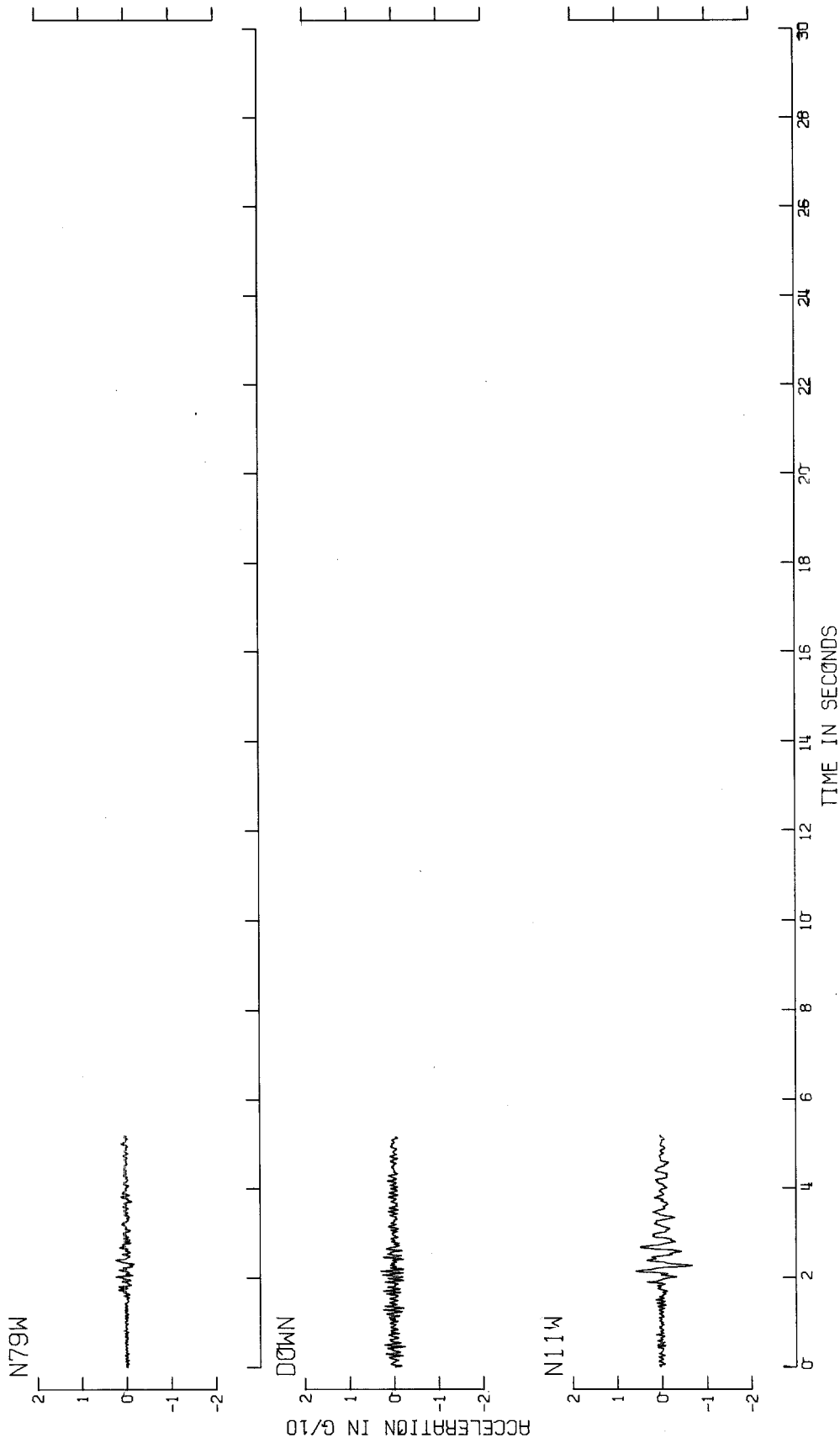
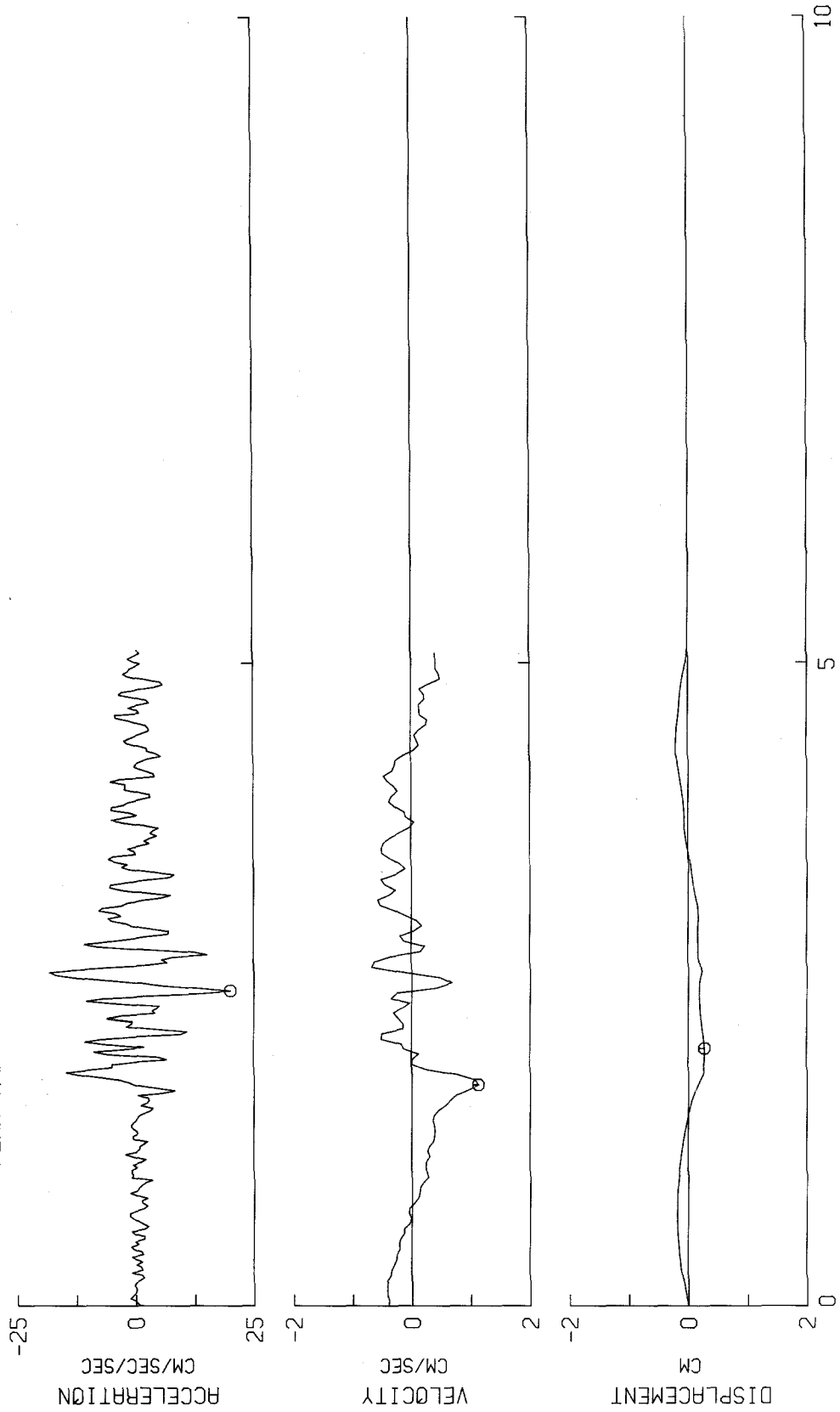


Fig. 84-b Uncorrected Accelerograms (Reservoir)

DIEMER FILTER PLANT, ADMINISTRATION BLDG., JAN. 1 1976-0920 PST
IN01440 DIEMER FILTER PLANT, ADMINISTRATION BLDG. COMP11E
PEAK VALUES : ACCEL = 20.0 CM/SEC/SEC VELOCITY = 1.1 CM/SEC DISPL = 0.3 CM



TIME - SECONDS

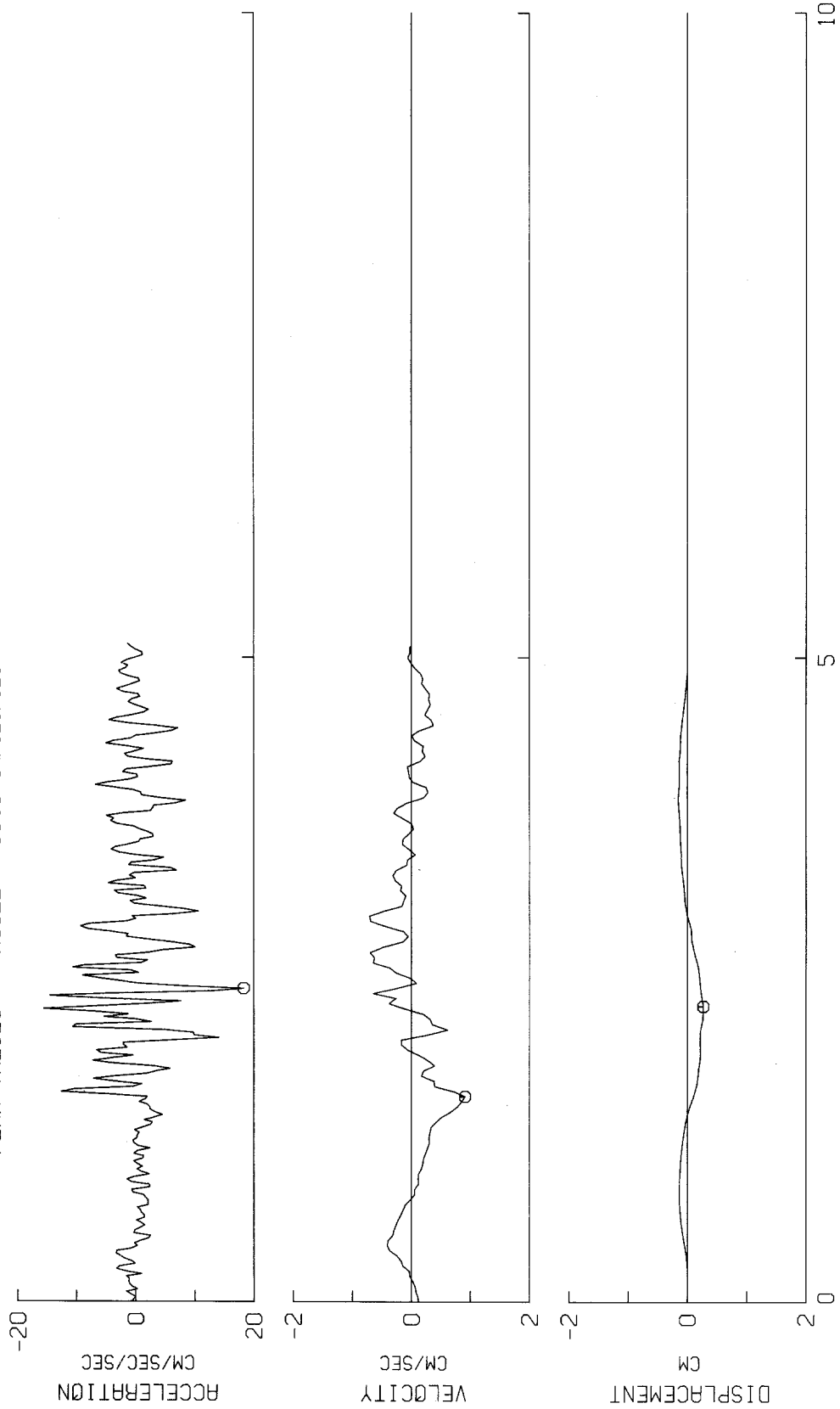
Fig. 85-a

DIEMER FILTER PLANT, ADMINISTRATION BLDG., JAN. 1 1976-0920 PST

IN01440

DIEMER FILTER PLANT, ADMINISTRATION BLDG. COMPS79E

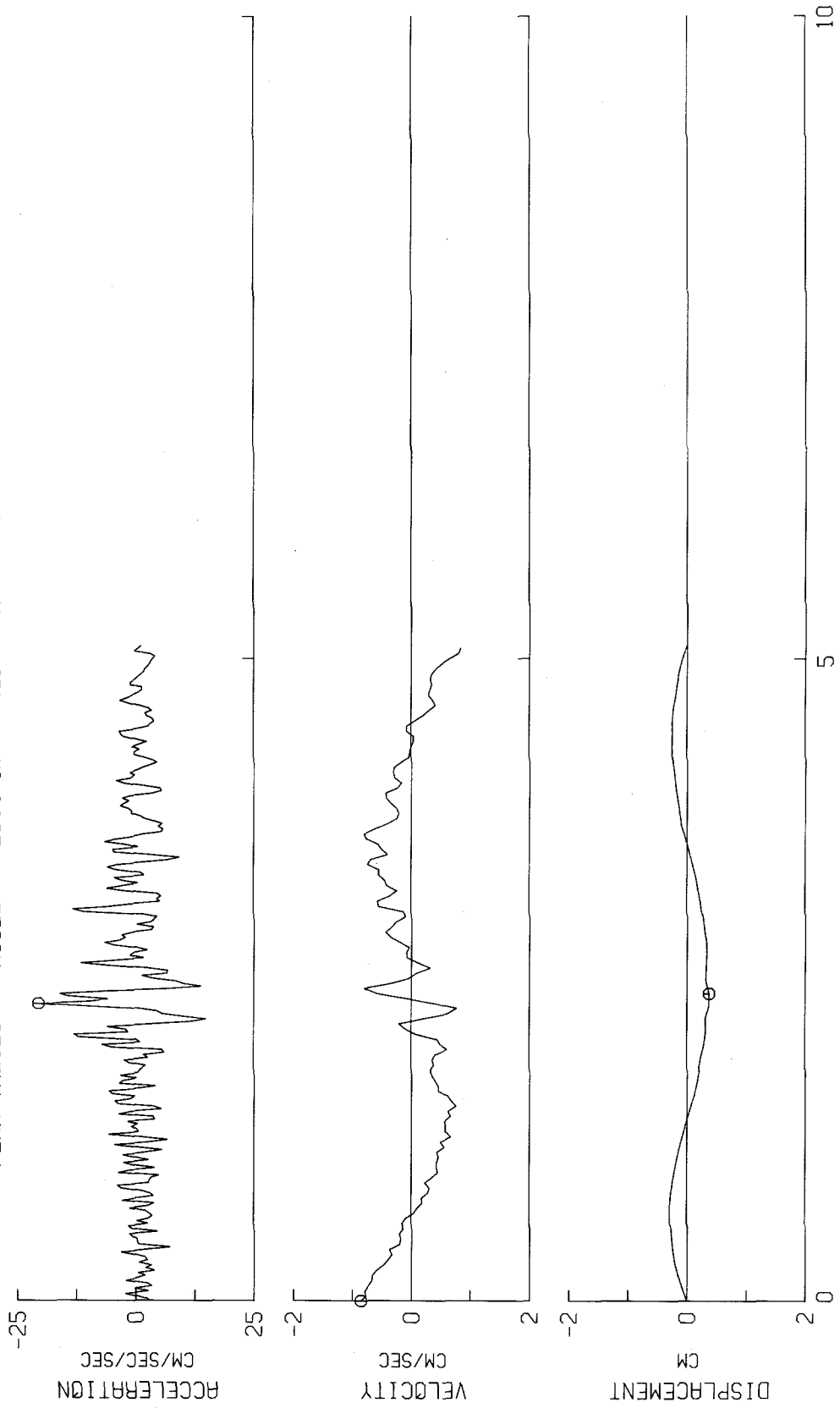
⊙ PEAK VALUES : ACCEL = 18.3 CM/SEC/SEC VELOCITY = 0.9 CM/SEC DISPL = 0.3 CM



TIME - SECONDS

Fig. 85-b

DIEMER FILTER PLANT, ADMINISTRATION BLDG., JAN. 1 1976-0920 PST
 IN01440 DIEMER FILTER PLANT, ADMINISTRATION BLDG. COMPDOWN
 PEAK VALUES: ACCEL = -20.4 CM/SEC/SEC VELOCITY = -.9 CM/SEC DISPL = 0.4 CM

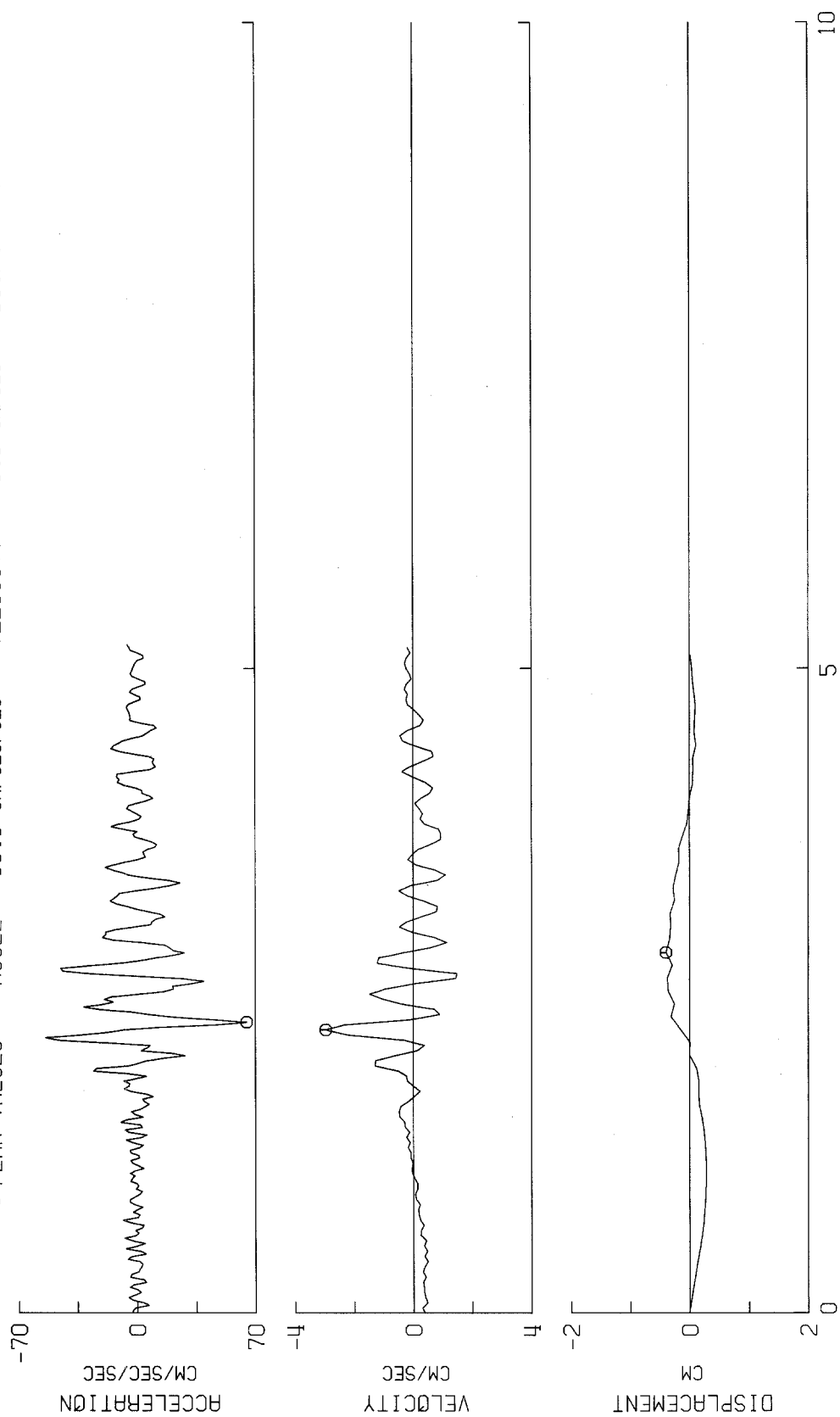


TIME - SECONDS

Fig. 85-c

DIEMER FILTER PLANT, RESERVOIR, JAN 1 1976-0920 PST
 IN01450 DIEMER FILTER PLANT, RESERVOIR COMPN:1W

Ø PEAK VALUES : ACCEL = 65.0 CM/SEC/SEC VELOCITY = -3.0 CM/SEC DISPL = -.4 CM



TIME - SECONDS

Fig. 86-a

DIEMER FILTER PLANT, RESERVOIR, JAN 1 1976-0920 PST
IN01450
DIEMER FILTER PLANT, RESERVOIR COMPS79E
⊙ PEAK VALUES : ACCEL = -19.6 CM/SEC/SEC VELOCITY = 0.7 CM/SEC DISPL = 0.2 CM

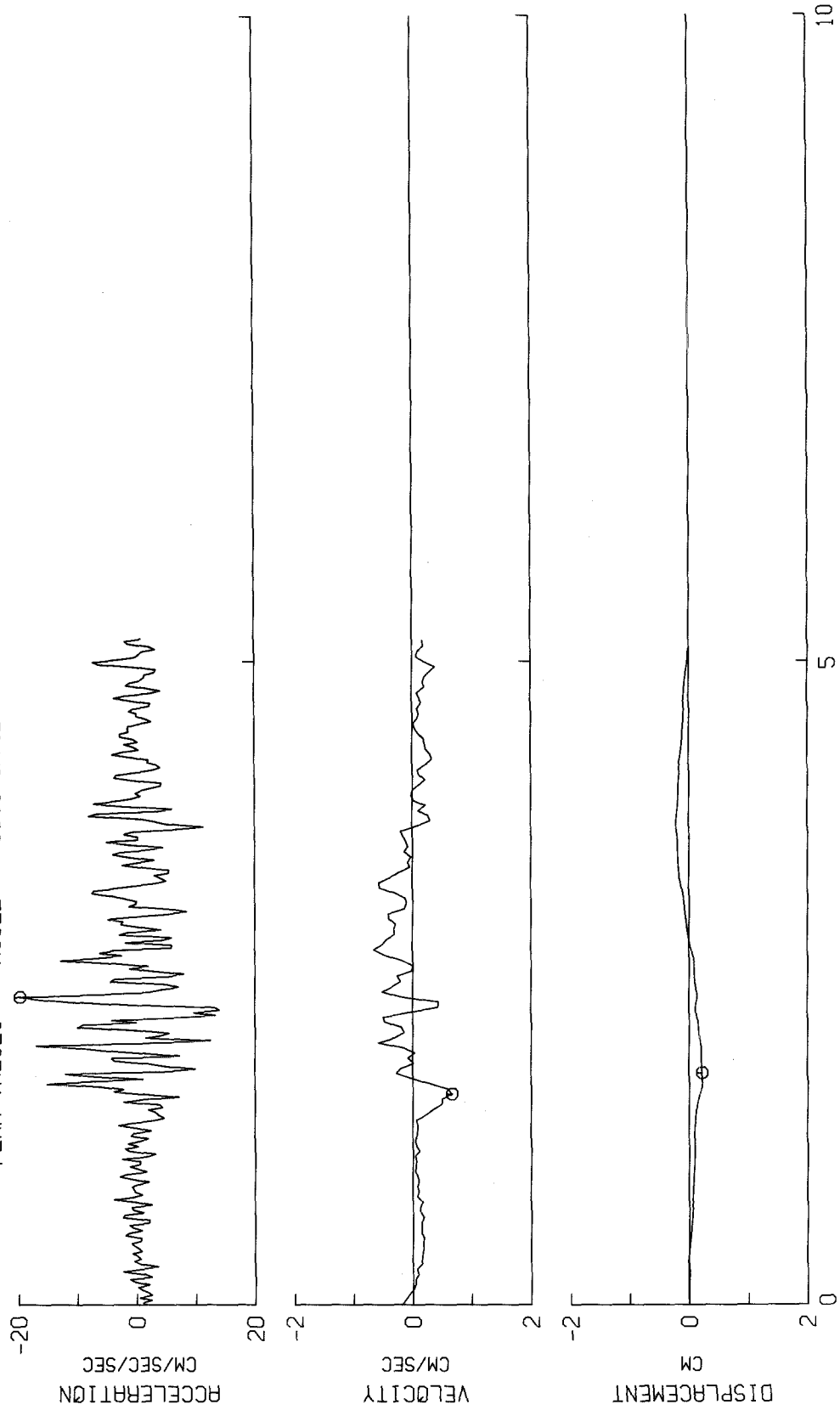
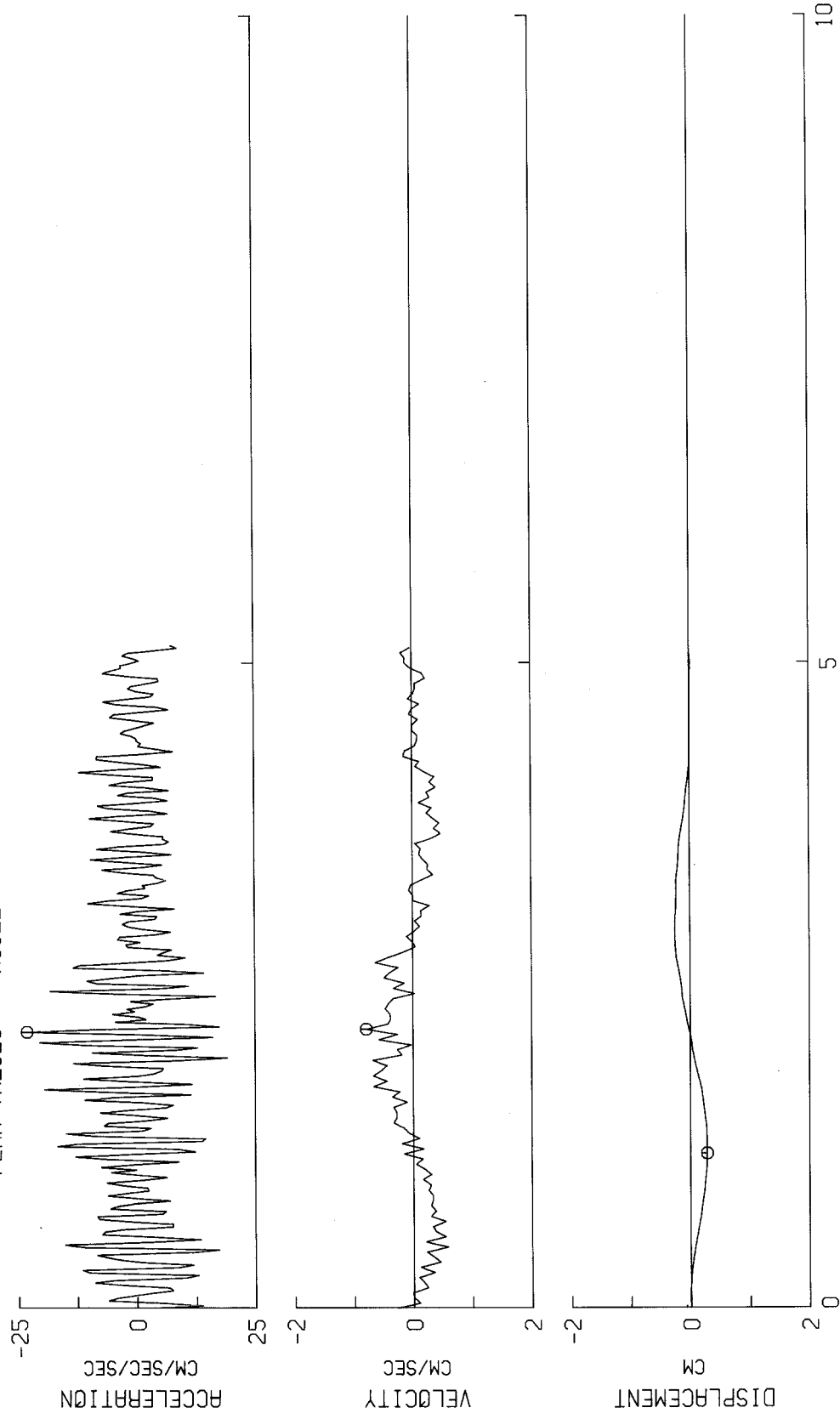


Fig. 86-b

DIEMER FILTER PLANT, RESERVOIR, JAN 1 1976-0920 PST
IN01450 DIEMER FILTER PLANT, RESERVOIR COMPDOWN
⊙ PEAK VALUES : ACCEL = -23.0 CM/SEC/SEC VELOCITY = -.8 CM/SEC DISPL = 0.3 CM



TIME - SECONDS

Fig. 86-c

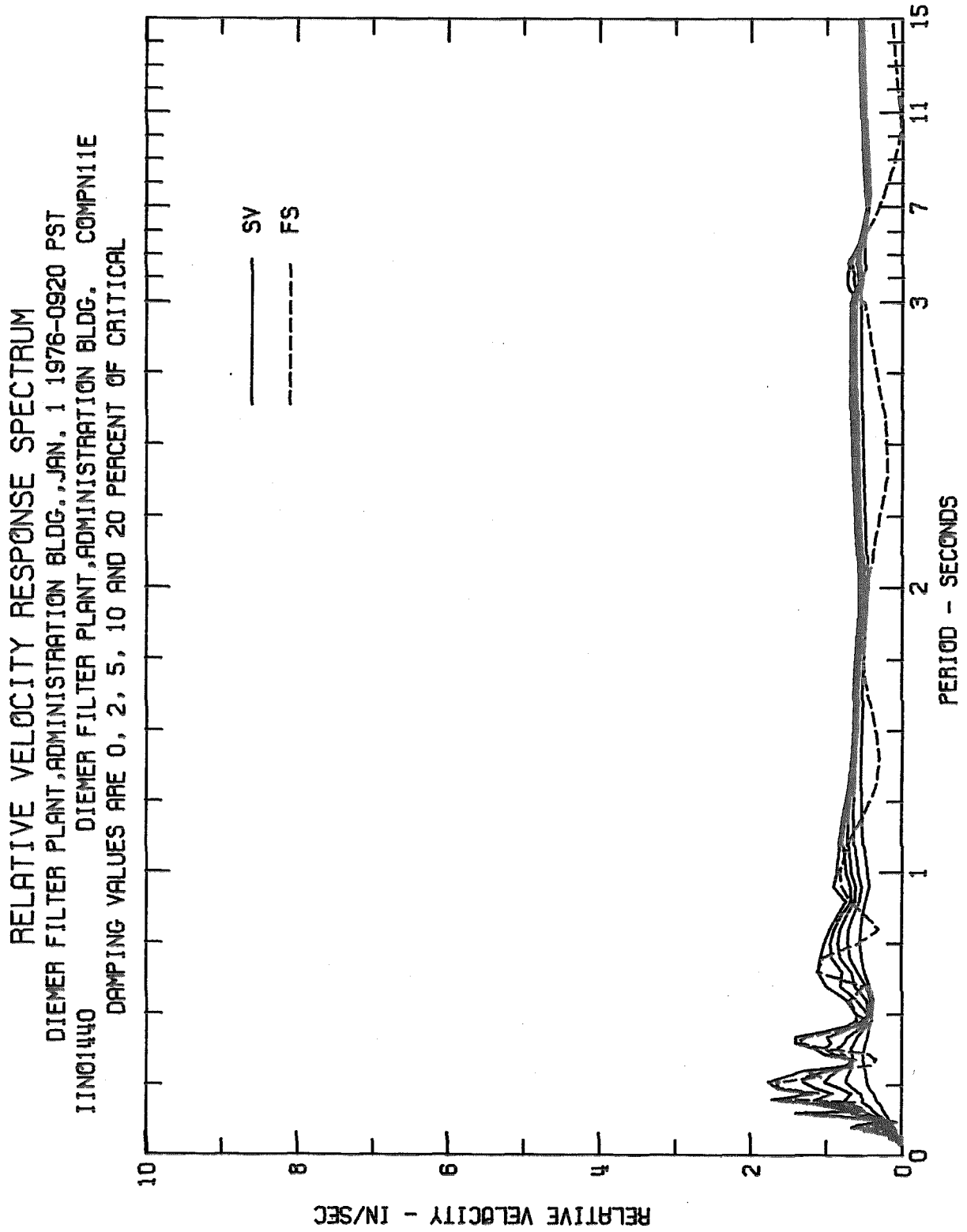


Fig. 87-a

RESPONSE SPECTRUM

DIEMER FILTER PLANT, ADMINISTRATION BLDG., JAN. 1 1976-0920 PST

IIN01440

DIEMER FILTER PLANT, ADMINISTRATION BLDG. COMPN11E

DAMPING VALUES ARE 0, 2, 5, 10 AND 20 PERCENT OF CRITICAL

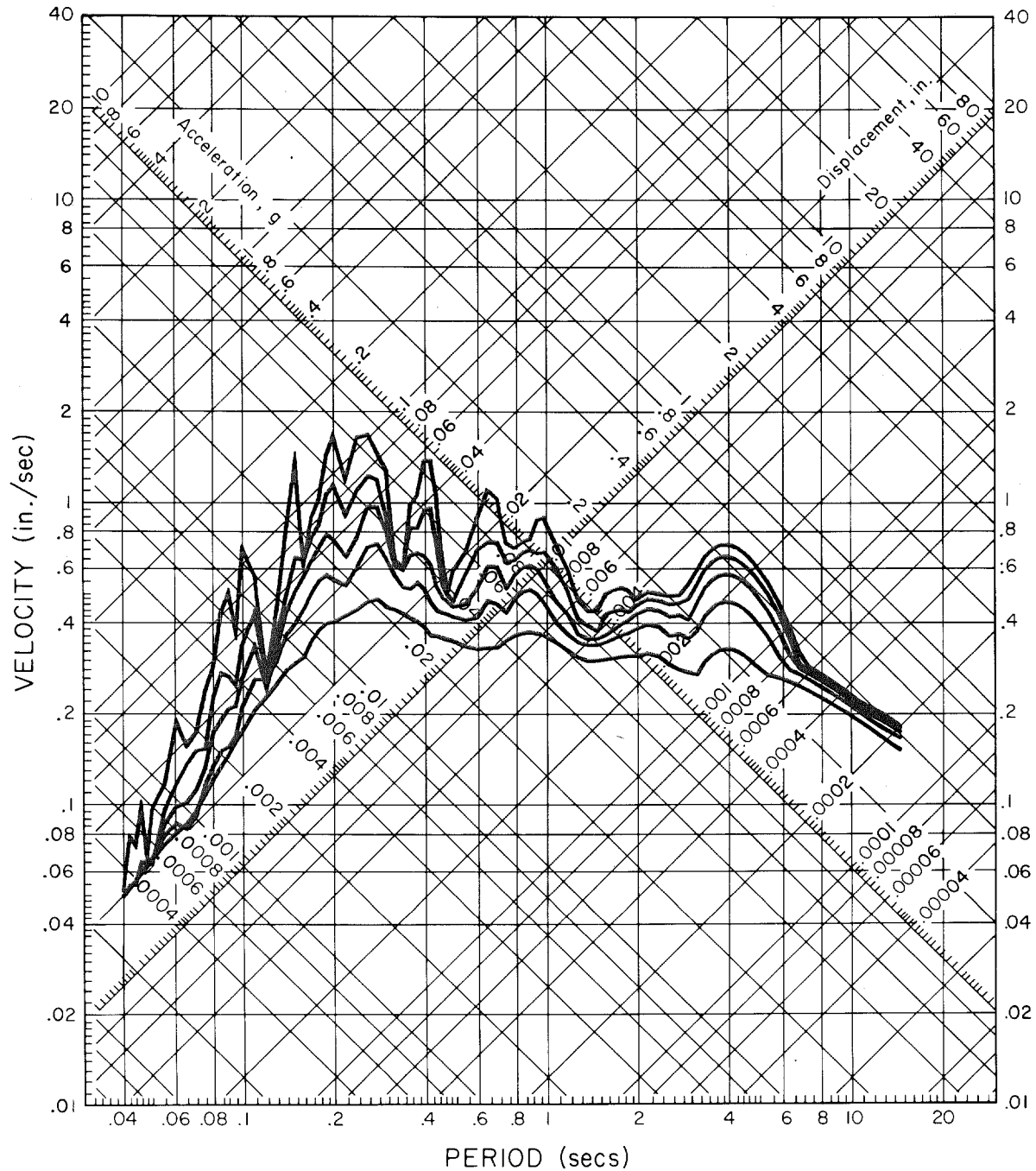


Fig. 87-b

RELATIVE VELOCITY RESPONSE SPECTRUM
DIEMER FILTER PLANT, ADMINISTRATION BLDG., JAN. 1 1976-0920 PST
11N01440 DIEMER FILTER PLANT, ADMINISTRATION BLDG. COMPS79E
DAMPING VALUES ARE 0, 2, 5, 10 AND 20 PERCENT OF CRITICAL

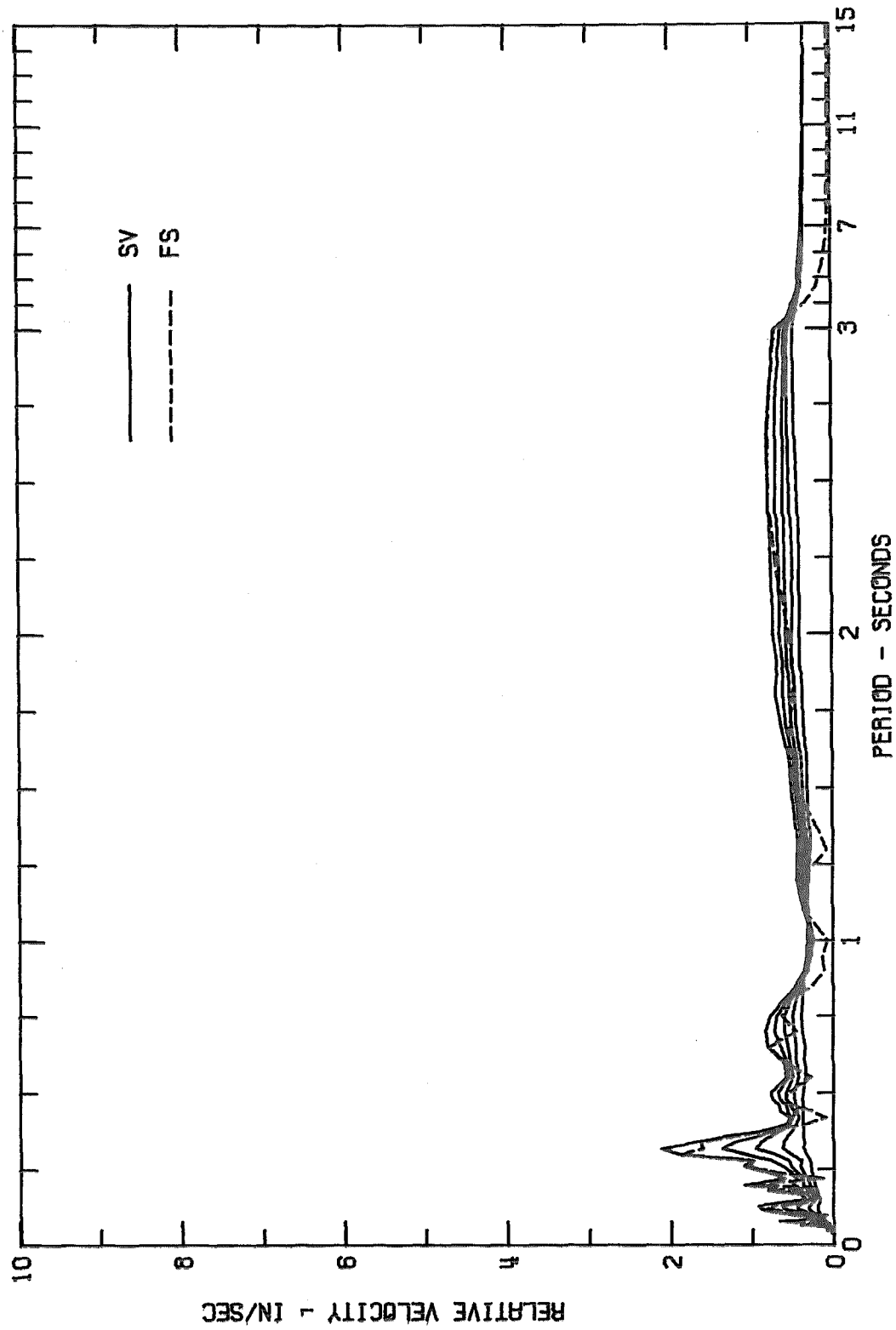


Fig. 88-a

RESPONSE SPECTRUM

DIEMER FILTER PLANT, ADMINISTRATION BLDG., JAN. 1 1976-0920 PST

IIN01440

DIEMER FILTER PLANT, ADMINISTRATION BLDG. COMPS79E

DAMPING VALUES ARE 0, 2, 5, 10 AND 20 PERCENT OF CRITICAL

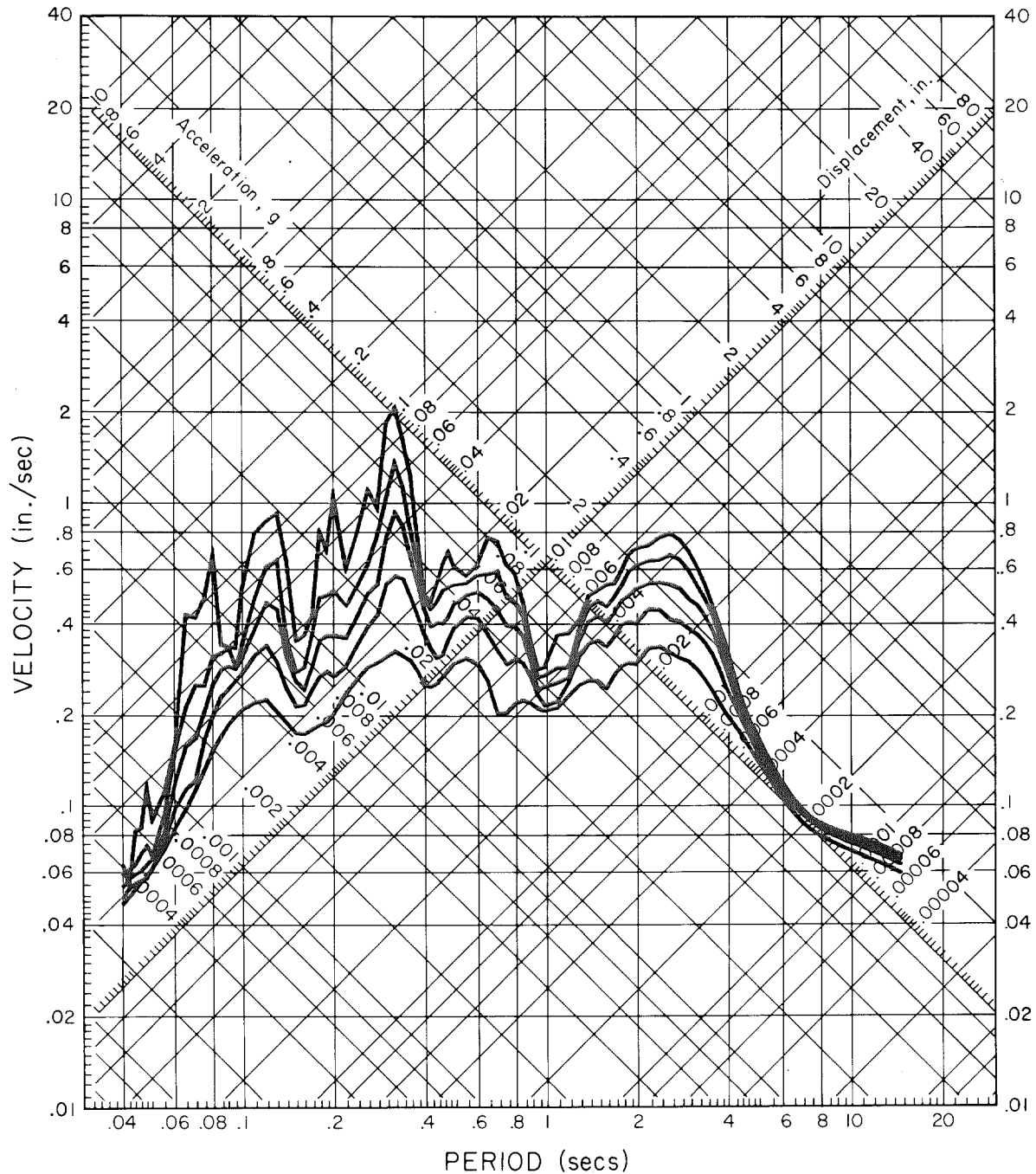


Fig. 88-b

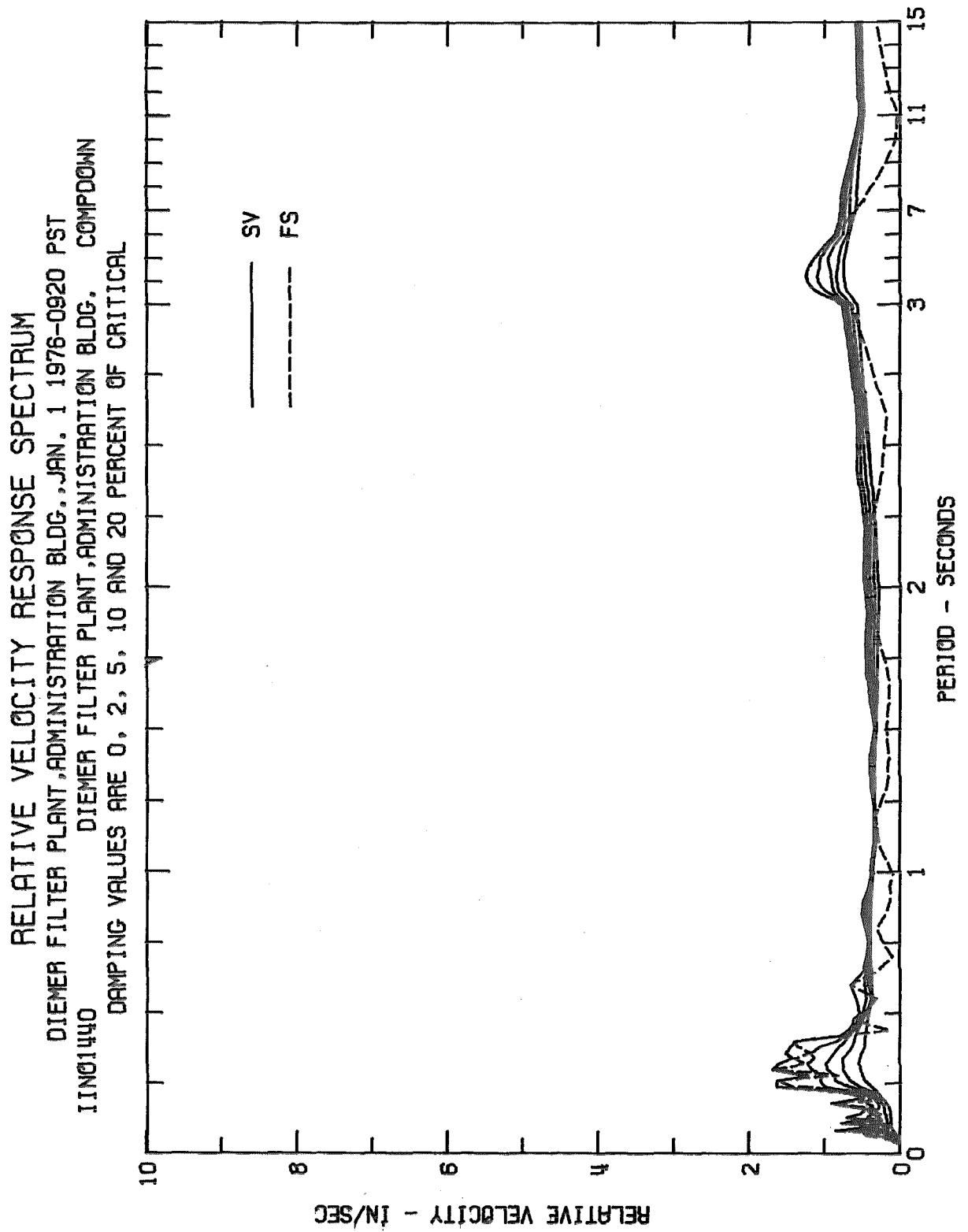


Fig. 89-a

RESPONSE SPECTRUM

DIEMER FILTER PLANT, ADMINISTRATION BLDG., JAN. 1 1976-0920 PST

IIN01440

DIEMER FILTER PLANT, ADMINISTRATION BLDG. COMPDOWN

DAMPING VALUES ARE 0, 2, 5, 10 AND 20 PERCENT OF CRITICAL

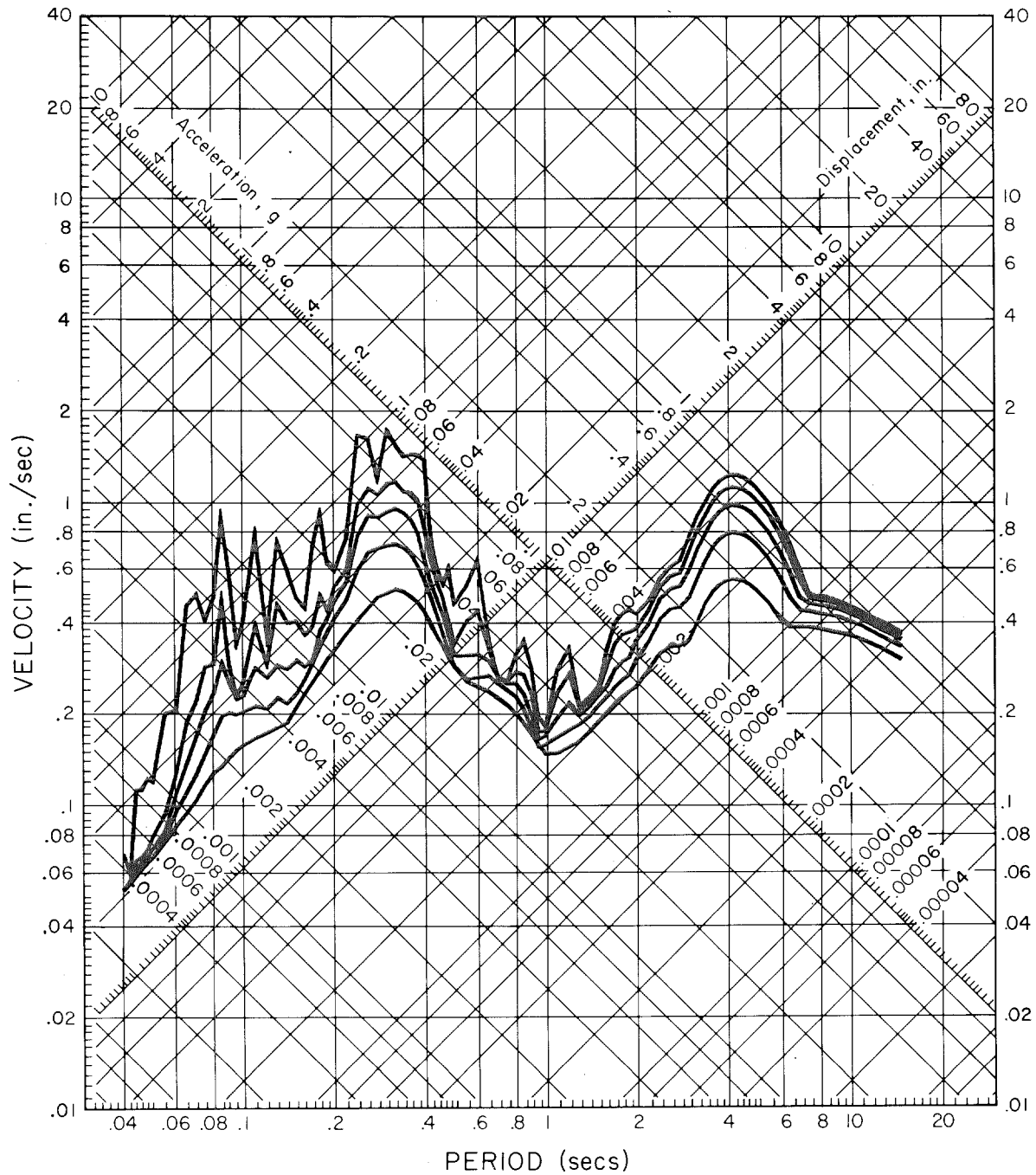


Fig. 89-b

RELATIVE VELOCITY RESPONSE SPECTRUM
DIEMER FILTER PLANT, RESERVOIR, JAN 1 1976-0920 PST
IIND01450 DIEMER FILTER PLANT, RESERVOIR COMP0111W
DAMPING VALUES ARE 0, 2, 5, 10 AND 20 PERCENT OF CRITICAL

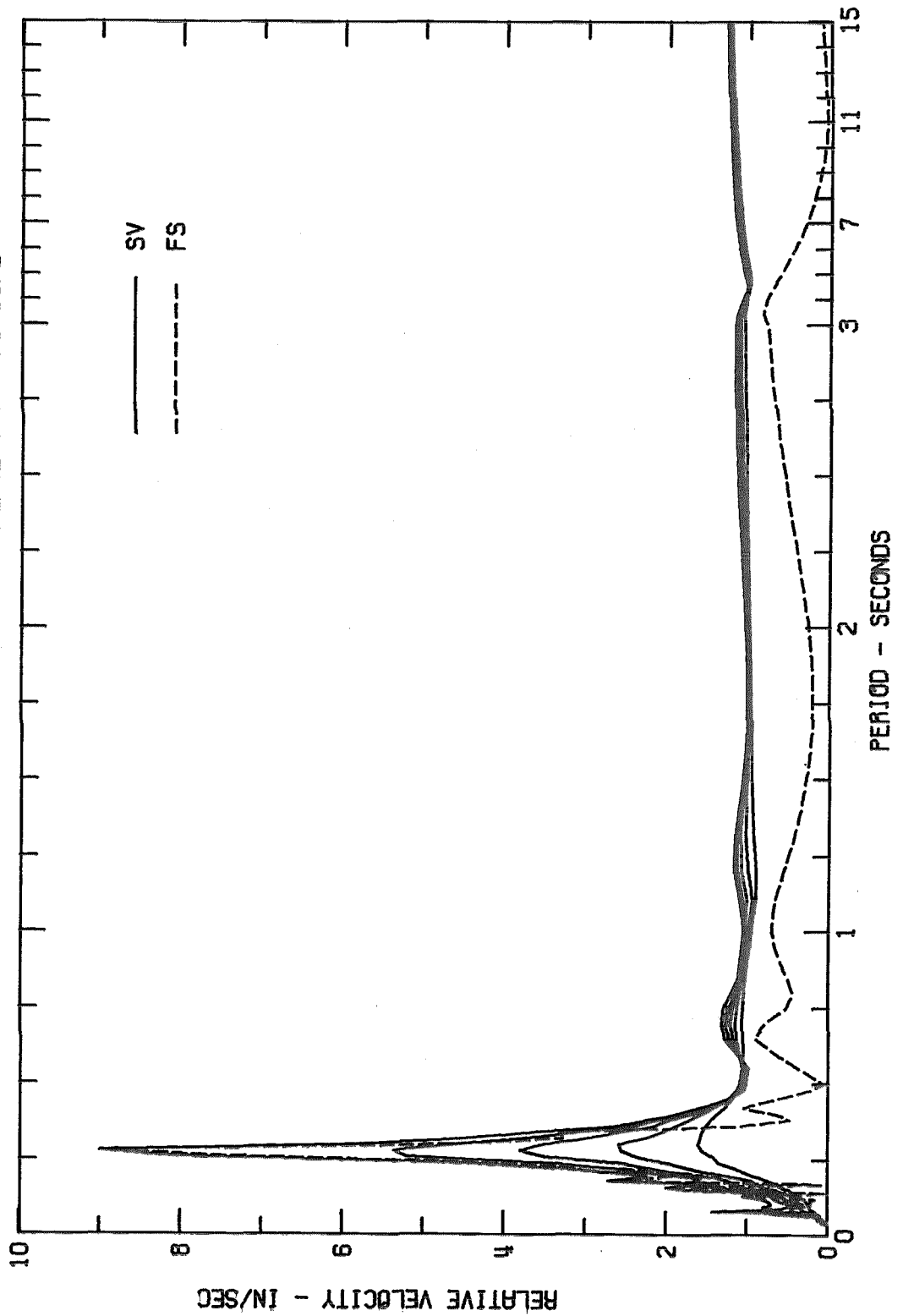


Fig. 90-a

RESPONSE SPECTRUM

DIEMER FILTER PLANT, RESERVOIR, JAN 1 1976-0920 PST

IIN01450

DIEMER FILTER PLANT, RESERVOIR COMPN11W

DAMPING VALUES ARE 0, 2, 5, 10 AND 20 PERCENT OF CRITICAL

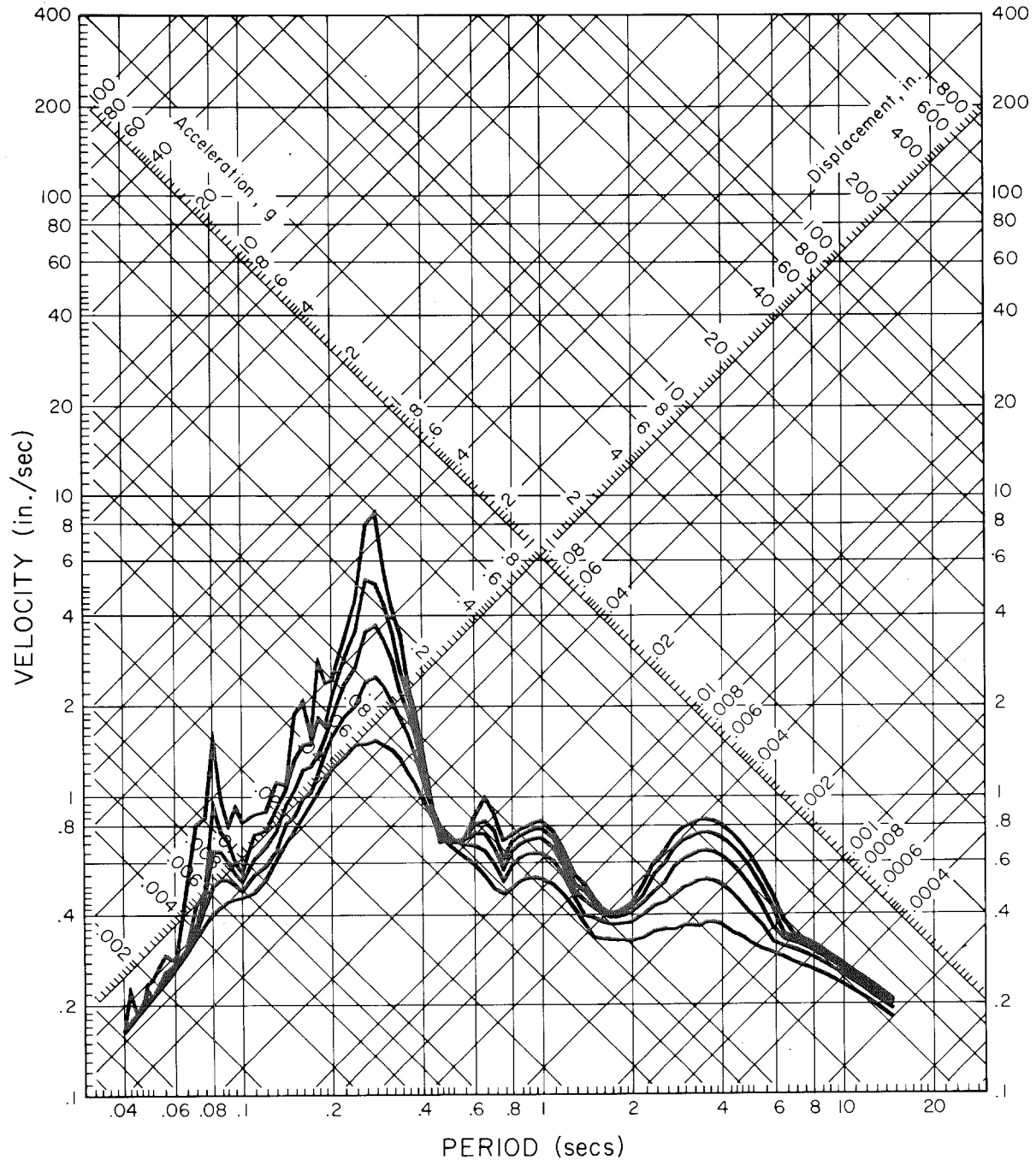
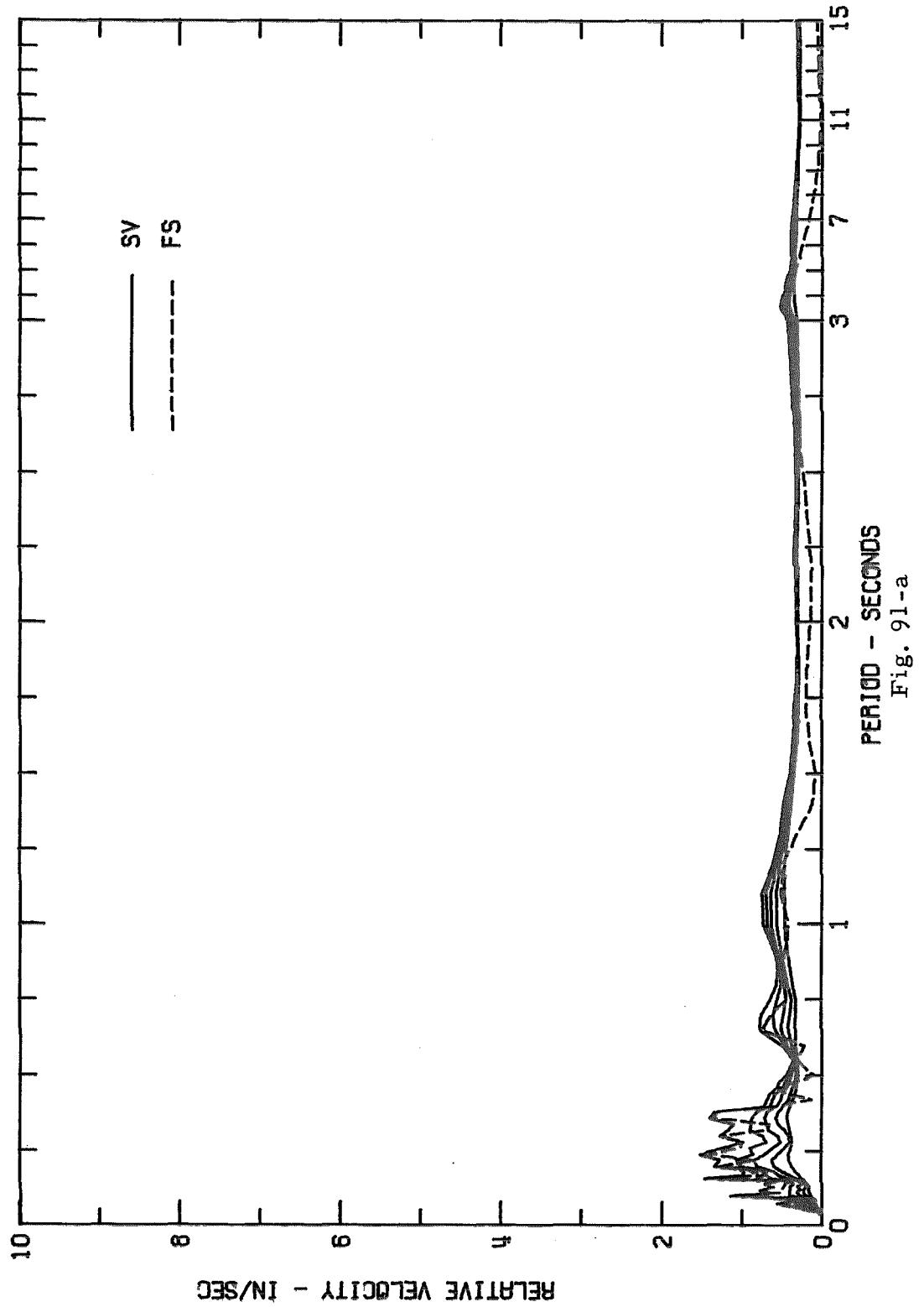


Fig. 90-b

RELATIVE VELOCITY RESPONSE SPECTRUM
DIEMER FILTER PLANT, RESERVOIR, JAN 1 1976-0920 PST
11N01450 DIEMER FILTER PLANT, RESERVOIR COMPS79E
DAMPING VALUES ARE 0, 2, 5, 10 AND 20 PERCENT OF CRITICAL



RESPONSE SPECTRUM

DIEMER FILTER PLANT, RESERVOIR, JAN 1 1976-0920 PST

IIN01450

DIEMER FILTER PLANT, RESERVOIR COMPS79E

DAMPING VALUES ARE 0, 2, 5, 10 AND 20 PERCENT OF CRITICAL

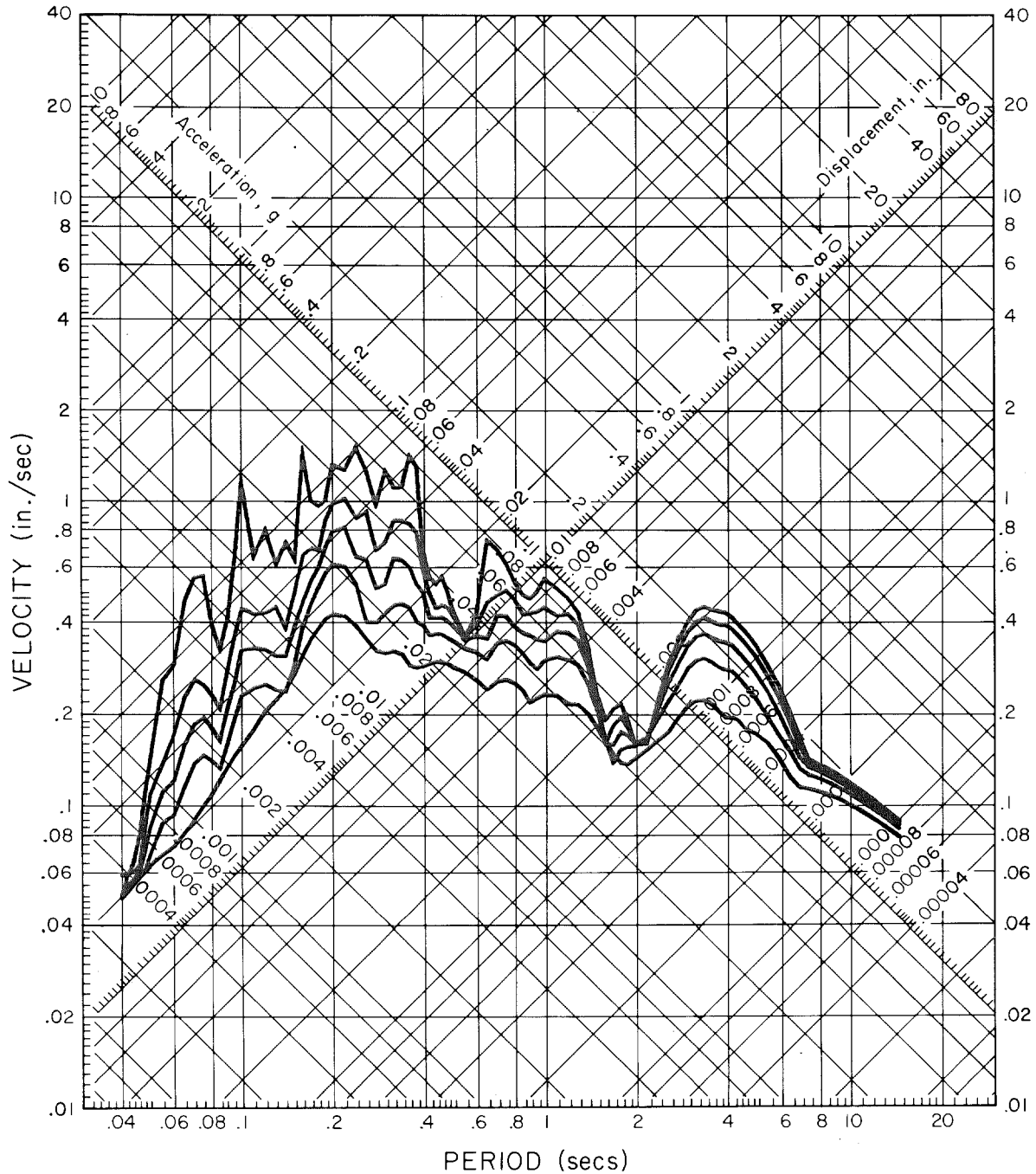
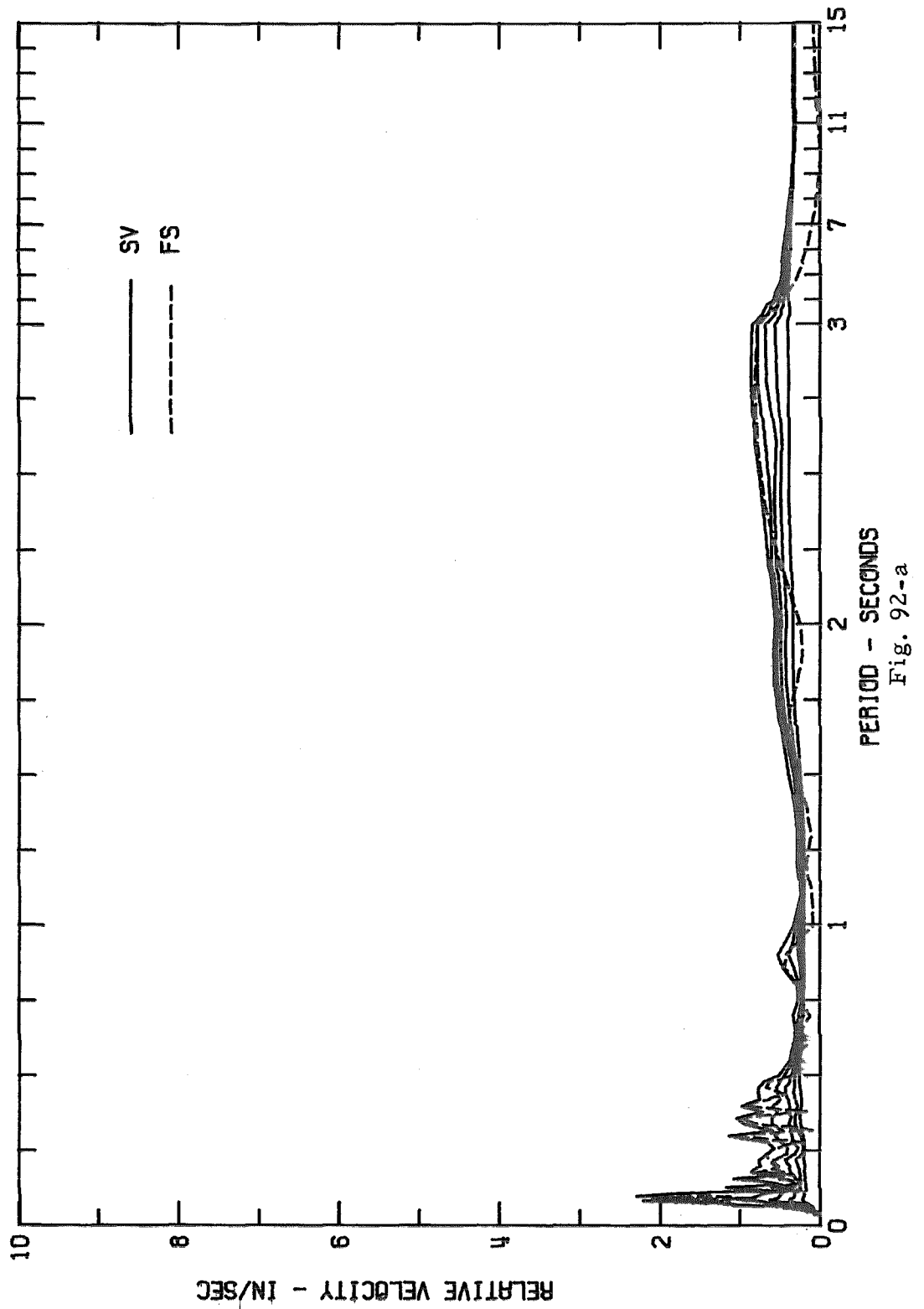


Fig. 91-b

RELATIVE VELOCITY RESPONSE SPECTRUM
DIEMER FILTER PLANT, RESERVOIR, JAN 1 1976-0920 PST
11N01450 DIEMER FILTER PLANT, RESERVOIR COMPOUND
DAMPING VALUES ARE 0, 2, 5, 10 AND 20 PERCENT OF CRITICAL



RESPONSE SPECTRUM

DIEMER FILTER PLANT, RESERVOIR, JAN 1 1976-0920 PST

IIN01450

DIEMER FILTER PLANT, RESERVOIR COMPDOWN

DAMPING VALUES ARE 0, 2, 5, 10 AND 20 PERCENT OF CRITICAL

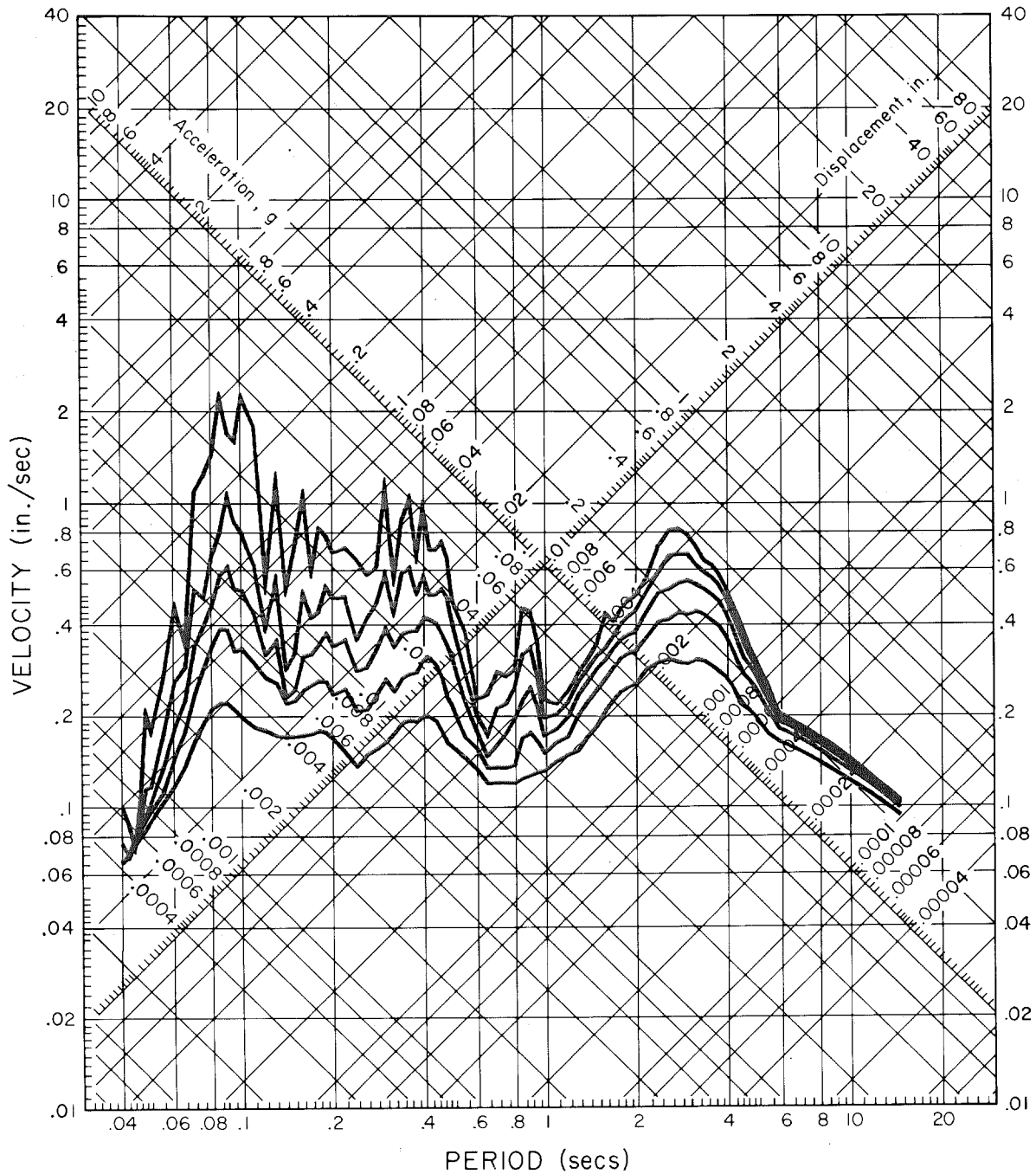


Fig. 92-b

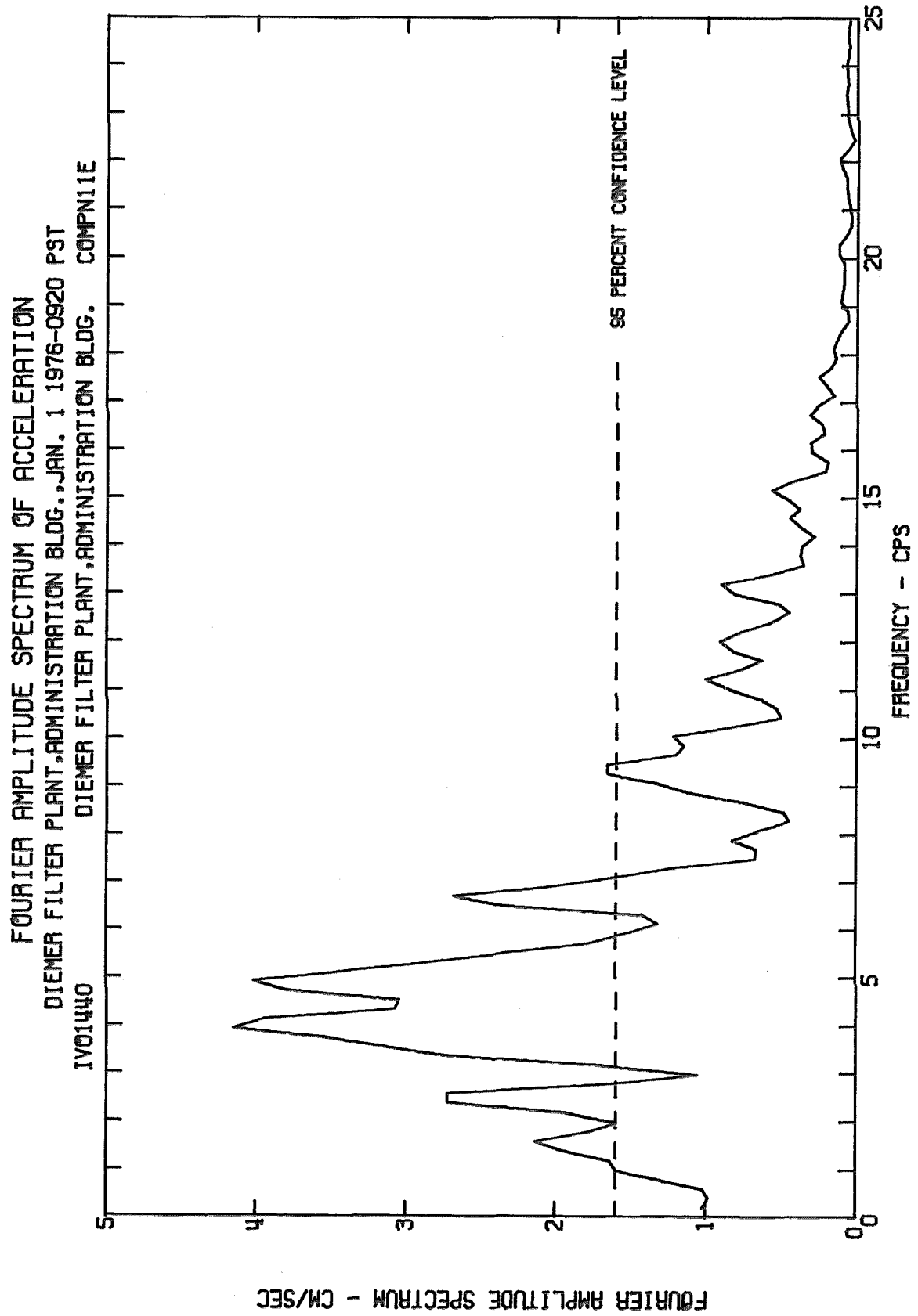
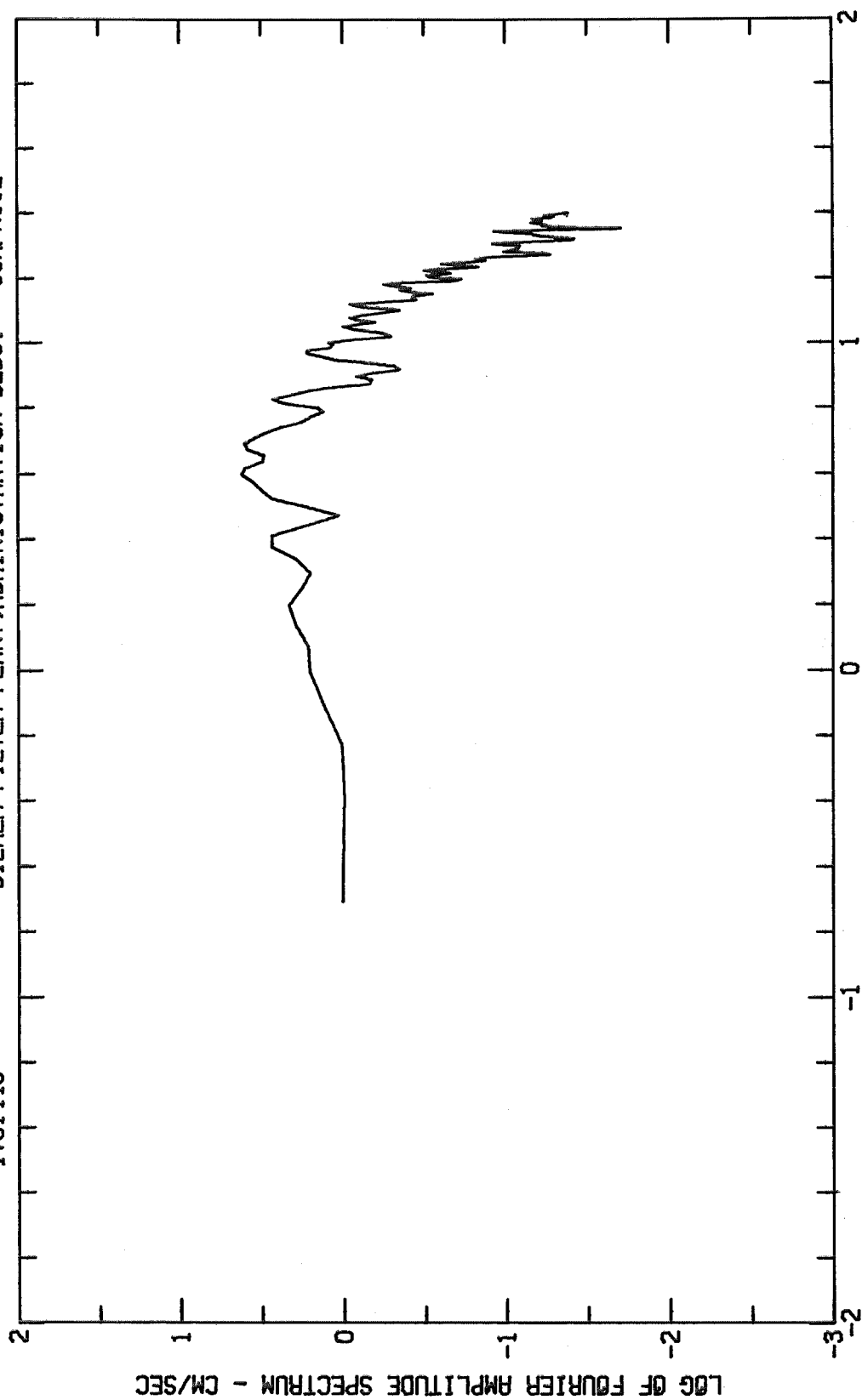


Fig. 93-a

FOURIER AMPLITUDE SPECTRUM OF ACCELERATION
DIEMER FILTER PLANT, ADMINISTRATION BLDG., JAN. 1 1976-0920 PST
IV01440 DIEMER FILTER PLANT, ADMINISTRATION BLDG. COMPN11E



LOG OF FREQUENCY - CPS
Fig. 93-b

FOURIER AMPLITUDE SPECTRUM OF ACCELERATION
DIEMER FILTER PLANT, ADMINISTRATION BLDG., JAN. 1 1976-0920 PST
IV01440 DIEMER FILTER PLANT, ADMINISTRATION BLDG. COMPS79E

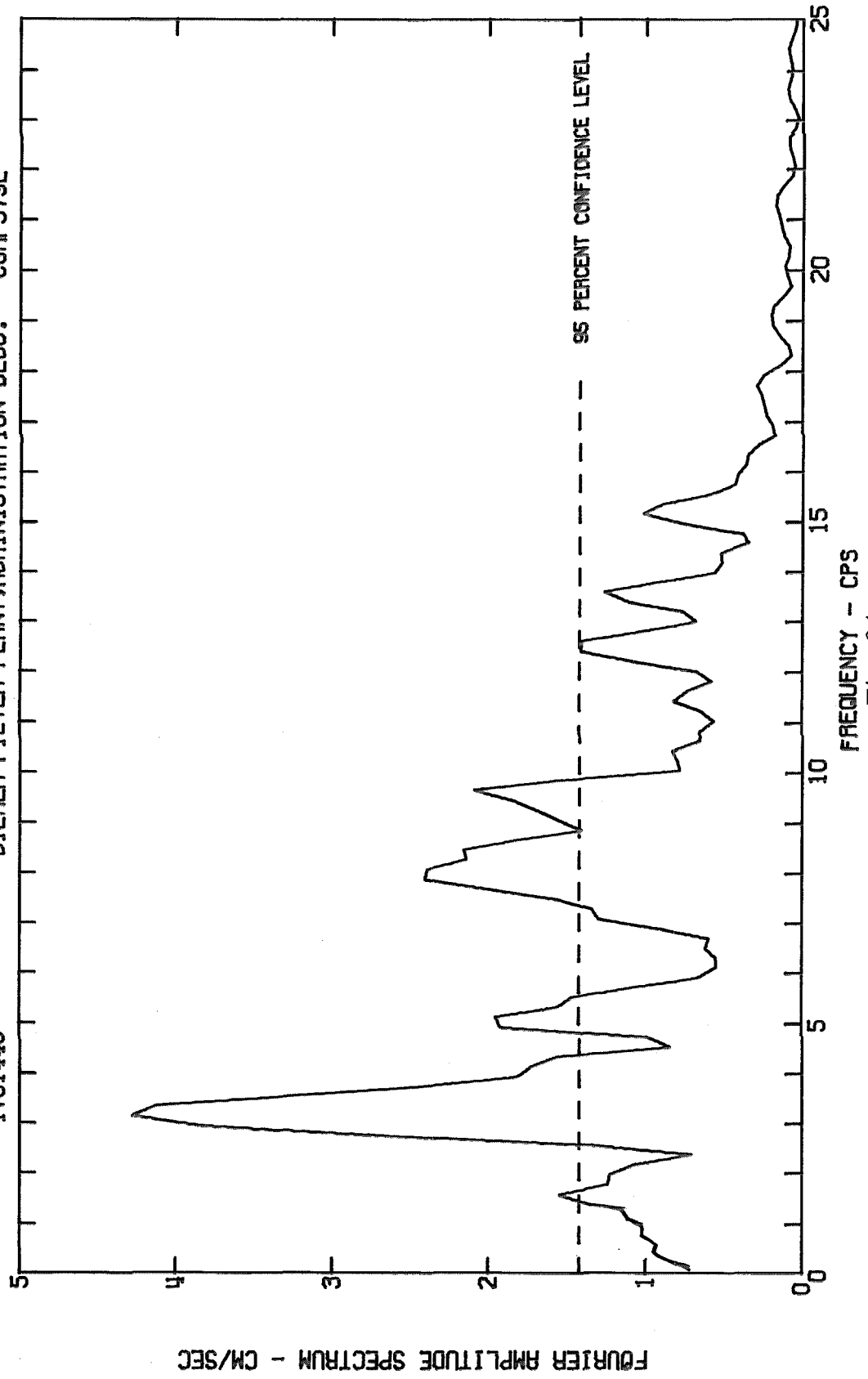
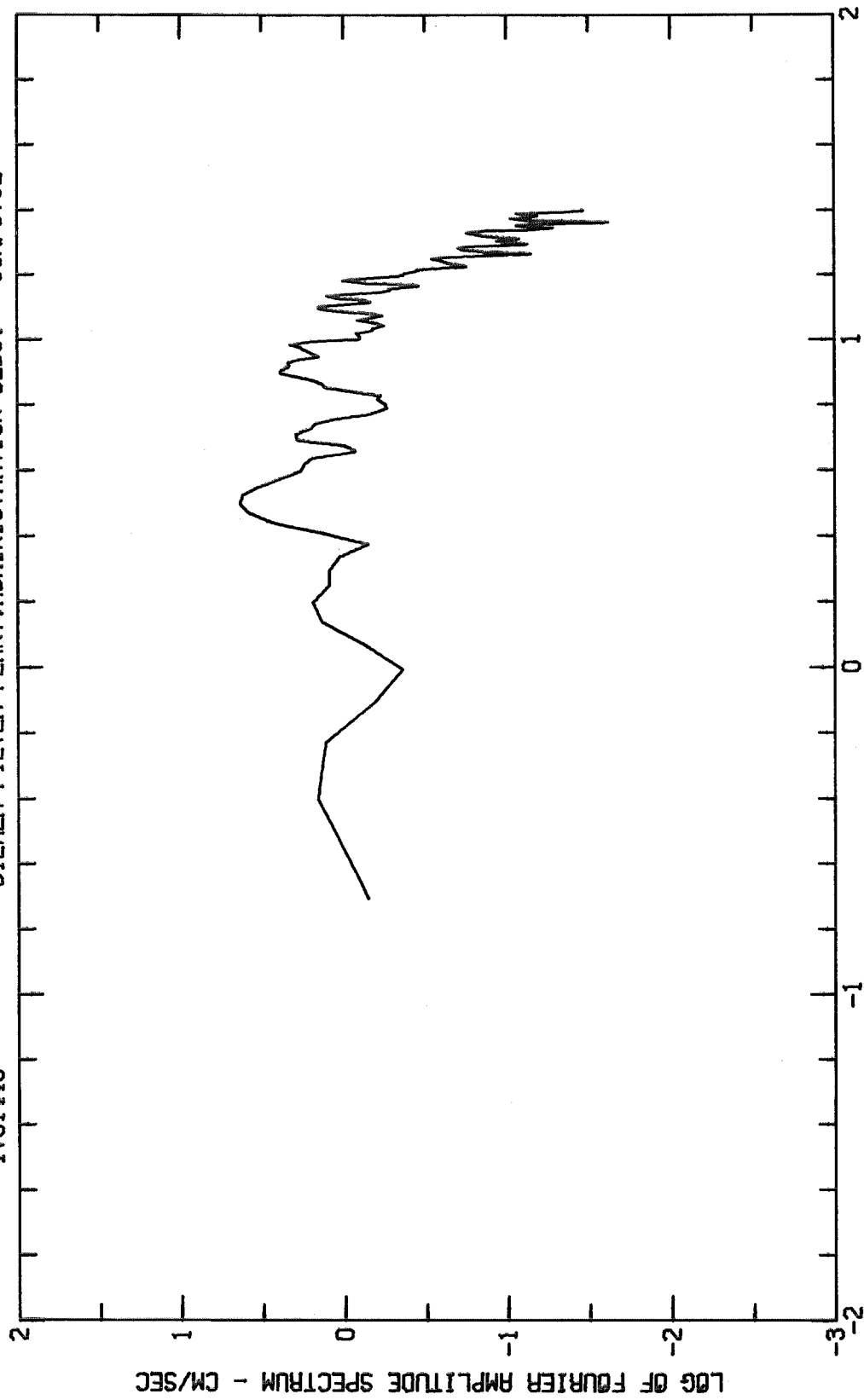


Fig. 94-a

FOURIER AMPLITUDE SPECTRUM OF ACCELERATION
DIEMER FILTER PLANT, ADMINISTRATION BLDG., JAN. 1 1976-0920 'ST
IVO1440 DIEMER FILTER PLANT, ADMINISTRATION BLDG. COMPS79E



LOG OF FREQUENCY - CPS
Fig. 94-b

FOURIER AMPLITUDE SPECTRUM OF ACCELERATION
DIEMER FILTER PLANT, ADMINISTRATION BLDG., JAN. 1 1976-0920 PST
DIEMER FILTER PLANT, ADMINISTRATION BLDG. COMPOUND

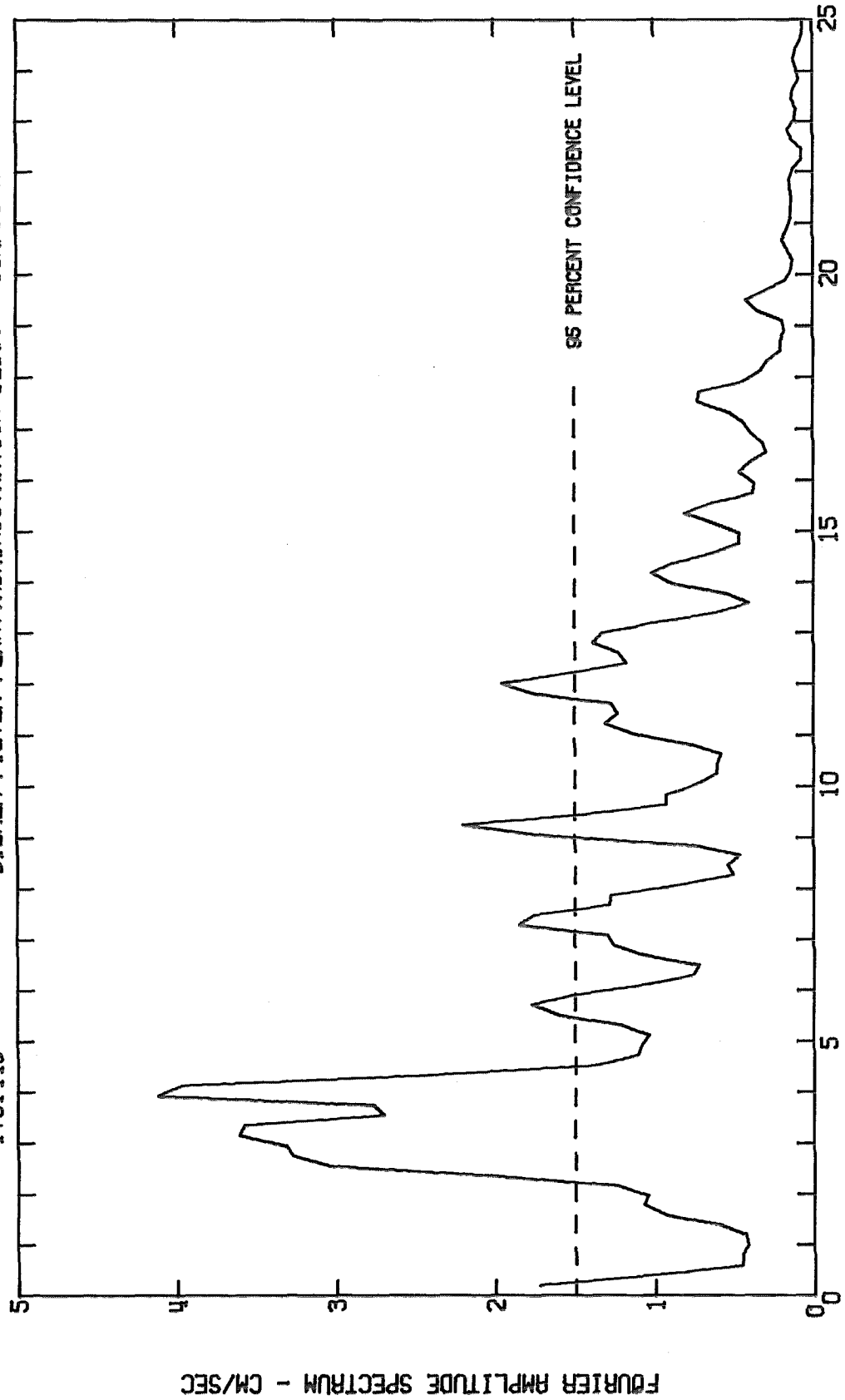
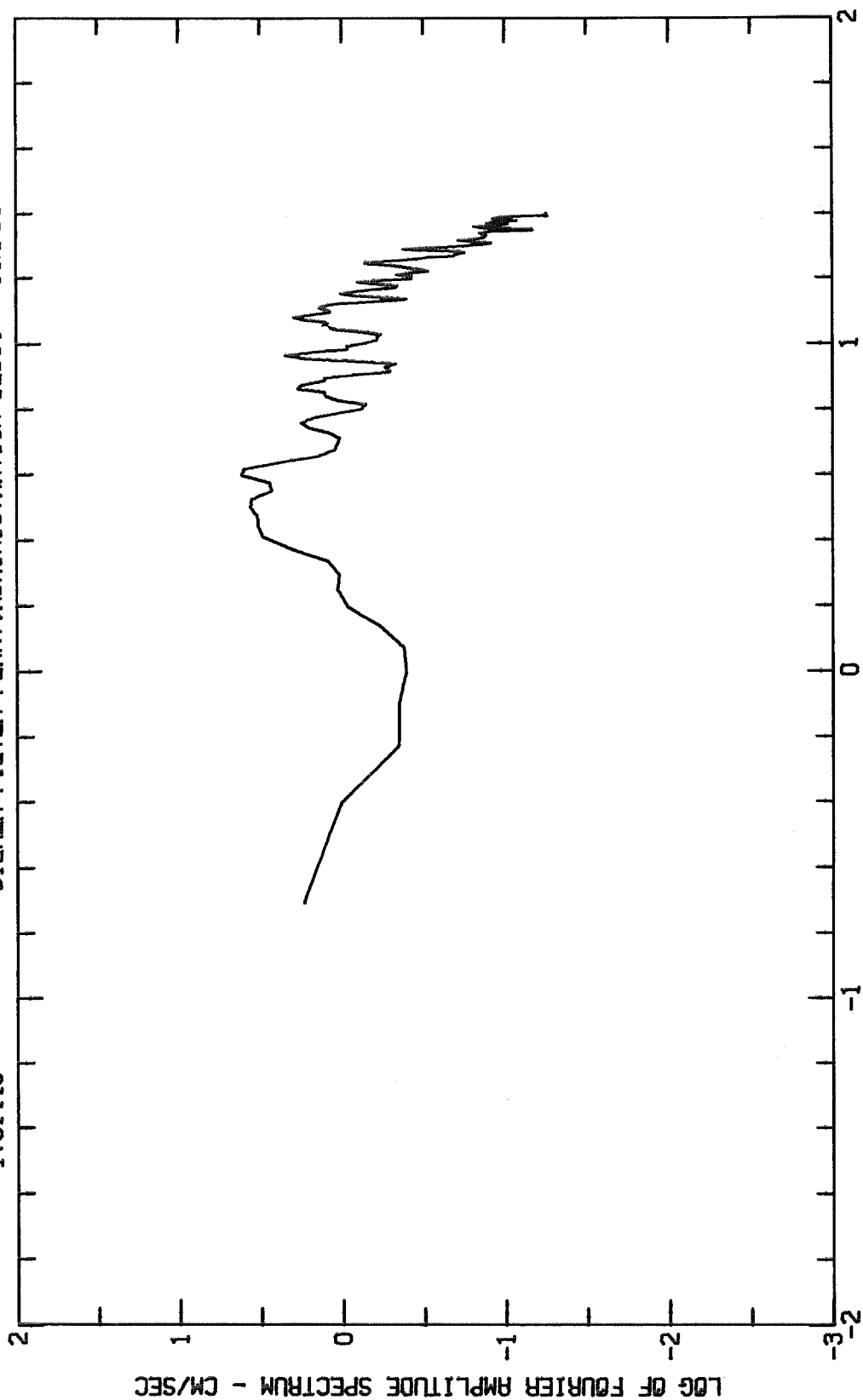


Fig. 95-a

FOURIER AMPLITUDE SPECTRUM OF ACCELERATION
DIEMER FILTER PLANT, ADMINISTRATION BLDG., JAN. 1 1976-0920 1ST
IV01440 DIEMER FILTER PLANT, ADMINISTRATION BLDG. COMPOUND



LOG OF FREQUENCY - CPS
Fig. 95-b

FOURIER AMPLITUDE SPECTRUM OF ACCELERATION
DIEMER FILTER PLANT, RESERVOIR, JAN 1 1976-0920 PST
IV01450 DIEMER FILTER PLANT, RESERVOIR COMP111W

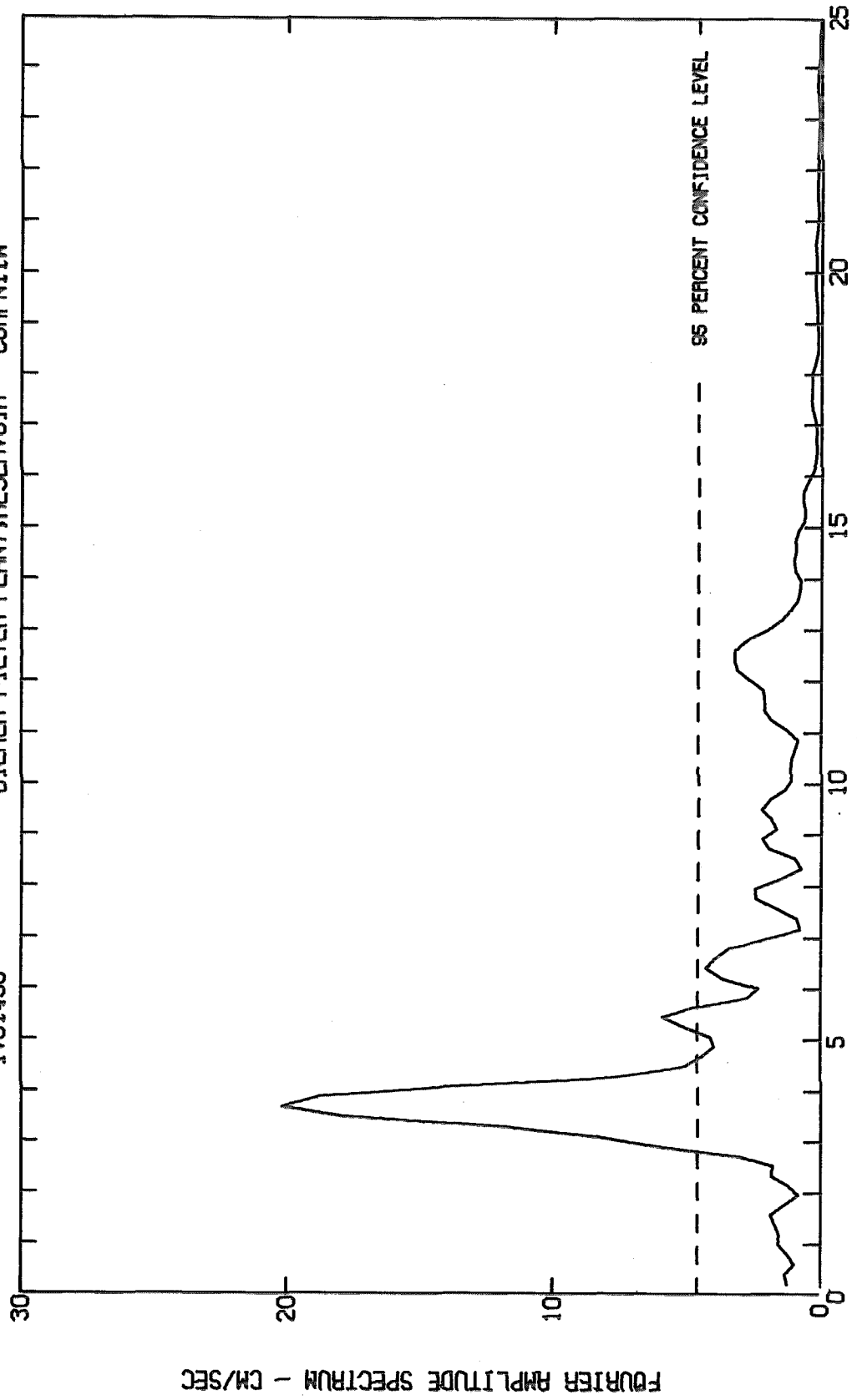
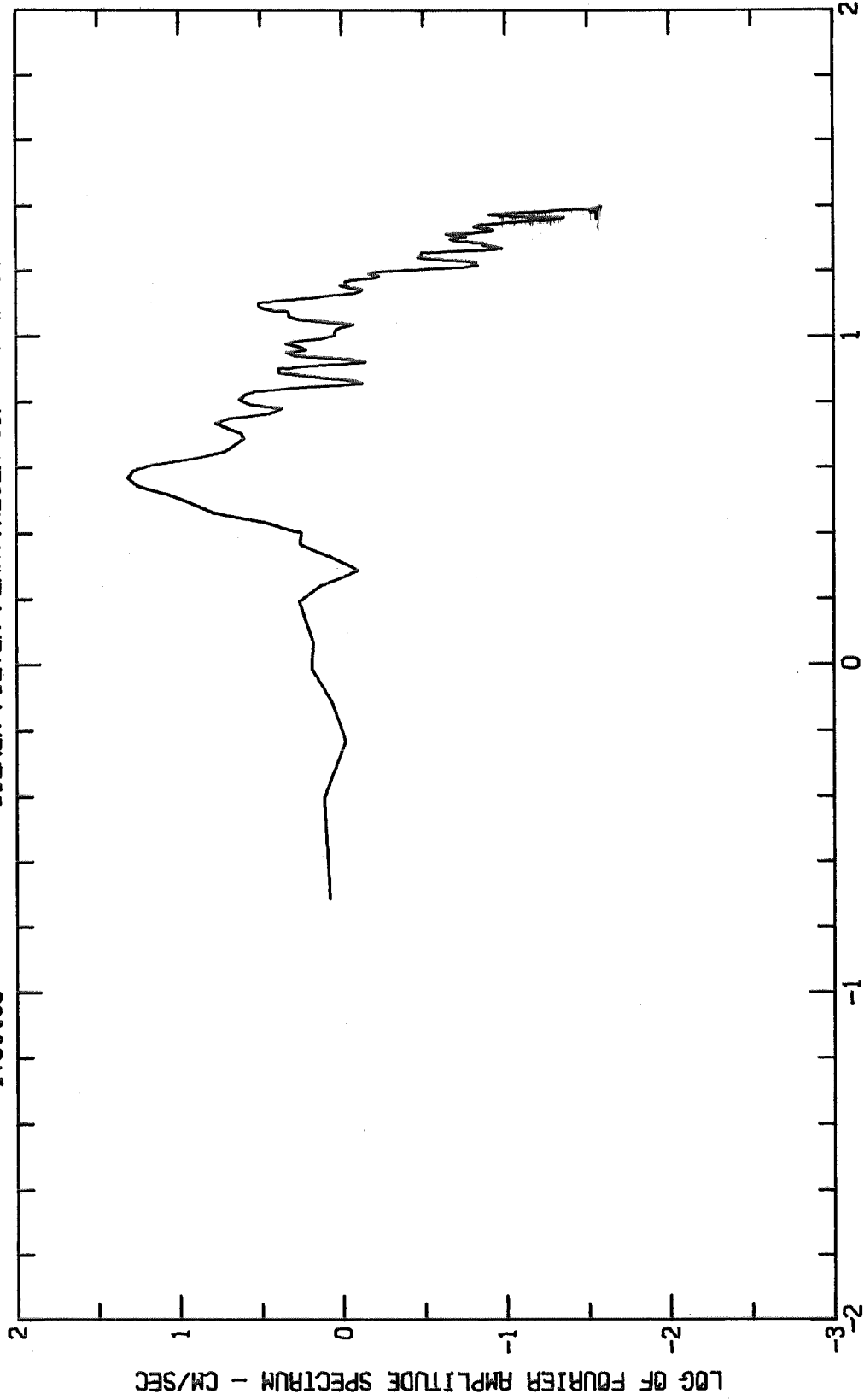


Fig. 96-a

FOURIER AMPLITUDE SPECTRUM OF ACCELERATION
DIEMER FILTER PLANT, RESERVOIR, JAN 1 1976-0920 PST
IV01450 DIEMER FILTER PLANT, RESERVOIR COMPN11W



LOG OF FREQUENCY - CPS
Fig. 96-b

FOURIER AMPLITUDE SPECTRUM OF ACCELERATION
DIEMER FILTER PLANT, RESERVOIR, JAN 1 1976-0920 PST
IV01450 DIEMER FILTER PLANT, RESERVOIR COMPS79E

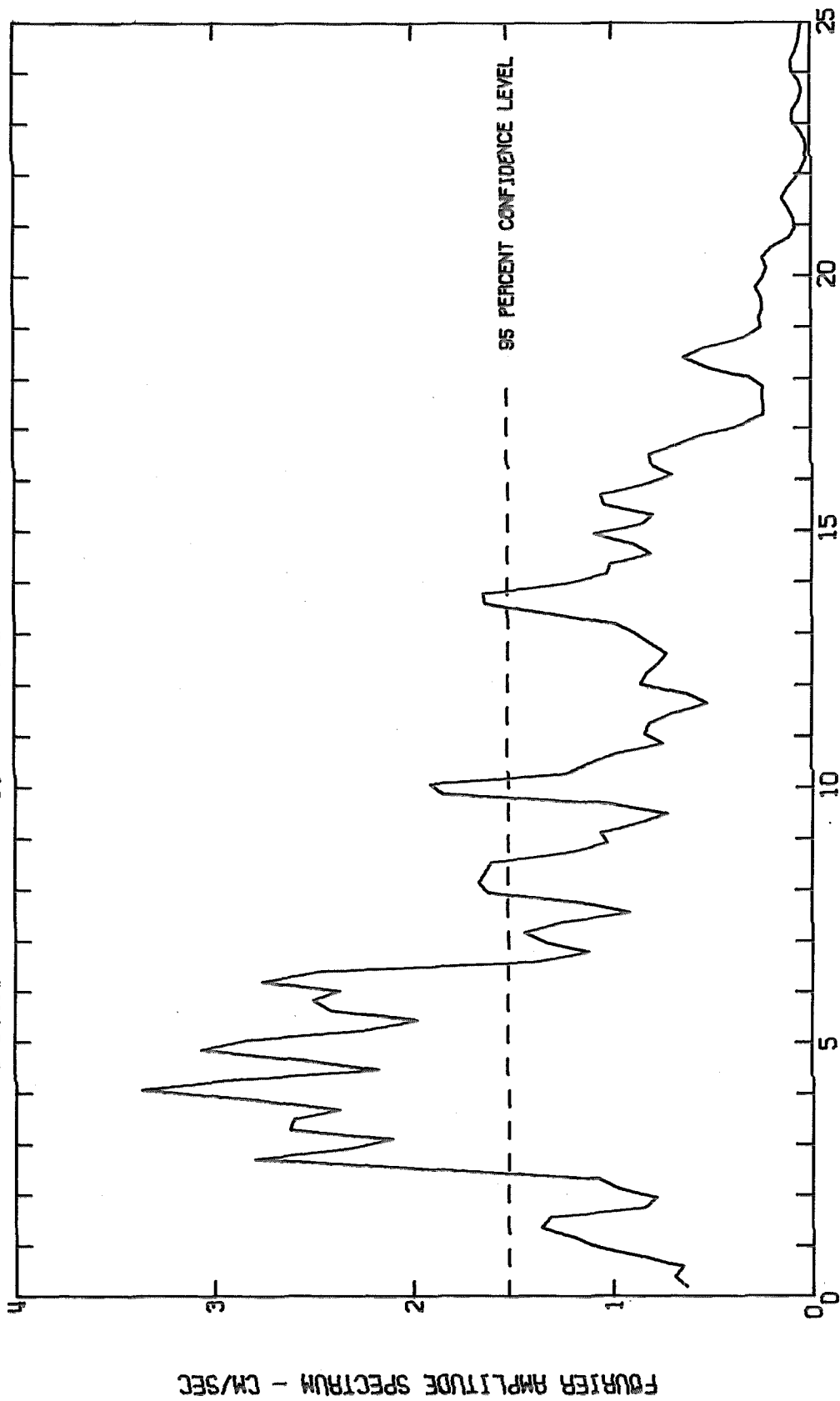
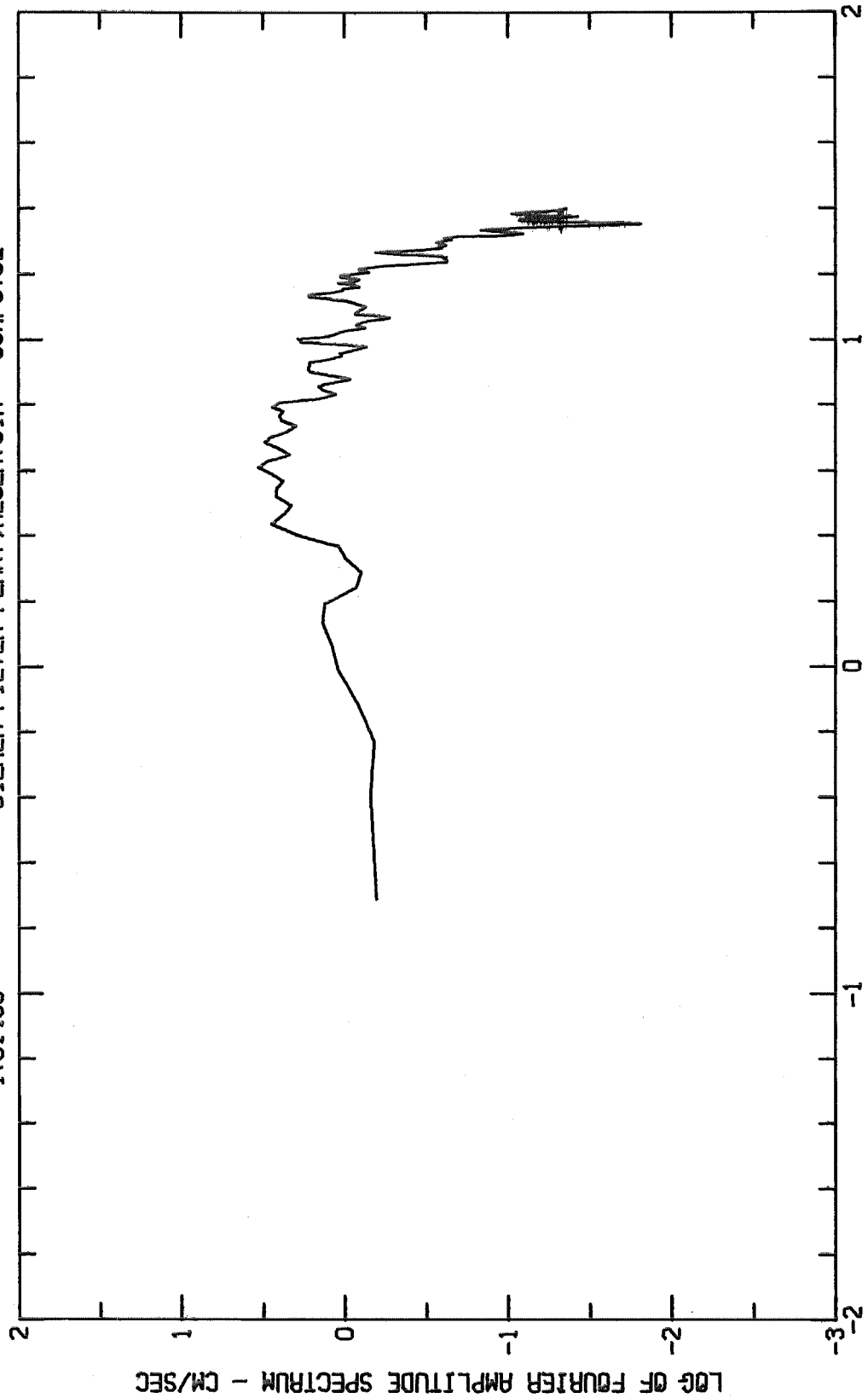


Fig. 97-a

FOURIER AMPLITUDE SPECTRUM OF ACCELERATION
DIEMER FILTER PLANT, RESERVOIR, JAN 1 1976-0920 PST
IV01450 DIEMER FILTER PLANT, RESERVOIR COMPS79E



LOG OF FREQUENCY - CPS
Fig. 97-b

FOURIER AMPLITUDE SPECTRUM OF ACCELERATION
DIEMER FILTER PLANT, RESERVOIR, JAN 1 1976-0920 PST
IVO1450 DIEMER FILTER PLANT, RESERVOIR COMPOUND

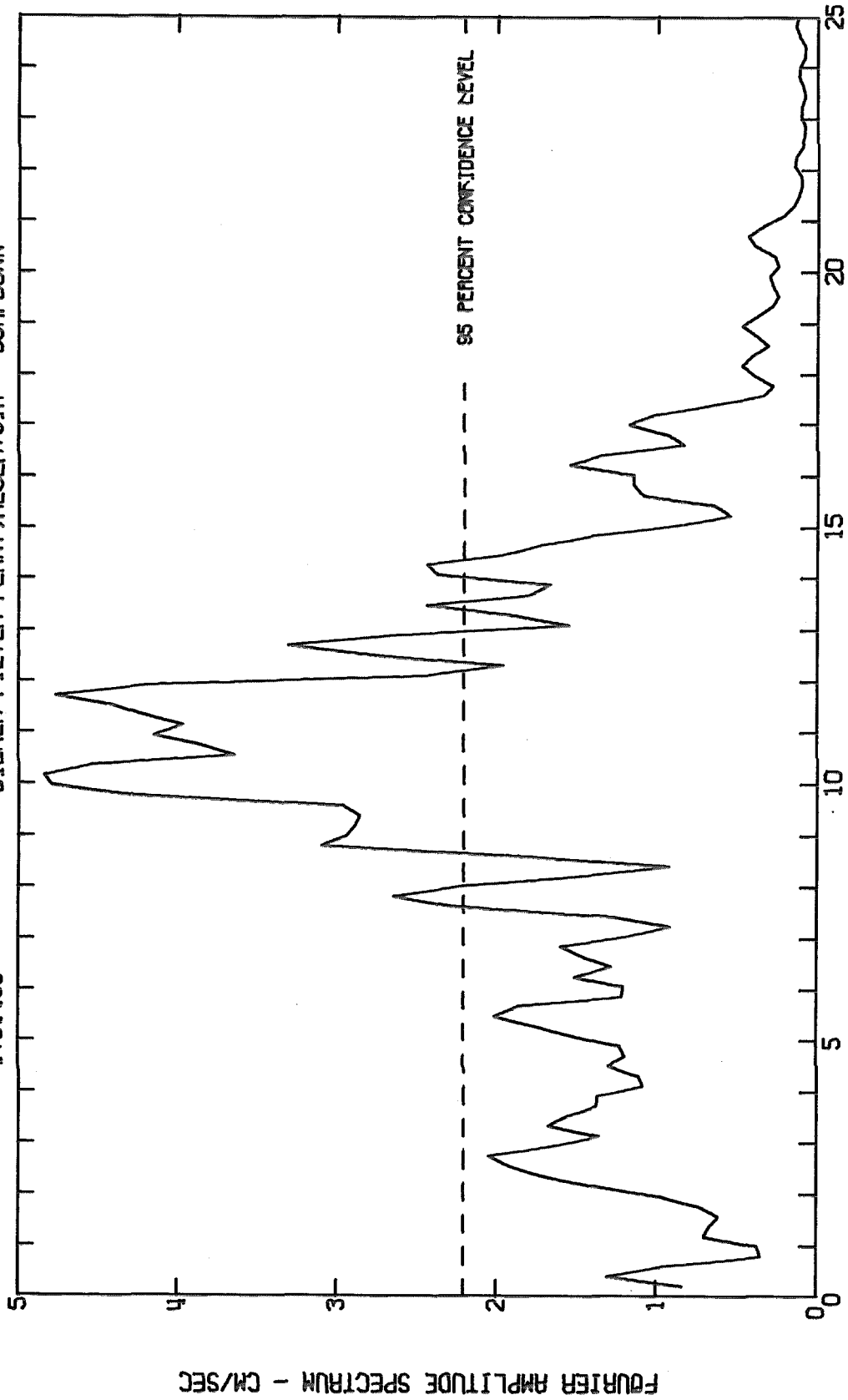
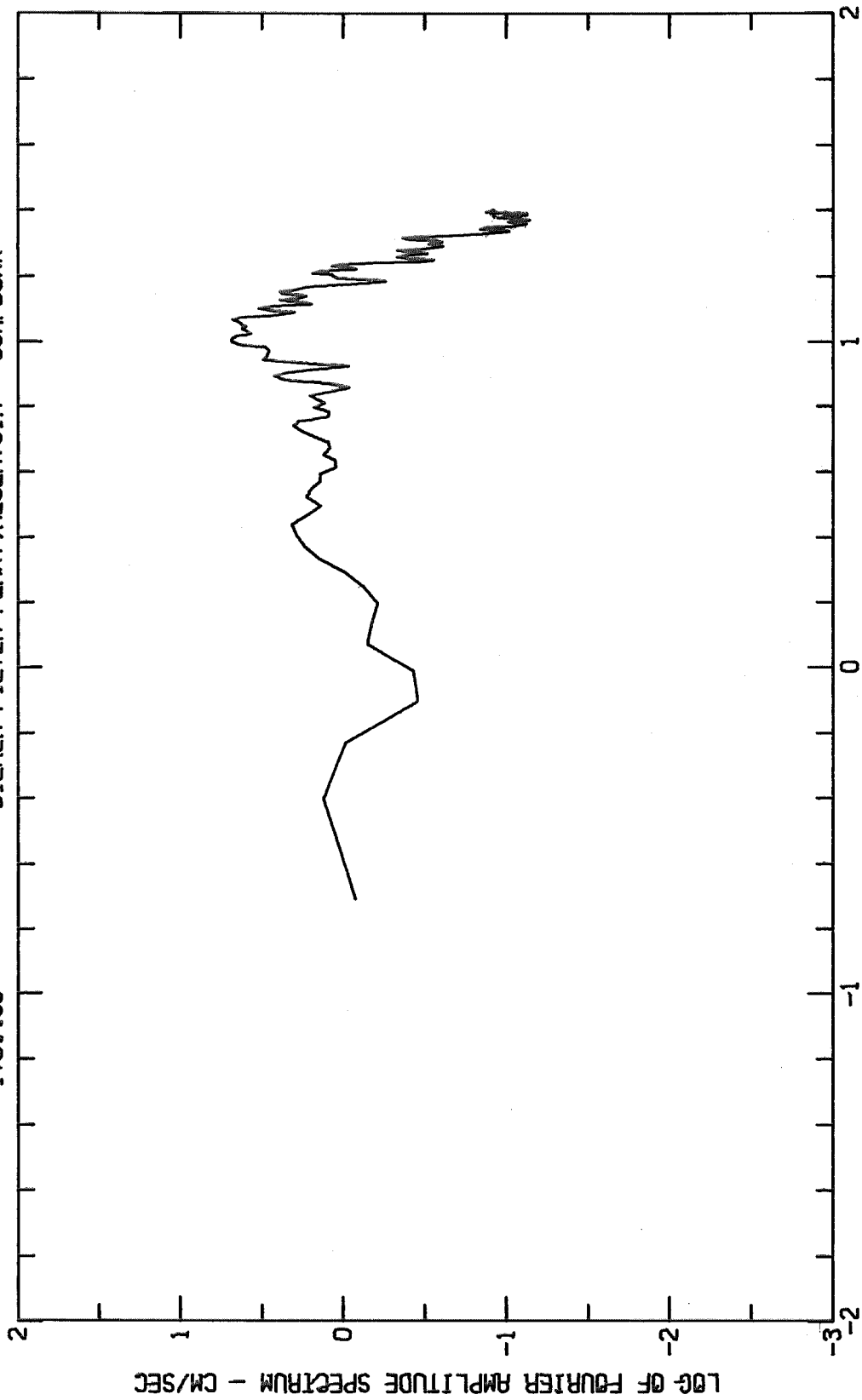


Fig. 98-a

FOURIER AMPLITUDE SPECTRUM OF ACCELERATION
DIEMER FILTER PLANT, RESERVOIR, JAN 1 1976-0920 PST
1V01450 DIEMER FILTER PLANT, RESERVOIR COMPOUND



LOG OF FREQUENCY - CPS

Fig. 98-b

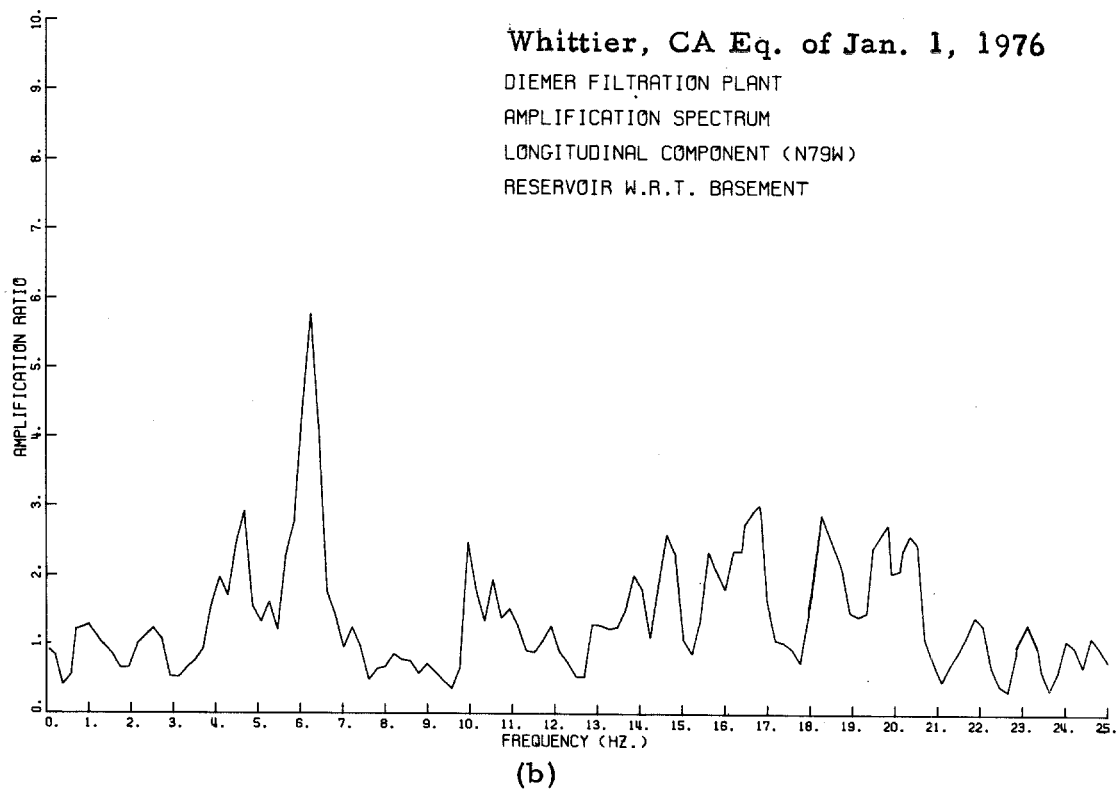
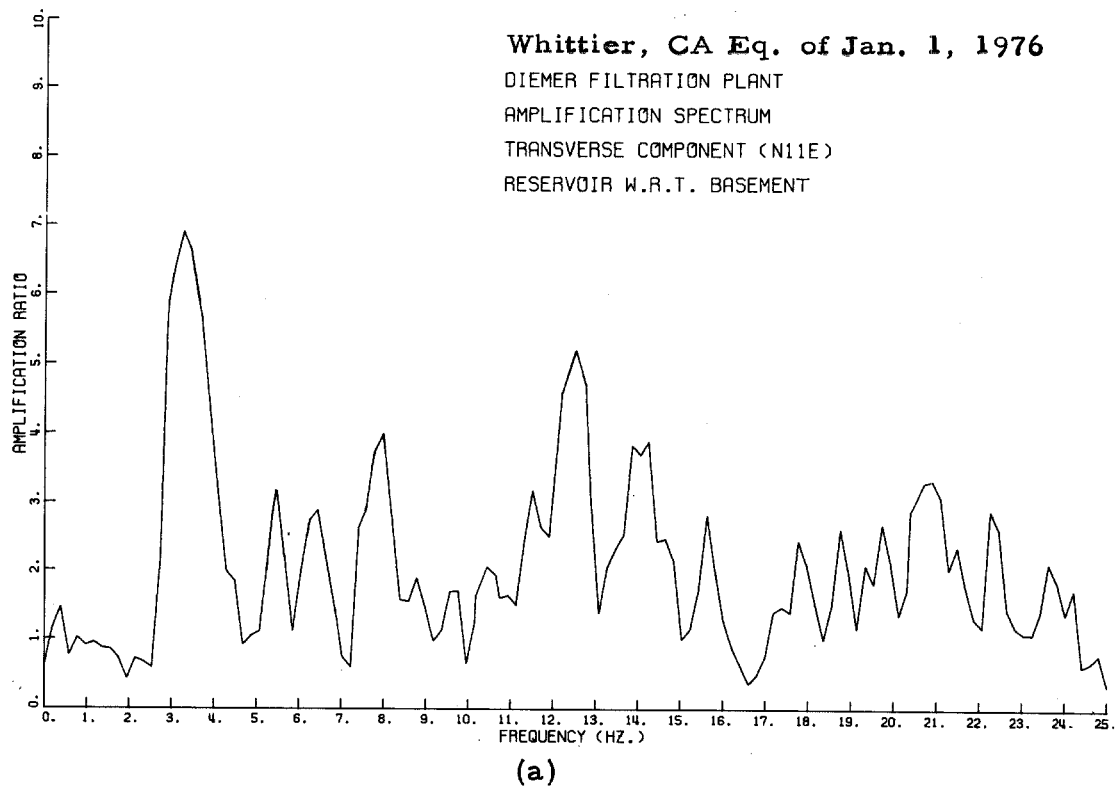


Fig. 99

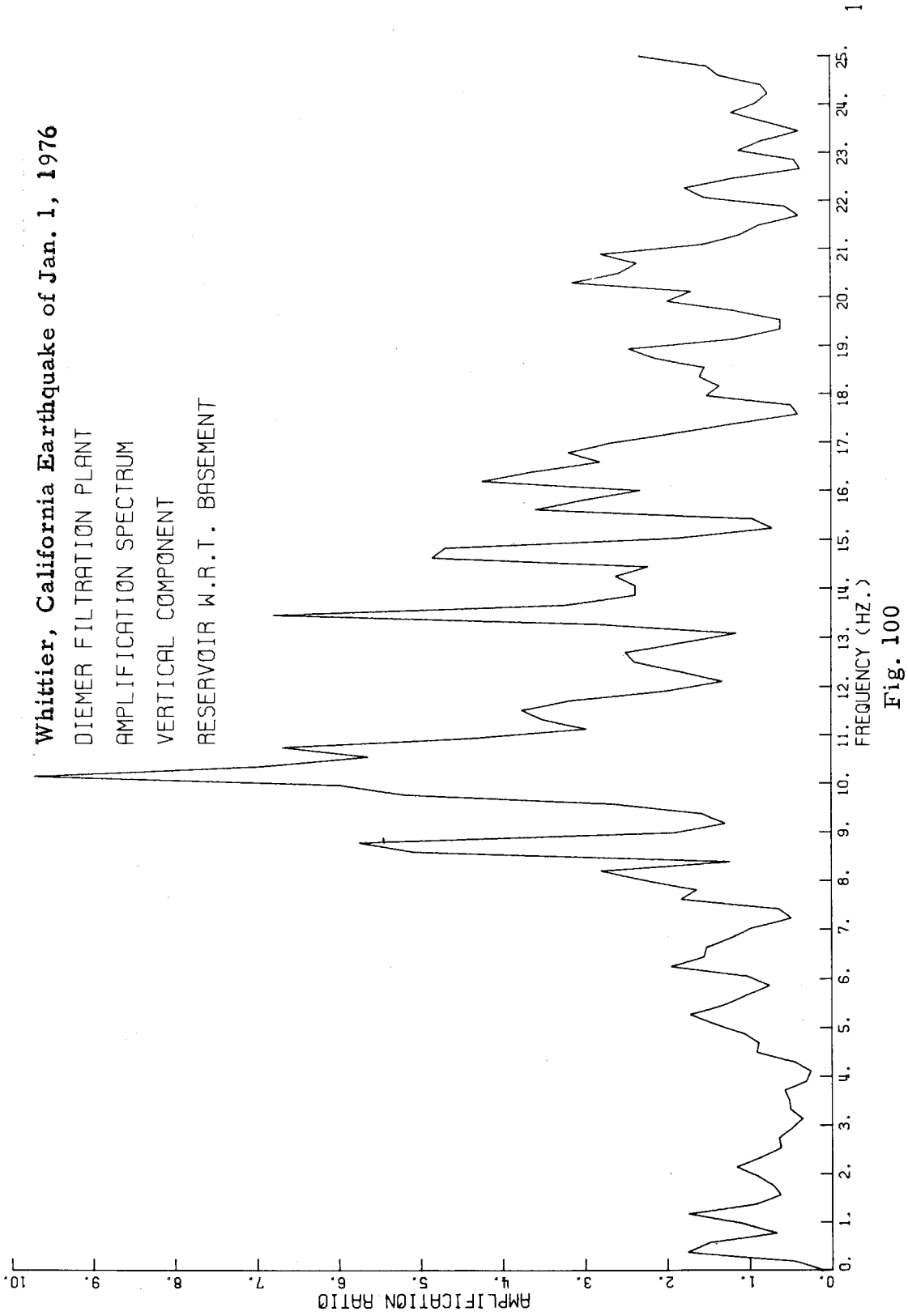


TABLE 11

Observed Natural Frequencies From the Fourier Amplitude Spectra
and the Amplification Spectrum
Whittier, California Earthquake of Jan. 1, 1976
Diemer Filtration Plant

Transverse Component (N11° E) of the Reservoir

Fourier Amplitude Spectrum of Acceleration (Basement)		Fourier Amplitude Spectrum of Acceleration (Reservoir)		Amplification Spectrum of the Reservoir		Modal Identification
Frequency (Hz)	Amplitude (cm/sec)	Frequency (hz)	Amplitude (cm/sec)	Frequency (Hz)	Amplification Ratio	
1.60	2.20	3.70	20.50	3.70	6.95	First Mode
2.50	2.85					
3.95	4.10	5.50 6.49	5.85 4.10	5.50 6.49	3.10 2.95	Second Mode Third Mode
4.95	4.00					
6.72	2.75	7.85 8.85	2.60 2.55	7.85 8.85	4.00 1.90	Fourth Mode Fifth Mode
7.85	0.66					
9.40	1.60	9.55	2.30	9.55	1.70	Sixth Mode
10.00	1.20	11.50	2.50	11.50	3.17	Seventh Mode
11.25	1.00					
12.0	0.92	12.50	3.50	12.50	5.20	Eighth Mode

TABLE 12

Observed Natural Frequencies From the Fourier Amplitude Spectra
and the Amplification Spectrum
Whittier, California Earthquake of Jan. 1, 1976
Diemer Filtration Plant

Longitudinal Component (N79° W) of the Reservoir

Fourier Amplitude Spectrum of Acceleration (Basement)		Fourier Amplitude Spectrum of Acceleration (Reservoir)		Amplification Spectrum of the Reservoir		Modal Identification
Frequency (Hz)	Amplitude (cm/sec)	Frequency (Hz)	Amplitude (cm/sec)	Frequency (Hz)	Amplification Ratio	
1.50	1.60	1.35	1.40			
3.15	4.30	2.70	2.80			
		3.35	2.60			
		4.00	3.40	4.00	2.00	First Mode
		4.80	3.10	4.80	3.05	Second Mode
5.05	2.00					
		5.80	2.50			
		6.15	2.80	6.15	6.00	Third Mode
8.00	2.40	7.10	1.40	7.10	1.30	Fourth Mode
9.60	2.0	8.15	1.60			
		10.00	2.00			
		11.10	0.85	10.00	2.20	
		12.05	0.90	10.55	1.80	Fifth Mode
12.50	1.40					
13.55	1.30	13.70	1.60			

CHAPTER VI

ORANGE COUNTY RESERVOIR

VI-1 Description of the Structure

The Orange County Reservoir is located very close to the Whittier Fault, approximately 3.5 Km south of the epicenter of the Jan. 1, 1976 earthquake, 3 Km (1.9 miles east of the city of Brea and about 36 Km (22.5 miles) southeast of Downtown Los Angeles. The reservoir is owned by the Metropolitan Water District of Southern California and is designed to supply the city of Brea. The reservoir is rectangular in shape with rounded corners, and it has four earth-fill embankments with average height of 15 m (49 ft). Figures 101 and 102 show a general view of the reservoir looking north and east, respectively. The reservoir is 85.4 m (280 ft) by 106.8 m (350 ft) in plan dimension at the bottom level (El. 613 ft) and is 176.9 m (580 ft) by 195.2 m (640 ft) in plan dimension at the crest level (El. 662.0 ft), as shown in Fig. 103-a. The cross section of the embankment consists of compacted random fill rested on sand and gravel drains (see Fig. 103-b).

One strong-motion accelerograph was located on the dam at the left abutment of the berm of the south embankment (El. 603 ft) in a piezometer terminal house, as is shown in Figs. 103 and 104. During the January 1, 1976 earthquake this instrument recorded a peak acceleration of 18% g in the N84°W direction. The peak acceleration of the other horizontal component (S06°W) was only 8% g.

Figures 105 and 106 show the uncorrected and corrected data of this single record, while Figs. 107-112 show the computed spectra.

It can be seen from Figs. 105 and 106-a that the strong ground shaking of the N84°W component lasted only about one second (approximately from second 1.5 to second 2.5 on the record). Similar observations have been made from the Whittier building (Chapter II) and Carbon Canyon Dam (Chapter III) records, suggesting that the fault released significant seismic energy in roughly the east-west direction, where impulsive-type ground shaking was recorded. It is difficult to analyze the structural response of the embankment from only one record. Therefore, for the future, it is suggested that at least two strong-motion accelerographs be placed at the reservoir site. One should be located on the original ground surface to recover the earthquake ground motion, and the other should be placed on the crest of the embankment (El. 662.0 ft) to recover the absolute motion of the structure.

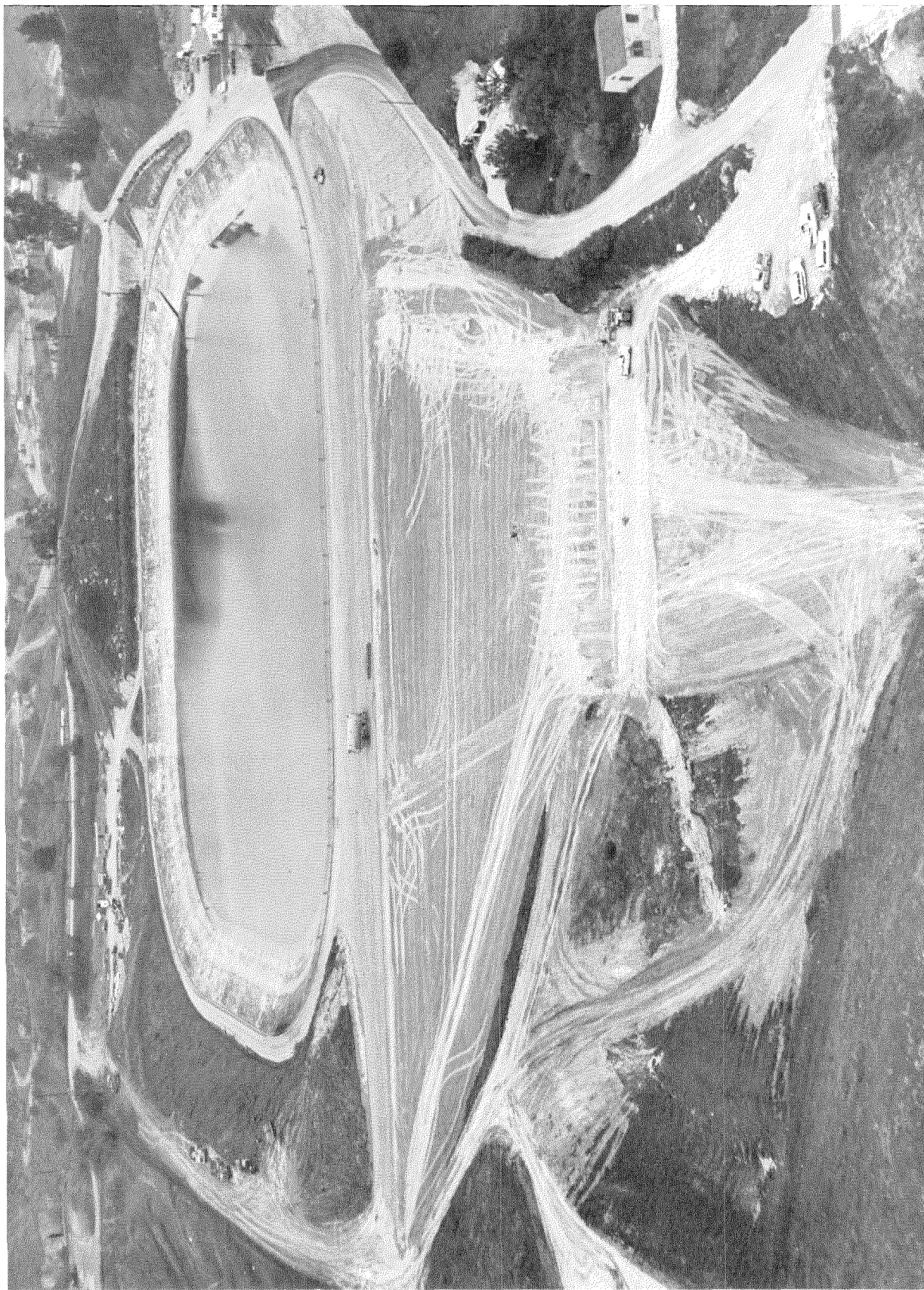


Fig. 101 Orange County Reservoir, View Looking North

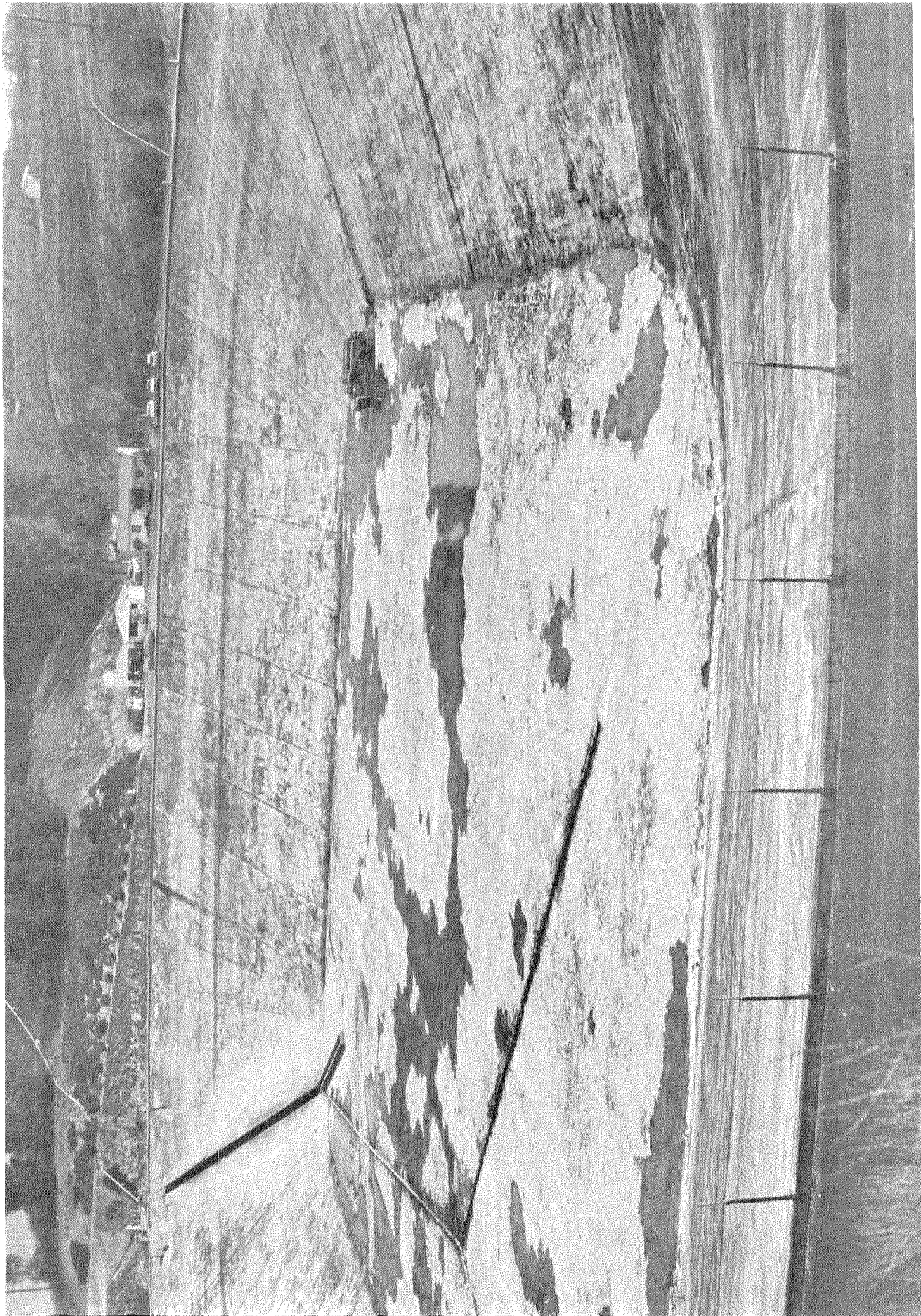
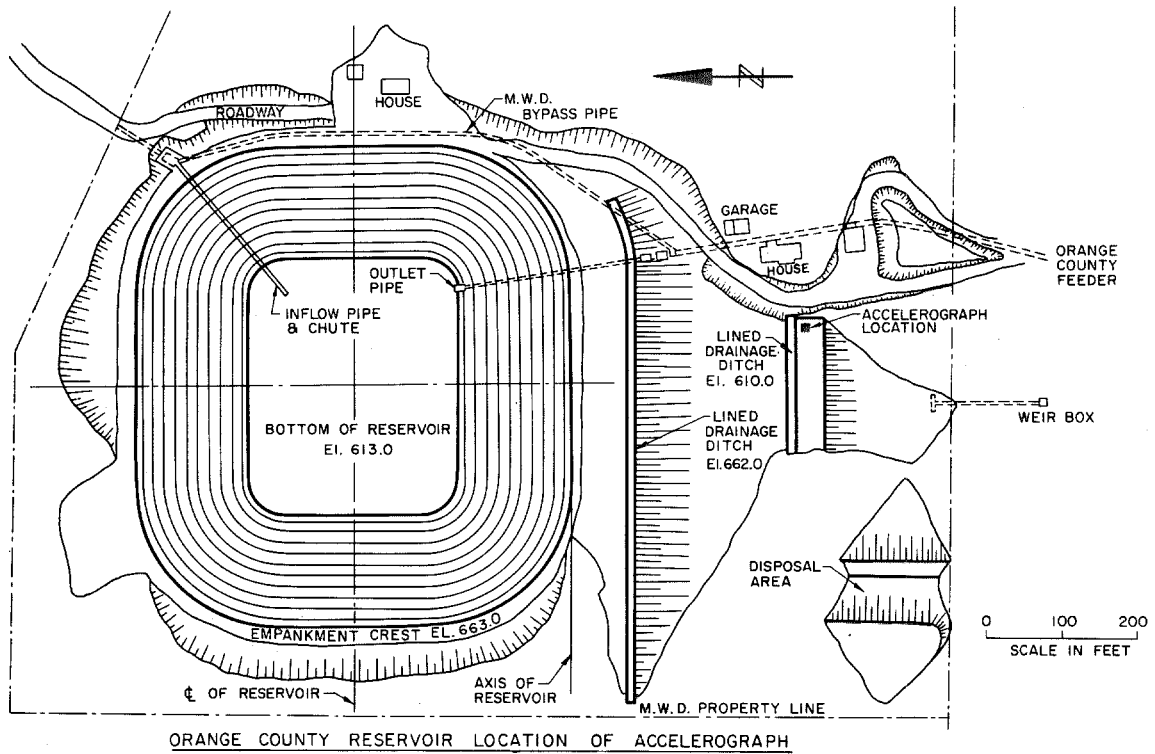
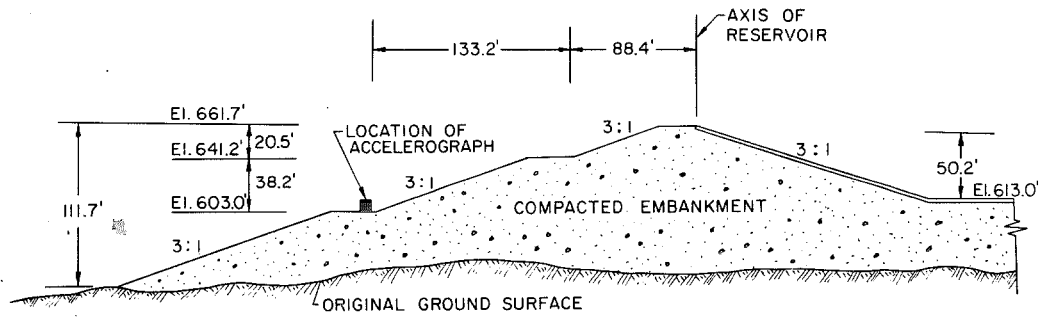


Fig. 102 Orange County Reservoir, View Looking East



(a)



(b)

0 50 100
SCALE IN FEET

Fig. 103



Fig. 104 Orange County Reservoir, Accelerograph in Small
White House on the Berm

ORANGE COUNTY RESERVOIR, ABUTMENT, JAN 1 1976 0920 PST

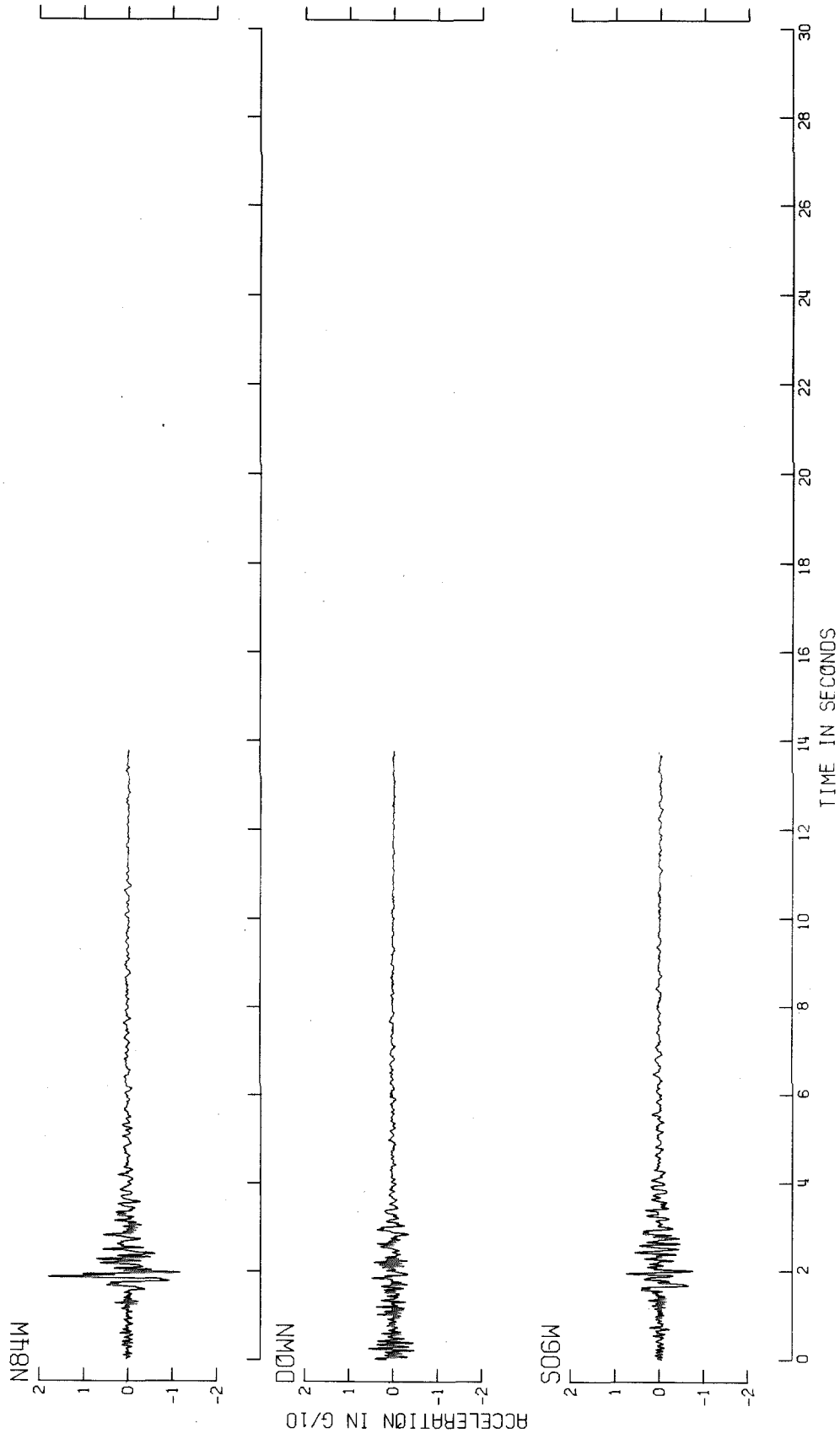


Fig. 105

ORANGE COUNTY RESERVOIR, ABUTMENT, JANUARY 1, 1976 - 0920 PST

IN00100

ORANGE COUNTY RESERVOIR, ABUTMENT N8411

PEAK VALUES : ACCEL = -160.7 CM/SEC/SEC VELOCITY = 4.8 CM/SEC DISPL = -1.7 CM

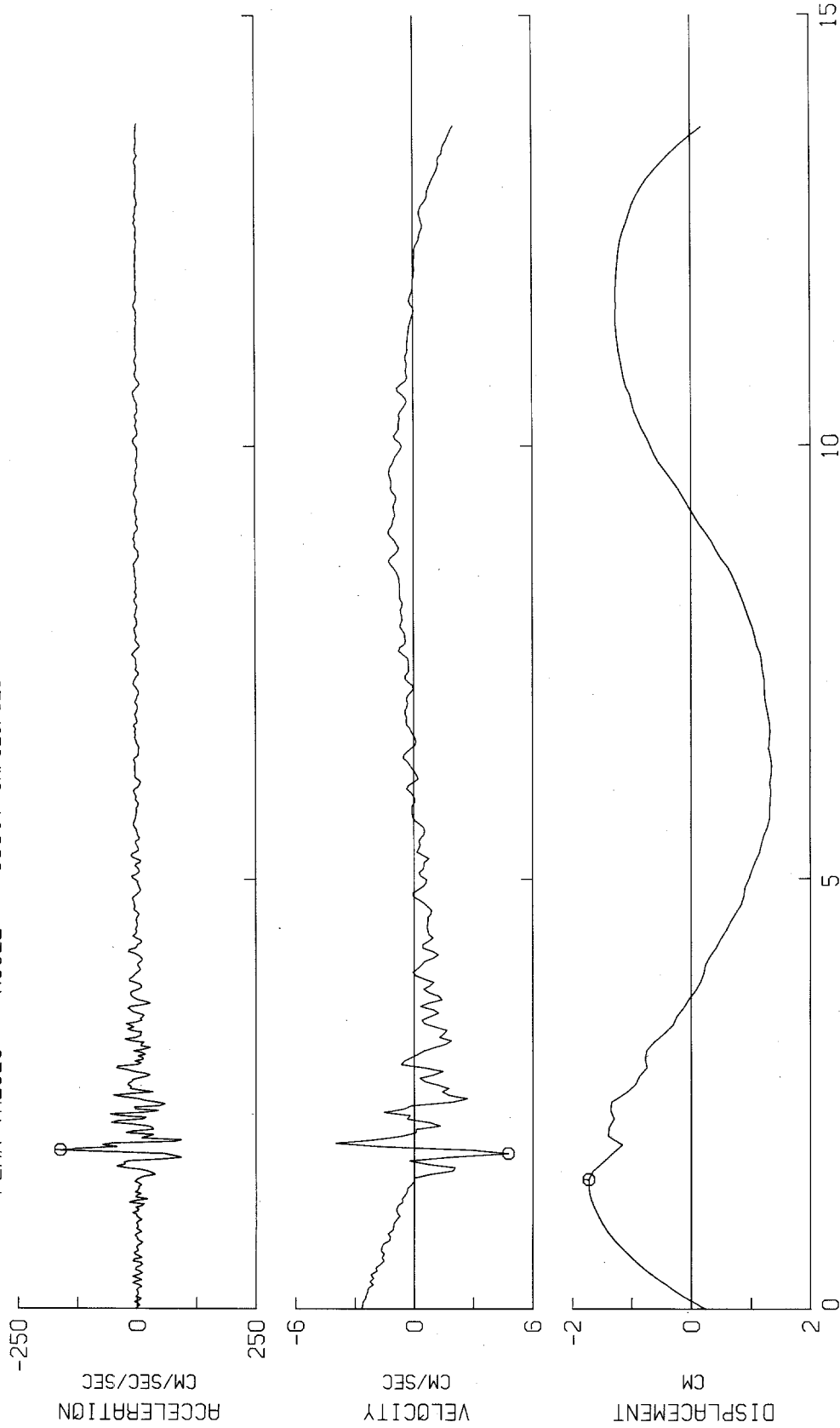
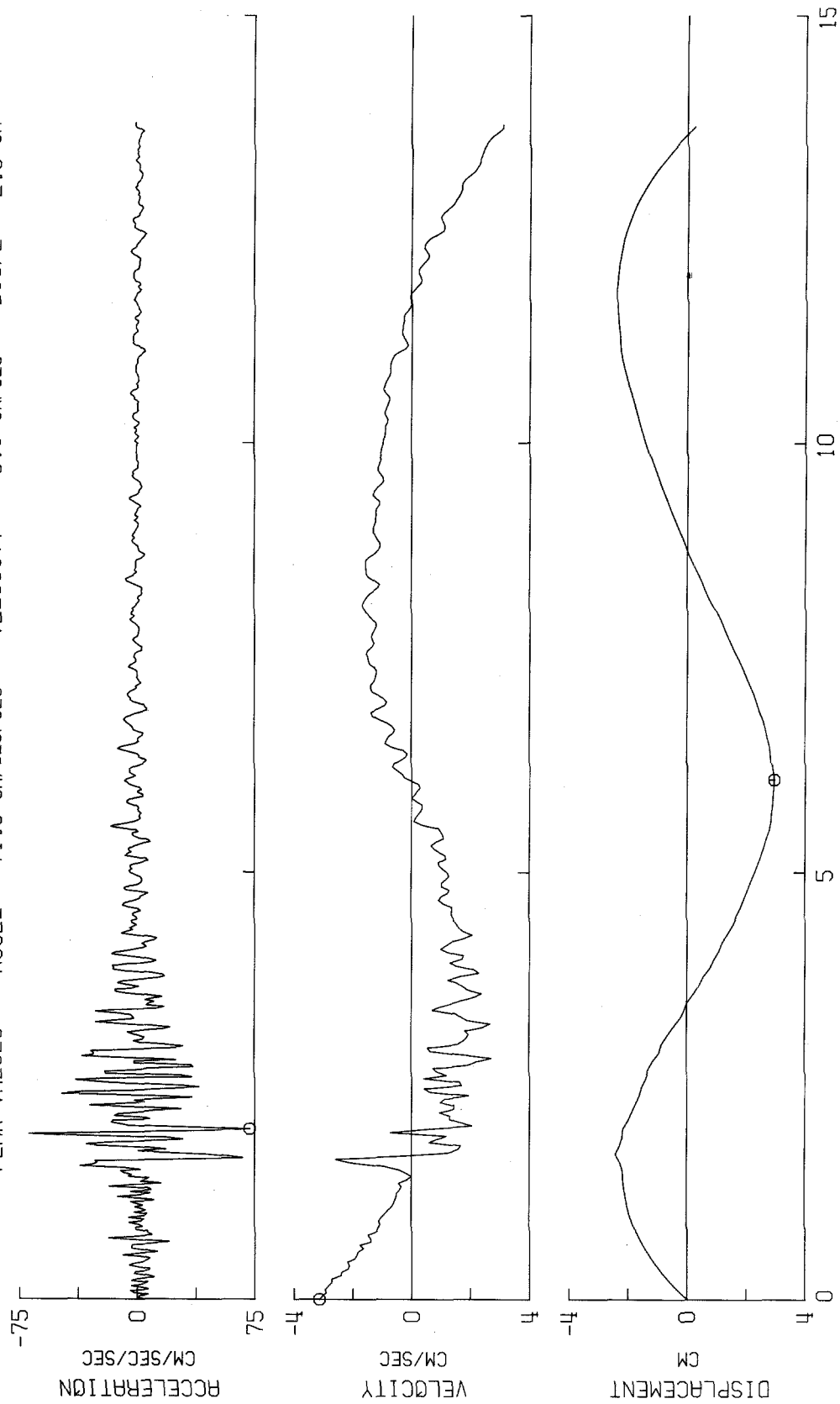


Fig. 106-a

ORANGE COUNTY RESERVOIR, ABUTMENT, JANUARY 1, 1976 - 0920 PST
 IN00100
 ORANGE COUNTY RESERVOIR, ABUTMENT S06W
 PEAK VALUES : ACCEL = 71.9 CM/SEC/SEC VELOCITY = -3.1 CM/SEC DISPL = 2.9 CM



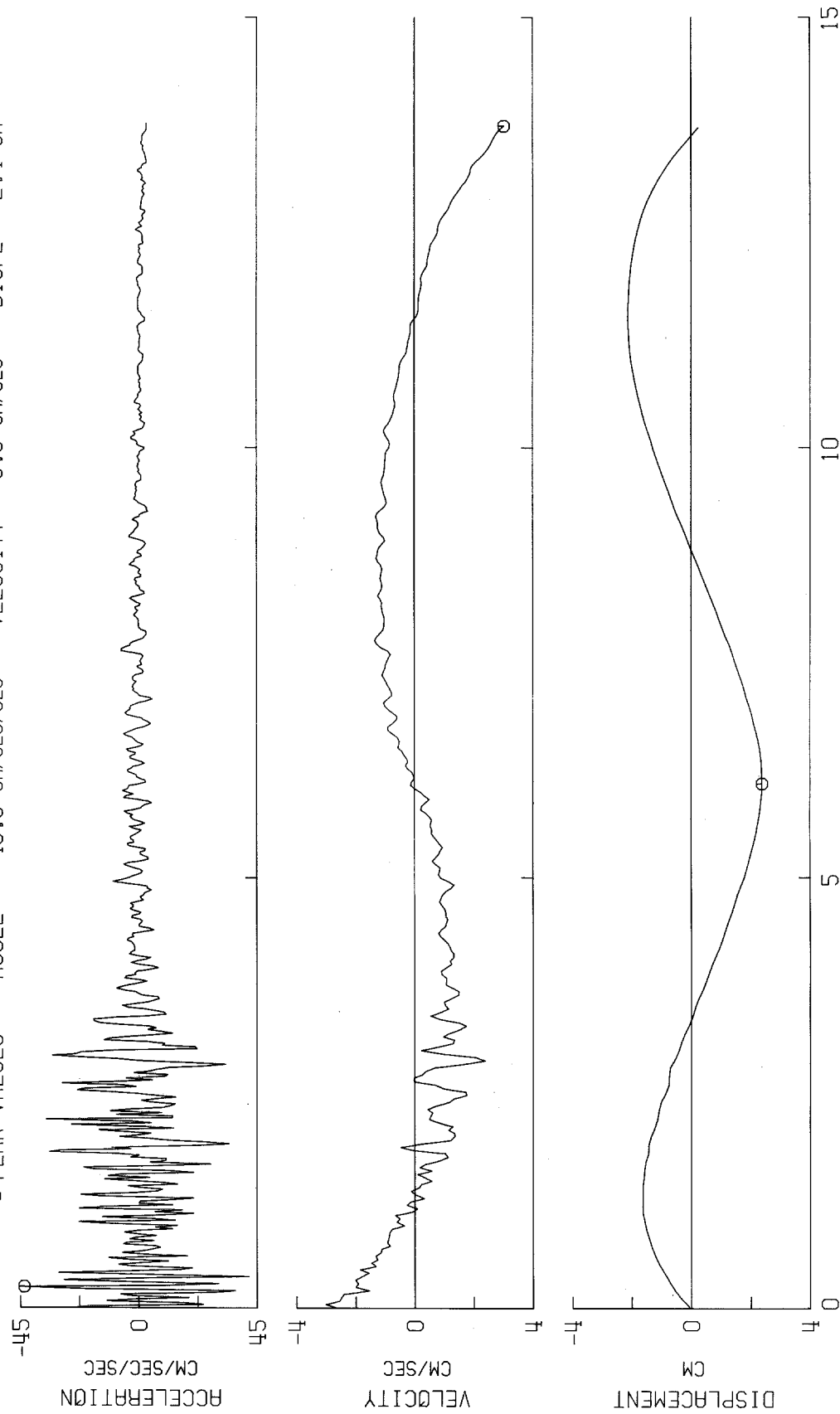
TIME - SECONDS
 Fig. 106-b

ORANGE COUNTY RESERVOIR, ABUTMENT, JANUARY 1, 1976 - 0920 PST

IN00100

ORANGE COUNTY RESERVOIR, ABUTMENT DOWN

PEAK VALUES : ACCEL = -43.5 CM/SEC/SEC VELOCITY = 3.0 CM/SEC DISPL = 2.4 CM



TIME - SECONDS
Fig. 106-c

RELATIVE VELOCITY RESPONSE SPECTRUM
ORANGE COUNTY RESERVOIR, ABUTMENT, JANUARY 1, 1976 - 0920 PST
IIN00100 ORANGE COUNTY RESERVOIR, ABUTMENT N84W
DAMPING VALUES ARE 0, 2, 5, 10 AND 20 PERCENT OF CRITICAL

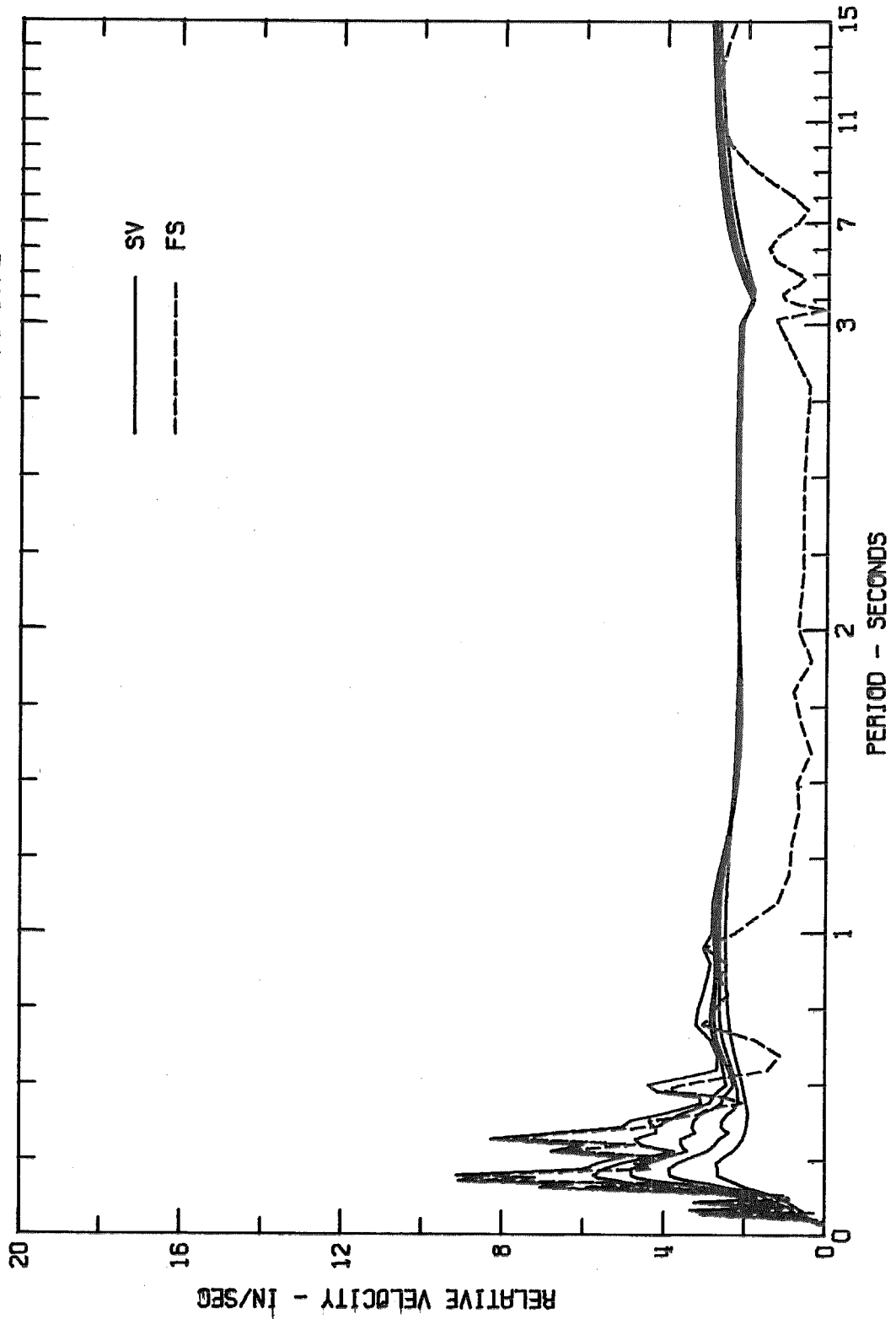


Fig. 107-a

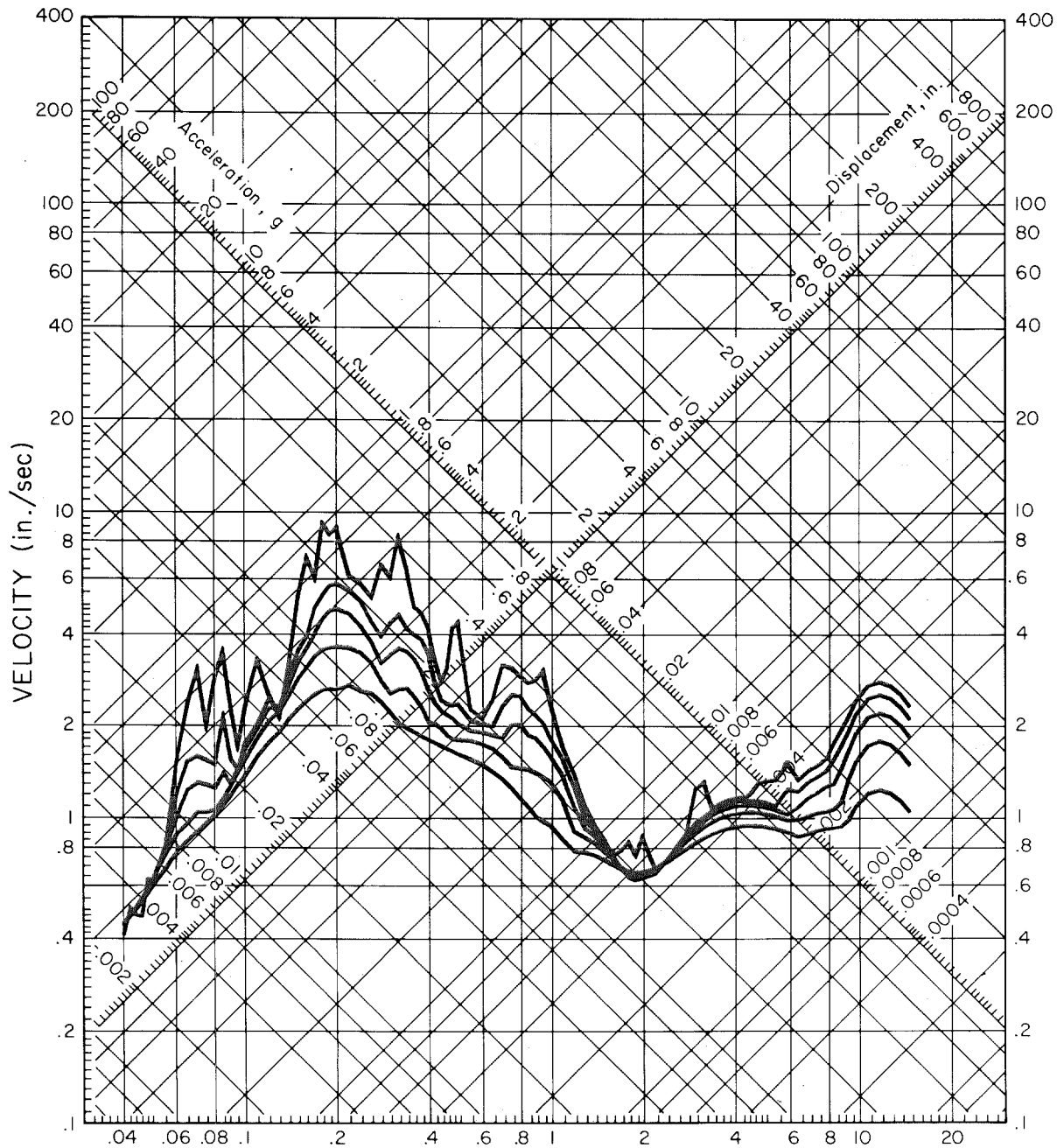
RESPONSE SPECTRUM

ORANGE COUNTY RESERVOIR, ABUTMENT, JANUARY 1, 1976 - 0920 PST

IIN00100

ORANGE COUNTY RESERVOIR, ABUTMENT N84W

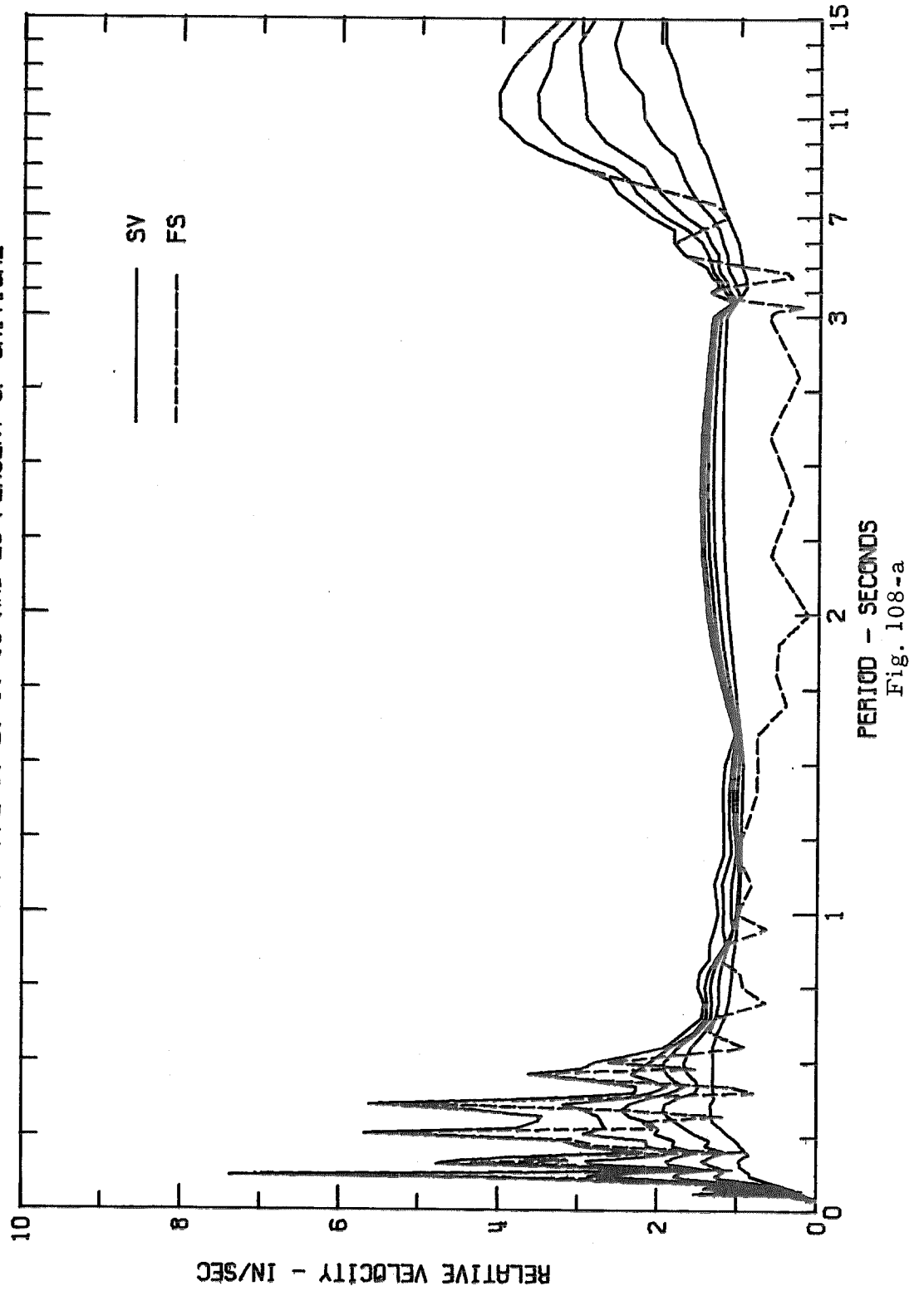
DAMPING VALUES ARE 0, 2, 5, 10 AND 20 PERCENT OF CRITICAL



PERIOD (secs)

Fig. 107-b

RELATIVE VELOCITY RESPONSE SPECTRUM
ORANGE COUNTY RESERVOIR, ABUTMENT, JANUARY 1, 1976 - 0920 PST
11N00100 ORANGE COUNTY RESERVOIR, ABUTMENT S06W
DAMPING VALUES ARE 0, 2, 5, 10 AND 20 PERCENT OF CRITICAL



RESPONSE SPECTRUM

ORANGE COUNTY RESERVOIR, ABUTMENT, JANUARY 1, 1976 - 0920 PST

IIN00100

ORANGE COUNTY RESERVOIR, ABUTMENT S06W

DAMPING VALUES ARE 0, 2, 5, 10 AND 20 PERCENT OF CRITICAL

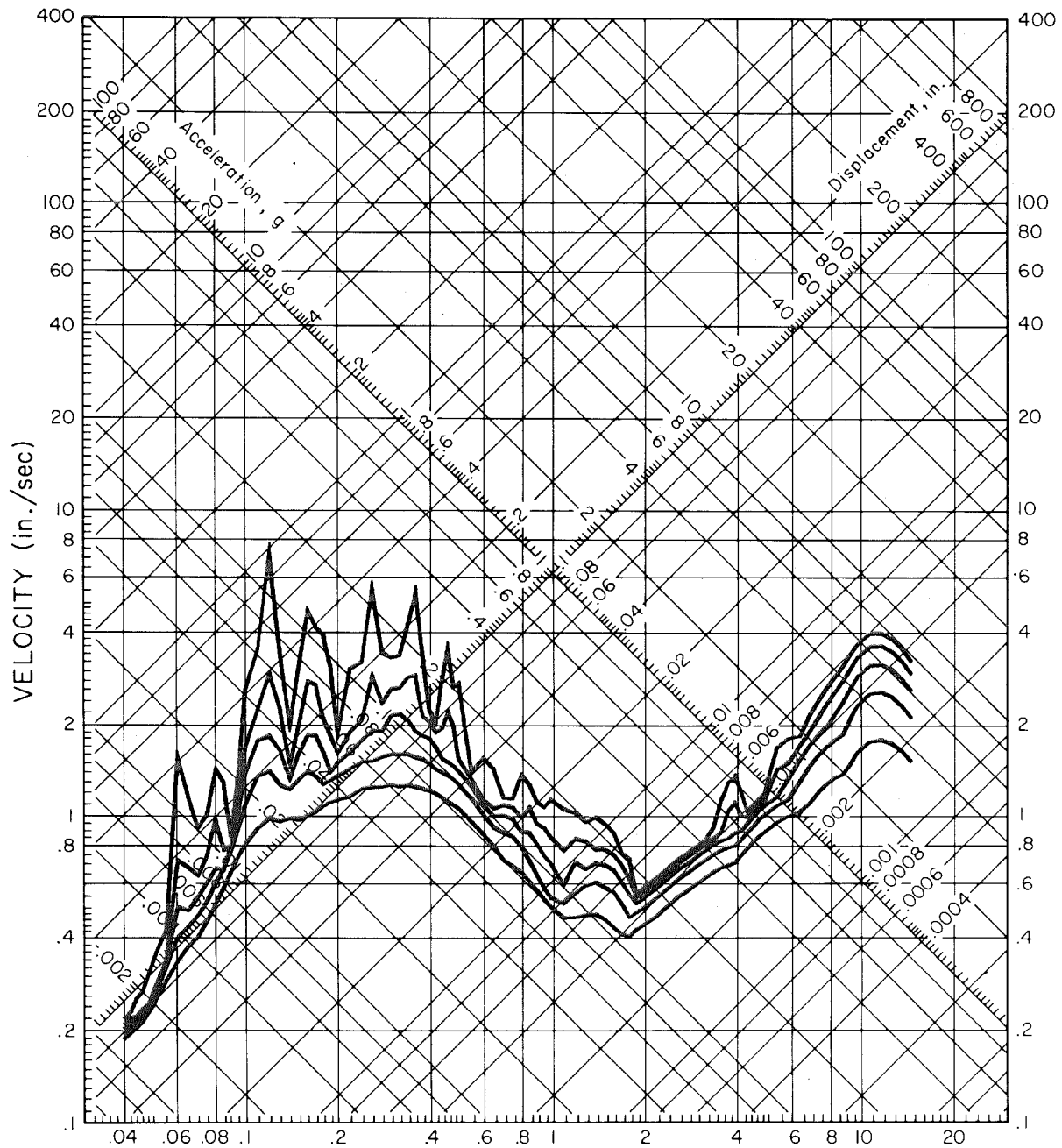
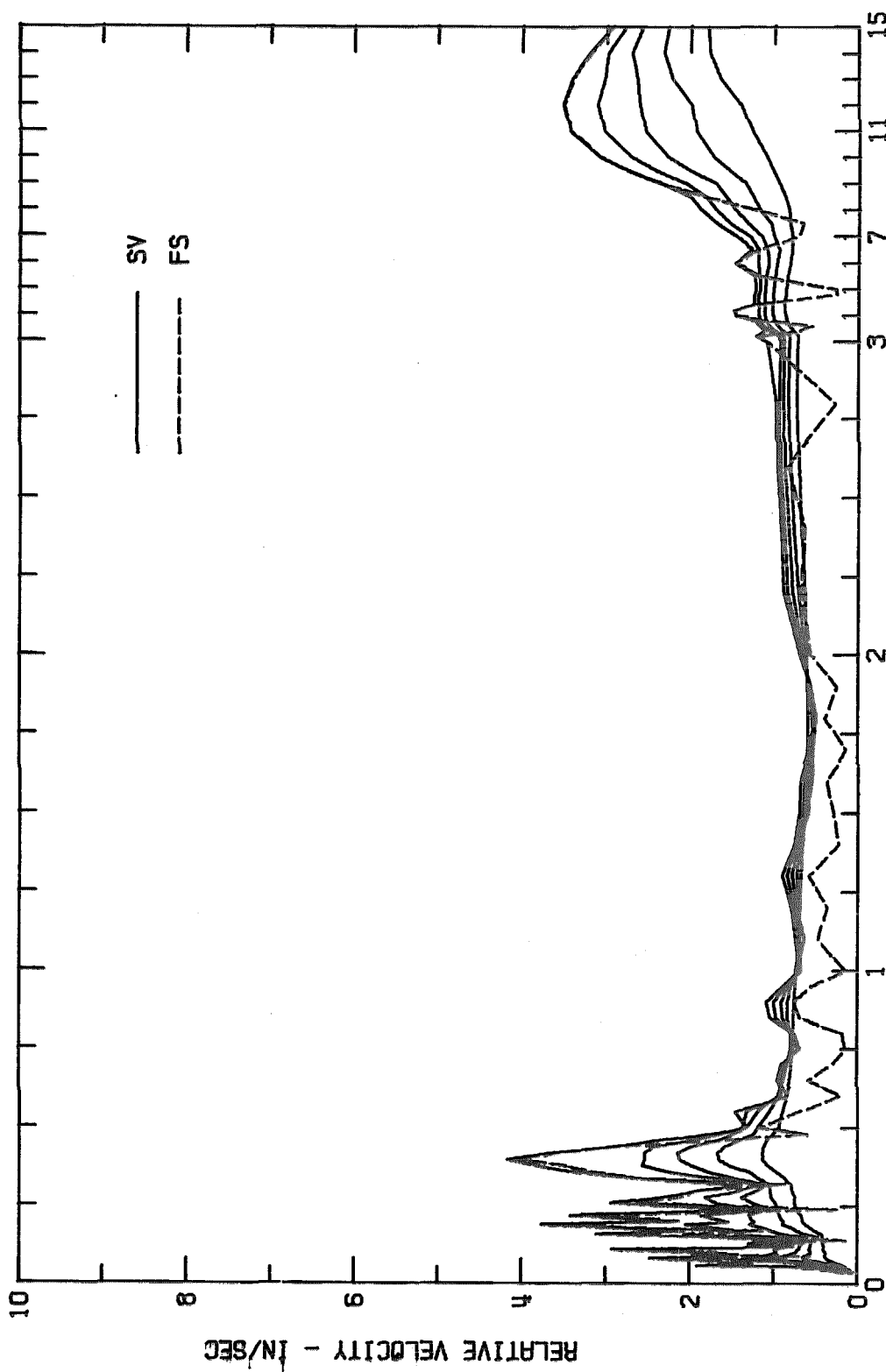


Fig. 108-b

RELATIVE VELOCITY RESPONSE SPECTRUM
ORANGE COUNTY RESERVOIR, ABUTMENT, JANUARY 1, 1976 - 0920 PST
11000100 ORANGE COUNTY RESERVOIR, ABUTMENT DOWN
DAMPING VALUES ARE 0, 2, 5, 10 AND 20 PERCENT OF CRITICAL



PERIOD - SECONDS
Fig. 109-a

RESPONSE SPECTRUM

ORANGE COUNTY RESERVOIR, ABUTMENT, JANUARY 1, 1976 - 0920 PST

IIN00100

ORANGE COUNTY RESERVOIR, ABUTMENT DOWN

DAMPING VALUES ARE 0, 2, 5, 10 AND 20 PERCENT OF CRITICAL

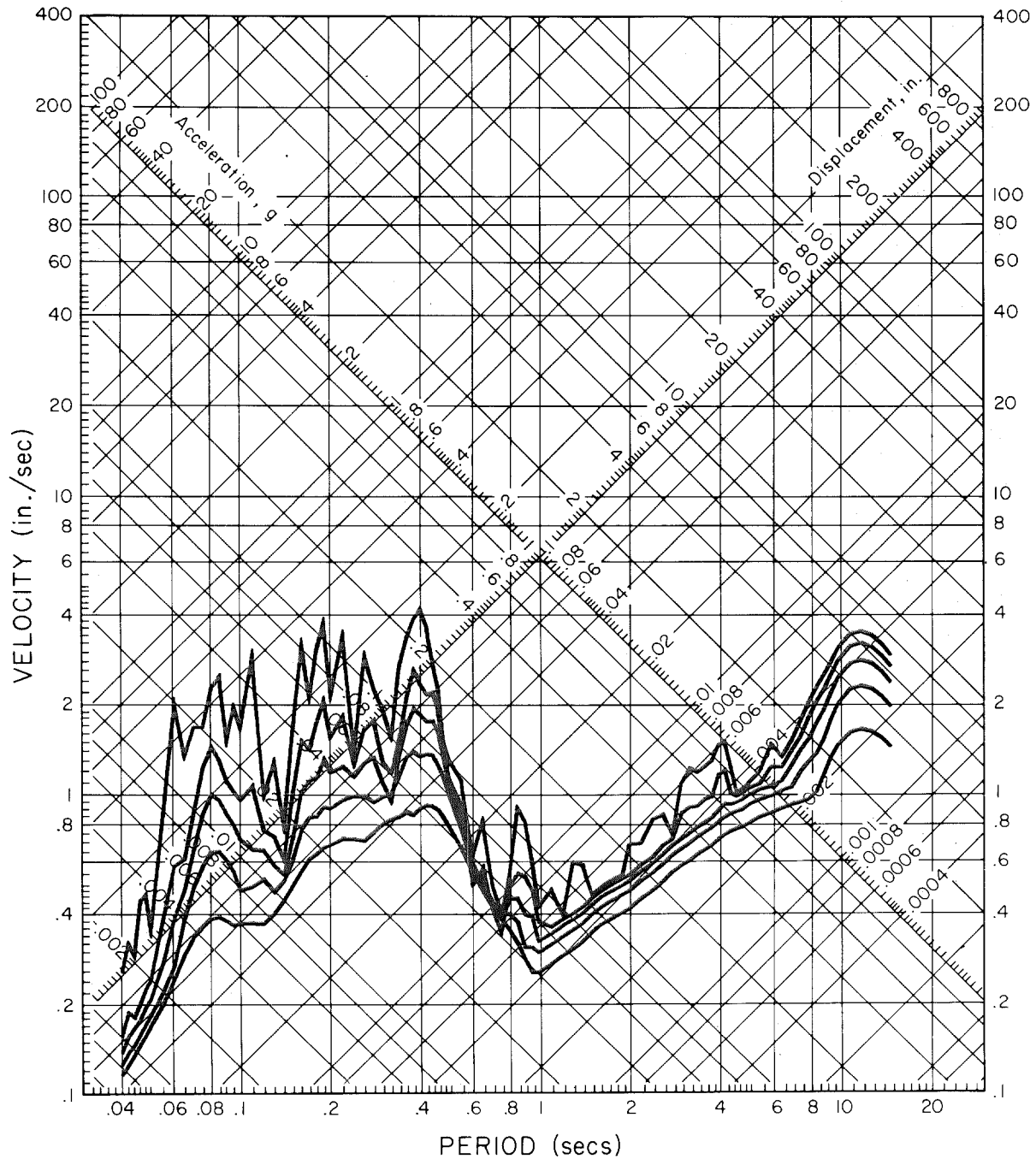
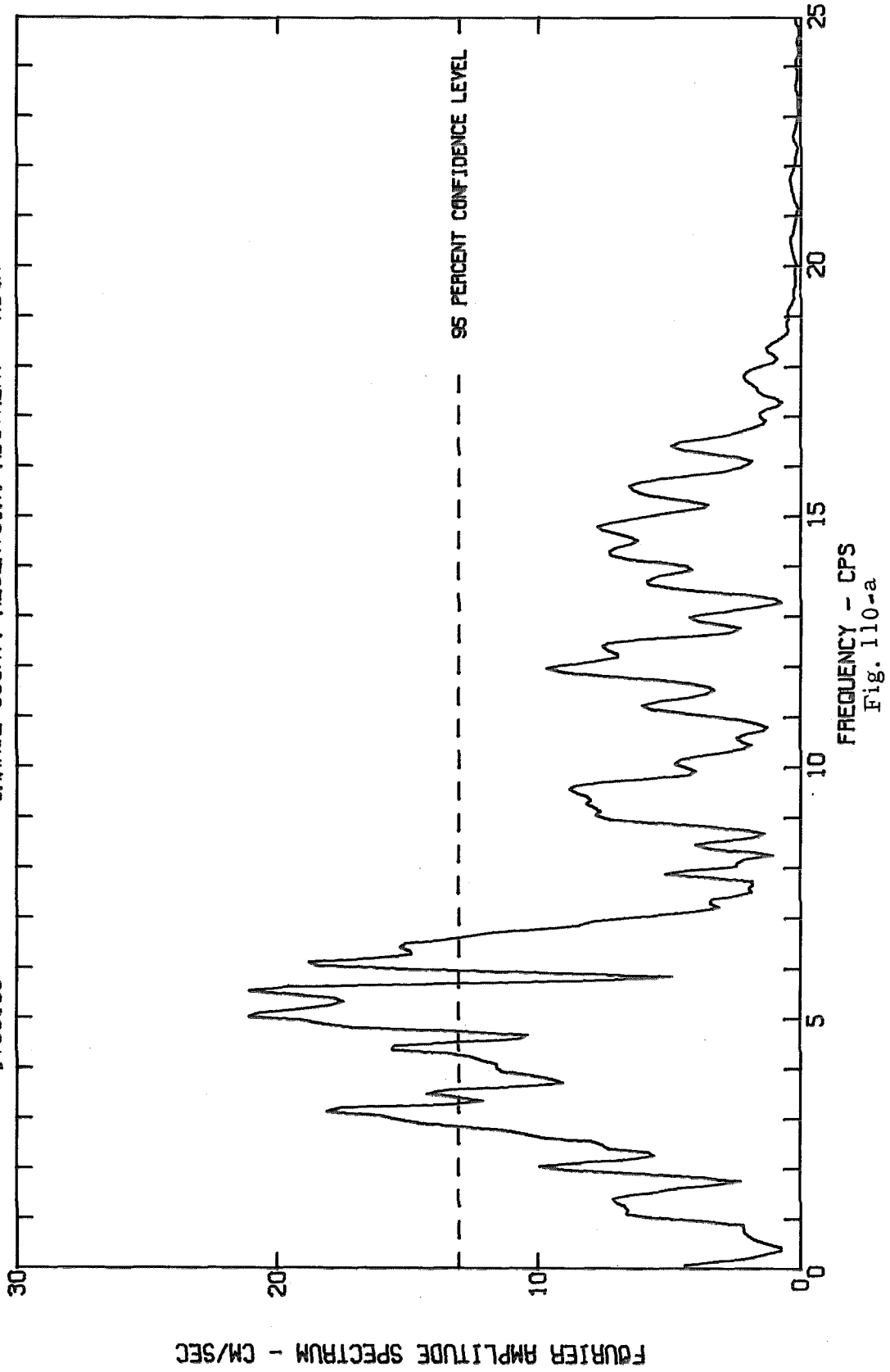
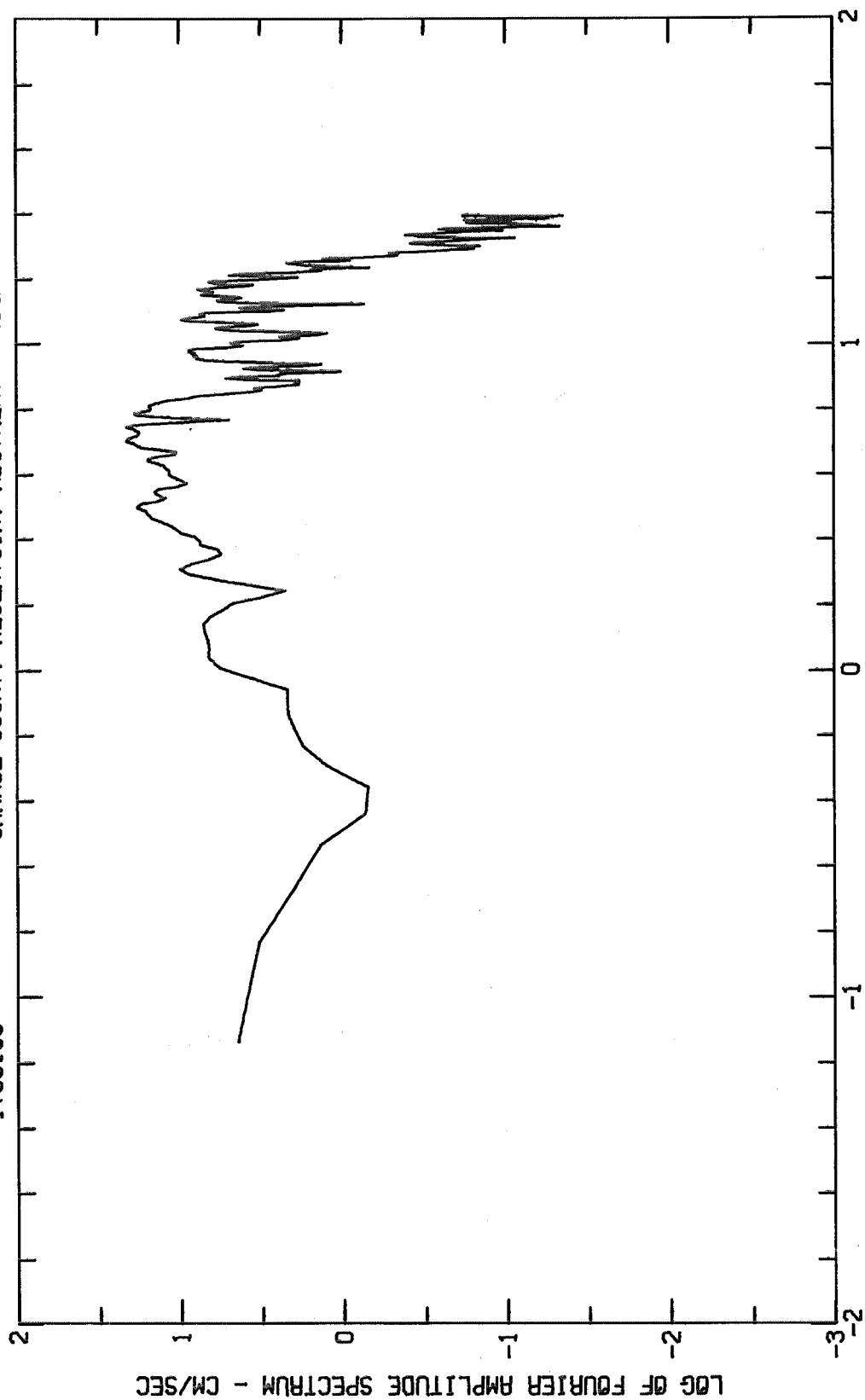


Fig. 109-b

FOURIER AMPLITUDE SPECTRUM OF ACCELERATION
ORANGE COUNTY RESERVOIR, ABUTMENT, JANUARY 1, 1976 - 0920 PST
IV00100 ORANGE COUNTY RESERVOIR, ABUTMENT N84W



FOURIER AMPLITUDE SPECTRUM OF ACCELERATION
ORANGE COUNTY RESERVOIR, ABUTMENT, JANUARY 1, 1976 - 0920 PST
1V00100 ORANGE COUNTY RESERVOIR, ABUTMENT N84W



LOG OF FREQUENCY - CPS
Fig. 110-b

FOURIER AMPLITUDE SPECTRUM OF ACCELERATION
ORANGE COUNTY RESERVOIR, ABUTMENT, JANUARY 1, 1976 - 0920 PST
1V00100 ORANGE COUNTY RESERVOIR, ABUTMENT S06W

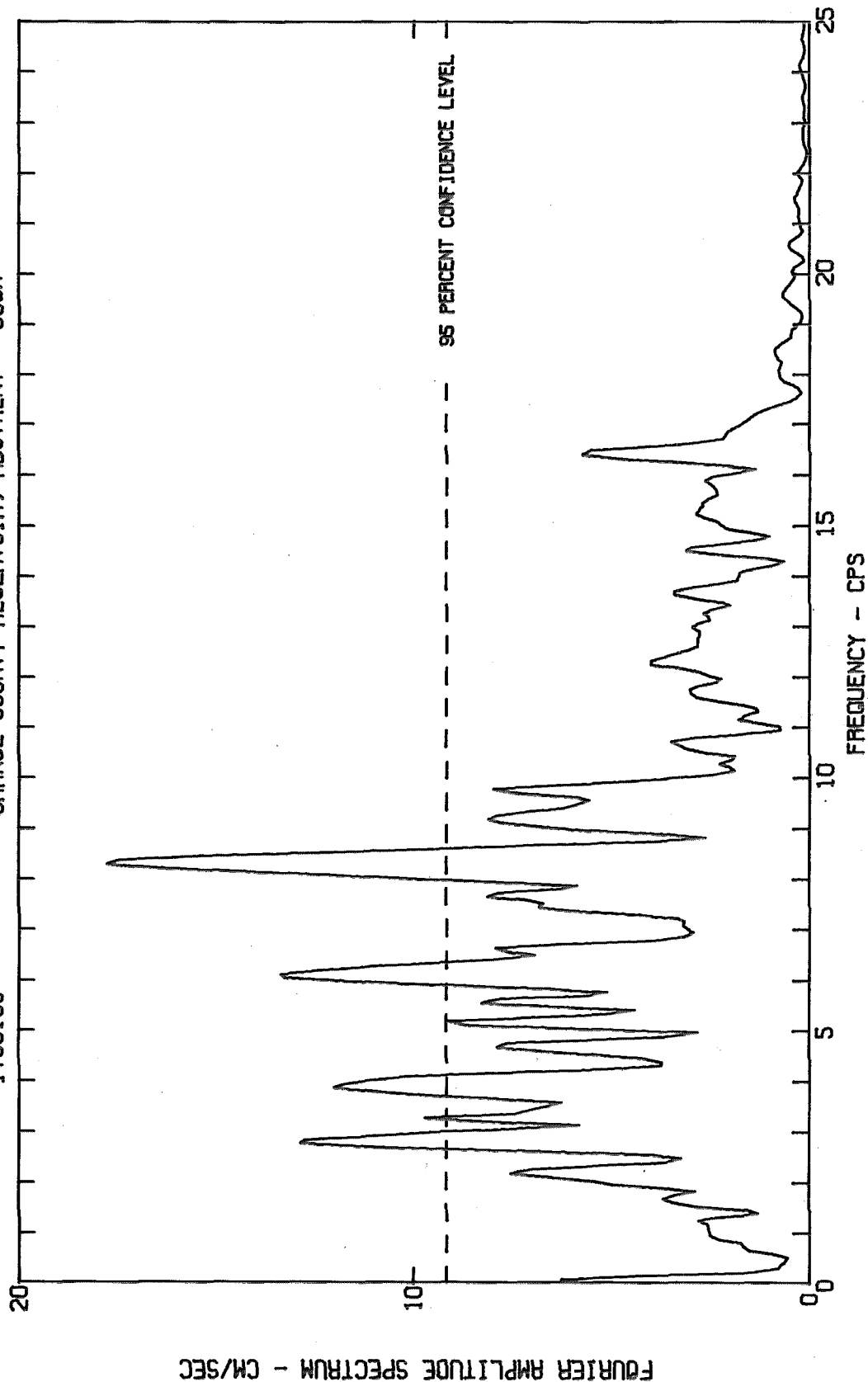
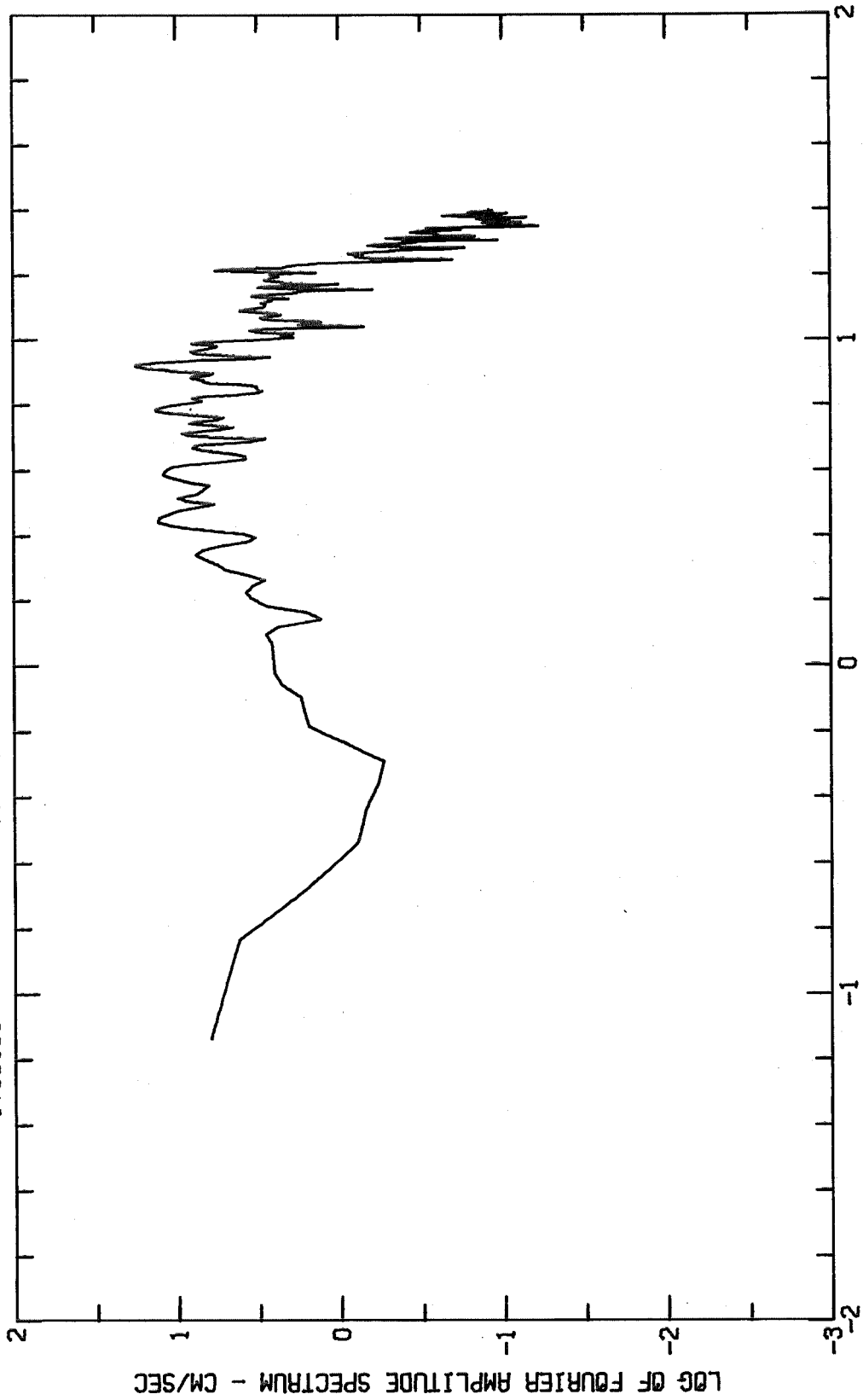


Fig. 111-a

FOURIER AMPLITUDE SPECTRUM OF ACCELERATION
ORANGE COUNTY RESERVOIR, ABUTMENT, JANUARY 1, 1976 - 0920 PST
IV00100 ORANGE COUNTY RESERVOIR, ABUTMENT S06W



LOG OF FREQUENCY - CPS

Fig. 111-b

FOURIER AMPLITUDE SPECTRUM OF ACCELERATION
ORANGE COUNTY RESERVOIR, ABUTMENT, JANUARY 1, 1976 - 0920 PST
ORANGE COUNTY RESERVOIR, ABUTMENT DOWN

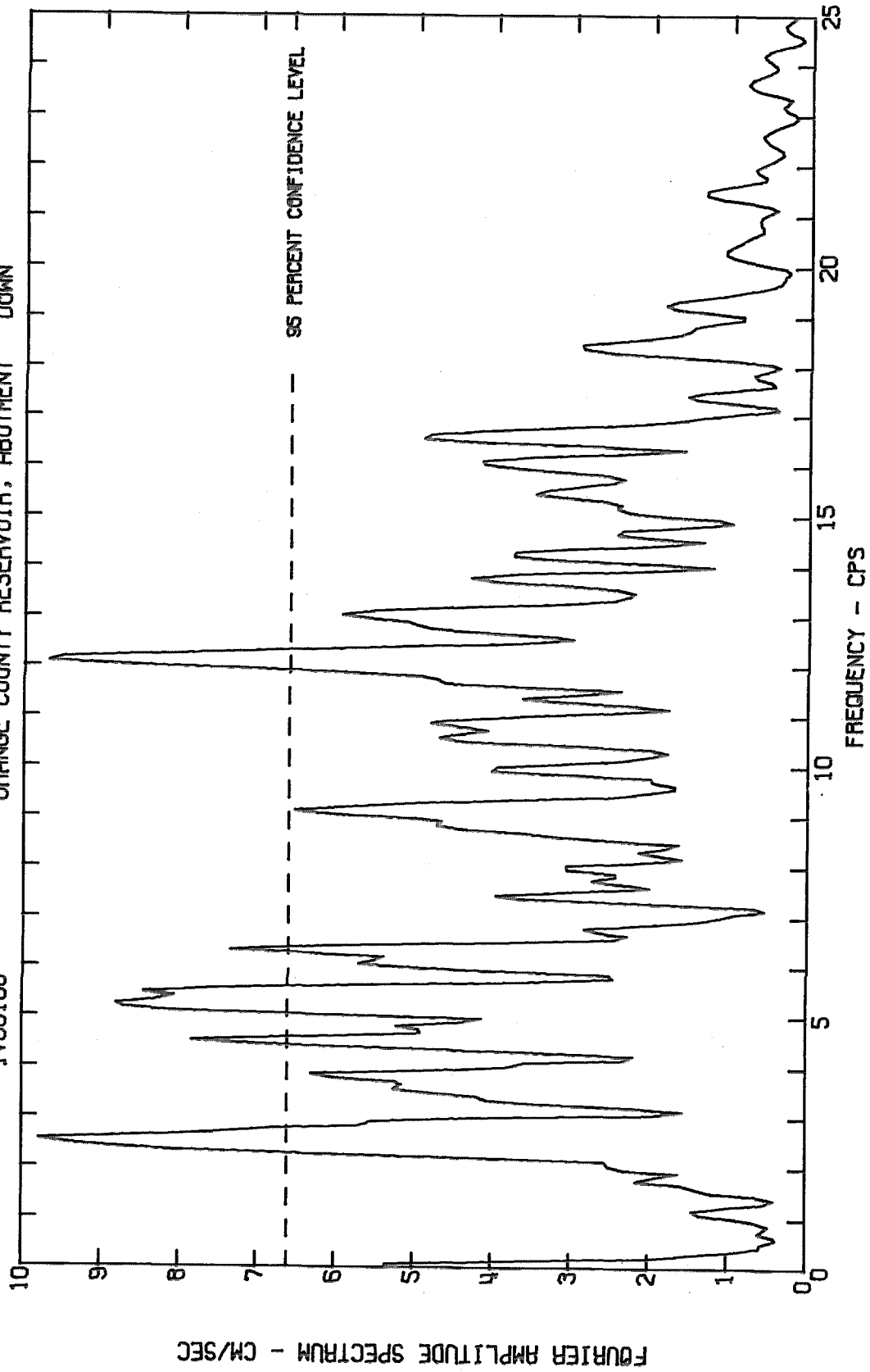
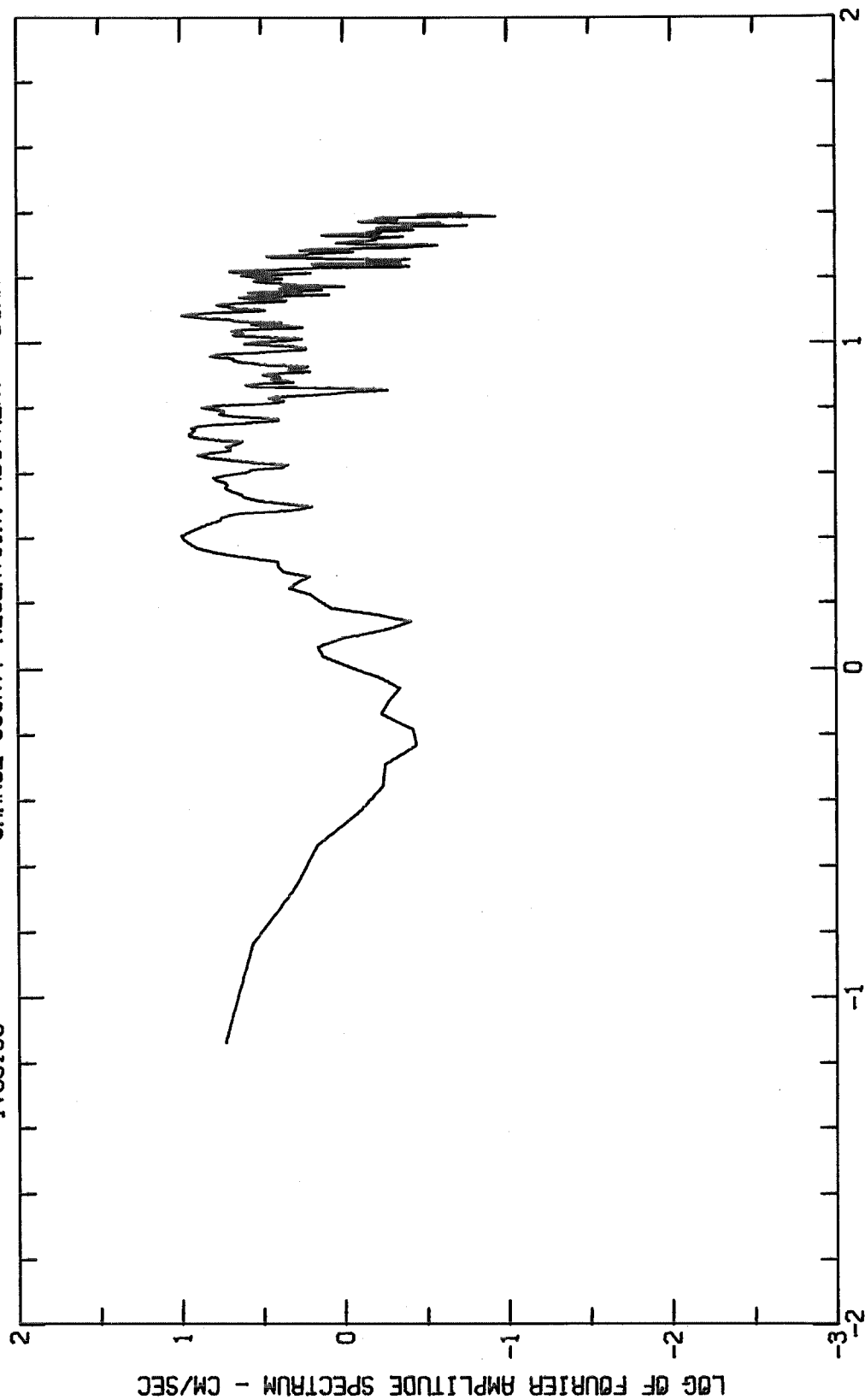


Fig. 112-a

FOURIER AMPLITUDE SPECTRUM OF ACCELERATION
ORANGE COUNTY RESERVOIR, ABUTMENT, JANUARY 1, 1976 - 0920 PST
IV00100 ORANGE COUNTY RESERVOIR, ABUTMENT DOWN



LOG OF FREQUENCY - CPS

Fig. 112-b

CONCLUSIONS

The eleven strong-motion accelerographs located near the epicenter of the Whittier earthquake of January 1, 1976 were installed in one multi-story building and on two dams and two reservoirs. Although the earthquake had a Richter magnitude of only 4.2, and thus does not qualify as a potentially destructive earthquake, a peak acceleration of 18% g was recorded by the closest accelerograph, 2.2 miles from the epicenter (at Orange County Reservoir). Having the earthquake motions recorded at five different locations, all within 10 miles of the epicenter, gives a good picture of the disturbance. The analysis of the records would, of course, have had a greater engineering significance if the magnitude of the earthquake had been greater so that the structural vibrations might have caused some overstress. However, even with ground motion of such short duration the recorded accelerations provided information of engineering significance. The analysis of the motions of the Whittier Building shows that even in such a relatively simple structure excited by moderate ground shaking, the vibrations are surprisingly complex. The recorded motion on the roof of the Diemer Reservoir clearly showed that the roof vibrated with appreciable beam-type deformations, thus revealing an undesirable flexibility of the structure. The two accelerographs on the two abutments of Carbon Canyon Dam provided valuable information on the degree of correlation between the earthquake motions of two ends of a dam.

ACKNOWLEDGEMENT

The author is grateful to several individuals and agencies for their assistance in providing much appropriate information and data. The author would especially like to thank Mr. R.P. Young and Mrs. J. Bridewell of the Army Corps of Engineers, Mr. D. Smith, Jr. and Mr. M. Dowd of the Metropolitan Water District of Southern California, Mr. R. Maley of the U.S. Geological Survey and Mr. R. Jensen of R. L. Jensen Associates of Los Angeles for providing structural details, drawings and data sheets of the different structures analyzed in this report. Gratitude is also extended to Sai-Man Li, Joannis Psycharis and Brian Murata of Caltech for the time and effort they contributed to the digitization and computer processing of the records.

Finally, the author wishes to thank Professor George Housner of the California Institute of Technology for his critical reading of the manuscript and for offering many valuable suggestions.